UNIVERSITY OF CALIFORNIA,
IRVINE

Progress Towards a Formal Enantiospecific Total Synthesis of Potent Antimalarial (-)-7-Isocyano-11(20),14-epiamphilectadiene and Preliminary Investigations of Carbene [2,3]-Wittig Reactions and Epoxypolyene Polycyclizations

THESIS

submitted in partial satisfaction of the requirements
for the degree of

MASTER OF SCIENCE

in Chemistry

by

Michael David Freidberg

Thesis Committee:
Professor Christopher D. Vanderwal, Chair
Professor David L. Van Vranken
Assistant Professor Sergey V. Pronin

2018

TABLE OF CONTENTS

	Page
LIST OF FIGURES	iii
LIST OF ABBREVIATIONS	vii
ACKNOWLEDGMENTS	ix
ABSTRACT OF THE THESIS	x
INTRODUCTION	1
CHAPTER 1: Towards an Enantioselective Formal Synthesis of an Antimalarial ICT	8
Devising improved route	25
CHAPTER 2: Carbene [2,3]-Wittig Investigations	34
CHAPTER 3: Exploration of Potential Radical and Cationic Polycyclization Methods for 2,2-Disubstituted Epoxide Substrates	50
REFERENCES	91
APPENDIX A: Experimental Details	101
APPENDIX B: Supporting Information	137

LIST OF FIGURES

		Page
Figure 1.	Examples of current antimalarials	1
Figure 2.	Precedented conversion of Shenvi intermediate **1** into ICT **2**	2
Figure 3.	Our lab's planned approaches to **2** (via Shenvi intermediate **1**)	3
Figure 4.	Potential use of carbene [2,3]-Wittig for installing a quaternary Stereocenter	5
Figure 5.	The only example of isolated 2,2-disubstituted epoxide in a Polycyclization	6
Figure 6.	IC_{50} values for selected ICTs and related compounds	10
Figure 7.	IC_{50} values of simplified structures of potent ICTs	12
Figure 8.	Overview of malaria life cycle in mammals and potential antimalarial drug interference of heme detoxification	13
Figure 9.	Shenvi retrosynthesis of intermediate **1** and our planned [4+2] reactions	17
Figure 10.	First and second generation retrosyntheses for comparison	18
Figure 11.	Bare amphilectane scaffold with traditional carbon numbering	20
Figure 12.	First attempt at enantiospecific formal synthesis of **2** (via **1**): Retrosynthesis	23
Figure 13.	Synthesis of monoprotected diol **13** and attempted elimination	23
Figure 14.	Synthesis of tosylate **34**, iodide **35** and elimination to give alkene **36**	24
Figure 15.	TBS-deprotection of **36** and subsequent attempted DMP oxidation	24

Figure 16. Attempted asymmetric Robinson annulation en route to DICA 25

Figure 17. Possible mode of Lewis acid-catalyzed decomposition of enone **5** 25

Figure 18. Second generation retrosynthesis of **2** (via **1**) 26

Figure 19. Jung's double Michael Addition precedence 28

Figure 20. Epimerization of *cis*-dione **10a** to *trans*-dione **10b** (presumed ground state conformations shown, with 2-propenyl group equatorial) 29

Figure 21. Hydroformylation of **10b** to give **30a** 31

Figure 22. X-ray diffraction crystal structure configuration of trans-dione **10b** 32

Figure 23. First sulfur-stabilized carbene [2,3] (Baldwin) 36

Figure 24. Late stage carbene [2,3]-Wittig in Evan's synthesis of bakkenolide-A 37

Figure 25. Jung & Parker use a bis(alkylthio)-stabilized carbene to install a hindered carboxylate group in the synthesis of an analogue of the antitumor agent, halomon 38

Figure 26. Büchi's use of the carbene [2,3]-Wittig to make amides 39

Figure 27. Thermal fragmentation pathways for 1,3,4-oxadiazolines 41

Figure 28. Mechanism of undesired radical [1,2]-Wittig rearrangement 41

Figure 29. Yields of nucleophilic carbenes from 1,3,4-oxadiazoline thermal Degradation 43

Figure 30. Synthesis of [2,3]-Wittig substrate **66** 43

Figure 31. Synthesis of [2,3]-Wittig substrate **68** 44

Figure 32. Brief optimization of solvent for the [2,3]-Wittig method with **66** 44

Figure 33. Optimization of temperature for thiol-derived 1,3,4-oxadiazolines; **68** reacting under optimized conditions for [2,3]-Wittig 45

Figure 34.	Synthesis of amine-derived [2,3]-Wittig substrate	46
Figure 35.	Graduated heating of amine-derived [2,3]-Wittig substrate	48
Figure 36.	Attempted synthesis of amide-derived [2,3]-Wittig substrate	49
Figure 37.	Polycyclization of farnesylacetic acid and monocyclic derivative	53
Figure 38.	All known precedence for 2,2-disubstituted epoxypolyene polycyclization	55
Figure 39.	Cyclopropylcarbinyl radical as analogue for Ti(III)-epoxide complex	58
Figure 40.	Summary of 1st generation retrosynthesis of initial model system	60
Figure 41.	Synthesis of phosphonate **94** (fragment **A1**)	61
Figure 42.	Literature synthesis of enone-aldehyde, **95**, and enone-acetal, **103**	62
Figure 43.	C Synthesis of (*E*,*Z*)-triene via an HWE olefination of fragments **A1** and **B1**	63
Figure 44.	Chemoselective mCPBA epoxidation of triene, **93**, and attempted (asymmetric) Shi epoxidation	64
Figure 45.	CBS reduction of **103** (prior to optimization) and Mosher's ester Analysis	66
Figure 46.	Improved synthesis of enone-tethered acetal **103**	66
Figure 47.	Synthesis of fragment **B2**, **108**, from **103**	67
Figure 48.	1st generation synthesis of epoxyphosphonate, **112** (fragment **A2**)	68
Figure 49.	Synthesis of epoxy iodide **111** from ethyl levulinate **109**	68
Figure 50.	Alkylation of **111** with **100** to obtain fragment **A2**, **112**	70
Figure 51.	2nd generation synthesis of epoxyphosphonate, **112** (fragment **A2**)	71
Figure 52.	Synthesis of epoxy tosylate, **116**, and attempted alkylation with **100**	72

Figure 53. Iodination of epoxy tosylate to give epoxy iodide, then alkylation to **112** 74

Figure 54. Summary of first two approaches to fragment **A2** 74

Figure 55. 3rd generation synthesis of epoxyphosphonate, **112** (fragment **A2**) 75

Figure 56. Wittig olefination attempt 76

Figure 57. Final improved synthesis of fragment **A2** 77

Figure 58. HWE coupling of fragments **A2** and **B2** 79

Figure 59. Simple aldehydes synthesized: fragments **B3**, **B4**, **B5**, and **B6** 83

Figure 60. Preliminary HWE couplings of fragments **A2**-**B3**, **A2**-**B4**, and **A2**-**B5** 84

Figure 61. The control reaction for Ti(III)-mediated radical cyclization 85

Figure 62. Example of attempted polycyclization with complex allylic acetate **92** 86

Figure 63. Attempted polycyclization of **126** under Lewis acidic conditions 87

Figure 64. Simple epoxy ketone **127** in radical-polar crossover polycyclization 89

LIST OF ABBREVIATIONS

Ac	acetyl
cat.	Catalytic
Cbz	carboxybenzyl
CDI	1,1'-carbonyl diimidazole
Coll.	collidine
d	day(s)
dr	diastereomeric ratio
ee	enantiomeric excess
h	hour(s)
HWE	Horner-Wadsworth-Emmons (reaction)
Imid.	imidazole
lit.	literature
LLS	longest linear sequence
mCPBA	*m*-chloroperbenzoic acid
MS	mass spectrometry
NHC	*N*-heterocyclic carbene
NMR	nuclear magnetic resonance (spectroscopy)
Ph	phenyl
Piv	pivaloyl
quant.	quantitative
SM	starting material

TBS	*t*-butyldimethylsilyl
Tf	trifluoromethylsulfonyl
TIPS	trimisopropylsilyl
TLC	thin layer chromatography
TMS	trimethylsilyl
Ts	*p*-toluenesulfonyl

ACKNOWLEDGMENTS

I would like to express the deepest appreciation to my committee chair, Professor Chris Vanderwal, who has been a steadfast champion for me during the most difficult times.

I would like to thank my committee members, Professors Dave Van Vranken and Professor Sergey Pronin, who have excitement for chemistry that is always contagious and have lent insight into organizational and chemical questions alike.

In addition, a thank you to Professor Jennifer Schomaker at the University of Wisconsin-Madison for allowing me to join her lab during my freshman year and for helping to cultivate a great love for chemistry.

Financial support was provided by the University of California, Irvine, NSF-GRFP Fellowship, which supported me for several quarters throughout my graduate career.

ABSTRACT

Progress Towards a Formal Enantiospecific Total Synthesis of Potent Antimalarial (-)-7-Isocyano-11(20),14-epiamphilectadiene and Preliminary Investigations of Carbene [2,3]-Wittig Reactions and Epoxypolyene Polycyclizations

By

Michael D. Freidberg

Master of Science in Chemistry

University of California, Irvine, 2018

Professor Christopher D. Vanderwal, Chair

Total synthesis and methodology are two large fields of study in synthetic organic chemistry which serve to expand available reactions and strategies with the overarching goal of revealing unique and concise solutions to complex chemical problems. Achievements in these fields are crucial for current and future reasonable syntheses of bioactive compounds of interest in order to evaluate potentially useful materials. Our efforts to contribute to these endeavors included the attempted formal synthesis of an antimalarial isocyanoterpene (ICT) and the investigation into the expansion of the carbene [2,3]-Wittig and polycyclization methodologies.

Malaria currently causes millions of infections yearly, and the drugs that are commonly used to treat it are losing efficacy. ICTs are a class of compounds that show great potential for becoming the basis of a new class of antimalarials that are believed to act via traditional and non-traditional routes to eliminate the malaria parasite. To improve upon the synthesis of one of the most potent ICTs, reported by Shenvi, we

chose to pursue an enantiospecific formal synthesis of (-)-7-Isocyano-11(20),14-epiamphilectadiene.

In the course of our investigations into two separate methodologies, we gained insight into the [2,3]-Wittig rearrangement of various carbenes and the polycyclization of 2,2-disubstituted epoxides and established reliable routes to substrates for the latter. It is our hope that this progress—in addition to future contributions from our lab—aids in the development of expedient and concise syntheses of useful bioactive compounds.

INTRODUCTION

It is commonly believed that with today's chemical knowledge, essentially all complex natural products are accessible using known reactions. However, the synthesis of these compounds using traditional well-established reactivity has many limitations, which can lead to synthetic routes that necessitate an excessively large number of individual reaction steps, with each step often requiring a different reaction setup, post-reaction extraction or "work-up", and one or more purification techniques. These issues, which result in a considerable amount of time, energy, and money expended synthesizing target compounds, culminate in an ongoing impetus to devise creative and concise solutions to synthetic problems. A new way to form chemical bonds (methodology) and novel, thoughtful sequence development (synthetic strategy)—for instance, a succinct route to a complicated scaffold—help contribute valuable knowledge to the scientific literature and expand the "repertoire" of reactions that organic chemists have at their disposal.

Figure 1. Examples of current antimalarials

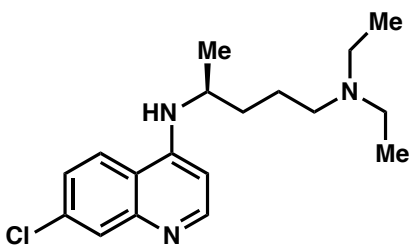

Chloroquine (racemate)

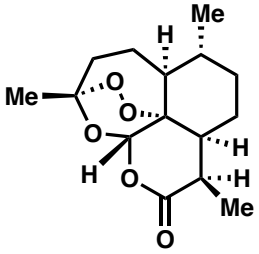

Artemisinin

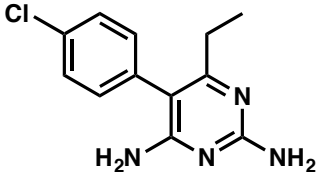

Pyrimethamine

Current antimalarials are losing efficacy and with hundreds of millions infected each year, new drugs are desperately needed (Fig. 1).[1-4] Isocyanoterpenes (ICTs) represent a unique potential solution, with many exhibiting potent antimalarial activity by attacking the parasite in multiple different ways.[3-6] In an effort to decrease the difficulty of synthesizing ICT analogues and streamline the efforts to find a suitable lead compound, many research groups have developed syntheses of the most potent antimalarials in the ICT family.[5,6] Our desire to contribute to this effort has led to a major focus in our lab on the synthesis of potent ICTs and their analgoues.[7-12] To this end, we pursued an enantiospecific formal synthesis of the potent ICT antimalarial (-)-7-isocyano-11(20),14-epiamphilectadiene, **2**, with a planned approach that intersects the previous (racemic) synthesis reported by Shenvi in 2012 at intermediate **1**.[13] Shenvi's synthesis of intermediate **1** was carried out in a total of 7 steps (LLS) from commercially available starting material (3-buten-2-ol), giving an overall step count (for the synthesis of **2**) of 11 steps (LLS) (Fig. 2).[13]

Figure 2. Precedented conversion of Shenvi intermediate **1** into ICT **2**

Shenvi's end game (summary):

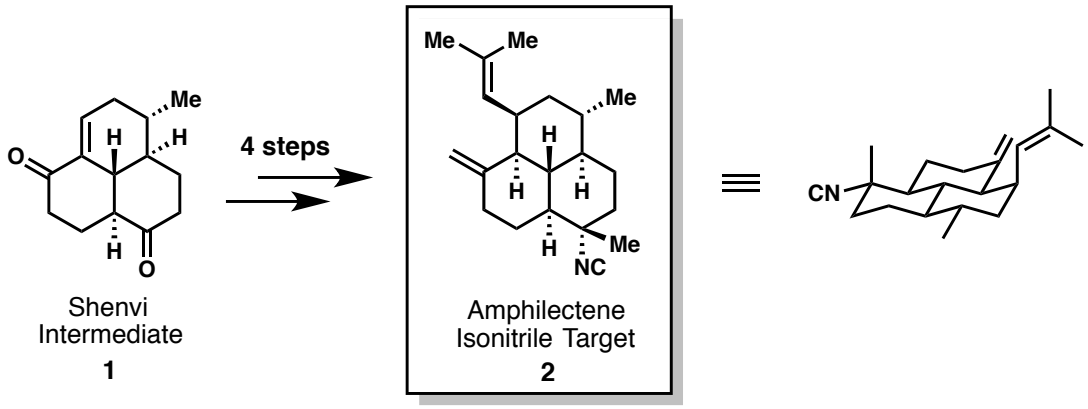

While the Shenvi synthesis relied on dendralene Diels-Alder reactions to form two of the three fused 6-membered rings, we planned to utilize an intramolecular aldol condensation and formal [4+2] cycloaddition to form two of these three rings (Fig. 3). In both of our attempted formal synthesis routes, we began with chiral pool starting material, which allowed for enantiospecific approaches. In the first route, the synthesis of aldehyde **7** from (*S*)-citronellol (**9**) was undertaken. Several functional group manipulations were accomplished toward this goal, but the use of aldehyde **7** in the Robinson annulation key step (**6+7→5**) was never attempted. Colleague Philipp Roosen found that Robinson annulations on these types of systems tend to lack diastereoslectivity, leading to the eventual abandonment of this route. We were encouraged to instead pursue a different route.

Figure 3. Our lab's planned approaches to **2** (via Shenvi intermediate **1**)

This work: 1st retrosynthesis:

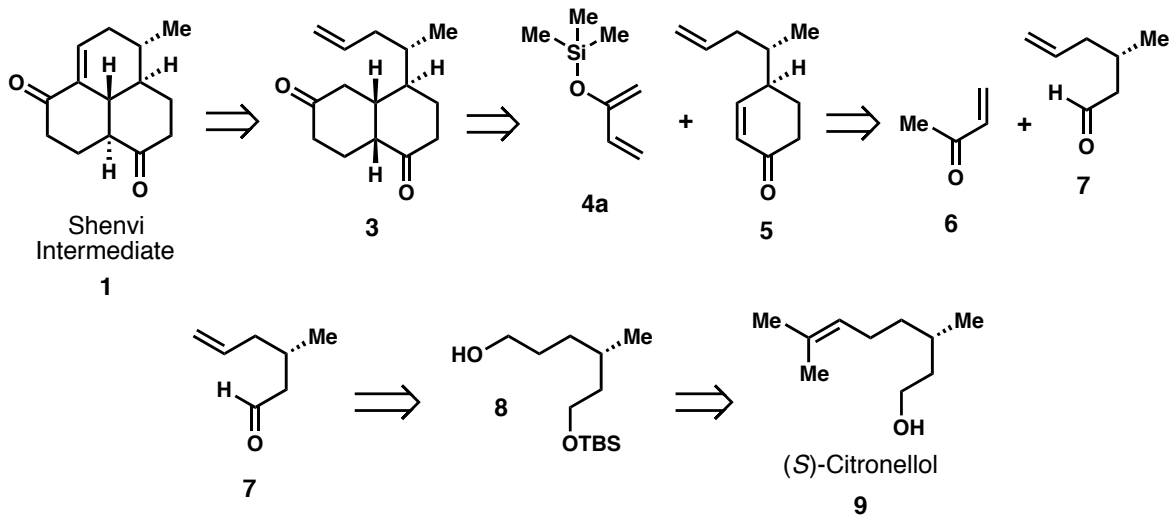

This work: 2nd retrosynthesis:

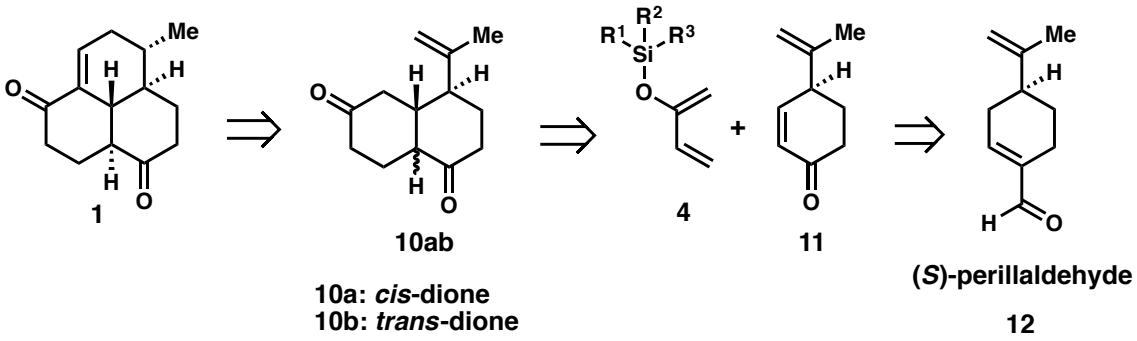

The second approach that we planned relied on a [4+2] of **4** and **11** and subsequent hydroformylation before a final ring-closing aldol condensation (Fig. 3). A vast array of conditions were tested before finding a method that accomplished the formal [4+2]. Fortunately, in a single step, the formal [4+2] was achieved, along with subsequent silyl enol ether hydrolysis and epimerization to *trans*-dione, **10b**, albeit in low yield. Product purification, however, was quite tedious. The next step, hydroformylation, proceeded very slowly under harsh conditions, making optimization difficult. The aldehyde product, obtained in low yields, was unfortunately found to possess the wrong stereochemistry at the methyl-containing stereocenter. Since these transformations are largely substrate-dependent, we chose to abandon this approach.

A relatively under-utilized methodology, the carbene [2,3]-Wittig,[14] represents a potentially unique way to install carboxylate-derived functional groups at hindered positions, with the stereospecificity of the transformation (e.g. diastereofacial selectivity) translating existing stereochemistry to a new stereocenter (Fig. 4).

Figure 4. Potential use of carbene [2,3]-Wittig for installing a quaternary stereocenter

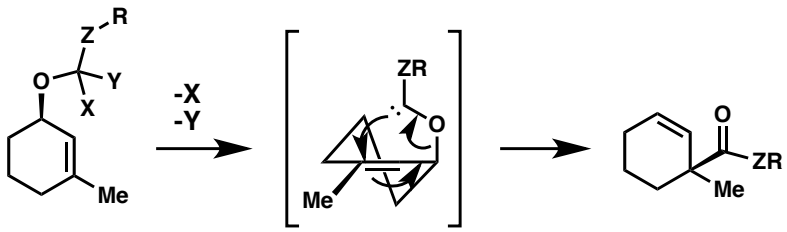

X,Y = carbene precursor; Z = O, NR', S, etc.

The expansion of the carbene [2,3]-Wittig methodology to include the generation of hindered α-carboxyl stereocenters has been, for many years, impeded by the high temperatures and harsh conditions required to form the intermediate carbenes and the steric limitations in forming the carbene precursors.[14] Unfortunately, the difficulty in applying this method to the installation of useful functionality at hindered positions has further limited the utility of this transformation. In an attempt to overcome these obstacles, our lab has begun investigating known methods of generating carbenes, with the option to differentially functionalize the divalent (carbene) species with heteroatoms of various stabilizing aptitude. Ideally, this could provide an alternative way to set α-quaternary and α-tertiary stereocenters in carboxylic acid derivatives in cases where features of the scaffold (e.g. sterics) do not permit easy access to the desired products via traditional reactivity (i.e. α-alkylation, α-protonation, etc.).

Our initial work on the carbene [2,3]-Wittig method led to some interesting findings. We prepared 1,3,4-oxadiazoline derivatives to be used as carbene precursors and found that allyloxy(alkylthio) carbenes are capable of undergoing a [2,3]-Wittig

rearrangement. As seen under ylide [2,3]-rearrangment conditions, the competing [1,2]-Wittig reaction is a common side reaction in this method, along with undesired pathways of oxadiazoline fragmentation. Further optimization is underway.

Polycyclizations of polyenes have been used for many years[15-20] by synthetic organic chemists to form a myriad of complex multi-ring carbocyclic molecules. The methodologies that have manifested from the development of these polycyclizations facilitate the rapid increase in molecular complexity in a purely synthetic setting without the need for enzyme catalysis.[15-31] While many avenues of polyene cyclization have been investigated in detail, epoxypolyene polycyclizations of 2,2-disubstituted epoxides—that do not contain adjacent (vicinal) functionality—have received very little attention. In fact, to the best of our knowledge, only one example exists in the literature which was published in 1969 by Goldsmith and Phillips (Fig. 5).[31] The reported conditions for their polycyclization was the result of a significant amount of reaction optimization; yet, poor yields were still obtained, likely due to the relatively harsh conditions employed for the cationic cyclization.

Figure 5. The only example of isolated 2,2-disubstituted epoxide in a polycyclization

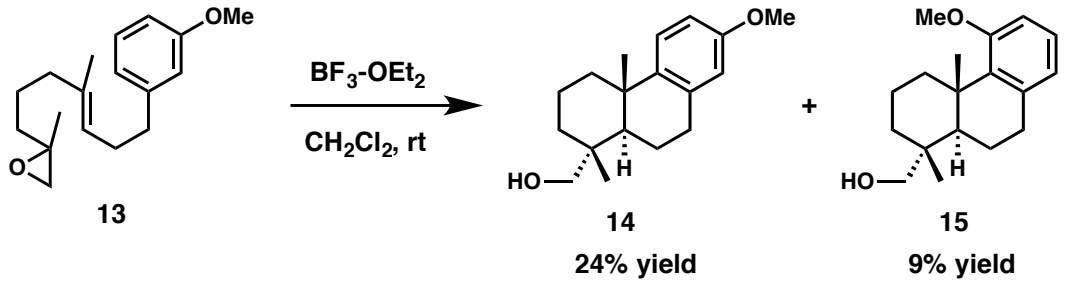

Even the polycyclization of 2,2-disubstituted epoxides with adjacent functionality is largely under-utilized, with only two reported examples: the racemic synthesis of aphidicolin by Van Tamelen and the enantioselective synthesis of neotripterifordin by Corey—both of these syntheses utilize cationic polycyclization conditions.[28,29] It is surprising that the use of this substitution pattern is not more widely recognized for its potential, especially considering that none of the three reports on cationic 2,2-disubstituted epoxypolyene polycyclizations mention the presence of a diastereomeric byproduct.[28,29,31] Also, the only high yielding cyclization (86%) was the only one of these reactions that was carried out at cryogenic temperatures (-94 °C, 10 min).[29] For these reasons, we became interested in exploring the untapped potential of this method.

The known reactivity of 2,2-disubstituted epoxides in the presence of Ti^{III} and the lack of reports on the polycyclization of these compounds made the pursuit of the radical version of this methodology particularly attractive.[31-42] Also, to date, no radical 2,2-disubstituted epoxide polycyclization has been reported. In our exploration of the potential of this method, we hope to gain insight into the diastereoselective—and perhaps even enantioselective—nature of both cationic and radical reaction manifolds. To accomplish this, we required reliable routes to polycyclization substrates. Achievements presented include the optimization of routes to two key fragments (A/B) and their derivatives for use in HWE olefination (coupling) reactions. Multiple substrates were made stereoselectively and several polycyclizations were attempted.

Chapter 1: Towards an Enantiospecific Formal Synthesis of an Antimalarial ICT

1.1 Introduction

Over 200 million malaria cases each year result in an estimated half a million deaths annually, which troublingly occur mostly in sub-Saharan African children under 5 years of age.[48-51] The fact that malaria most disproportionately effects undeveloped and developing regions of the world has contributed to a lack of funding and research for innovative treatments.[49,51,52] The three main classes of antimalarial drugs in current use today, quinolines/arylamino alcohols, antifolates, and endoperoxides, have been known to cause severe side effects (e.g. cinchonism, blood diseases, etc.), especially at higher dosages.[53,54] Also, resistance to antifolates has been a long-standing issue and recently, chloroquine-resistance has been observed in a number of endemic regions.[55,56] Startlingly, artemisinin resistance, in the last 10 years, has also been encountered which could mean the three main classes of antimalarials are becoming obsolete.[2]

In 2009, Dondorp et al. conducted a study along the Thai-Cambodian border that provided the first evidence of emerging resistance to artemisinin-combination therapies.[2] Drug-resistant strains have been found to possess mutations in the genome that affect the phenotypic propeller region of the parasite, which is believed to be the mechanistic origin of drug-insensitivity in many cases.[57] Undoubtedly, this pathogen

displays a high degree of genetic adaptability, demonstrated by its development of resistance to such a wide array of antimalarials.[2,55-57]

Numerous studies have shown that this endemic disease has become a major issue of concern in an increasing number of southeast Asian countries, with drug price volatility accompanying the failed treatments.[58-61] From these reports, and the fact that nearly half of the world's population lives in the 91 countries and territories effected by endemic malaria, the need to explore alternative antimalarial drug candidates is evident.[62]

Isocyanoterpenes (ICTs) are a class of structurally diverse natural products that exhibit a broad range of bioactivities including antibacterial, anti-inflammatory, and most prominently, antimalarial activity.[5,6,63-65] They are found largely in the marine environment as secondary metabolites of various sea creatures including sponges, nudibranchs, and sea cucumbers.[5,6] The ICT class of compounds represent an appealing entry into new antimalarial drug investigations for several reasons. Initial findings have shown that several simple compounds containing the isonitrile moiety were administered to rodents orally and subcutaneously in doses of up to 5 g/kg with little toxicity, indicating the relatively benign nature of the isonitrile functional group.[66] ICTs also generally display rather weak mammalian cytotoxicity (high μM) and certain ICTs have been found to exhibit very potent (low nM) antimalarial activity against *Plasmodium falciparum*, largely regarded as the most deadly species of the parasite (Fig. 4).[67-69] Importantly, the potent antimalarial activity ascribed to several ICTs has been verified by independent research groups and found to be equipotent against both

chloroquine-sensitive (HB3 and D6) *and* drug-resistant (W2 and Dd2) strains, showing further promise as a new drug class.[3,5,6,67,70-78]

1.2 Structure-Activity Relationship

The proposed mechanism of action for many of the currently prescribed antimalarial drugs (e.g. quinolines/arylamino alcohols, endoperoxides) involves their interaction with free heme.[3,78-80] The small molecule-heme interaction is also believed to play a role in the antimalarial activity of ICTs since the isonitrile group, being isoelectronic to carbon monoxide, exhibits strong binding as a ligand in the coordination to transition metal (TM) ions, such as the Fe ion in heme.[3,5,6,76,80] While the isonitrile group is—with one important known exception—required for anti-parasitic activity, the structure-activity relationship (SAR) and other data show that the entire pharmacological action of these ICTs does *not* rely solely on their ability to form strong non-covalent (dative) bonds with heme's Fe center (Fig. 6).[4,5,66]

Figure 6. IC_{50} values for selected ICTs and related compounds

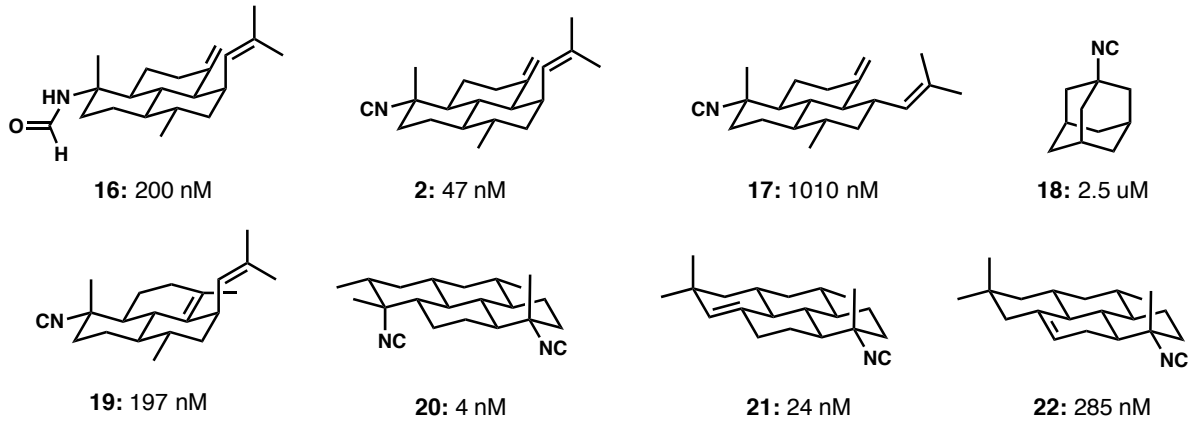

The theory that ICTs fully derive their activity from binding to heme is not consistent with either the observation that formamide amphilectane **16** has an IC_{50} of 200 nM (since formamide is a poor TM ligand) or the observation that the variation in the stereochemistry of a hydrocarbon moiety distal to the isonitrile in **2** and **17** is responsible for a >20-fold difference in anti-parasitic activity against *Plasmodium falciparum*.[5] The SAR indeed reveals a complex relationship between distal functionality and potency.[5] For instance, an alkene isomerization effects a significant change in potency, giving rise to a >10-fold difference in activity between **21** and **22** and a 4-fold difference in activity between **2** and **19** (Fig. 6).[80] Endocyclic alkene isomers of **2** exhibit lower antiplasmodial activity with almost no change to their KB cytotoxicity.[67] Additionally, simple isonitriles in general possess much lower activity than ICTs.[74] The most potent simple isonitrile is adamantyl isonitrile, **18**, which has an IC_{50} value of only 2.5 μM.[5,74,81,82] However, Schwartz et al. found that simplified versions (**23-26**) of potent natural product ICTs (e.g. **2**)—that retain the isonitrile functionality and (*6,6,6*)-tricyclic core—exhibit sub-micromolar IC_{50} values, adding further evidence that the antimalarial activity of these compounds relies on features other than the isonitrile moiety alone (Fig. 7).[75] Interestingly, the replacement of the isonitrile in **24** with a cyanide group (to give **26**) causes a drastic decrease in potency (Fig. 7). While the isonitrile group is not the only factor contributing to high potency, it is clear from these findings that this moiety maintains great importance in these structures with regard to their activity against malaria.[3,5,6,81,82]

Figure 7. IC_{50} values of simplified structures of potent ICTs

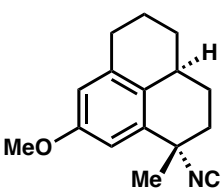

23: 462 nM

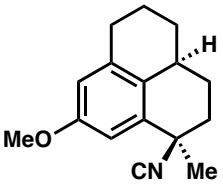

24: 866 nM

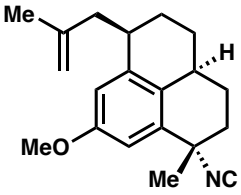

25: 354 nM

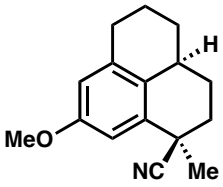

26: >16 uM

1.3 The mechanisms of action of ICTs

Malaria has proved incredibly challenging to eradicate largely due to its genetic and life cycle complexity (Fig. 8).[83-85] After an infected *Anopheles* misquito transmits sporozoites to a mammalian host, liver cells are the first to be infiltrated. Upon growing, reproducing, and maturing into schizonts, the parasite increasingly harms the cell to the point of rupture. Merozoites are then released and proceed to the blood stream to attack red blood cell hosts, initiating the symptom-causing phase of the infection. Once a red blood cell has been overtaken, the food vacuole of the blood-stage parasite catabolizes hemoglobin, releasing free heme, a "redox-active" complex that is toxic to the parasite.[55,59,60,85] The pathogen then detoxifies the free heme it creates by converting it into hemozoin (β-hematin) by a process known as biocrystallization; preventing hemozoin formation in some way is understood to be beneficial in destroying the parasite (Fig. 8).[3,55,80,85] In fact, many currently used antimalarials target and interfere with this process and introducing new ways to effect this interference is still considered to be a worthwhile mechanistic goal.[79] It is expected to remain a major

goal for future antimalarial drugs, too, because the parasite heavily relies on hemoglobin as (a food source) and this detoxification pathway to mitigate the toxicity threat. The features (e.g. proteins) necessary to enact the metabolysis-detoxification process originate in genes of the parasite that are "integral…for its survival".[80]

Figure 8. Overview of malaria life cycle in mammals and potential antimalarial drug interference of heme detoxification

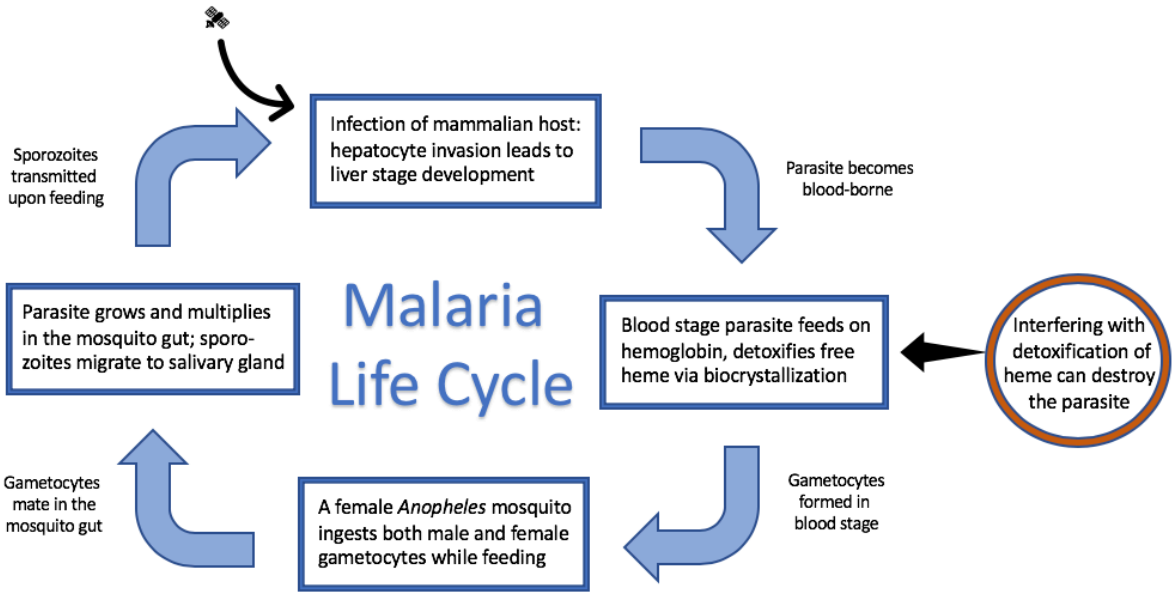

The ability of the isonitrile functional group to bind both Fe (II) and Fe (III) in heme (especially the former) is believed to contribute to the prevention of the formation of hemozoin, reducing the parasite's protective detoxification.[3,5,76,80] In 2001, Wright proposed that the ability of ICTs to exhibit potent antimalarial activity exclusively relies on their propensity to coordinate with heme to form complexes.[3] Wright found that stronger binding to heme correlated with increased antimalarial

activity.[3,80] The computational studies conducted by Wright support the notion that ICTs inhibit parasite-driven heme biocrystallization and other heme-detoxifying pathways in blood-stage malaria via this mechanism.[3,67] When the sequestration of toxic free heme is averted, colloidal osmotic instability of *P. falciparum* leads to premature hemolysis of the host cell, effectively arresting parasite development and proliferation.[3,6,76,80,83] In 2001, Wright also proposed that by binding to heme's Fe ion, ICTs likely impede the parasite's ability to properly degrade the toxic H_2O_2 that is formed during heme degradation.[3,6,80] Later, in a 2011 study, Wright's group reported a computational analysis that is consistent with an alternative theory. Wright suggested that anti-plasmodial functions of ICTs may actually be derived from the allosteric binding of these compounds to the "heme trench," a cavity within the hemoglobin protein tertiary structure, rather than simply the direct binding of the isonitrile moiety to the Fe ion in heme.[6,76] However, since their publication, no experimental evidence has accrued to support this theory. In fact, the low toxicity of isonitriles serves as counterevidence that their bioactivity relies heavily on disrupting hemoglobin functioning, an important biological process in humans.[80] A more recent publication by Wright's group, in 2015, provides further insight on the topic and lends support to a third proposal: the ring stacking of ICTs and heme prevents biocrystallization.[80] First, they use a purely chemical heme crystallization inhibitory assay to assess the ability of ICTs and related compounds to prevent heme polymerization in a nonbiological environment as a model for the parasite-driven process. Multiple ICTs exhibited significant inhibitory properties in this setting. Upon computational examination, they found that in the presence of heme or heme-dimers, the electrostatic potential

indicated that the ICT isonitrile groups and the nitrogens near the heme center possessed partial negative charges. They suggest that, for this reason, it is unlikely that the isonitrile carbon is acting as an Fe ion ligand.[80] Instead, they assert that the isonitrile moiety is faced away from the Fe center due to Columbic repulsion, giving rise to their new (third) proposal that ring stacking of the terpene scaffold and the heme porphyrin ring system prevents heme from further crystallizing.[80] In this publication, they also denounce their initial proposal, stating that a direct isonitrile-Fe ion dative bond is less likely than ring stacking to be responsible for the observed activity of ICTs.[80]

The gap in knowledge of the mechanisms involved in the biocrystallization of free heme by *P. falciparum* makes the search for the source of blood-stage antimalarial activity in ICTs an arduous task.[3,67,80] However, as mentioned above, recent evidence suggests that the blood-stage inhibition of biocrystallization is not the only mechanism of action that imparts such high antimalarial activity to ICTs and their analogues.[6] In 2016, thoughful research on this topic emerged from Shenvi's group.[4] Upon completion of a concise enantioselective synthesis of DICA, (+)-**20**, they carried out bioassays on this and similar chemical species, including (±)-**2**.[4] The results demonstrated the potent activity of these compounds against the *liver-stage* parasite.[4] As emphasized in their publication, this finding serves to provide further evidence against the theory that free heme detoxification is the sole mechanism of action of ICT antimalarials since *Plasmodium* spp. do not use hemoglobin as a food source in the liver stage.[4,86] This multi-mechanistic feature of ICTs is most likely responsible for the convolution of their SAR. Nonetheless, it makes the synthetic pursuit of these compounds even more

attractive, since there is much still to discover, and the known characteristics of ICTs show great promise for their future use in medicine development.[5,6,76]

The evidence presented supports the notion that the pharmacology of this class of compounds is broader and more complex than initially proposed by Wright.[3,5] Still, the elucidation of the full mechanistic profile of these compounds and a coherent understanding of their SAR trends remain unfinished goals of the research community.[3-6,76,80] This is largely due to the difficulty in obtaining suitable quantities of ICTs for further biological studies.[3,5,6] Because of the scarcity of ICTs in nature, the total synthesis of potent or untested ICTs has become a fundamental way to facilitate further investigation into the SAR of these compounds and provide new insights into the synthetic strategies needed to access these molecules in a concise, reliable manner. Investigating the effects that subtle changes to ICT structures have on potency is key to lead compound development. Having one or more new mechanisms to destroy the malaria parasite in combination with the well-researched prevention of hemozoin formation would be a huge improvement to current treatment options. Therefore, ICTs present an excellent starting point for developing new and unique lead compounds for further development towards novel efficacious antimalarial agents. For these reasons, we became motivated to investigate a formal enantiospecific approach to a potent member of this natural product class, **2**, that could also be applicable to its unnatural enantiomeric isomer, (+)-**2**. The focus of this project was to utilize the end game of Shenvi and Pronin's synthesis of (±)-**2** to enable access to (+)-**2** and its analogues in an enantiospecific manner so that bioactivity analysis and further investigative testing could be carried out on these compounds.[13]

1.4 Precedence from previous approaches to ICTs

Previously reported syntheses of ICTs have successfully incorporated [4+2] cycloadditions, Robinson annulations, and aldol condensations to form the 6-membered carbocycles common in the ICT scaffold. We planned to also utilize these reactions in our proposed routes to **2**.

Shenvi's lab and our lab both designed routes that incorporated the intermolecular Diels-Alder transformation. However, the Shenvi synthesis of (±)-**2** relied on a very electron-rich diene (dendralene **29**) and very electron-poor dienophile (**28**) for this reaction, whereas our planned syntheses relied on a less electron-rich diene (**8**) and less electron-poor dienophilic cyclohexenone derivatives (**5**, **11**) (Fig. 9).

Figure 9. Shenvi retrosynthesis of intermediate **1** and our planned [4+2] reactions

Shenvi approach via dendralene Diels-Alder

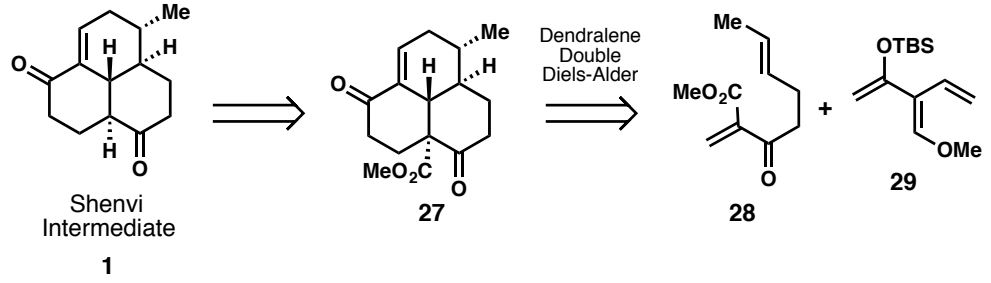

This work: planned [4+2] reactions:

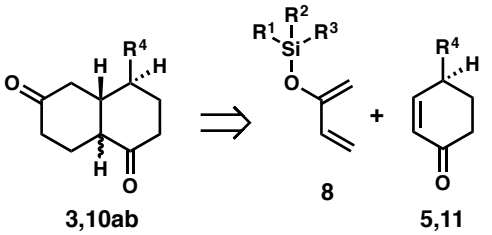

Additionally, the cyclohexenone dienophiles we planned to utilize (**5**, **11**) both possessed a chiral center at the 4-position with set stereochemistry (Fig. 9 & 10). This allowed for an enantiospecific formal synthesis, but with the hurdles of a sterically encumbered dienophile and a much smaller HOMO-LUMO gap. It was expected that increasing the HOMO-LUMO gap (e.g. with Lewis acid) would be required for the Diels-Alder to proceed in acceptable yields.[87-89]

Figure 10. First and second generation retrosyntheses for comparison

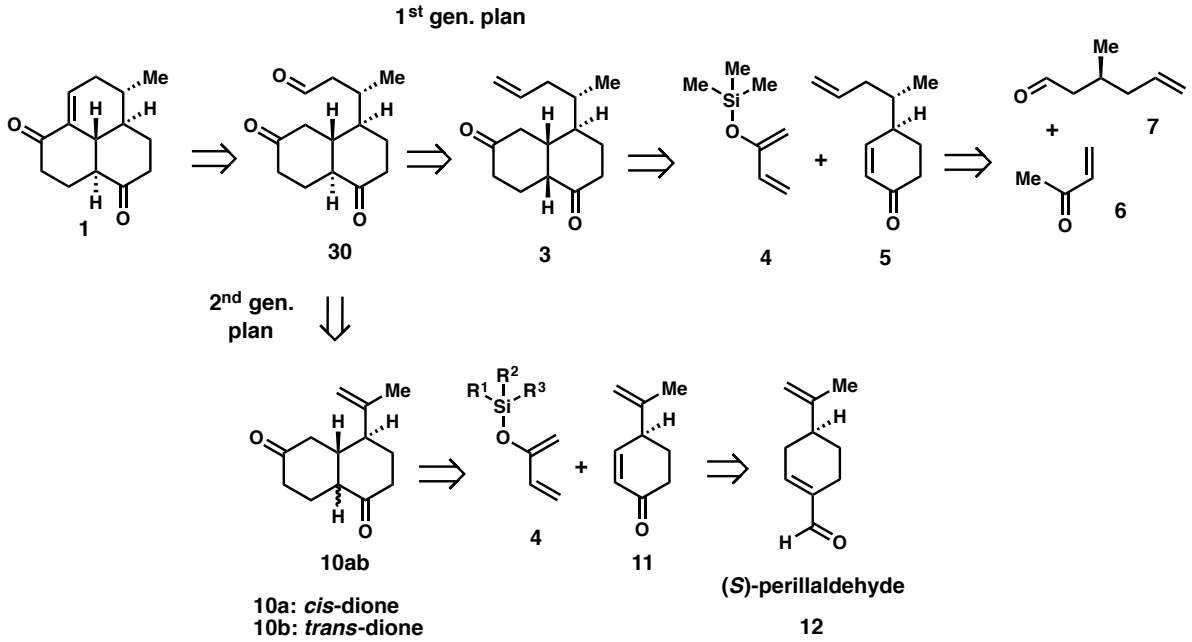

The Robinson annulation is another commonly used tactic in the synthesis of natural products, including ICTs. Both the Robinson annulation and the Diels-Alder reaction are not only common ways to quickly increase complexity, set stereocenters, and create 6-membered carbocycles in the general literature, but they have also been successfully employed in the various ICT syntheses.[4-6,8,9,12,87,90] Our lab has applied the

Robinson annulation method to the synthesis of highly decorated and largely unfunctionalized ICT systems in the synthesis of kalihinol B (and its simplified analogues) and pustulosaisonitrile-1, respectively.[8,12] We hoped to utilize insight gleaned from the development of these Robinson annulations in the first proposed synthetic route (**6**+**7**→**5**) (Fig. 10).

Additionally, the aldol condensation *en route* to DICA was found in our lab to proceed smoothly to the expected cyclic enone, as is found in the synthesis of other types of compounds with little functionality present.[7,12,91] In the first retrosynthesis, we intended to utilize the Robinson annulation, but in both planned retrosyntheses, we envisioned utilizing an intramolecular aldol condensation and Diels-Alder transform or similar formal [4+2] (Fig. 3, 9, & 10). Due to the reversibility of aldol reactions, under acidic conditions, the three possible undesired aldol reactions (forming bridged aldol products) were expected to be easily reversible. Only the single possible aldol *condensation* of **30** should prevail, with water removal as a potential way to shift equilibrium toward the desired product, **1** (Fig. 10).

Another methodology, hydroformylation, has also found an abundance of use as a one carbon-homologating tool in commercial chemical synthesis (from petroleum-derived starting materials) and, to some extent, in the total synthesis of natural products.[92,93] Unfortunately, unactivated 1,1-disubstituted alkenes[94-96] are substrates for which developing asymmetric reactions of this type is incredibly challenging. Generally, a directing group or electron-withdrawing group is required to impart high stereoselectivity for 1,1-disubstituted alkene substrates. In the literature, hydroformylations of these unactivated moieties (e.g. the 2-propenyl group in

limonene and carvone) are almost exclusively substrate-dependent.[94-96] Stereoselectivity is very difficult to predict and generally neither stereoisomer is favored over ~2.3:1 for these substrates. However, switching selectivity for one stereoisomer over another can sometimes be achieved by altering the conditions.[96]

Figure 11. Bare amphilectane scaffold with traditional carbon numbering

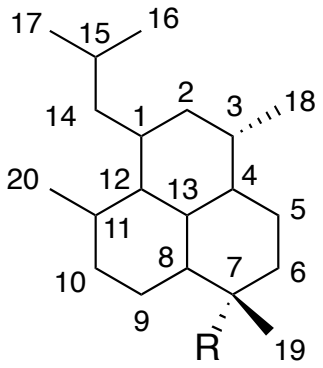

In our 2nd generation planned synthesis of **2**, we decided to use a hydroformylation reaction to form and set the methyl-containing C-3 stereocenter (Fig. 10 & 11). In this approach, we relied, in part, on the substrate-dependent stereochemical preference of the hydroformylation of substrate **10b** to form the desired diastereomer in excess. We hoped this would allow for the elaboration of the underdeveloped hydroformylation methodology (of unactivated 1,1-disubstituted alkenes) into more complex settings. Acknowledging that even a lack of stereochemical preference (i.e. dr ≈ 1:1) would still give a workable sequence, we set forth to investigate the potential of this method. During our analysis of potential retrosynthetic pathways, we realized that the stereocenter to be formed upon hydroformylation is

otherwise particularly difficult to set (as either diastereomer) without significantly lengthening our formal synthesis. Also, hydroformylation of the *cis*-dione **10a** could potentially give different (better) selectivity if the *trans*-dione **10b** gave undesired or poor selectivity. Moreover, altering the ligand(s) and/or metal in the catalyst could potentially help slightly increase the amount of the desired diastereomer formed in comparison to the undesired stereoisomer (Fig. 10).[96]

1.5 First generation approach to 2

In 1980, Kazlauskas first isolated the diterpene isonitrile natural product **2**, (1R,3S,4R,7S,8S,12S,13S)-7-isocyanoamphilecta-11(20),14-diene, from a marine sponge of the *Adocia* genus.[76,97] In 1996, Wright isolated **2** from a different marine sponge, *Cymbastela hooperi*.[67] In nearly four decades since the initial discovery of this potent antimalarial, only a single synthesis has been carried out. This synthesis of **2**, reported by Shenvi in 2012, is a racemic synthesis that rapidly builds complexity and sets multiple stereocenters by employing two Diels-Alder cycloadditions of different dienophiles onto a Danishefsky diene-like dendralene scaffold (Fig. 8).[13] The employment of the correct initial dienophile, however, required considerable optimization to achieve acceptable yields for the double Diels-Alder procedure. The precise nature of the reactants suggests that this route may not be amenable to analogue synthesis. Also, the ability to render the synthesis enantioselective was not mentioned in the report, which indicates another limit to the utility of the Shenvi route. These observations serve as further incentives to pursue an enantiospecific version of

the synthesis of **2**. Since the last 4 steps of the Shenvi synthesis were amenable to changes required for constructing analogues of **2**, we decided to investigate a formal synthesis of **2**, with our focus on approaching Shenvi intermediate **1** in an enantiospecific, anologue-amenable fashion.[13] We saw this venture as a way to further the research into the SAR and mechanism of action details of **2** and other similar compounds via analogue synthesis. These potential findings could lend valuable insight into the exact nature of how these chemical species exhibit such potent antimalarial activity.

Initiating the formal synthesis of **2** with a chiral pool precursor that possesses enantiomers which are both commercially available allows for an enantiospecific synthesis of either enantiomer (natural or unnatural) of the final product. By deriving all other stereocenters from that of the chiral pool precursor, our synthesis negates the need for an enantioselective reaction or other method of selectively isolating a single enantiomer. Both retrosyntheses rely on this feature to be amenable to accessing each enantiomer of **2** as an enantiopure compound (Fig. 3, 10, & 12). Furthermore, since installing the methyl-containing stereocenter at C-3 in Shenvi intermediate **1** was perceived to be a challenging task, we chose *β*-citronellol **9** to be the chiral pool starting material in this route so that this stereocenter was set from the beginning of the synthesis (Fig. 12).

Figure 12. First attempt at enantiospecific formal synthesis of **2** (via **1**): retrosynthesis

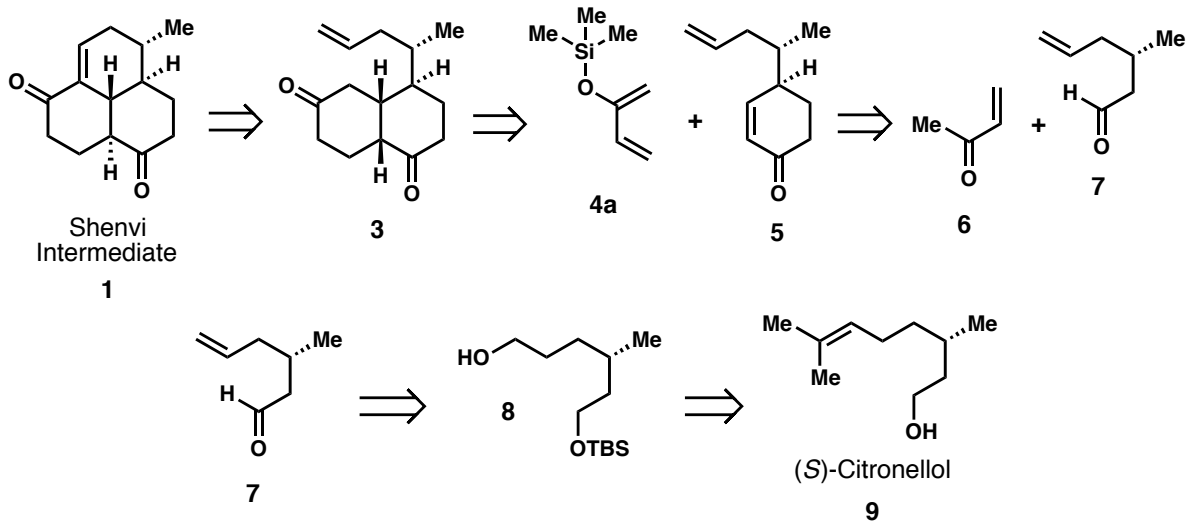

Progress on the first route began with the TBS-protection of starting material (*S*)-(−)-*β*-citronellol with a literature precedent of 98% yield.[98] Due to prior success in the lab with EtOH as a cosolvent for ozonolysis, a modification of the literature procedure to use EtOH instead of MeOH gave the monoprotected diol **31** in 66% yield (Fig. 13).[99]

Figure 13. Synthesis of monoprotected diol **13** and attempted elimination

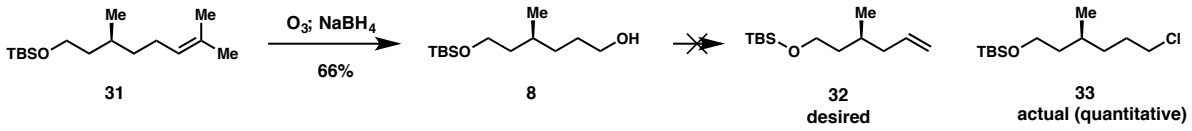

Attempted elimination with $SOCl_2$ and pyridine gave undesired alkyl chloride **33** in quantitative yield. As a workaround, a tosylation-elimination sequence was attempted. Tosylation of **8** gave **34** in 55% yield (Fig. 14). Attempted elimination of tosylate **34** was unsuccessful, giving a multitude of products. Instead, the alkyl iodide, **35**, was

made in 95% yield from **34** via a Finkelstein reaction. Following, **35** was then subjected to E2 elimination conditions to give alkene **36** in 60% yield via a literature procedure (Fig. 14).[100,101]

Figure 14. Synthesis of tosylate **34**, iodide **35** and elimination to give alkene **36**

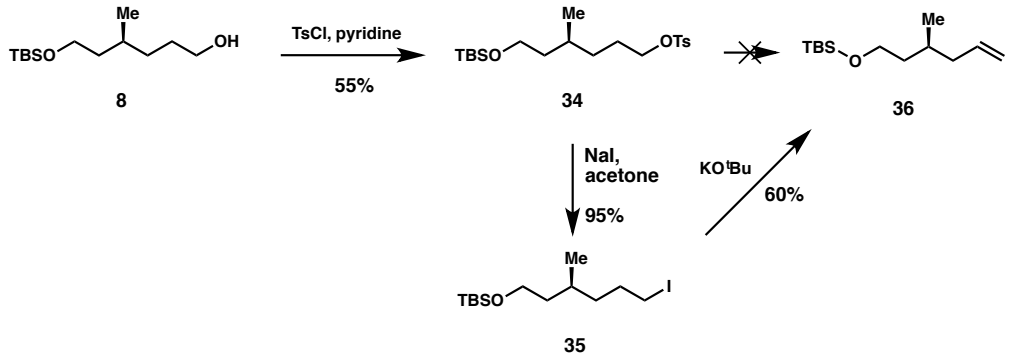

With alkene **36** in hand, literature TBS-deprotection was carried out to give the free alcohol in 35% yield on a small scale (single step yield not reported in literature; Fig. 15).[102] The free alcohol, **37**, was then subjected to DMP oxidation which gave a mixture of several products, but further analysis was not conducted for reasons listed below.

Figure 15. TBS-deprotection of **36** and subsequent attempted DMP oxidation

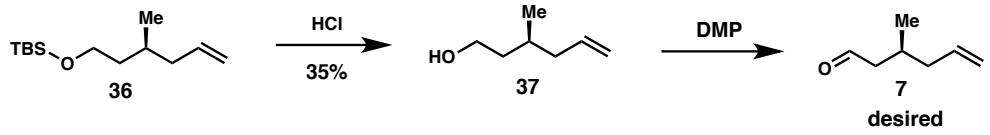

During the development of this route, the difficulty in obtaining stereoselectivity in an asymmetric Robinson annulation with **38** (to obtain enone **39**, which is very similar to enone **5**) was discovered by colleague Philipp Roosen during his investigation of various synthetic routes toward DICA (Fig. 16).[9] Furthermore, colleague Bryan Ellis

found that treating the desired (racemic) 4-substituted cyclohexenone **5** with Lewis acid led to a variety of decompositions products (Fig. 17). This would likely cause severe problems when attempting Lewis acid-catalyzed [4+2] reactions with **5**.

Figure 16. Attempted asymmetric Robinson annulation en route to DICA

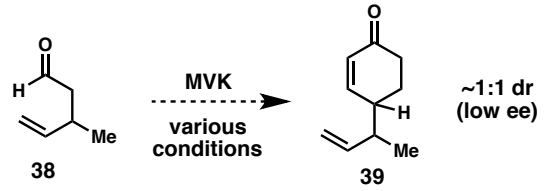

Figure 17. Possible mode of Lewis acid-catalyzed decomposition of enone **5**

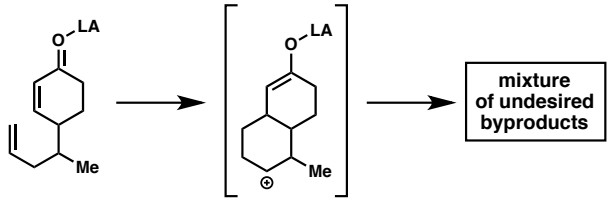

Other drawbacks of this route include its high step count and the need for several transformations and purifications to achieve the isolation of the aldehyde substrate for the Robinson annulation key step (**6**+**7**→**5**). For these reasons, our focus shifted to a newly devised retrosynthesis that was simpler and more concise (Fig. 18).

1.6 Second generation approach to 2

In the second generation approach, we envisioned initiating the synthesis from the chiral pool precursor, perillaldehyde, since in the synthesis of a related ICT in our lab, DICA, the enone **11** (as its (*S*)-enantiomer) was able to be produced from

(*S*)-perillaldehyde, **12**, in 62% yield over 3 steps.[9] A formal [4+2] cycloaddition of **11** with a 2-silyloxybutadiene derivative (**4a-c**) was deemed worthwhile in the planning stages since the regioselectivity and stereoselectivity would help construct the scaffold as desired (Table 1, Fig. 18).

Figure 18. Second generation retrosynthesis of **2** (via **1**)

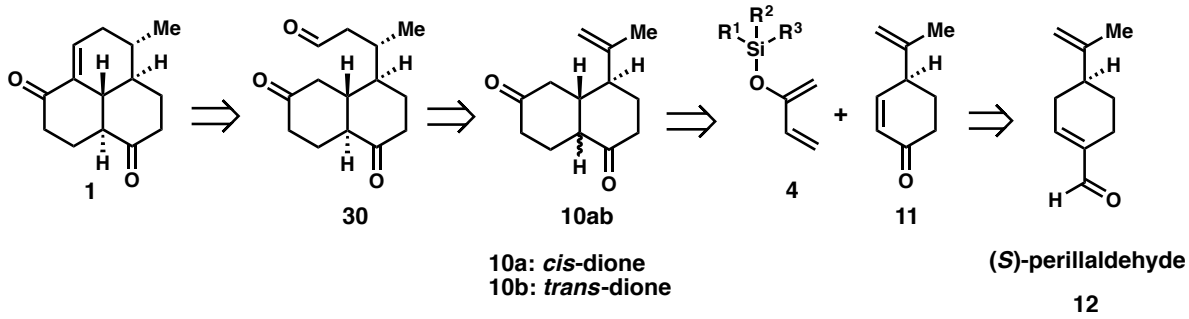

Known enone **11** was synthesized and in turn subjected to an enormous array of Diels-Alder conditions with various 2-silyloxy-1,3-butadiene derivatives (Table 1).[103-106] A control reaction was performed with **4b** and (*S*)-carvone which, upon acidic workup, gave the dione product within 5-10% of literature (^{1}H NMR) yields.[107] This ensured that proper technique was being used for these air and water sensitive reactions. The vast majority of attempted Diels-Alder and formal [4+2] reactions gave either returned starting material (enone **11**) or multiple indiscernible products from which no desired product could be isolated (Table 1).

Table 1. Selected formal [4+2] reactions (changed variables are underlined)

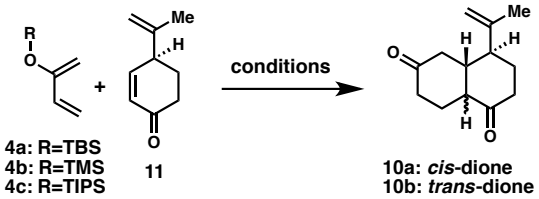

Entry	Equivalents	Conditions	Outcome
1	1.0 **11**, 1.5 4**a**, 1.05 LA	LA = Et_2AlCl, 0.1 M $PhCH_3$, 24 h, 0 °C to rt, 1.0 M HCl workup	Mostly enone **11**
2	1.0 **11**, 1.5 4**a**, 2.10 LA	LA = Et_2AlCl, 0.1 M $PhCH_3$, 12 h, 0 °C to rt, 1.0 M HCl workup	Complex mixture
3	1.0 **11**, 3.0 4**a**, 1.05 LA	LA = Et_2AlCl, 0.1 M $PhCH_3$, 12 h, 0 °C to rt, 1.0 M HCl workup	Complex mixture
4	1.0 **11**, 1.5 4**a**, 1.05 LA	LA = Et_2AlCl, 0.5 M $PhCH_3$, 12 h, 0 °C to rt, 1.0 M HCl workup	Complex mixture
5	1.0 **11**, 1.5 4**a**, no LA	0.1 M $PhCH_3$, 20 h at 95 °C	Mostly enone **11**
6	1.0 **11**, 1.5 4**a**, no LA	1.0 M $PhCH_3$, 20 h at 145 °C	Mostly enone **11**
7	1.0 **11**, 5.0 4**a**, no LA	Neat, 6 h at 190 °C	Complex mixture
8	1.0 **11**, 1.5 4**a**, 1.05 LA	LA = $MeAlCl_2$, 0.33 M $PhCH_3$, 12 h, 0 °C to rt, 1.0 M HCl workup	Complex mixture
9	1.0 **11**, 1.5 4**a**, 1.05 LA	LA = $EtAlCl_2$, 0.33 M $PhCH_3$, 21 h, 0 °C to rt, sat. $NaHCO_3$ (-78 °C) workup	Complex mixture
10	1.0 **11**, 2.0 4**b**, 0.5 LA	LA = $EtAlCl_2$, 0.33 M $PhCH_3$, 21 h, 0 °C to rt, sat. $NaHCO_3$ (-78 °C) workup	Complex mixture
11	1.0 **11**, 1.5 4**a**, 1.05 LA	LA = *i*$BuAlCl_2$, 0.2 M CH_2Cl_2, 4 h, 0 °C to rt, sat. $NaHCO_3$ (-78 °C) workup	Reduction products
12	1.0 **11**, 1.5 Danishefsky's diene, 0.05 LA	LA = $Eu(FOD)_3$, 0.6 M CH_2Cl_2, 20 h, rt	Mostly enone **11**
13	1.0 **11**, 1.5 4**a**, 0.5:0.1 LA	LA = $AlBr_3$:$AlMe_3$, -15 °C, 5 days, silica pad filtration workup	Double bond isomerization
14	1.0 **11**, 1.5 4**a**, 0.10 LA	LA = $TBSNTf_2$ (made *in situ*), -78 °C 2h, 0 °C 10 min, Et_3N quench,	10 % isolated *trans*-dione **10b**

Even the highly electron-rich Danishefsky's diene gave either returned starting material or decomposition.[106] Fortunately, utilizing a Lewis acid generated *in situ*, in a procedure developed by Jung to accomplish a double Michael Addition with hindered diene-dienophile pairs, led to an initial hit with ~10% isolated dione, which was believed to possess the *cis*-decalin configuration (**10a**) (Fig. 19).[108] After optimization, the yield of the dione was increased to 29% on a small scale.

Figure 19. Jung's double Michael Addition precedence

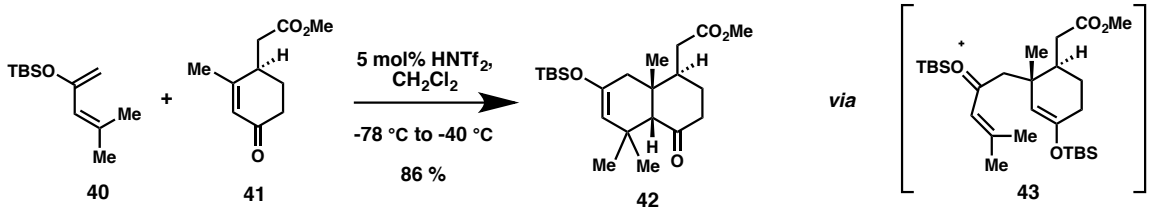

The epimerization of a variety of *cis*-1-decalone derivatives to their *trans*-1-decalone isomers under thermodynamic equilibrium conditions has been at the core of many ICT syntheses, often allowing for high *trans*-selectivity even in various tricyclic and perhydrindane scaffolds.[5,8,9,90,109] However, due to the complex nature of predicting the relative stabilities of the conformation(s) of the *cis* compound and the rigid *trans* structure—especially in the midst of other fused rings in the scaffold—it is not guaranteed that the equilibrium will always greatly favor the *trans* product. Epimerizations are highly substrate-dependent and can afford drastically different results for only slightly different compounds.[8,90] Fortunately, during the course of investigating this route, we found that under epimerizing conditions (e.g. TsOH, residual acid in $CDCl_3$, etc.), the desired *trans*-diastereomer **10b** was preferred (Fig.

20). In fact, simply quenching the reaction by filtering through silica gel usually caused both protodesilylation and epimerization to give the *trans*-dione **10b**, predominantly. This was confirmed by obtaining an X-ray crystal structure of the **10b** product. Only upon rapid quenching and very brief flash chromatography on pH 7 silica gel was the *cis*-dione intermediate **10a** able to be isolated (see SI).

Figure 20. Epimerization of *cis*-dione **10a** to *trans*-dione **10b** (presumed ground state conformations shown, with 2-propenyl group equatorial)

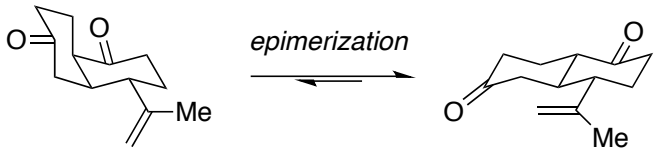

10a **10b**

The penultimate step to the Shenvi intermediate **1** was a hydroformylation reaction. The first mechanistic step of the Rh-catalyzed hydroformylation, hydrorhodation, is the stereochemistry-determining step of this transformation.[110] The stereoselectivity of the reaction is determined in this step since a new stereocenter is formed. The preference for one stereoisomer over another is also largely due to steric constraints. Also, because of steric congestion, hydrometallation of a 1,1-disubstituted alkene tends to be slower than that of a 1,2-disubstituted or monosubstituted alkene.[111] Thus, the high temperatures and pressures required for even modest reaction rates contributed to the practical difficulty of optimizing this reaction. Demonstrating this, a solution of *trans*-dione (alkene) **10b**, catalytic $RhH(CO)(PPh_3)_3$, and catalytic PPh_3 in benzene (0.4 M) was subjected to 40 bars of pressurized syn gas

(H_2:CO ratio of 1:1) at 60 °C for 4 days, giving only ~15% yield of a single identifiable aldehyde product with starting material comprising the remainder of the mass balance (Fig. 21).

The desired diastereomer of the aldehyde product of hydroformylation, **30**, was previously synthesized en route to (±)-7-isocyanoamphilecta-11(20),15-diene, by Miyaoka, albeit in approximately 20 steps (LLS).[90] Access to the spectral data of this compound was crucial for identifying the stereochemistry of the C-3 stereocenter formed during the hydroformylation of **10b**. Discrepancies between the ^{1}H- and ^{13}C-NMR spectral data of our aldehyde product, **30a**, and the aldehyde obtained by Miyaoka's group, **30**, were too large to reasonably consider them identical. The ^{1}H-NMR spectra for both Miyaoka's aldehyde (**30**) and our product (**30a**) were recorded on 400 MHz ^{1}H-NMR instruments. The ^{1}H-NMR spectrum we obtained of **30a** shows a distinct doublet (J = 3.2 Hz) for the aldehyde peak—as opposed to a singlet observed for **30**—at a very similar chemical shift to that of **30a** (δ_{30} = 9.74 ppm, δ_{30a} = 9.75 ppm). Also, a substantial difference in methyl group chemical shifts was observed with Miyaoka's reported at 0.77 ppm and ours found at 1.05 ppm (though both methyl doublets exhibited identical coupling constants: J = 6.9 Hz). Furthermore, the ^{13}C-NMR peak chemical shifts varied significantly between the two compounds. The four most upfield peaks in the ^{13}C-NMR data reported for **30** were: 12.9 ppm, 24.9 ppm, 25.2 ppm, and 25.9 ppm; whereas our product gave the following four most upfield peaks: 19.1 ppm, 25.1 ppm, 26.3 ppm, and 29.8 ppm. In fact, almost every

^{13}C-NMR signal was different from the spectral data of the desired compound. This led us to conclude that we had obtained—almost exclusively—the opposite (undesired) stereochemistry at the methyl-containing stereocenter (Fig. 21).

Figure 21. Hydroformylation of **10b** to give **30a**

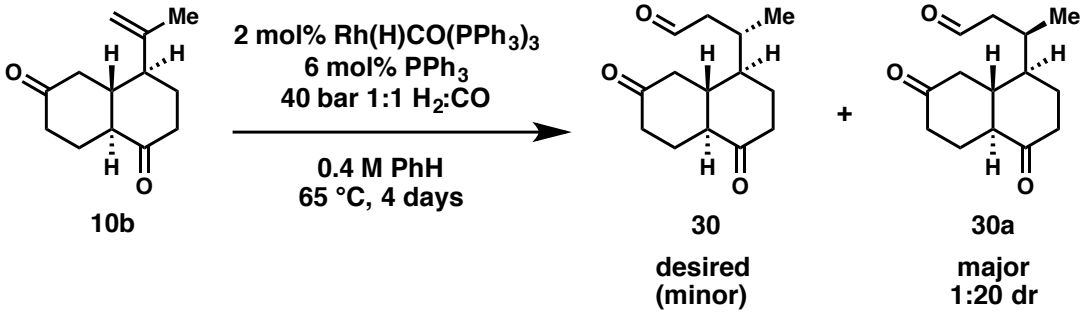

Post-reaction analysis led us to propose that the observed high selectivity for the wrong epimer at C-3 could be explained by a simple allylic 1,3-strain reducing model.[112] This proposal is supported by the configuration of the 2-propenyl substituent in the X-ray crystal structure obtained for trans-dione **10b** (Fig. 22). The geometry of this crystal structure showed the 2-propenyl group's C-C double bond to be roughly periplanar with the adjacent allylic methine C-H bond. We posit that this ground-state conformer represents a satisfactory approximation of the geometry of the alkene during hydrorhodation. The majority of the trans-decalin system sterically hinders the *re* face of the alkene in this configuration which strongly disfavors attack from this (*re*) face. Thus, hydrorhodation occurs predominantly on the more accessible *si* face of the alkene, which ultimately yields the undesired epimer, preferentially, with (*S*)-stereochemistry at C-3 (Fig. 21 & 22).

Figure 22. X-ray diffraction crystal structure configuration of trans-dione **10b**

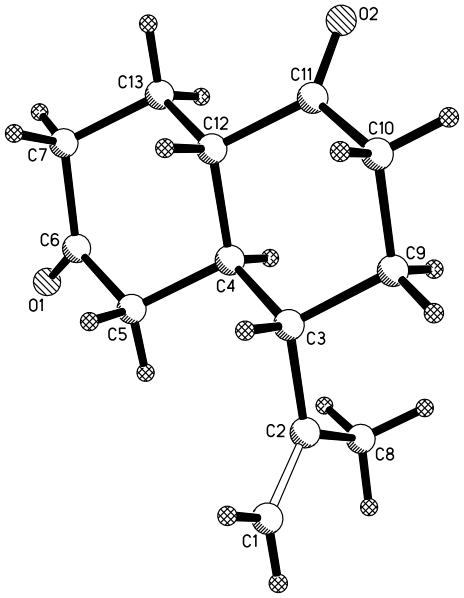

Despite many attempts at trying to obtain the key intermediate **1** from enone **11** via the 2nd generation retrosynthesis outlined above, this route was finally abandoned due to 3 main reasons: 1) the low optimized yield (29%) of the transformation of enone **11** to *trans*-dione **10b** (even after extensive investigation); 2) the low conversion (~15%) of **10b** to the hydroformylated product under harsh conditions over a long period of time; and 3) the high selectivity in the hydroformylation reaction (irreversibly setting the stereochemistry at the methyl-containing stereocenter) for the *undesired* diastereomer, **30a**, most likely due to the substrate-dependence of the hydroformylation[94] reaction as discussed above. While altering the conditions could potentially slightly change the stereochemical

preference of the hydroformylation, the pursuit of such a drastic change in preference needed to give a satisfactory dr was decidedly not a sensible endeavor.

1.7 Future directions

This project was undertaken during the 2015-2017 time period, but since then, in 2018, a remarkable achievement was made in the subfield of asymmetric hydroformylation: a chiral ligand has been designed for Rhodium that enables a >10:1 dr for the methyl-containing stereocenter of the linear aldehyde resulting from the hydroformylation of either (R)-limonene or (S)-limonene in a catalyst-controlled (as opposed to substrate-controlled) fashion![113] This finding has implications in the synthesis of **2** using the second approach detailed above since the substrate-dependent stereoselectivity of the hydroformylation of trans-dione **10b** could potentially be switched to favor the desired stereochemistry at C-3 with a catalyst-controlled hydroformylation, which would enable the synthesis of **30**. If **30** was obtained, only one step would remain to complete an enantiospecific formal synthesis of **2**.

Chapter 2: Carbene [2,3]-Wittig Rearrangements

2.1 Introduction

Setting stereocenters at sterically congested positions has remained a difficult prospect in organic chemistry. Particularly, the challenges associated with selectively forming all-carbon quaternary stereocenters, and to some degree tertiary carbon stereocenters, represent substantial hurdles to overcome when pursuing a concise total synthesis of a compound with these characteristics. With the goal of contributing a solution for this longstanding chemical problem, we undertook a project focused on expanding the utility of the carbene [2,3]-Wittig methodology.[114-123] We envisioned that this unique avenue of reactivity would address some of the difficulties involved with setting congested stereocenters.

Many variations of radical and carbocation propagation as well as numerous pericyclic reaction manifolds have been employed to access sterically congested scaffolds. While carbenes are among the most reactive chemical species, their use in synthesis has been relatively limited, primarily for this exact reason. We planned to harness the reactive—yet tunable—nature of carbenes and increase the synthetic versatility of these intermediates by employing them in the [2,3]-Wittig methodology.

Generally, due to the high energy nature of carbenes, the formation of these species often demands rather harsh conditions. For example, generating carbenes often require strong base (for deprotonation) or high temperatures (for radical disproportionation, fragmentation, etc.).[14,114-119] In fact, there are a number of ways to

generate nucleophilic carbenes, which work to varying degrees. However, the two established methods[14,114,119] of making carbene intermediates that undergo the [2,3]- rearrangement (discussed below) both have significant drawbacks (Fig. 23-26).

2.2 Precedence for the carbene [2,3]-Wittig rearrangement

In order to obtain the desired reactivity—the [2,3]-sigmatropic rearrangement of allylhetero(alkylhetero) carbenes—there are several factors to consider. Forming the carbenes reliably is the first objective. In the earliest reported carbene [2,3]-Wittig reaction, developed by Baldwin and Walker in 1972, the authors used a tosylhydrazone derivative as the carbene precursor (Fig. 23).[114] At relatively low temperatures, strong base (sodium hydride) reliably generated the intermediate allylthio(alkylthio) carbene. With two adjacent divalent sulfur atoms, the carbene is sufficiently stabilized, nucleophilic, and the strain in the transition state is decreased due to two long C-S bonds, which ultimately allows for the formation of quaternary centers. Also, the thiocarbonyl functionality produced upon rearrangement causes the [2,3]-Wittig reaction of allylthio(alkylthio) carbenes to be less exothermic than, for instance, a carbonyl group. These factors contribute to a later transition state, which means the intermediate carbenes do not react as rapidly as certain other heteroatom-stabilized carbenes (discussed below). Therefore, with these rearrangements, achieving high selectivity (such as stereoselectivity) is, to a degree, more easily attained. Indeed, multiple reports of stereoselective allylthio(alkylthio) carbene [2,3]-Wittig rearrangements have been published.[115,116,122,123]

Figure 23. First sulfur-stabilized carbene [2,3] (Baldwin)

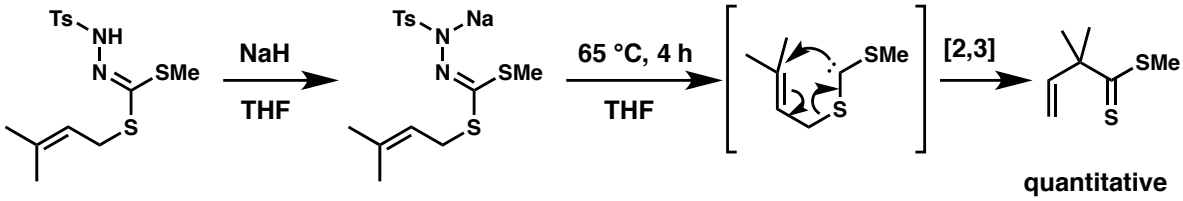

The current scope of the carbene [2,3]-Wittig method—in the case of allylthio(alkylthio) carbenes—is limited by certain requirements for the substrates as well as the nature of the products. While the precedence for bis(alkylthio)-stabilized carbene derivatives undergoing the [2,3]-Wittig rearrangement under rather mild conditions is encouraging, the dithioester products are not generally useful intermediates in total synthesis. With that said, there are a few examples of bis(alkylthio)-stabilized carbenes undergoing a [2,3]-Wittig rearrangement in natural product synthesis.[115-117] Shortly after the initial report by Baldwin and Walker that shows that these types carbenes are excellent precursors for the [2,3]-Wittig reaction, Evans incorporated a diastereoselective variant of the method into the total synthesis of bakkenolide-A, **50** (Fig. 24).[114,115] The carbene preferentially attacked the convex face of the bicyclic system (**47**) to install a quaternary carbon stereocenter with the thiocarbonate moiety on the top face (**48**). Due to the synthetic route chosen (**44** → **46**) , both (*E*)- and (*Z*)-geometries of the alkene are present in the starting material, **46**. Both alkene diastereomers differentiate between the two diastereotopic faces to give the same product, **48**, as a single diastereomer in 62% yield (Fig. 24).[114,115] Unfortunately, superstoichiometric quantities of two mercuric salts are required to

convert dithioester **48** into the desired methyl thioester, **49**, in order to accomplish the final step of the synthesis of bakkenolide-A (**50**). The requirement for one or more additional steps after the [2,3]-Wittig, especially utilizing highly toxic reagents, represents a major drawback of this method.

Figure 24. Late stage carbene [2,3]-Wittig in Evan's synthesis of bakkenolide-A

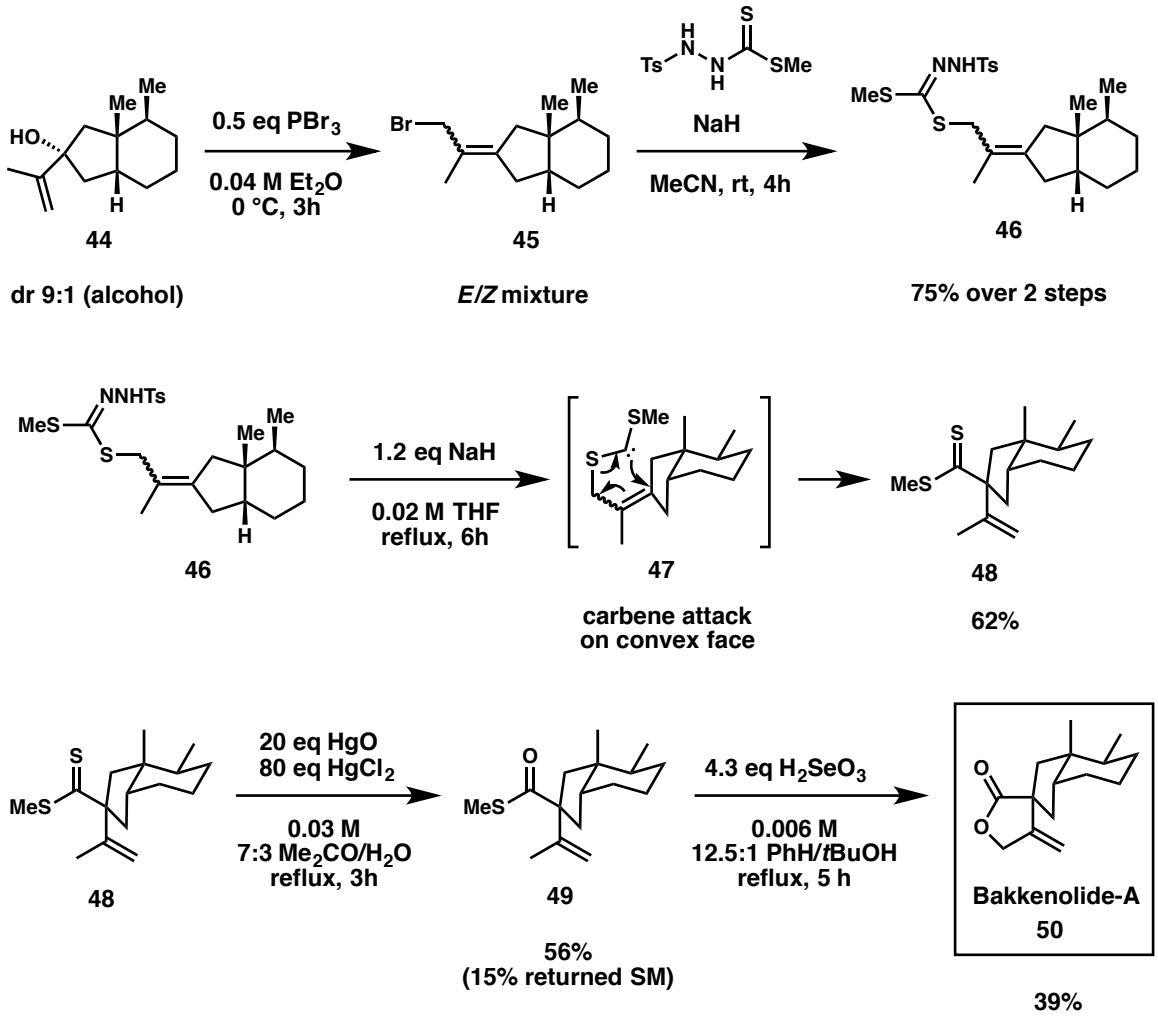

In another natural product total synthesis, Jung and Parker utilize the allylthio(alkylthio) carbene [2,3]-Wittig method (Fig. 25).[117] In their approach to the

racemic antitumor halomon analogue, **55**, they utilize this transformation to obtain functionality at a position that otherwise would be very difficult to achieve. This illustrates another favorable quality of the carbene [2,3]-Wittig; it can be used as an alternative to traditional reactions when certain features of the molecule prohibit this type of approach.[118]

Figure 25. Jung & Parker use a bis(alkylthio)-stabilized carbene to install a hindered carboxylate group in the synthesis of an analogue of the antitumor agent, halomon

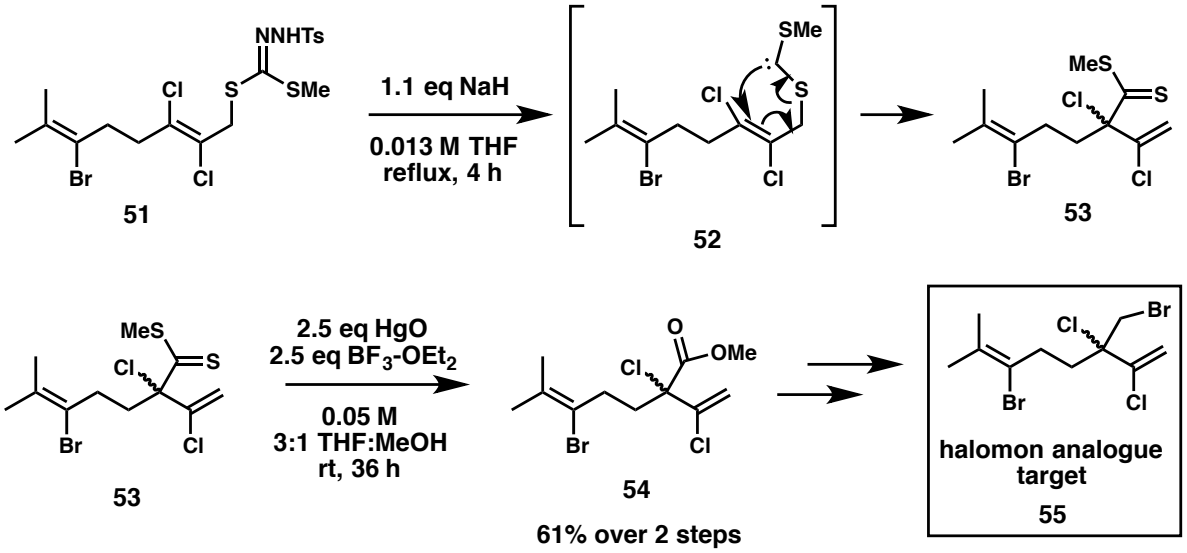

It is crucial that the heteroatoms covalently bonded to the divalent carbon stabilize the carbene to the extent that they do not undergo β-scission; but if the adjacent groups are too stabilizing, the carbenes may remain dormant under the reaction conditions (e.g. NHCs). In the method developed by Büchi, often referred to as the Büchi rearrangement, allyloxy(alkylamino) carbenes were reported to undergo the [2,3]-sigmatropic reaction (**58** → **59**, Fig. 26).[14,119,120] Unfortunately, this reaction

manifold suffers from multiple limitations as well, including high temperatures, long reaction times, and reaction rates that are exceedingly sensitive to substrate sterics.[14,119] However, achieving this type of transformation with oxygen- and nitrogen-stabilized carbenes represents a surprising elaboration of this chemistry since the previously used carbene intermediates were stabilized by two sulfur substituents. The C-O bonds in allyloxy(alkylamino) carbenes are significantly shorter than the C-S bonds in allylthio(alkylthio) carbenes, yet—as long as steric hindrance remains at a minimum—Büchi has shown that the [2,3]-Wittig rearrangement of these species will proceed (albeit at higher temperatures) (Fig. 26).

Figure 26. Büchi's use of the carbene [2,3]-Wittig to make amides

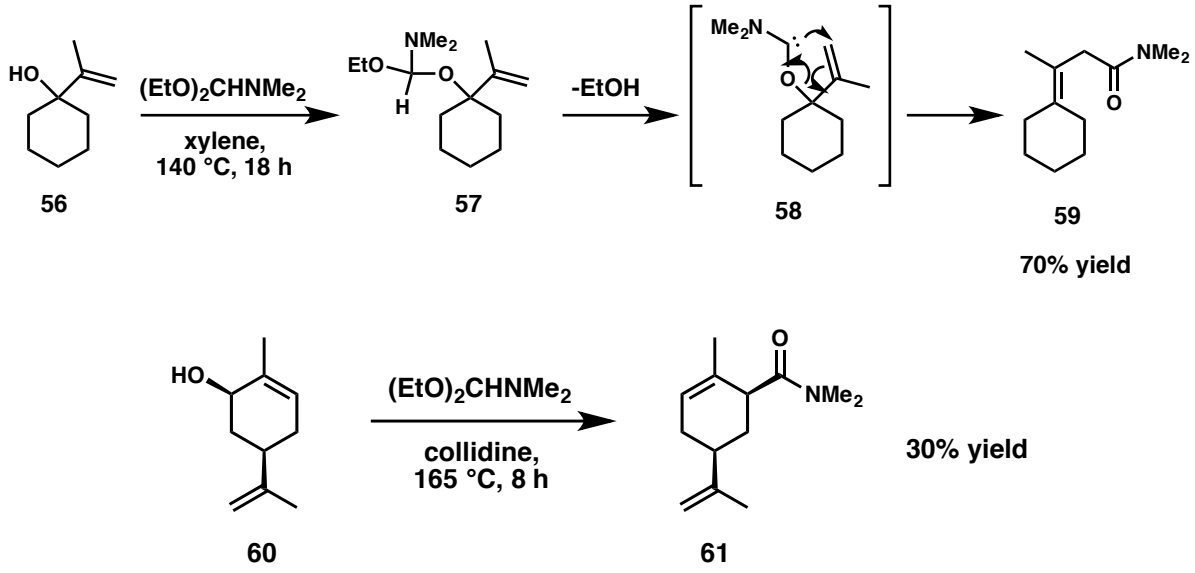

As mentioned above, one serious disadvantage of Büchi's [2,3]-rearrangement is that low yields are obtained when attempting to form hindered tertiary or quaternary centers, demonstrated by the reaction of **60** to **61**, with more hindered

systems frequently affording little to no product at all.[14] Also, the high temperature reactions necessitate the use of solvents with very high boiling points. This negatively impacts both the practicality and utility of the method by requiring a painstaking post-reaction removal of these solvents by distillation. However, this method proves that the carbene [2,3]-Wittig is possible when 2 C-O bonds—that are substantially shorter than C-S bonds—are present in the 5-membered cyclic transition structure. Additionally, a carbonyl moiety is produced instead of the thiocarbonyl, making the reaction more exothermic. This contributes to an earlier transition state, which may somewhat counteract the higher degree of steric hindrance caused by the shorter C-O bonds. Also, the amide products are of greater synthetic use than the dithioester in Baldwin and Walker's method.

2.3 Oxadiazoline thermolysis and experimental procedure

Due to the limitations of the Büchi method and the method set forth by Baldwin and Walker, we planned to develop a new tactic to approach the carbene [2,3]-Wittig. First, we chose to pursue a different way to form the intermediate carbenes, utilizing the 1,3,4-oxadiazoline scaffold as a carbene precursor via an innovative methodology that has been largely developed by Warkentin (Fig. 27-29).[124-129] These heterocycles are able to form carbenes at much lower temperatures than the Büchi method and, using allyloxy(alkylhetero) carbenes, the carboxylate-derived products, **D**, have greater direct synthetic utility than the dithioesters products of allylthio(alkylthio) carbenes.

Figure 27. Thermal fragmentation pathways for 1,3,4-oxadiazolines

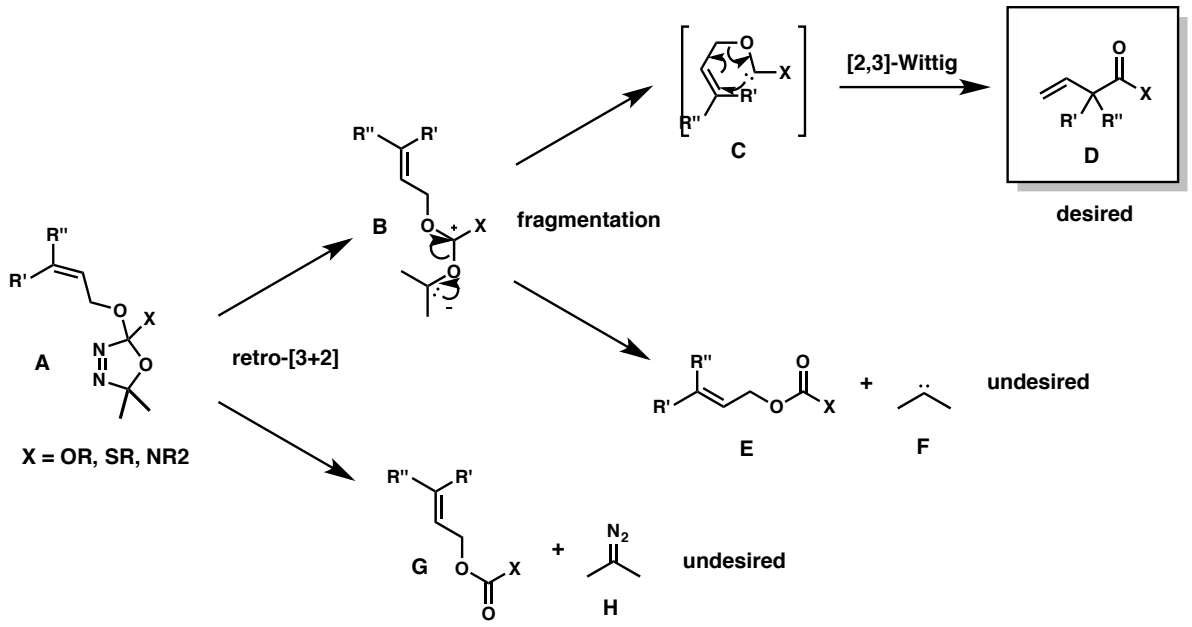

Figure 28. Mechanism of undesired radical [1,2]-Wittig rearrangement

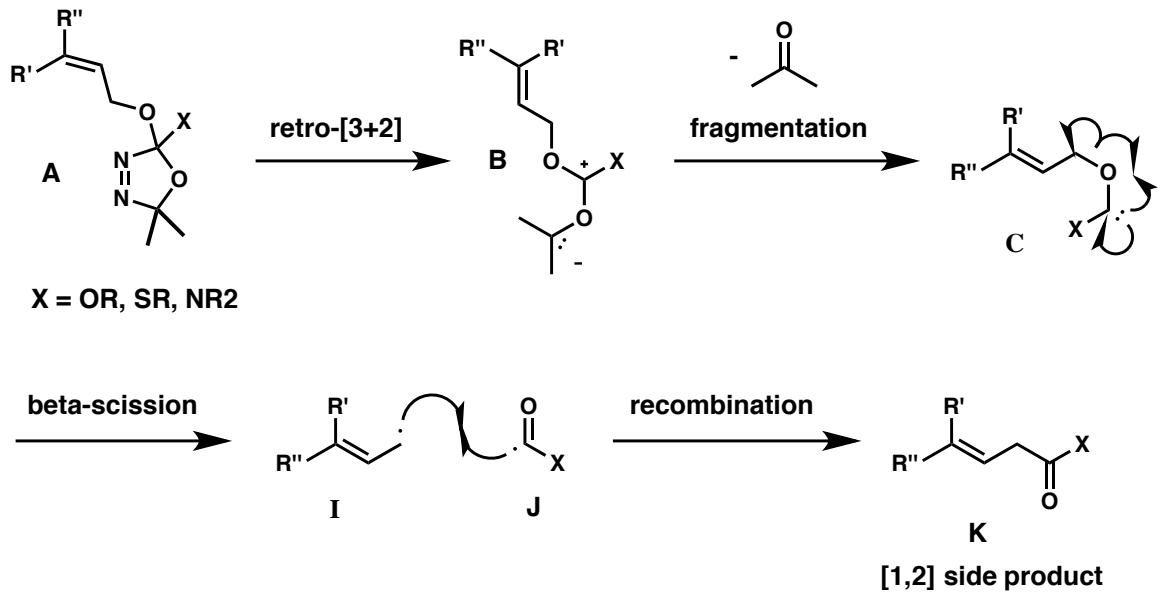

The thermal degradation of the 1,3,4-oxadiazoline structure, **A**, is able to undergo two different retro-[3+2]-cycloadditions, to give either **B** (desired) or **G** (undesired) (Fig. 27).[125-128] The former pathway again diverges, either losing acetone to give the desired allyloxy(hetero) carbene, **C**, or losing isopropyl carbene to give the undesired carbonate derivative, **E**. The stabilized carbene, **C**, then rearranges via either a [2,3]- or [1,2]-Wittig reaction (Fig. 27 & 28).

Fortunately, a variety of carbenes have been successfully made from 1,3,4-oxadiazoline thermal degradation. Warkentin employed PhOH and PhNCO to trap a number of different carbenes created from thermolysis of various 1,3,4-oxadiazoline derivatives (Fig. 29).[125-128] Most bis(hetero)-stabilized carbenes were formed in good yields. While the ability to form carbenes is sensitive to heteroatom type, the alkoxy(acylamino) carbene yields are reliably high, and the alkoxy(alkylthio) and bis(alkoxy) carbenes are generally formed in relatively good yields (Fig. 29). Since alkylthio groups, when adjacent to the divalent carbon, tend to significantly stabilize carbenes, we decided to first pursue the synthesis of substrates **66** and **68** (Fig. 30 & 31). With the 1,3,4-oxadiazoline scaffold, these starting materials should be able to fragment into their respective carbenes at relatively low temperatures.[125-128] Also, the carbenes generated will be stabilized by both oxygen and sulfur lone pairs, in addition to the stabilization afford by the large sulfur atom's polarizability.[114-116]

Figure 29. Yields of nucleophilic carbenes from 1,3,4-oxadiazoline thermal degradation

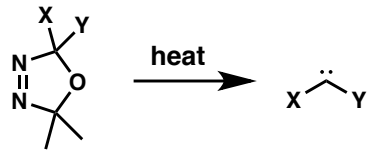

Entry	X	Y	yield range
1)	OR	OR	65-90%
2)	OR	NR_2	0-90%
3)	OR	SR	55-65%
4)	OR	NRCOR'	89-100%

*All yields determined by trapping with PhOH

Figure 30. Synthesis of [2,3]-Wittig substrate **66**

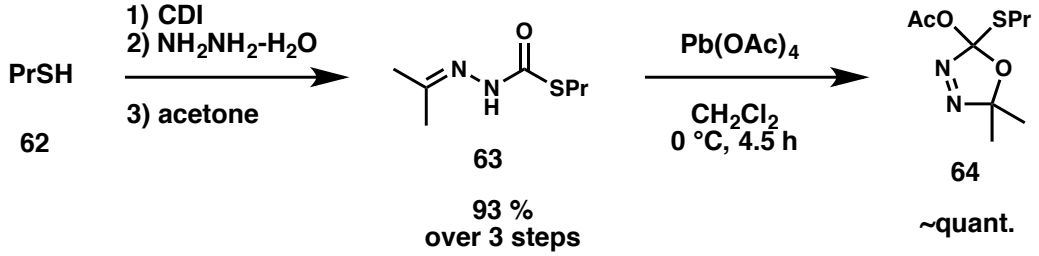

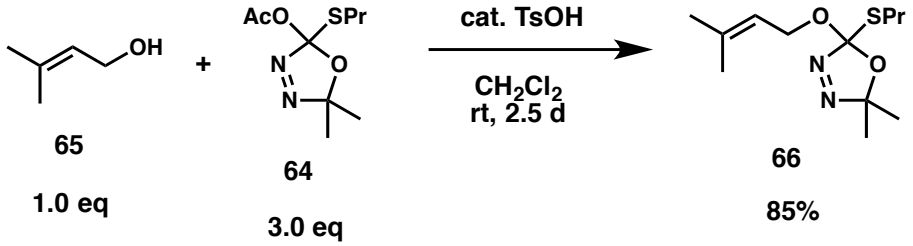

Following literature precedent, propanethiol, **62**, underwent monothioesterification with carbodiimidazole (CDI) followed by a reaction with hydrazine monohydrate and condensation with acetone to give semicarbazone

derivative **63** (Fig. 30).[130] Oxidation of **63** to give 1,3,4-oxadiazoline acetate **64** proceeded in quantitative yield, also via literature precedent.[130] Toluenesulfonic acid-catalyzed transacetalization of **64** with allylic alcohol **65** gave carbene precursor **66** in 85% yield after 2.5 days in a solution of CH_2Cl_2 at rt.

Figure 31. Synthesis of [2,3]-Wittig substrate **68**

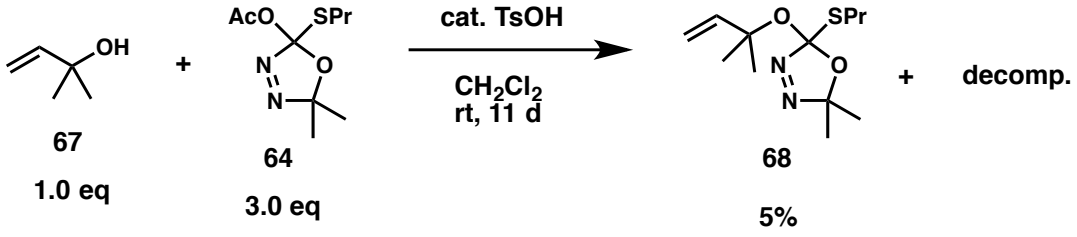

The synthesis of substrate **68** proved much more challenging. Allylic alcohol **67** was, expectedly, very sensitive to acidic conditions. Transacetalization with **64** took 11 days at room temperature to reach completion, affording only 5% of the substrate **68**, with the remaining mass balance comprised of decomposition products (Fig. 31).

Figure 32. Brief optimization of solvent for the [2,3]-Wittig method with **66**

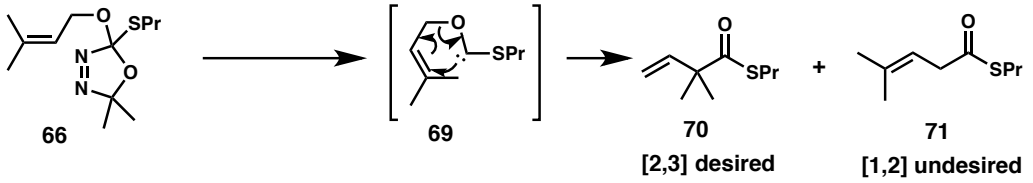

Entry	Solvent	Conditions*	[2,3]**	[1,2]**	Other
1)	PhCl	60 °C, 1h; 100 °C, 1 h	12%	9%	
2)	THF	100 °C, 1 h	-	-	side prod. only
3)	PhF	100 °C, 1 h	24%	12%	

*All reactions were performed in sealed vials with microwave heating
**NMR yields

Next, a brief optimization of solvent for the [2,3]-Wittig was undertaken with **66** as the carbene precursor (Fig. 32). Completion of the reaction was reached at 100 °C within an hour. The use of chlorobenzene as a solvent was not ideal due to its high boiling point (BP 132 °C) and the use of THF was problematic due to its presumed reaction with intermediates. Fortunately, using fluorobenzene (BP 85 °C), more promising results were obtained, with 24% of the desired [2,3]-sigmatropic rearrangement taking place to produce the quaternary carbon in **70**, although 12% of the [1,2]-Wittig product, **71**, was observed as well. Subsequent to this, another brief optimization of temperature was carried out to find the lowest temperature at which the reaction would take place (Fig. 33).

Figure 33. Optimization of temperature for thiol-derived 1,3,4-oxadiazolines; **68** reacting under optimized conditions for [2,3]-Wittig

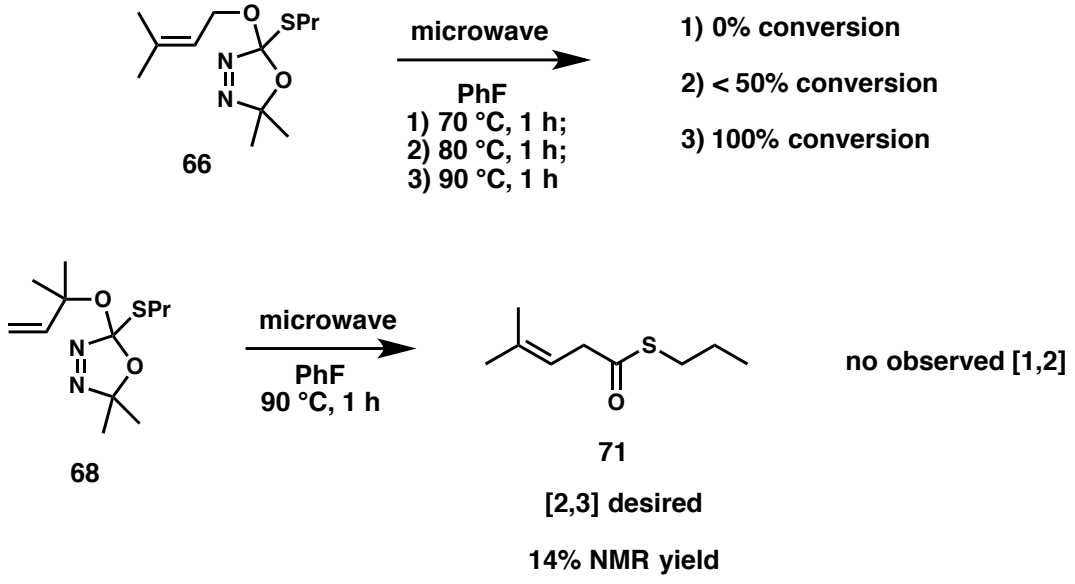

At very high temperatures (≥ 250 °C), allyloxy carbenes become more likely to homolyze into radicals in an entropy-driven process, rearranging into undesired byproducts (e.g. via the [1,2]-Wittig reaction).[129] At 60-110 °C, allyloxy carbenes are expected to instead preferentially rearrange via the desired[124] [2,3]-Wittig pathway. Fortunately, thermal degradation of **66** and **68** was complete at 90 °C after 1 h (Fig. 33). However, while just a single product (**71**) was observed from the thermolysis of **68**, arising from the [2,3]-Wittig rearrangement, only a 14% yield was obtained. No other side products were observed in these reactions. These results indicate that perhaps either the products or side products are volatile enough to leave the reaction mixture upon evaporative workup, even though the boiling points of the products were expected to be above 200 °C. Also, the 1.3-2.0:1 ratio of [2,3]:[1,2] products obtained from **66** is likely lower than that of **68** (from which only [2,3] products were observed) due to the increase in strain associated with producing a quaternary center from the former and the strain-releasing nature of the [2,3]-rearrangement of the latter.

Figure 34. Synthesis of amine-derived [2,3]-Wittig substrate

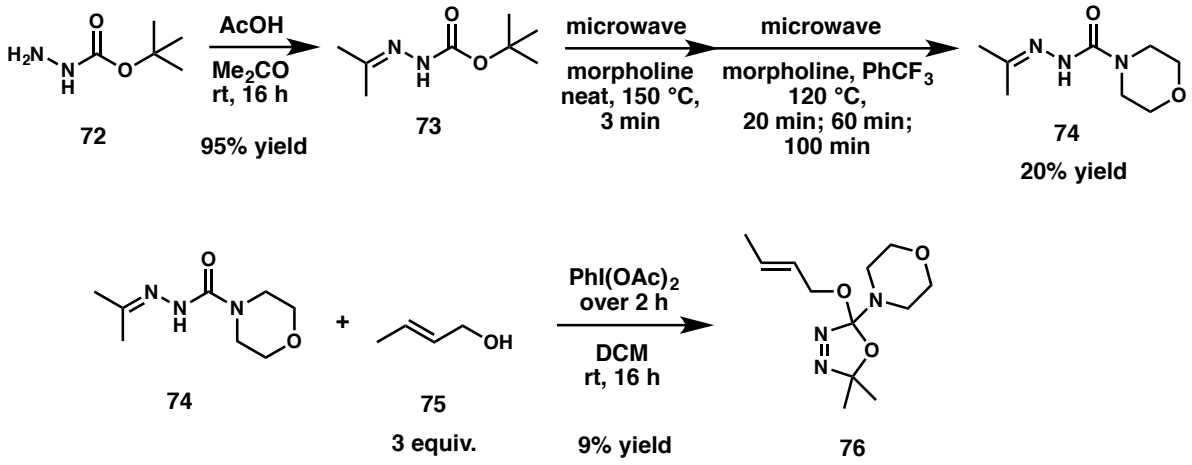

To evaluate the potential of allyloxy(alkylamino)-derivatives of 1,3,4-oxadiazolines to undergo the [2,3]-Wittig reaction, the synthesis of substrate **76** was also carried out (Fig. 34). Carbazate **72** was condensed with acetone to give carbazate hydrazone **73** in 95% yield. After subjecting a mixture of **73** and morpholine to microwave radiation under a variety of conditions, semicarbazone **74** was eventually obtained, albeit in poor yield (20%).[131] Oxidative cyclization of **74** proved incredibly challenging. With stoichiometric $PhI(OAc)_2$, in the presence of 3 equivalents of allylic alcohol **75**, only single digit yields of oxadiazoline **76** were obtained.[127,128] Finally, with substrate **76** in hand, thermolysis of the material in fluorobenzene at a variety of temperatures was carried out (Fig. 35). Only after slowly increasing the temperature in 10 °C increments to 110 °C and maintaining this temperature for 1 h 45 min was complete conversion observed. Unfortunately, the only isolable product was undesired carbamate **78**, arising as a major side product (12% NMR yield), likely from undesired fragmentation pathways (Fig. 27). One or more non-isolable products were visible in the NMR spectra, but no [2,3]-Wittig product was observed.

As mentioned above, alkoxy(acylamino) carbenes can be reliably obtained from 1,3,4-oxadiazoline precursors.[127] However, the methods used to make substrates for carbene trapping (Fig. 29) utilized amines tethered to alcohols, which caused them to entropically favor the spirocyclic oxadiazoline derivatives.[127,128] We attempted to form this type of carbene precursor without the entropic advantage of intramolecular cyclization (Fig. 35).

Figure 35. Graduated heating of amine-derived [2,3]-Wittig substrate

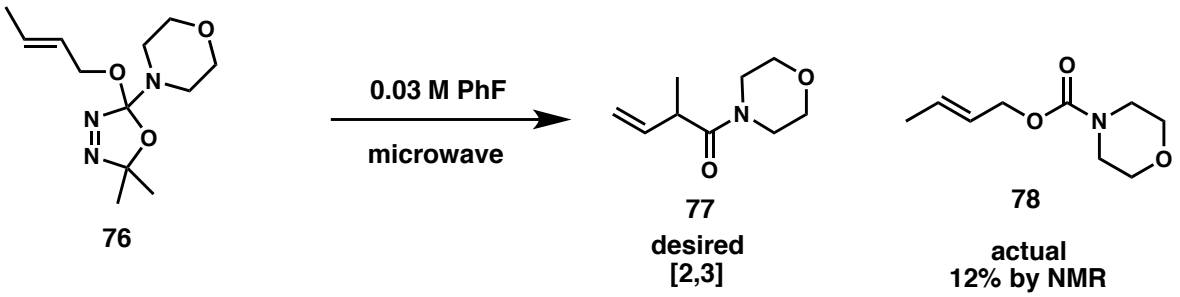

Entry	Conditions	Results
1	60 °C, 1 h	polar spot barely visible
2	70 °C, 1 h	polar spot barely visible
3	80 °C, 1 h	polar spot barely visible
4	90 °C, 1 h	slightly more polar spot
5	100 °C, 1 h	slightly more polar spot
6	110 °C, 1 h	>50 % conversion by TLC
7	110 °C, 30 min	almost complete by TLC
8	110 °C, 15 min	single polar spot on TLC

Semicarbazone **79** was obtained in 50% yield from **73** by heating with aniline in a solution of $PhCF_3$ via microwave radiation for 140 min at 120 °C, using a procedure designed by Garland's group.[128,131] Oxidative cyclization of **79** to **80** via literature precedent was accomplished in 81% yield.[127] But attempts to acylate the isourea nitrogen of **80** and add crotyl alcohol to the N-acyliminium ion to afford amide-derived oxazoline **81** were unsuccessful, giving ester **82** instead.

Figure 36. Attempted synthesis of amide-derived [2,3]-Wittig substrate

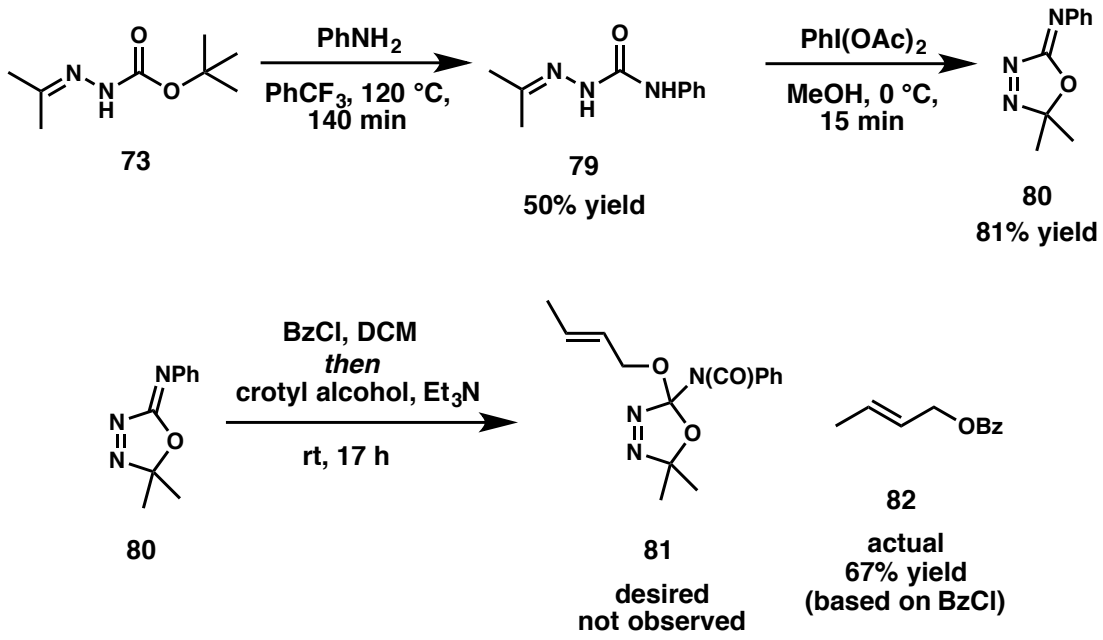

2.4 Future Directions

Although only preliminary investigations were carried out, valuable insight into the [2,3]-Wittig reaction for these types of systems was still gained. Allyloxy(alkylthio) carbenes remain a promising intermediate for undergoing the [2,3]-Wittig rearrangement and allyloxy(alkoxy) carbenes may be of interest as well. Additional optimization and substrate scope expansion is of continued interest to us in pursuit of a useful [2,3]-Wittig rearrangement methodology. Further work on this topic has been conducted by colleague Kimberly Buck, and it is our hope that this research will culminate in a versatile reaction manifold with great synthetic utility.

Chapter 3: Initial Exploration of Potential Radical and Cationic Polycyclization Methods for 2,2-Disubstituted Epoxide Substrates

3.1 Introduction

Cationic and radical polyene cyclization methods have been known for several decades with enormous advancements made during this time.[15-24,30] There are a number of advantages that these types of polycyclizations have over other methods of cyclization. For instance, both of these reactions often proceed with high stereoselectivity in the formation of C-C bonds. They can be configured to afford products with multiple fused 6-membered carbocycles—allowing selective access to *trans*- or *cis*-configurations at ring junctures—and set several stereocenters (including quaternary centers), all with largely predictable outcomes.[15-32,36,38,43,44,47,132-136] Also, 1,3-diaxial methyl groups are easily installed in these cyclizations and a number of functional groups are tolerated, though generally not required (except near the source of the cation or radical to be generated).[137-141] Overall, these polycyclization methods have demonstrated the ability to rapidly build complexity, which has aided in the concise synthesis of countless natural products[25-31,33-35,42-47,139-160] and their congeners. These polycyclic compounds have found use in the pharmaceutical and agricultural industries due to their biological and societal importance. For these reasons, we have embarked on an effort to fill in the gaps in knowledge of radical and cationic polycyclizations by exploring the under-developed areas of this research, with our focus largely on (terminal) 2,2-disubstituted epoxide substrates.

Both cationic and radical polyene cyclizations are largely kinetically controlled, exergonic processes.[144] Transforming a single chain into a compound containing multiple rings causes a relatively minor decrease in entropy as opposed to annulations, which combine two or more different molecules into one (poly)cyclic structure. In terms of enthalpy, polyene cyclizations ultimately benefit from the forging of 2 or more C-C σ-bonds from C-C π-bonds (or activated C-X σ-bonds; X = heteroatom). These polycyclizations, once completed, are thus usually irreversible, affording kinetic products, although there are cases where substrates, under certain circumstances (e.g. attack of electron-poor alkene onto a carbocation), undergo polycyclizations proceed in a step-wise fashion and may therefore exhibit reversibility.[15] However, this does not necessarily preclude a highly stereoselective reaction. Also, cationic polycyclization substrates may[145] or may not[15,144] pre-align in a conformation conducive to facile polycyclization (e.g. all-chair pre-organization), depending on the substrate and reaction conditions.

Barring any activating groups attached to the alkene that would stabilize intermediates, C-centered radicals and carbocations tend to undergo 6-*endo*-trig cyclizations onto tethered trisubstituted alkenes to afford a cation or radical that is trisubstituted. Therefore, in this mode of cyclization, both radicals and cations exhibit the same regiochemical preference. This trend has been known[132-136] for several decades, established and analyzed initially by Stork and Eschenmoser (cationic) and later expanded by Beckwith, Houk, and RajanBabu (radical).

The stereoselectivities for radical and cationic (poly)cyclizations are determined by similar factors as well. Both types of polycyclization frequently tend to

proceed through all-chair transition structures in a concerted fashion.[15] When the cyclizations occur simultaneously, stereochemical features that control the transition state conformation of one ring therefore also—to a large degree—dictate the stereochemistry of other forming rings due the sp^3 nature of the carbon atoms involved in bond formation. Remarkably, for both radical and cationic transformations, the presence of chirality on one of the pro-carbocycles (either proximal or distal to the initial ring formed) can act as a sort of stereodifferentiating group, encouraging a preference for a particular stereochemical outcome.[137-140] Steric factors often guide the diastereoselectivity in this manner[141,143,145,148-151] (e.g. sterically demanding substitutents exhibit a preference to sit pseudo-equatorial in the transition structure).

Since 6,6-fused systems are of great practical importance to synthetic chemists, many polycyclizations have been developed with this motif in mind to provide a linear framework by which multiple rings can be generated in a single transformation.

3.1.1 Cationic polycyclizations of epoxypolyenes

Cationic polycyclizations were first investigated by Stork and Eschenmoser and then initially developed by van Tamelen, Goldsmith, and Johnson.[28,31,132,133,152] In Stork's paper,[132] farnesylacetic acid and (monocyclo)farnesylacetic acid were individually subjected to Lewis acidic conditions ($SnCl_4$). Both polyenes cyclized to afford the same diastereomer, with *trans*-configured ring junction. This finding, as well as others in Stork's and Eschenmoser's 1955 publications,[132,133] showed that multiple rings could be formed from the polycyclization of polyenes, taking place in a single

mechanistic step. The *anti*-addition of electrophiles and nucleophiles to the alkenes provided evidence for a concerted reaction: the (*E*)-configured γ,δ-unsaturated carboxylic acid gave a *trans* ring junction and the (*Z*)-configured γ,δ-unsaturated carboxylic acid gave a *cis* ring junction between the final two rings formed (Fig. 37).

Figure 37. Polycyclization of farnesylacetic acid and monocyclic derivative

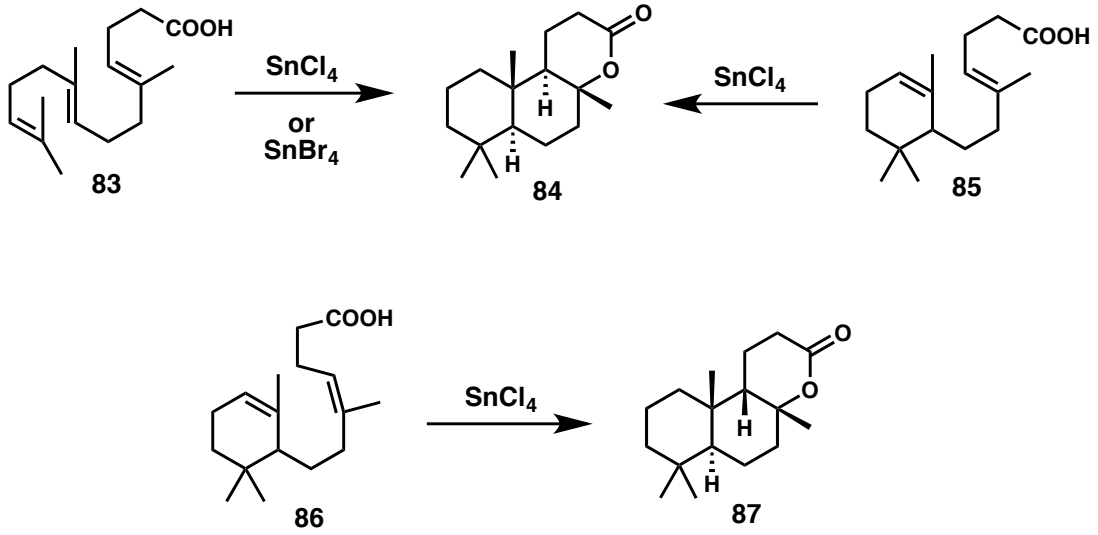

The *anti*-relationship between the attack of an electrophile by an alkene and the adjacent attack of a nucleophile is a crucial feature for understanding the nature and predictability of transition state (and thus product) stereochemistry. This *anti*-stereospecificity is constant in various concerted cationic polyene cyclizations. The minimization of steric hindrance and the orbital preference for *anti*-addition to alkenes can be strategically utilized to favor the assembly of *trans*-fused ring systems via all-chair transition states (e.g. polyisoprenes). The preset (*E*)- or (*Z*)-configuration of each internal alkene, along with the penchant for electrophile-nucleophile

anti-addition across these alkenes, allows the relative stereochemistry at ring junctures (*trans* or *cis*) to be derived from the respective alkene geometry in the substrate. This preference for *anti*-addition takes priority over a variety of unfavorable steric interactions, including 1,3-diaxial interactions between methyl groups. Non-concerted cationic cyclizations generally only take place when formidable steric congestion and/or prohibitive electronic effects (e.g. electron-poor or electron-neutral arene nucleophiles or over-stabilized carbocation electrophiles) prevent or decrease the rate of a particular cyclization. Some cationic polycyclizations are only partially concerted, with one or more non-concerted cyclizations.[143,144]

The stereochemistry of starting epoxides in an epoxypolyene scaffold is almost always inverted at the carbon that is attacked during the first cationic cyclization (usually the most substituted, electrophilic carbon).[153] This inversion takes place in such a way that the resulting alcohol products from 2,2,3-trisubstituted epoxides end up equatorial.[27-29,31,138,143,145] This stereochemical outcome tends to takes priority over other sterically demanding groups that would typically prefer to be equatorial in the first ring and subsequent rings. Our focus on 2,2-disubstituted epoxide polycyclization arose from a combination of an interest in the subject and a paucity of literature on the topic, particularly regarding product stereochemistry.

After an extensive survey of the literature, only three examples were found of 2,2-disubstituted epoxides undergoing polycyclizations, all of which were cationic and afforded *trans*-decalin derivatives (Fig. 38).[28,29,31] The transformations that took place at rt gave much lower yields than the cryogenic polycyclization reported by Corey.

Figure 38. All known precedence for 2,2-disubstituted epoxypolyene polycyclization

Goldsmith and Phillips (1969)[31]:

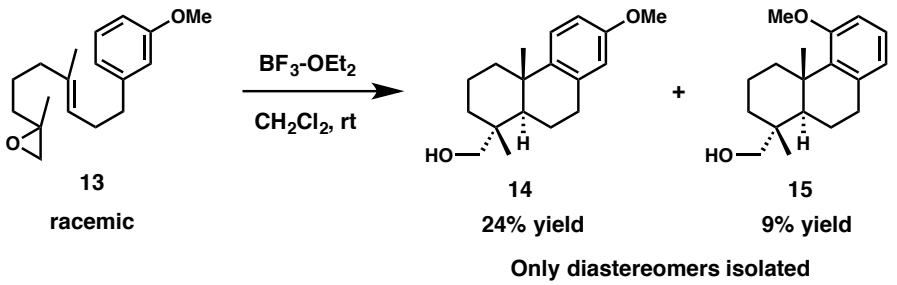

Van Tamelen (1983)[28]:

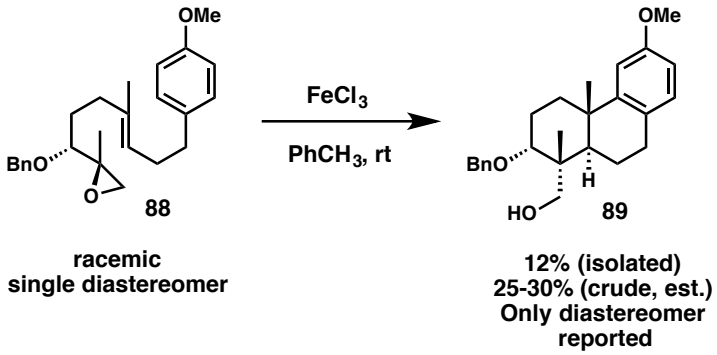

Corey (1997)[29]:

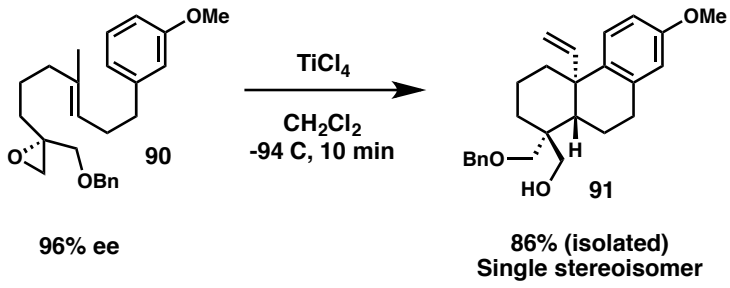

The only products isolated, in every case, were single diastereomers that had the distinguishing feature of an equatorial hydroxymethylene (-CH_2OH) group. While this precedence intrigued us, a great deal of investigation must be done to assert that these findings are general for other cationic polycyclizations of 2,2-disubstituted

epoxides. We were most curious about which reactive conformation (transition structure) would generally dominate and what implications this had for product stereochemistry (e.g. equatorial or axial hydroxymethylene). In addition, a key objective of ours was to employ a functionalizable moiety other than a methyl group on the center olefin.

While most carbonyl and carboxylic acid derivatives are likely too deactivating towards cation-propagation to use as functional handles, the nitrile group has been shown to be significantly less deactivating, and in certain cases, even very slightly activating (with respect to hydrogen).[161-164] This stabilizing effect has been shown to be derived from its ability to stabilize carbocations through resonance. Since secondary carbocations have been successfully employed as intermediates in cationic polycyclizations, it may indeed be possible to employ α,β-unsaturated nitriles in these reactions.[137] Although the effect of neighboring alkene participation is somewhat convoluted, in certain cases, the rate of alpha-cyano carbocation formation is faster with π-donation from nearby alkenes.[164] If the developing carbocation alpha to the nitrile is indeed stabilized by donation of electron-density from a tethered electron-rich π-system, the desired polycyclization would become more likely. With these ideas in mind, we intended to investigate the possibility of employing the nitrile group, as stated, in our polycyclization method. Since this moiety is known to be an excellent functional handle for further manipulation, the implementation of this idea would provide a great advantage.[43-46]

3.1.2 Radical polycyclizations of epoxypolyenes and congeners

Radical polycyclizations have garnered a great deal of attention from synthetic chemists in recent years. Polycyclizations initiated by the reduction of an epoxide moiety are of great interest to our lab. In particular, we have chosen to focus on developing radical and radical-polar crossover polycyclizations of 2,2-disubstituted epoxypolyenes and their congeners to form poly(carbo)cycles.[36,154] To the best of our knowledge, research into this area (using these substrates) is scarce. The three literature examples above detail the *cationic* polycyclization of 2,2-disubstituted epoxide-containing substrates, whereas the *radical* polycyclization of this class of compounds has no precedence (Fig. 38). There is, however, precedence by Cuerva's group and others that demonstrates the radical *mono*cyclization of 2,2-disubstituted epoxy olefins as well as the radical mono- and polycyclization of various other epoxypolyenes and similar systems, including one especially intriguing example of a radical-polar crossover polycyclization (termination via aldol).[23,26,32-44] In these transformations, the reagent of choice is typically Cp_2TiCl_2, which, when reduced to its Ti^{III} state (i.e. Cp_2TiCl), coordinates to epoxides and homolyzes the C-O bond that forms the most stable carbon radical.

Nugent and RajanBabu first introduced this reagent as an efficient regioselective epoxide reducing agent in 1988, and since then, it has since gained widespread interest[23,26,32-42,136,149-151,155-160] for various transformations of epoxides. These include intermolecular additions to electron-poor olefins (e.g. acrylonitrile) and shortly after, *intra*molecular additions to a variety of alkenes, including 5-*exo*-trig

α,β-unsaturated nitriles (4 examples).[146,147]

The idea of finding a metal-bound epoxide analogue to the cyclopropylcarbinyl radical was first described by RajanBabu and Nugent (Fig. 39).[155] The Ti(III)-coordinated epoxide was a remarkable manifestation of their initial concept, since it possessed a metal with a half-filled d-orbital (which approximates radical character) and epoxide ring cleavage occurs with high regioselectivity for most substitution patterns. In 1998, Gansäuer's group developed a catalytic version of this methodology that employed superstoichiometric quantities of cheap metal powders, Mn or Zn, and substoichiometric amounts of the Ti(IV) precatalyst.[165]

Figure 39. Cyclopropylcarbinyl radical as analogue for Ti(III)-epoxide complex

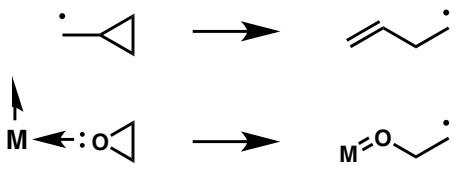

Barring any stabilizing groups, in the Ti(III)-mediated reduction of epoxides, tertiary radicals are generally highly preferred over secondary and primary radicals. This causes selective radical formation to occur at the most substituted carbon. Consequently, the ensuing radical cyclization (of epoxypolyprenes) tends to follow the same regiochemical preference as cationic cyclizations. One major difference between cationic and radical polycyclizations is that the latter tends to be more facile when the eletron-density of olefin radical acceptors alternates[24,25,43,44] throughout the molecule. More specifically, when electron-poor radicals attack electron-rich alkenes and vice

versa, Coulombic interactions and molecular orbital effects (usually) decrease the barrier to intramolecular radical propagation.[43,44] However, radical intermediates can apparently be "too stable" to react further[36] (e.g. certain systems with α-keto radicals). This occurs when a stabilizing group is responsible for decreasing the energy of the radical species by significantly more than it decreases the total barrier energy ($\Delta\Delta G^{\ddagger}$) of the cyclization of this radical (to form the next ring).[43] In this setting, the nitrile group's ability to act as a moderately stabilizing electron-withdrawing group ultimately allows for facile radical propagation.[24,25,43,44,47,142] Proper placement of the nitrile moiety can therefore facilitate the consecutive inversion of electron-density of queued olefin radical acceptors (in polyenes) and prevent the "over-stabilization" of radical intermediates.[43] This makes the nitrile group well suited for accelerating radical cyclizations. Notably, as mentioned above, nitriles can be easily manipulated into a variety of other common moieties which allows them to serve as excellent functional handles.[24,43-47] For these reasons, we chose to investigate the radical polycyclization of 2,2-disubstituted epoxypolyenes and related systems that possess strategically placed α,β-unsaturated nitriles.

A major advantage of the Ti^{III}-induced radical cyclization method, in comparison to cationic cyclization, is the large array of functional groups that can be tolerated under the reaction conditions. Free hydroxyl groups and other polar functionality that is labile in the presence of Lewis acid or oxidizing agents (e.g. Br_2, Cu^{2+}, etc.) remain intact under mild RajanBabu-Nugent conditions. Developing a radical polycyclization method for 2,2-disubstituted epoxides therefore serves to complement current and future cationic polycyclization methods.[154]

3.2 First approach towards the first model system for polycyclization, 92

All approaches to the polycyclization substrates were developed in a convergent manner, each relying on the coupling of two fragments (**A** & **B**) with an HWE olefination (generally at the end of a given route) (Fig. 40). The HWE reaction between pre-functionalized (cyanoalkyl)phosphonates and aldehydes, under the right conditions (KHMDS, $PhCh_3$, -78 °C), is known to favor the formation of (*Z*)-α,β-unsaturated nitrile products,[24,25,43,44,46,47,142] usually in high yield and good dr.

Figure 40. Summary of 1st generation retrosynthesis of initial model system

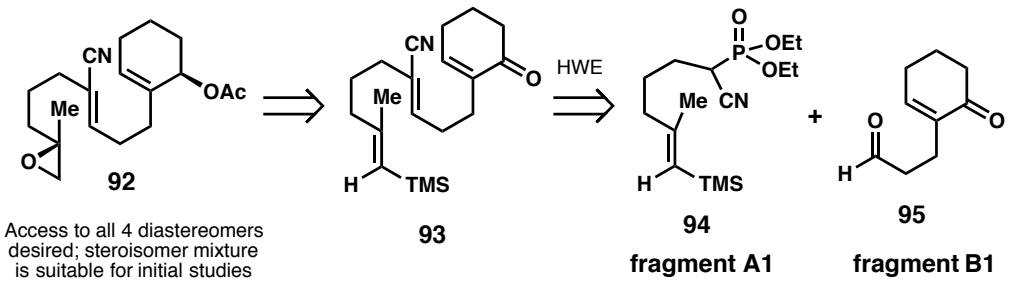

The first route towards the initial polycyclization precursor began with the TMS-protection of alkyne **96**, which was carried out using a literature procedure to give **97** in 95% yield (Fig. 41).[166] Next, a highly regioselective zirconocene-catalyzed carboalumination-isomerization of **97** (followed by protodemetalation) afforded the vinylsilane-tethered alcohol, **98**, in 70% yield; only the desired regioisomer, **98**, was observed. This transformation was carried out on the same substrate and under the same initial reaction conditions as in Negishi's 1997 paper on carboalumination but

treated with a proton source as the electrophile during reaction work-up instead of iodine.[167] As anticipated, the *(E)*-diastereomer of **98** was obtained predominantly, with excellent stereoselectivity (23:1 dr, (*E*):(*Z*)) (Fig. 41).

Figure 41. Synthesis of phosphonate **94** (fragment **A1**)

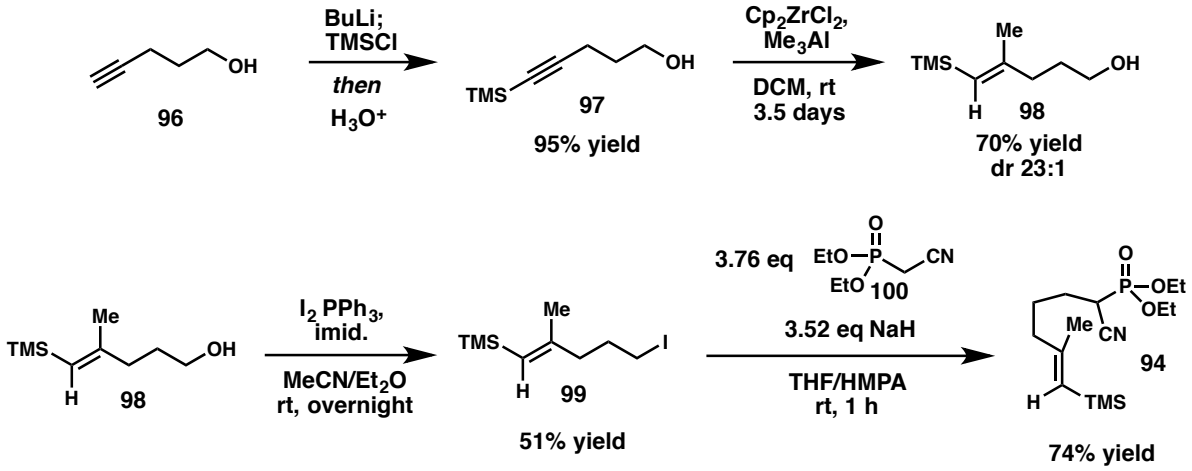

Iodination of vinylsilane-tethered alcohol **98** was carried out under Appel conditions, following a procedure employed in the literature for a very similar substrate (Fig. 41).[168] The primary iodide, **99**, was obtained in 51% yield from this reaction. Using conditions similar to a literature example for monoalkylation, the reaction of diethyl (cyanomethyl)phosphonate, **100**, with this electrophile was accomplished by adding a solution of **99** to an excess of the nucleophilic phosphonate anion derived from NaH and **100**.[169] The S_N2 reaction was finished in just 1 h, affording the desired monoalkylated product, **94**, in 74% yield, which completed the synthesis of fragment **A1**.

Figure 42. Literature synthesis of enone-aldehyde, **95**, and enone-acetal, **103**

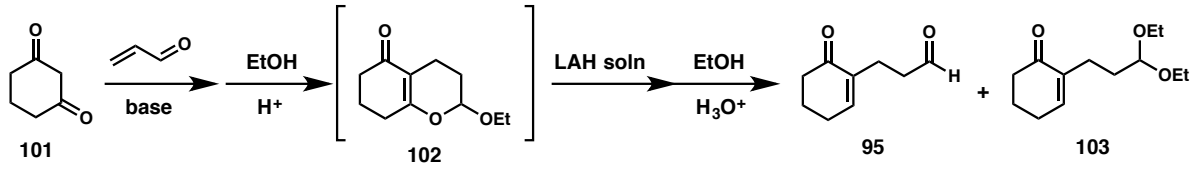

The synthesis of **95** was carried out following literature[170] precedent (Fig. 42). Strangely, while usable quantities of **95** were obtained and the diethyl acetal (of the aldehyde), **103**, was also isolated as a side product, much lower yields were observed than reported. The yield of the desired product, **95**, was only 14% (lit. yield 84%) and the yield of the byproduct, **103**, was only 3% (lit. yield 10%) (Fig. 42). The low purity of the starting material, 1,3-cyclohexadione (**101**), is suspected to be the source of this result. Fortunately, however, the two products were easily separated by chromatography on silica gel. Purified **95** (fragment **B1**) was carried forward while isolated **103** was set aside for potential future use (see subsections **3.3** & **3.8**).

Nitrile-stabilized phosphonate anions have been known to react with α,β-unsaturated ketones via both 1,2- and 1,4-addition and are capable of reacting with saturated ketones as well, but their reaction with aldehydes are typically much faster since aldehydes are more electrophilic and generally less sterically encumbered than ketones.[171-173] Also, forming an alkene and a soluble phosphate derivative upon HWE coupling with an aldehyde serves as a convenient thermodynamic well, from which conjugate additions do not benefit.

Figure 43. Synthesis of (*E,Z*)-triene via an HWE olefination of fragments **A1** and **B1**

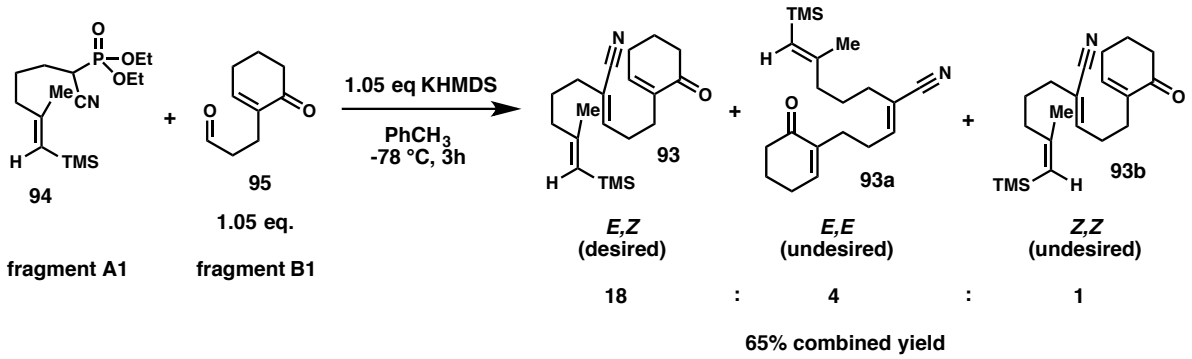

With fragments **A1** and **B1** in hand, an HWE reaction was carried out. Utilizing conditions known to favor the (*Z*)-configuration of the forming alkene (i.e. the resulting α,β-unsaturated nitrile), this geometry was generated preferentially in the product mixture (with a ~4.4:1 dr for the forming alkene) (Fig. 43).[174] A solution of the potassium phosphonate in toluene, generated *in situ*, was treated with 1.05 eq fragment **B1** at -78 °C, which ultimately gave mostly the desired (*E,Z*)-diastereomeric product. However, unsurprisingly, a small amount of the (*Z,Z*)-product derived from the minor (*Z*)-diastereomer of the vinylsilane (present in fragment **A1**, (as 23:1, (*E*):(*Z*) mixture) was also detected. The (*E*)- and (*Z*)-stereoconfigurations of the α,β-unsaturated nitrile and the vinylsilane double bonds were discerned using a combination of spectral data from the literature on these types of trisubstituted alkenes and spectral data (including 2D-NOESY) analysis of the products (see SI). The combined yield of diastereomeric products of **93** was 65%, but the 3 diasteromers obtained—(*E,Z*), (*E,E*), and (*Z,Z*), formed in a ratio of 18:4:1—proved largely inseparable, even with the use of a variety of chromatographic techniques (e.g.

argentation chromatography, preparative TLC, etc.). Thus, the product mixture was carried forward without complete separation.

Figure 44. Chemoselective mCPBA epoxidation of triene, **93**, and attempted (asymmetric) Shi epoxidation

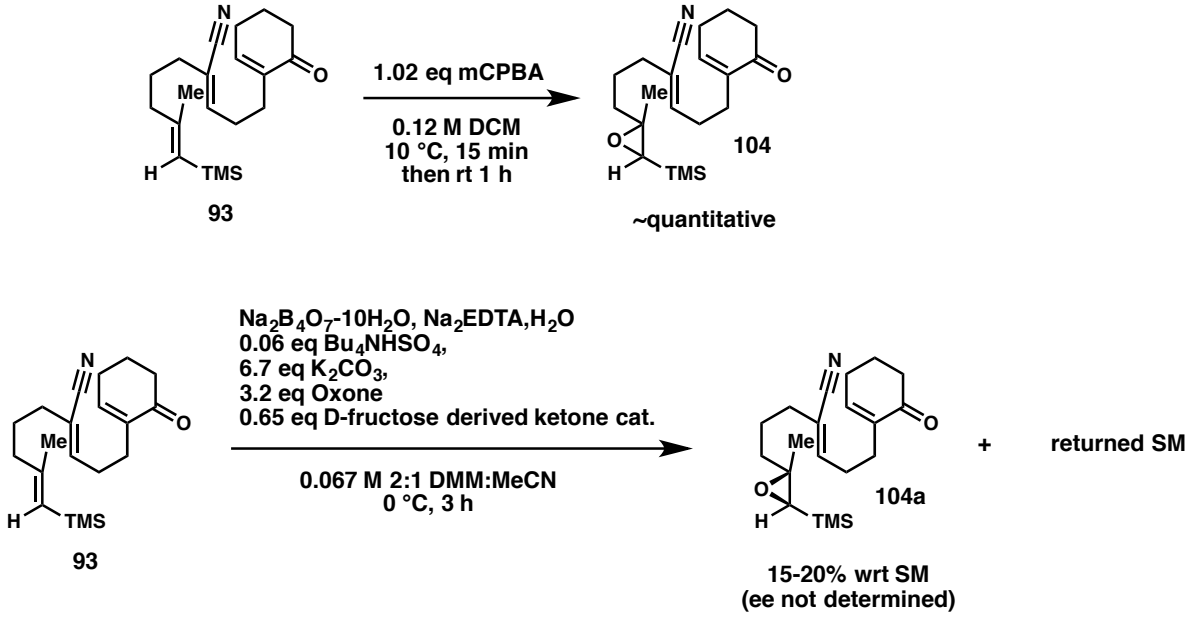

Under ambient conditions, and using only slightly more than 1 equivalent of mCPBA, the most nucleophilic alkene (the vinylsilane) in compound **93** was selectively epoxidized in just 1 h (rt), giving a quantitative yield of the desired racemic product, **104**, on a small scale (Fig. 44).[175]

While utilizing Shi epoxidation conditions for trisubstituted vinylsilanes gave the desired chemoselectivity for this substrate, the reaction suffered from low reactivity with < 20% conversion in every attempt. Using different Shi conditions did not favorably influence this outcome (Fig. 44).[176] Thus, no attempt was made to

ascertain the absolute stereochemistry of the product, **104a**. Instead, we sought to formulate an alternative route to the initial polycyclization precursor.

3.3 First approach to epoxyphosphonate 112 (fragment A2) & synthesis of allylic acetate-tethered aldehyde 108 (fragment B2)

With enone-tethered acetal **103** available, the convenience of performing multiple functional group manipulations to make the allylic acetate moiety prior to performing an HWE coupling was viewed as a viable alternative in terms of scale-up and overall practicality. This way, more complexity could be added (to the aldehyde fragment) prior to coupling the fragments. Also, this averted the need for devising conditions (to asymmetrically reduce **104(a)** to the corresponding allylic alcohol) that would require several different aspects of chemoselectivity. The enone moiety in **104(a)** would need to be converted to an allylic alcohol, without reduction of either C-C double bond, the nitrile, or the epoxide, and without otherwise affording unwanted byproducts (e.g. by isomerization of the unsaturated nitrile, opening the epoxide with Lewis acid, etc.). Thus, we chose to employ a CBS reduction of **103**, since this compound was inadvertently obtained in the synthesis of **95** and therefore available for use in the new route (see subsection **3.2**).[177]

Figure 45. CBS reduction of **103** (prior to optimization) and Mosher's ester analysis

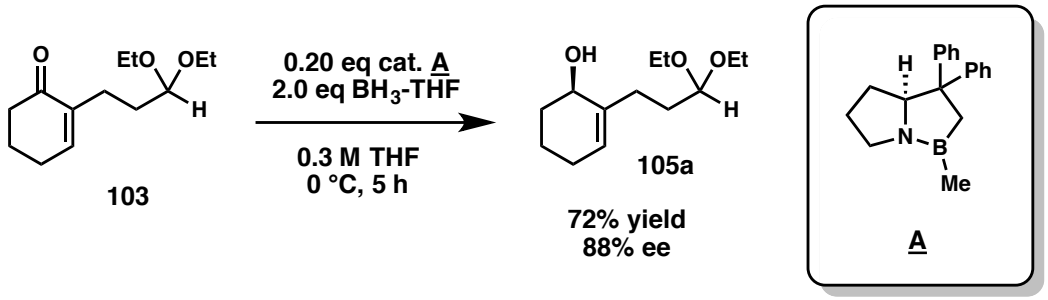

The CBS reduction of enone **103** in fact gave an appreciable preference for the expected (and desired) enantiomer, verified by performing a Mosher's ester analysis (Fig. 45).[178-180] Since the first equivalent of BH_3-THF did not fully reduce the enone, additional reducing reagent was added in small amounts until the reaction reached completion (2.0 eq total).[181] The (*R*)-alcohol **105(a)** was obtained in good yield (72%) and with good ee (88% ee), considering the procedure was unoptimized for the substrate, **103**. This reaction, by elaboration, provides access to each enantiomer of **105a** as well as its functionalized derivatives (acetates, carbonates, etc.) which is a necessary component of both stereoselective substrate synthesis and future stereochemical analysis of 2,2-disubstituted epoxide polycyclizations.

Figure 46. Improved synthesis of enone-tethered acetal **103**

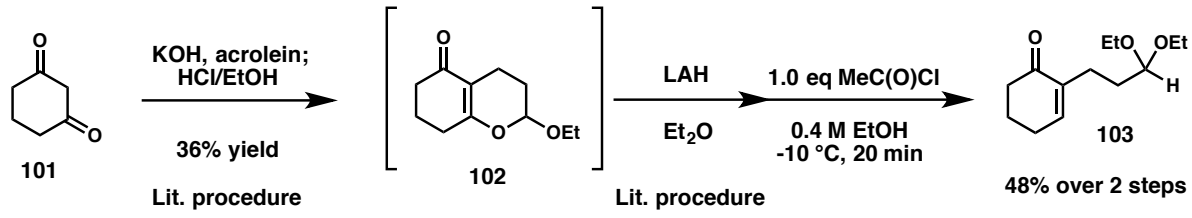

The previously mentioned unintended formation of **103** as a side product in the (literature) preparation of **95** afforded only a small amount of **103**, a compound that we chose to employ in our revised synthesis of the first model system (Fig. 47). Optimization of the last step of the 3-step sequence led to an increased yield (17% over 3 steps on gram-scale, previously 3%) of the newly desired acetal product, **103**, which provided usable quantities of this compound (Fig. 46).

Figure 47. Synthesis of fragment **B2**, **108**, from **103**

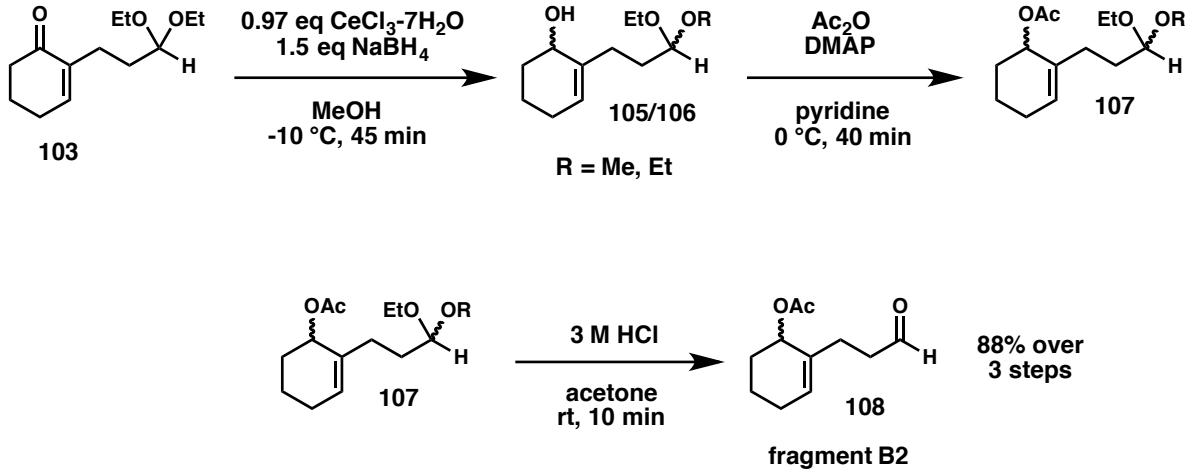

The synthesis of allylic acetate-tethered aldehyde **108** from **103** was comprised of 3 simple transformations: Luche reduction of enone **103**, acetylation of **105/106**, and deacetalization of **107**. The Luche reduction afforded both the diethyl acetal and the mixed methyl/ethyl acetal (**105/106**), but this was of no concern since both compounds served to protect the aldehyde from reacting in the subsequent reaction and were easily cleaved, afterwards, to the aldehyde. The desired allylic acetate-

tethered aldehyde, fragment **B2**, was obtained in 88% yield over 3 steps, and only one purification, after the final step, was required (Fig. 47).

Figure 48. 1st generation synthesis of epoxyphosphonate, **112** (fragment **A2**)

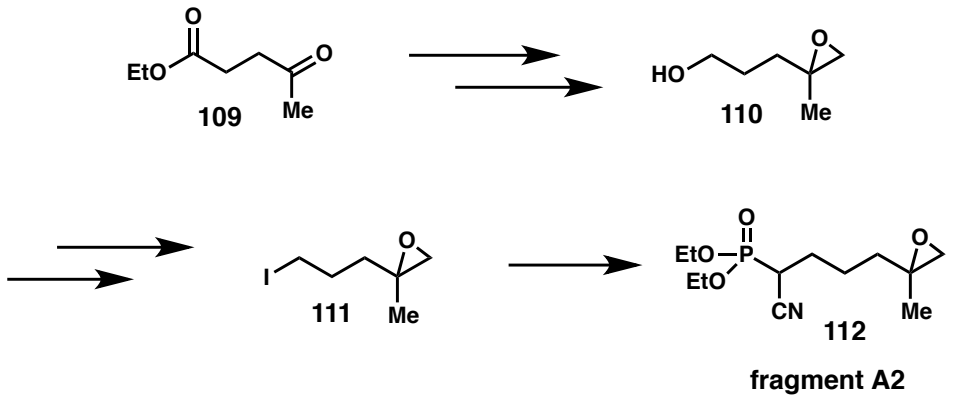

Figure 49. Synthesis of epoxy iodide **111** from ethyl levulinate **109**

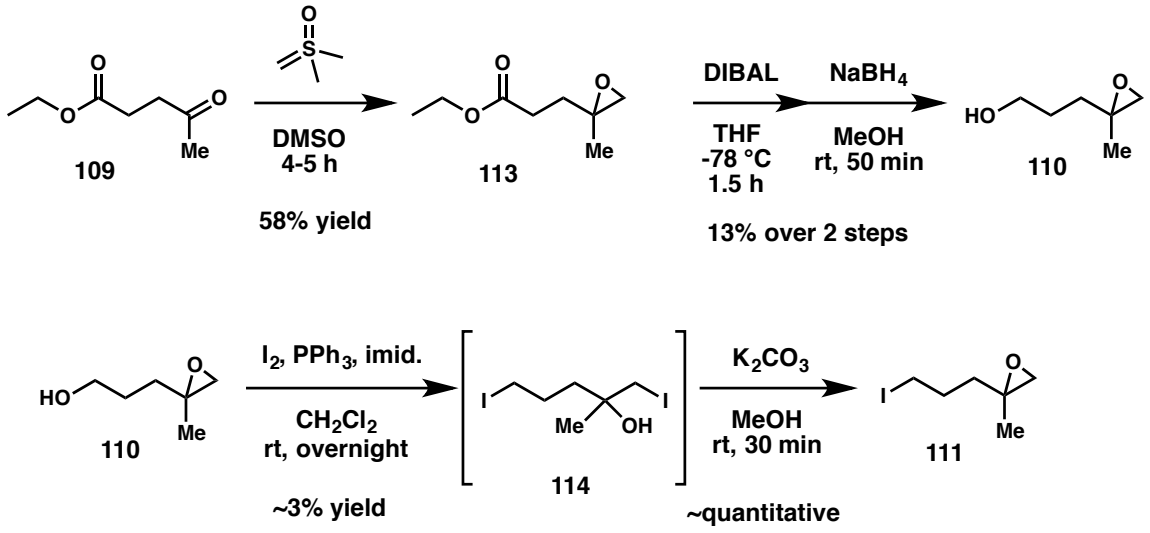

After the synthesis of fragment **B2** was complete, we set out to procure the epoxy phosphonate, fragment **A2** (**112**) (Fig. 48). We chose this fragment as the coupling partner for a variety of aldehydes because it possessed all the desired

features of the substrates we wished to make—no further functionalization was required on this portion of this molecule after the HWE coupling.

The epoxidation of ethyl levulinate was carried out under standard Johnson-Corey-Chaykovsky conditions to give a 58% yield of epoxy ester, **113**[182,183] (Fig. 49). Notably, similar methyl ketone systems have been epoxidized in an asymmetric version of this reaction, the Shibasaki epoxidation.[184] We plan to incorporate this methodology in the future to render the synthesis of the epoxide moiety enantioselective; once the routes to racemic substrates have been established, this will become a crucial element of our planned strategy. Carrying epoxy ester **113** forward, DIBAL reduction at -78 °C afforded the aldehyde (not drawn) as the only identifiable product (though in low yield, est. ~40%), with longer reaction times and excess reducing agent ultimately leading to decomposition.[183] Due to the proclivity of the product to decompose under mild conditions (e.g. on SiO_2), the next step was carried out without purification. Since the epoxy alcohol could not be obtained directly from the ester by reduction with DIBAL, crude epoxy aldehyde was reduced with $NaBH_4$, under conditions used in the literature for a very similar compound, to afford the desired epoxy alcohol, **110**, albeit in a low 2-step yield (13% over 2 steps).[185]

The direct iodination of epoxy alcohol **110** proved to be a mostly unfruitful endeavor. A presumed epoxide-cleaved bis(iodo) compound was obtained on a small scale, when **110** was subjected to standard Appel conditions, in only ~3% (crude) yield (Fig. 49).[180] Unfortunately, 2,2-disubstituted epoxides are prone to nucleophilic opening under rather mild conditions, including in the presence of iodophosphonium salts.[186] Upon exposing the crude material from the attempted iodination to a solution

of K_2CO_3 in MeOH—known iodohydrin cyclization conditions—the desired epoxy iodide **111** was indeed obtained, supporting our initial proposed structure for **114**.

Figure 50. Alkylation of **111** with **100** to obtain fragment **A2**, **112**

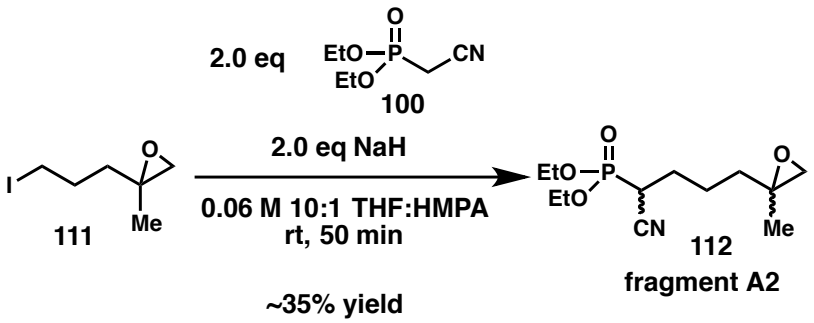

Finally, the synthesis of **112** (fragment **A2**) was attempted, and a variety of conditions were compared. The best yield (~35%) was obtained with 2 equivalents each of NaH and **100** (Fig. 50). If less of the nucleophile (anion derived from **100**) was used, undesired dialkylation dominated, and with more of the nucleophile, a large amount of unreacted **100** was present in the crude product mixture. Both of these scenarios caused serious issues during separation because, most unfortunately—**100**, **112**, and the dialkylated side product all coeluted on silica, even under drastically different chromatographic conditions. Isolation of the product was only possible when the presence of the other coeluting species were minimized.

A number of issues with this route led to very low yields (0.08% overall yield of fragment **A2**) and the clear need for a better substrate route. Thus, further optimization was halted and a new route to fragment **A2** was envisaged.

3.4 Second approach to epoxyphosphonate 112 (fragment A2)

Figure 51. 2nd generation synthesis of epoxyphosphonate, **112** (fragment **A2**)

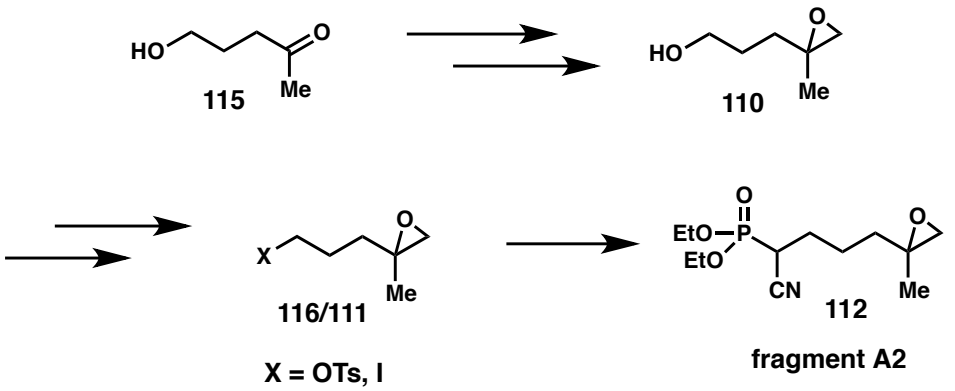

In our second approach to **112**, we started with 3-acetyl-1-propanol, **115**, again using a Johnson-Corey-Chaykovsky epoxidation to install the epoxide moiety, and conducting other functional group manipulations to provide a suitable electrophile for monoalkylation of **100** (Fig. 51).

The TBS-protection of **115** was carried out following literature precedent to give 54% of the silyl ether, **117** (Fig. 52). In the literature procedure for this reaction, a much higher yield (89%) was reported, but higher yields could not be obtained by following this protocol.[187] However, in the subsequent reaction, using twice recrystallized trimethylsulfoxonium iodide (using H_2O, then washing with acetone), the epoxide, **118**, was obtained in quantitative yields, reproducibly—in high purity, on gram-scale, and without purification—using literature conditions, even though the reported yield for this reaction was only 45%.[188] Following this successful epoxidation,

TBAF-mediated deprotection of the TBS-ether, **118**, was carried out under typical mild conditions to give **110** (in est. ~80% yield).[189]

Figure 52. Synthesis of epoxy tosylate, **116**, and attempted alkylation with **100**

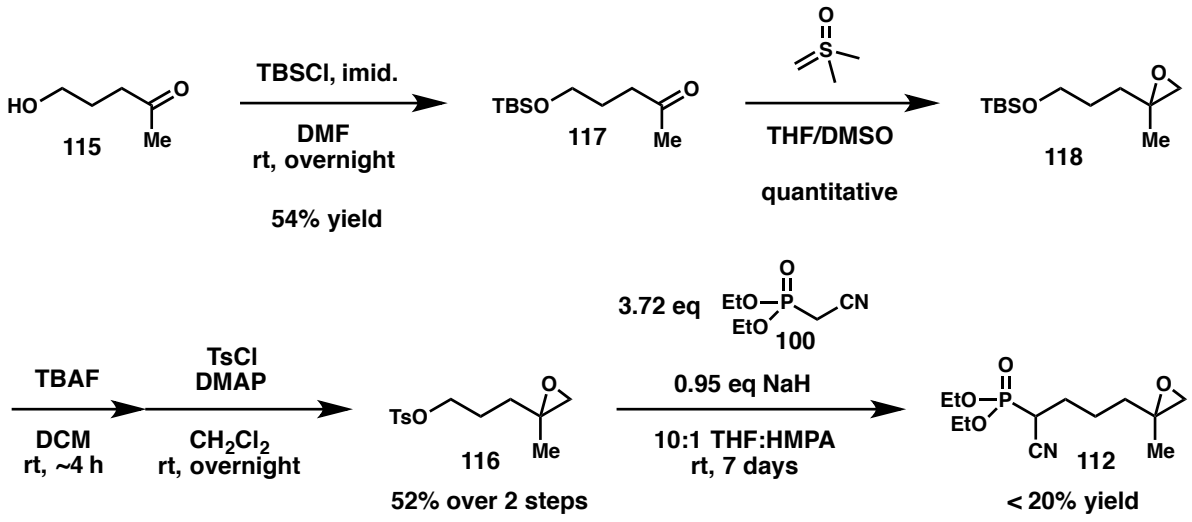

Since direct conversion of alcohol **110** to epoxy iodide **111** was unsuccessful in the previous route (see subsection **3.3**) and monoalkylation of **100** with **111** proved troublesome, we chose to instead make epoxy tosylate **116** to use as the electrophile in the alkylation of **100**. Tosylation of the free alcohol, **110**, afforded epoxy tosylate, **116**, which was obtained in a 52% 2-step yield (single step yields of ~79% for TBS-deprotection then ~64% for tosylation) using conditions that were employed for a similar primary alcohol (4,5-epoxy-1-ol) substrate (Fig. 52).[190] While the resulting tosylate could be purified on silica gel, the neat compound quickly decomposed, becoming an intractable mixture (in < 24 h at rt), even at cryogenic temperatures. Thus, the phosphonate alkylation was attempted with freshly produced **116**. Unfortunately, the alkylation of **100** with **116** gave only a ~20% yield of **112** after

stirring for a total of 7 days, although decomposition did not take place; mostly starting material remained.

To the best of our knowledge, there is no literature precedent for the alkylation of **100** with a tosylate and only one procedure details the intermolecular alkylation of **100** with an alkyl mesylate. In the latter case, 24 hours at room temperature were required to obtain a 62% reported yield of monoalkylated product from deprotonated **100** and an unhindered primary activated (allylic) mesylate.[191] It was conceived that the soft resonance-stabilized phosphonate anion nucleophile does not easily displace a hard electrophilic tosylate or mesylate via S_N2 due to the lack of hard/soft pairing.[192] It makes sense that the anion produced by deprotonating **100** would be soft when considering that it is highly stabilized by resonance with two adjacent electron-withdrawing species, fulfilling the requirements of being "large", having low charge density, and exhibiting strong polarizability.[193] In the previously mentioned alkylations of **100** with alkyl iodides (**99** and **111**)—which are much softer electrophiles—we observed reaction times that were indeed significantly shorter than alkylation with the tosylate (7 days, ~20% conversion); complete consumption of the corresponding iodides occurred in just ≤ 1 h (Fig. 41 & 50). In our investigations, we determined that alkylation of **100** with the tosylate must be hundreds of times slower than with the analogous iodide. With this in mind, a Finkelstein reaction was carried out with **116**, affording epoxy iodide **111** in 79% yield (Fig. 53). The reaction was complete after just 10 min in refluxing acetone and, fortunately, no iodinative opening of the epoxide was detected. The product, **111**, was used as before in the alkylation of **100** (in ~35% yield) to complete the second route to fragment **A2**.

Figure 53. Iodination of epoxy tosylate to give epoxy iodide, then alkylation to **112**

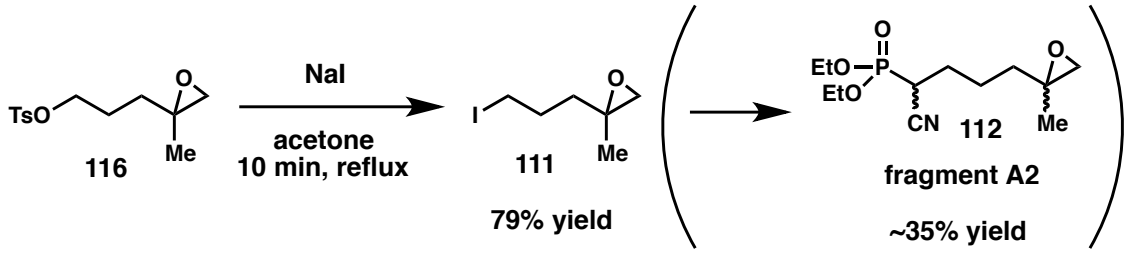

Unfortunately, further attempted optimization of the alkylation of **100** with **111** (see subsection **3.3**) did not increase the yield of this transformation. The overall yield of this route was therefore calculated to be 6% over 6 steps (Fig. 54).

Figure 54. Summary of first two approaches to fragment **A2**

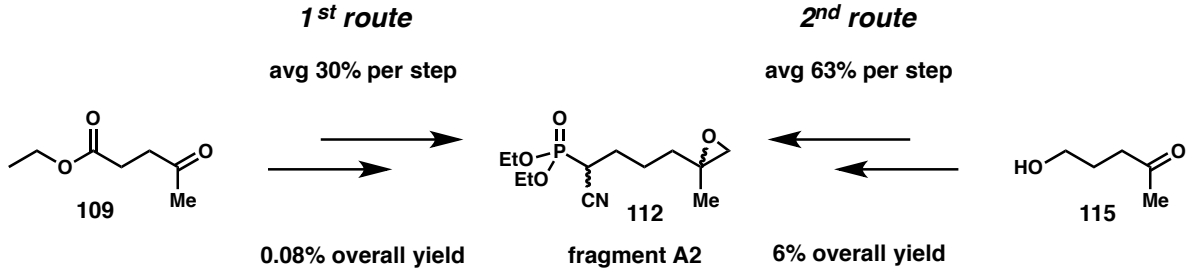

The two approaches to fragment **A2** (**112**) detailed thus far were 6 steps each, but the yield for the 2nd route was 75 times higher than the 1st, signifying a huge improvement (Fig. 54). However, with the low yielding final step (phosphonate alkylation with **111**, ~35%) and the timely purification of the product from this reaction, further development was still needed for a fast, reliable synthesis of fragment **A2** (as a racemic mixture of diastereomers).

3.5 Third approach to epoxyphosphonate 112 (fragment A2) and completion of first substrate (93) synthesis

Figure 55. 3rd generation synthesis of epoxyphosphonate, **112** (fragment **A2**)

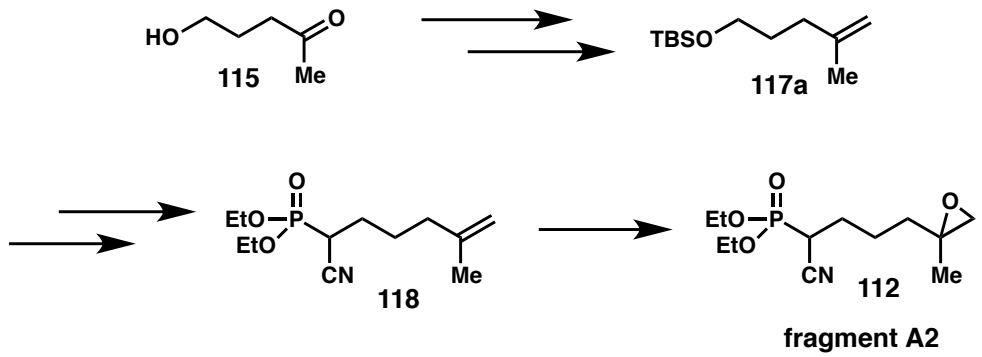

The next and final route to the desired epoxyphosphonate, fragment **A2**, was devised to increase the overall yield of the synthesis and ensure scalability and purification issues remained minimal (Fig. 55).

We hoped that the (alkene-tethered) primary iodide, **120**—accessible directly from the alcohol in this route—would provide an ideal starting material for the phosphonate alkylation for two main reasons. First, the products and starting material were expected to have different polarities than those produced from alkylation with epoxy iodide **111** (in which they all co-eluted on silica gel; see subsection **3.3**). Thus, we anticipated that the polarities of the starting material, monoalkylated product, and dialkylated side product in this new route would be different enough to allow for separation using flash chromatography (Fig. 41 & 50). Second, monoalkylation and product isolation were successful (74% isolated yield) in the reaction of phosphonate **100** with the vinylsilane-tethered primary iodide **99** (see subsection **3.2**). Since the

only difference between the two primary iodide electrophiles (**99** and **120**) was the presence of a TMS-group (in **99**) instead of a hydrogen (in **120**), we expected similarly successful results—the presence of a vinyl proton instead of a TMS-group should only very slightly change the polarity of the molecule. We hoped this strategy would circumvent the issues encountered with the phosphonate alkylation of epoxy iodide, **111**, and consequently provide fragment **A2** in higher overall yield from commercially available starting materials.

Figure 56. Wittig olefination attempt

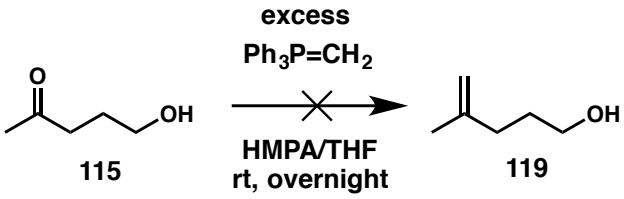

The Wittig olefination of 3-acetyl-1-propanol did not provide any of the desired alkene using the literature procedure that purported to provide access to the product when 4+ equivalents of ylide were used (Fig. 56).[194] Perhaps the cause of these fruitless attempts can be traced back to faulty reagents (e.g. wet THF, etc.). In any case, a workaround was devised, utilizing available **117** from the prior approach to fragment **A2** (see subsection **3.4**).

Figure 57. Final improved synthesis of fragment **A2**

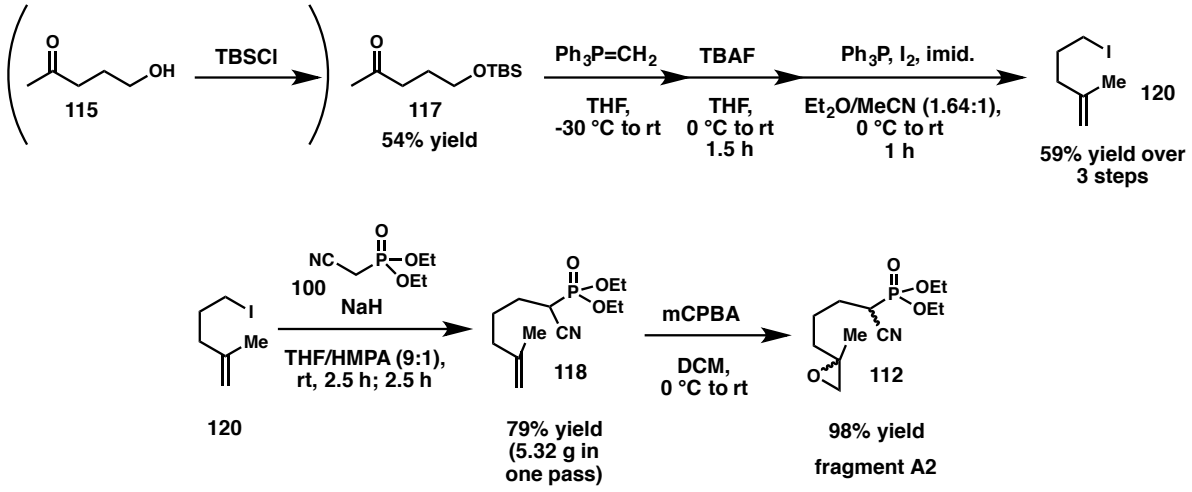

The aforementioned TBS-protection of 3-acetyl-1-propanol gave silyl ether **117** in 54% yield.[187] This ketone was then subjected to a Wittig olefination using 1.24 equivalents each of *n*-BuLi and the freshly made iodophosphonium salt, $(Ph_3PMe)^+(I^-)$, affording the TBS-protected alkenyl alcohol, **117a** (est. ~quantitative yield; not drawn) (Fig. 57).[195,196] Deprotection with TBAF gave free unsaturated alcohol **119** (not drawn; est. ~78% yield), which was subsequently subjected to Appel conditions to give the desired unsaturated primary iodide, **120**, in 59% yield over 3 steps (Appel reaction est. ~75% yield, lit. yield of 69%).[197] The conditions used for this iodination were nearly identical to the literature procedure for this reaction except for the substitution of MeCN/Et_2O as the solvent system (instead of PhH) since previous investigations into the iodination of the similar alcohol, **98** (which possesses an even more electrophile-sensitive alkene), showed promising results with this solvent mixture (see subsection **3.2**).[168]

Alkylation of **100** with the soft electrophile, primary iodide **120**, proceeded to give the monoalkylated product, **118**, in good yield (79%) on a multigram-scale. No issues were encountered with separation of the product from side products, byproducts, or starting material, which was in line with our prediction. Since an epoxyphosphonate similar to **112** was formed by alkene epoxidation with mCPBA in the literature, we used somewhat similar mild conditions to effect the epoxidation of **118** (1.5 d, rt, 1.02 eq mCPBA).[198] Epoxidation was accomplished in excellent yield (98%) to afford **112** in very high purity (Fig. 57).

To render this method enantioselective, the alkene moiety in one of the intermediate species (e.g. **118**) could be oxidatively cleaved (e.g. with O_3; DMS) and the resulting methyl ketone subjected to Shibasaki conditions to (presumably) set the absolute stereochemistry of the epoxide stereocenter with only a minor adjustment to the route.[184,200] Alternatively, the alkyl bromide analogue of electrophile **120** could be synthesized from **119** (via a simple bromide-substitution reaction). This alkenyl bromide is a known compound[201] and has been shown to undergo an enzyme-catalyzed enantioselective epoxidation in the presence of chloroperoxidase (in 58% yield and 95% ee after just 1 h, without further optimization).[202] However, since we wished to tackle the foundational problems of our polycyclizations before probing stereochemical ones, the racemic route detailed above was utilized first.

Figure 58. HWE coupling of fragments **A2** and **B2**

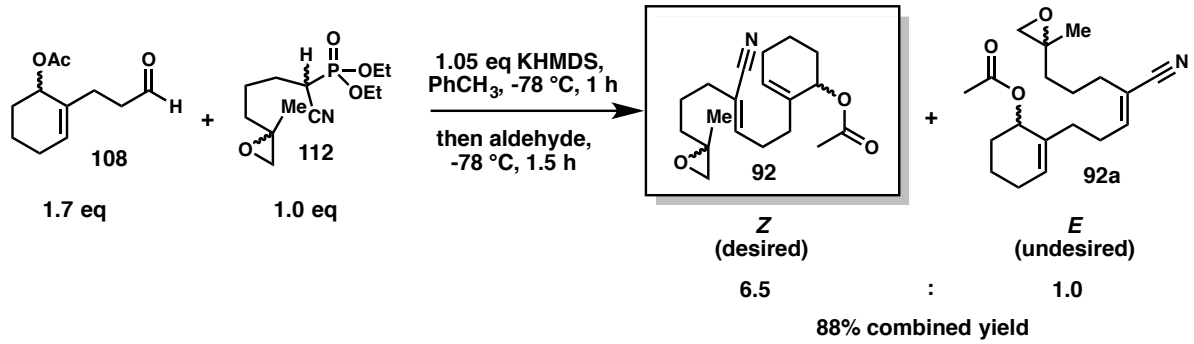

HWE olefination of epoxyphosphonate **112** and the aldehyde-tethered allylic acetate, **108**—following the protocol used most often for analogous (*Z*)-selective HWE reactions—proceeded in good yield (88% combined) and good dr (6.5:1, (*Z*):(*E*)) and provided the desired compound as the major product (Fig. 62). While the yield and dr were slightly lower upon scale-up (87% NMR yield—78% isolated—and 4.1:1 dr on 10-fold scale-up), the larger amount of product was much easier to purify. On a larger scale, the mixture of diastereomers at the chiral centers coeluted and overlapped favorably to allow some separation of (*E*)- and (*Z*)-configured products by flash chromatography (up to 18:1 dr). Thus, the synthesis of the first model system, **92**, was complete (Fig. 58).

The ease of separation of the alkene-tethered phosphonate alkylation product from other species represents a major advantage of this route, enabling a significant increase in alkylation yield. When phosphonate **100** was alkylated with primary iodoalkene **120**, a 74% yield of product **118** was obtained, whereas alkylation with epoxy iodide **111** gave only a ~35% yield (see subsection **3.3**). Furthermore, the former reaction was scaled to multigram-size batches with no change in yield while

scale-up of the latter proved difficult and time-consuming in practice due to the extensive chromatography required for product purification. Of the three routes to fragment **A2**, this 3rd approach was the most reliable, high-yielding, and scalable. This synthesis provided a concise, reproducible path to epoxyphosphonate **112** in 23% overall yield (avg 78% per step) over 6 steps, demonstrating significant further improvement to the previous approach (6% overall yield). Also, importantly, asymmetric epoxidation at some point during substrate synthesis could be used to generate 2,2-disubstituted epoxide stereocenters in high ee, enabling access to either stereochemical configuration of the tetrasubstituted carbon in the epoxide.

While this route served to provide us with usable quantities of the desired epoxyphosphonate, **112**, and the polycyclization substrate, **92**, other variations may be used in the future (such as 2-methallyl Grignard addition to ethylene oxide or ethyl levulinate olefination-reduction to give alkenyl alcohol **120**).[197,201,203] However, the chosen route has proved incredibly useful for accessing racemic mixtures of 2,2-disubstituted epoxide polycyclization precursors and, therefore, will likely serve as a template for other future substrate syntheses.

3.6 Synthesis of aldehydes (fragments B3-B6) and HWE couplings carried out (thus far) to form substrates

While the allylic acetate substrate, **92**, was synthesized as the initial model substrate for Ti(III)-induced radical polycyclization/acetate-elimination, we hoped to also pursue the cationic variant of 2,2-disubstituted epoxypolyene polycyclization with

a suitable corresponding cationic leaving group (e.g. TMS+, $Ph(Me)_2Si$+, etc.) (Fig. 59). We expected the cationic reactivity to in some ways mirror the radical reactivity, resulting in the same regiochemical preference for *6,6,6*-fused tricyclic products—that is, if the polycyclization efficiently proceeded through an intermediate (or transition structure) that possessed an alpha-cyano cation. If the nitrile group is tolerable (i.e. stabilizing or not prohibitively destabilizing towards the carbocation), we planned to glean information about the stereochemical features pertinent to the cationic reaction (see subsection **3.1**).

The nitrile group in alpha-cyano radical intermediates is known to be only somewhat electron-withdrawing, allowing for facile cyclization of these radicals onto alkenes ranging from electron-rich to slightly electron-poor (see subsection **3.1**). In fact, the 6-*endo* mode of addition of tertiary cyclic alpha-cyano radicals have been shown to undergo cyclizations onto mono-, di-, and trisubstituted alkenes.[24,43,44,46,47] In one particularly notable polycyclization, an alpha-cyano radical attacked a slightly electron-poor allylic benzyl ether at the sp^2 carbon gamma to the benzyloxy group (in a 6-*endo*-trig cyclization).[142] This reported cyclization is analogous to the desired final cyclization of **92**, in which the intermediate alpha-cyano radical attacks the somewhat electron-poor alkene of the allylic acetate at the sp^2 carbon gamma to the acetate. Considering this precedence, the ability to accomplish the second (and final) cyclization of **92** may actually be feasible since allylic acetates possess alkenes that are only slightly more electron-poor than allylic benzyl ethers.

Our initial tactic was to generate an analogue of **92** for use as a model substrate for cationic polycyclization, with an allylsilane terminating group. However,

preliminary *radical* polycyclization attempts with the ring-containing substrate, **92**, unfortunately gave undesired results (e.g. epoxide opening, possible monocyclization; see subsection **3.7**). After discovering the difficulties involved with obtaining tricyclic product from **92**—and deliberating on how to bypass these and similar challenges—we embarked on a more simplified approach to continue our investigation into the cyclization chemistries. We chose to pursue simpler model systems with fewer variables in play to explore the fundamentals of both radical and cationic polycyclizations (of 2,2-disubstituted epoxides) more effectively. Reactions of more complex systems could be examined after suitable conditions had been established for more rudimentary substrates.

Fortunately, the simplified structures we planned to construct could potentially be efficiently accessed utilizing the same epoxy phosphonate fragment (**A2**), **112**, that served as a vital coupling partner for the synthesis of the first model system, **92**. Four aldehydes (**121**-**124**) were prepared following literature procedures, with the goal of incorporating each one into the general HWE olefination procedure with fragment **A2** (Fig. 59).[204-207] We hoped this would provide a substrate for each type of polycyclization we intended to study: cationic, radical, and radical-polar crossover. In addition, precedence laid out in the introduction showed that electron-rich (and perhaps even electron-poor) arenes can sometimes, in fact, also serve as radical acceptors when using Ti(III), providing rearomatized products upon oxidation-deprotonation.[158-160] Therefore, arene termination may be a viable option for the radical epoxypolyene polycyclization of **125**.

Figure 59. Simple aldehydes synthesized: fragments **B3**, **B4**, **B5**, and **B6**

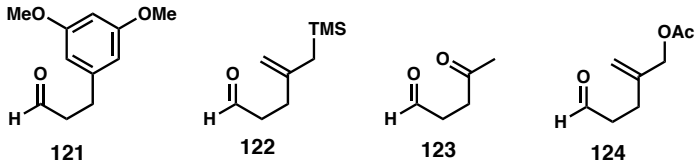

Colleague Darius Vrubliauskas graciously synthesized and provided the arene-tethered aldehyde for use in the HWE coupling.[204] The other three aldehydes were synthesized following literature precedent, as mentioned above.[205-207] However, thus far only three of the above four aldehyde fragments (**121**-**123**) were subjected to HWE coupling conditions (in this case with epoxyphosphonate **112**, fragment **A2**) that were analogous to the previous (*Z*)-selective α,β-unsaturated nitrile syntheses. The fourth aldehyde, **124**, unexpectedly decomposed upon workup of the final (Claisen) reaction. This was presumably caused by drying a solution of the compound (in CH_2Cl_2) with $MgSO_4$ instead of Na_2SO_4, during which the solution turned purple and showed newly formed compounds by TLC and NMR.

Under HWE coupling conditions, aldehyde **121** and fragment **A2** reacted to give an approximate ~2.5:1 ratio of (*Z*)- and (*E*)-diastereomers of α,β-unsaturated nitrile **125**, in an estimated ~81% combined NMR yield (unoptimized, based on [product]:[phosphonate SM] ratio in crude product residue—see SI) (Fig. 60). Both the allylsilane-tethered aldehyde and the ketoaldehyde were also subjected to largely unoptimized HWE olefinations with **112** using similar conditions. The yield for the HWE reaction with aldehyde **122** was 38% (dr 2.9:1, (*Z*):(*E*)), while the yield for the analogous reaction with ketoaldehyde **123** was 77% (dr 2.4:1, (*Z*):(*E*)). Thus, the

synthesis of two more substrates, **126** and **127**, was accomplished. The latter reaction entailed a very chemoselective olefination of the aldehyde (over the ketone).

Figure 60. Preliminary HWE couplings of fragments **A2**-**B3**, **A2**-**B4**, and **A2**-**B5**

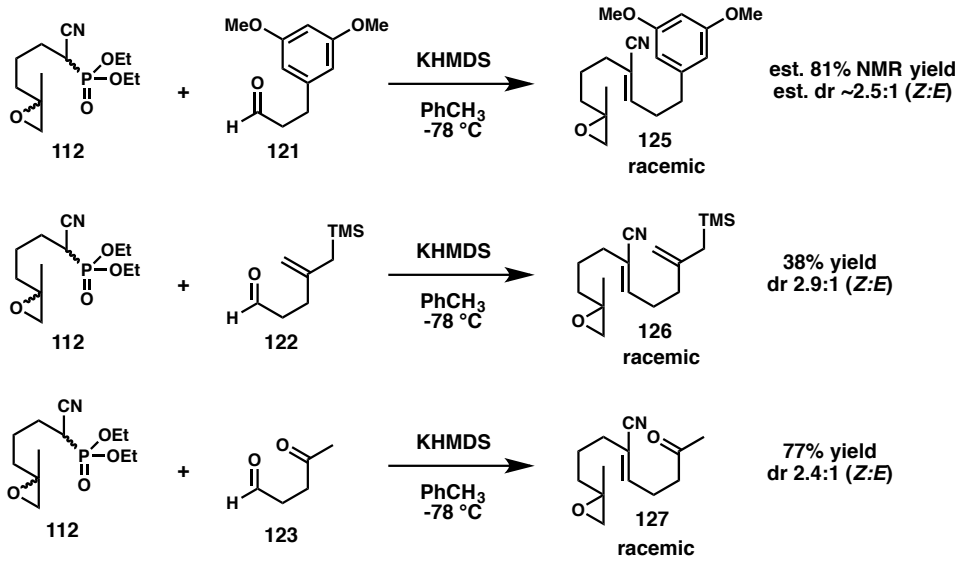

Due to the preliminary nature of our cyclization investigations, the stereoisomers of the substrates were not separated (unless otherwise stated) if flash chromatography failed to afford diastereomerically enriched product, though only major (racemic) diastereomers are depicted as substrates in polycyclization reaction figures. In cases where systems possess two chiral centers (e.g. **92**), a statistical mixture of the RR/SS/RS/SR diastereomers and enantiomers is expected.

Future experiments using these substrates may require either separation of (*E*)- and (*Z*)-isomers or reactions (conditions) that impart higher stereoselectivity. Also, enantio- and diastereoselective transformations that culminate in stereoisomer-

enriched substrates are expected to facilitate the detailed stereochemical analysis of these reactions. Further research into the polycyclization of 2,2-disubstituted epoxides is ongoing in our lab and these substrates may yield insight into the lengths this chemistry can be taken.

3.7 Complex and simple substrates used in initial polycyclization investigations

Most of the efforts reported in this chapter are focused on the synthesis of polycyclization substrates for cationic and radical (including radical-polar crossover) methodologies. However, a few polycyclizations were attempted before the conclusion of this work, and continued experimentation is ongoing in the lab. Given the time constraints, only one substrate for each polycyclization method of interest (radical, cationic, and radical-polar crossover) was able to be briefly investigated thus far under conditions used in the closest analogous reactions.

Figure 61. The control reaction for Ti(III)-mediated radical cyclization

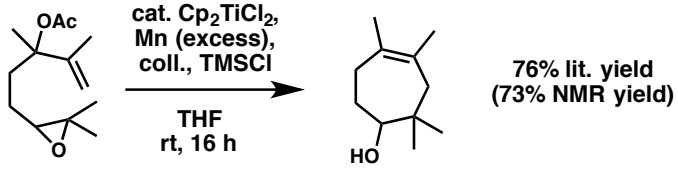

128 129

Due to the highly oxygen-sensitive nature of the Ti(III) species required for radical chemistry, a control reaction was set up to ensure proper technique was being

utilized during these radical cyclization procedures. A simple yet appropriate control substrate was chosen from compounds within Cuerva's report featuring novel Ti(III)-mediated 7-*endo*-trig cyclizations with subsequent (acetate) elimination (Fig. 61).[40] The control substrate employed was easily accessed via literature procedures and had demonstrated the desired reactivity under Cuerva's radical conditions. Thus, we sought this compound for use in a control reaction for confirmation that the radical cyclization-elimination reactions carried out under similar (Ti(III)-mediated) conditions were sufficiently oxygen-free. This was especially crucial since the corrosiveness of TMSCl—which was utilized in some of our conditions—prohibited its introduction into the glovebox, requiring the reaction set-up to be completed outside of the glovebox (under a stream of Ar). Fortunately, on a small scale (12.9 mg), following the literature cyclization procedure afforded the cycloheptenol product, **129**, in 73% NMR yield, which is within 5% of the isolated yield reported (76% lit. yield) This served as confirmation that the technique involved was being properly executed.

Figure 62. Example of attempted polycyclization with complex allylic acetate **92**

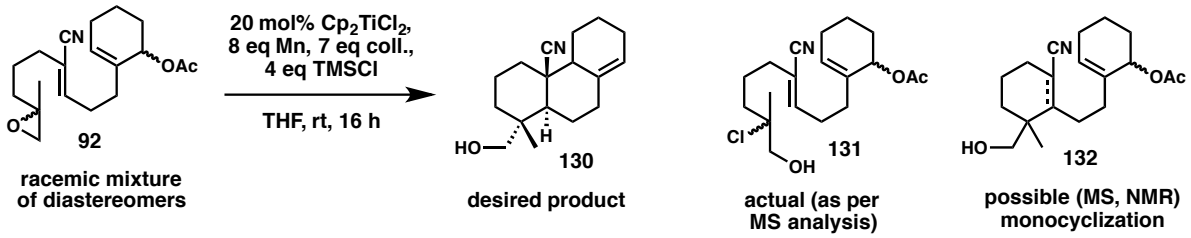

Several attempts to achieve radical polycyclization of the first model system, **92**, were carried out under conditions known to work for systems with similar scaffolds

(Fig. 62). However, upon subjecting **92** to these conditions,[40,41,146,147,149,208] a number of problems were encountered and a complex assortment of compounds were observed in the crude product material. These products and side products could not be sufficiently separated to enable full characterization, but mass spectrometry and ^{1}H-NMR analysis of the crude product mixture indicated that issues of chlorinative opening of the epoxide, monocyclization, and possibly allylic alcohol formation contributed to the lack of desired polycyclization products observed. As mentioned in subsection **3.6**, we then chose to pursue simpler, more manageable polycyclization precursors, through which productive processes could be more easily discerned.

Continuing our pursuit of the polycyclization of 2,2-disubstituted epoxides via the unsaturated nitrile moiety, we chose to undertake a cationic approach. Using substrate **126**, in combination with Lewis acids, we set forth to attempt the cationic polycyclization of this scaffold.

Figure 63. Attempted polycyclization of **126** under Lewis acidic conditions

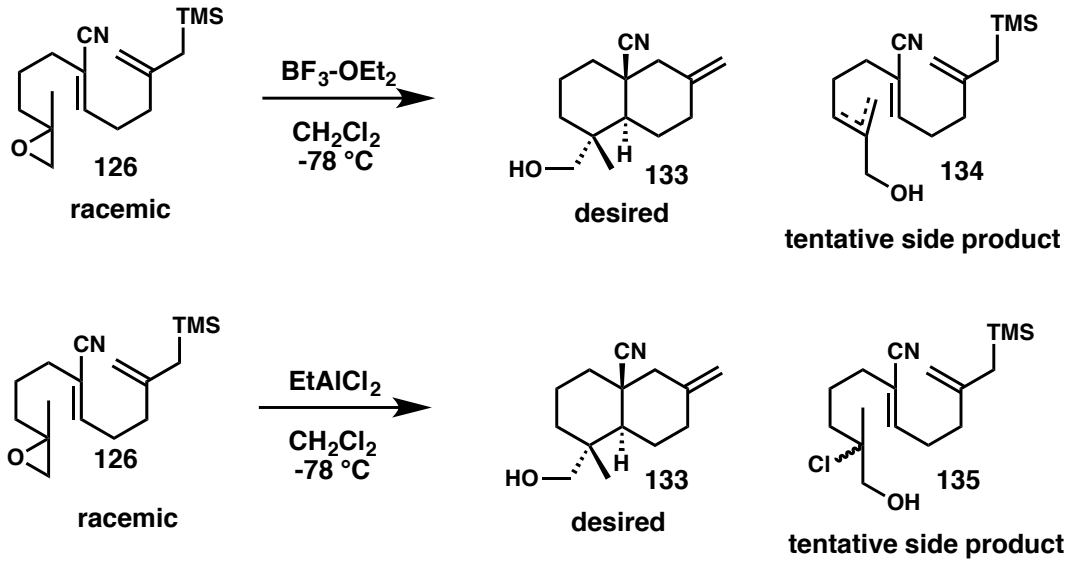

Two different Lewis acids were utilized in the attempted polycyclization of **126**, $EtAlCl_2$ and BF_3-OEt_2 (Fig. 63). These were chosen by surveying the literature for suitable Lewis acids that were capable of enabling the cationic polycyclization of 2,2-disubstituted epoxypolyenes without substantial rearrangement at the epoxide moiety. Since only three examples are known for 2,2-disubstituted epoxide substrates,[28,29,31] we chose to first attempt to initiate the transformation with a Lewis acid that has given encouraging results in literature reactions of other epoxypolyenes with allylsilane terminating groups.[148] The reaction of **126** and $EtAlCl_2$ mostly afforded returned starting material and epoxide degradation (likely chlorinative opening). With the hope of avoiding the chlorinative opening of the epoxide, BF_3-OEt_2 was employed next. Again, however, nonproductive epoxide opening occurred, along with a multitude of other side reactions, ultimately giving an intractable mixture of compounds.

Finally, the radical-polar crossover polycyclization was attempted with substrate **127**. This reaction was carried out under the same conditions used in Cuerva's paper on ketoepoxypolyenes, in which he reported the successful 1,4-addition of a β-titanoxy radical to an α,β-unsaturated ketone, followed by a 5-(enolexo)-*exo*-trig aldol addition in the second cyclization. Also, our substrate was similar to the singular literature example of this type of polycyclization. Using catalytic Ti(III) (formed *in situ*) to cyclize **127**, we indeed obtained encouraging results (Fig. 64). The major product (proposed to be **136**) was significantly more polar than the starting material and, upon isolation, was found to possess ^{1}H- and ^{13}C-NMR peaks that were consistent with a

6,5-fused carbocyclic aldol product (also, with no epoxide and olefin peaks). Since only a small amount of substrate was used in the reaction, though, and the isolated yield was 18%, very little product was obtained, making further (stereochemical) analysis difficult. However, the presence of ^{1}H-NMR peaks alpha to the (primary) alcohol at 3.58 ppm and 3.98 ppm—about 0.50 ppm higher than equatorial hydroxymethylene groups should be—suggests either an axial hydroxymethylene group (in the deshielding cone[43] of the axial nitrile), or perhaps even intramolecular lactonization onto the nitrile to give a tricyclic product. The former appears more likely though, since analogous lactone protons are generally more downfield (4.0-4.5 ppm) than the observed methylene chemical shifts (3.58, 3.98 ppm). Additionally, the two methyl group ^{1}H-NMR peaks were observed at 0.89 ppm and 1.55 ppm, a finding which is consistent with a respective correlation to the α-methyl group on the 6-membered ring and the α-methyl group on the 5-membered ring. The latter methyl group would likely be downshifted significantly (~1.81 ppm) if it were on the same face of the ring system as the nitrile, since it would be in closer proximity to the deshielding cone of that moiety.[209] Therefore, from the data currently available, we propose **136** as the major diastereomer formed in this polycyclization.

Figure 64. Simple epoxy ketone **127** in radical-polar crossover polycyclization

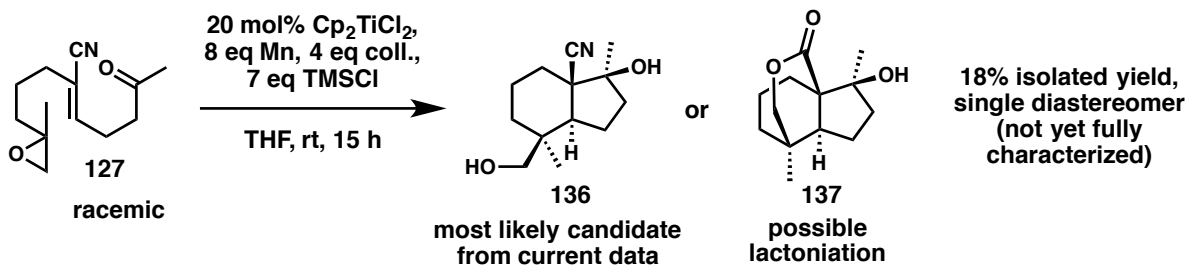

3.8 Future directions

The next step will likely be to scale up the polycyclization of **127**, with the goal of definitively discerning the stereochemistry of the diastereomer obtained. Upon optimization of this protocol, we hope to determine the elements of this reaction that are important regarding the yield and stereochemical outcome. Additionally, we plan to expand this method to encompass the polycyclization of substrates that form 6,6-fused systems and more fused ring systems (e.g. tricyclic products, etc.).
Also, other functional handles besides nitriles may be investigated for use in cationic cyclization chemistry.

References

1. *Infect. Dis. Rep*. **2009**, *11* (1), 59–65.
2. *J. N. Engl. J. Med*. **2009**, *361* (5), 455-467.
3. *J. Med. Chem*. **2001**, *44* (6), 873–885.
4. *J. Am. Chem. Soc.* **2016**, *138* (23), 7268–7271.
5. *Nat. Prod. Rep*. **2015**, *32* (4), 543–577.
6. *Mar. Drugs* **2016**, *14* (1), 16, 1-83.
7. *Org. Lett*. **2014**, *16,* 4368–4371.
8. *J. Am. Chem. Soc*. **2015**, *137*, 4912–4915.
9. *Chem. Int. Ed.* **2016**, *55*, 7180–7183.
10. *ACS Med. Chem. Lett.* **2017**, *8*, 355–360.
11. *J. Org. Chem.* **2017**, *82*, 4533–4541.
12. *J. Org. Chem.* **2017**, *82*, 13313–13323.
13. *J. Am. Chem. Soc*. **2012**, *134*, 19604–19606.
14. *J. Am. Chem. Soc*. **1974**, *96* (17), 5563-5565.
15. *Chem. Rev.* **2005**, *105* (12), 4730–4756.
16. *Tetrahedron* **1968**, *24* (2), 859-876.
17. *Nat. Prod. Rep*. **2015**, *32* (6), 841-864.
18. *Angew. Chem. Int. Ed.* **1976**, *15* (1), 9–17.
19. *Tetrahedron Lett*. **1985**, 26, (3), 343-346.
20. *Acc. Chem. Res.* **1971**, *4* (11), 386-392.
21. *J. Am. Chem. Soc.* **2010**, *132* (40), 14303-14314.

22. *Chirality* **2013**, *25*, 692–700.

23. *J. Org. Chem*. **2005**, *70* (21), 8265–8272.

24. *J. Am. Chem. Soc.* **2010**, *132* (14), 5027-5029.

25. *J. Org. Chem.* **1998**, *63* (21), 7213–7217.

26. *Eur. J. Org. Chem.* **2006**, *2006* (7), 1627-1641.

27. *Org. Lett*. **2010**, *12* (15), 3548-3551.

28. *Nat. Prod. Rep.* **2011**, *28* (6), 1035–1053.

29. *Chem. Rev.* **2006**, *106* (8), 3142–3442.

30. *Bioorg. Chem*. **1976**, *5* (1), 51-98.

31. *J. Am. Chem. Soc.* **1969**, *91* (21), 5862-5870.

32. *J. Org. Chem. Front*. **2014**, *1* (4), 373-381.

33. *J. Org. Chem*. **2009**, *74* (16), 6151-6156.

34. *J. Org. Chem*. **2012**, *77* (1), 341-350.

35. *Chem. Soc. Rev.* **2011**, *40*, 3525-3537.

36. *J. Am. Chem. Soc*. **2014**, *136* (19), 6943-6951.

37. *J. Org. Chem*. **2002**, *67* (8), 2566-2571.

38. *Chem. Eur. J.* **2004**, *10* (7), 1778-1788.

39. *Tetrahedron* **2009**, *65* (52), 10837-10841.

40. *Chem. Soc. Rev.* **2011**, *40*, 3525–3537.

41. *Chem. Eur. J.* **2013**, *19* (43), 14484-14495.

42. *Org. Chem. Front*. **2014**, *1*, 15-33.

43. *Tetrahedron Lett*. **1996**, *37* (11), 1751-1754.

44. *Tetrahedron Lett*. **1996**, *37* (44), 7909-7912.

45. *J. Am. Chem. Soc.* **1967**, *89* (25), 6794-6796.

46. *Tetrahedron Lett.* **1994**, *35* (10), 1581-1584.

47. *J. Org. Chem*. **1998**, *63* (4), 1162-1167.

48. *Malar. J*. **2015**, *14*, 265.

49. *Soc. Sci. Med*. **2008**, *67*, 854-862.

50. *J. Trop. Med. Int. Health* **2008**, *13*, 771-783.

51. *Pathogens* **2019**, *8* (1), 11.

52. *Ann. N.Y. Acad. Sci*. **2008**, *1136* (1), 32–37.

53. *Infect. Dis.* (4th Ed.) **2017**, *2*, 1345-1372.

54. *Malar. J.* **2011**, *10*, 144.

55. *J. Clin. Pharmacol.* **2006**, *46* (12), 1487-1497.

56. *Pharmacol. Rev.* **2005**, *57* (1), 117-145.

57. *Science*. **2015**, *347* (6220), 428-31.

58. *Malar. J.* **2014**, *13*, 284.

59. *PLoS ONE* **2009**, *4* (2), e4551.

60. *Nature* **2012**, *484*, S16-S18.

61. *N Engl J Med*. **2014**, *371* (5), 411-423.

62. *N. Engl. J. Med*. **2011**, *365* (12), 1073–1075.

63. *Bioorg. Med. Chem*., **2012**, *20* (1), 279–282.

64. *J. Am. Chem. Soc*. **1987**, *109* (20), 6119–6123.

65. *Tetrahedron* **2004**, *60* (33), 6981–6988.

66. "Isonitrile Chemistry" Academic Press. New York, 1971, p. 1-278.

67. *J. Nat. Prod*. **1996**, *59* (7), 710–716.

68. *Pharmaceuticals* **2011**, *4*, 681-712.

69. *J. Infect. Dis*. **2001**, *184* (6), 770-776.

70. *J. Nat. Prod*. **1992**, *55* (12), 1787–1789.

71. *J. Org. Chem*. **1996**, *61*, 3259–3267.

72. *Aust. J. Chem*. **1997**, *50*, 1123–1127.

73. *Tetrahedron* **1998**, *54*, 13467– 13474.

74. *Bioorg. Med. Chem. Lett*. **2002**, *12*, 2277–2279.

75. *Tetrahedron Lett*. **2002**, *43*, 1009–1013.

76. *Org. Biomol. Chem*. **2011**, *9*, 400–407.

77. *J. Nat. Prod*. **2012**, *75* (4), 789–792.

78. *J. Med. Chem*. **2013**, *56*, 5231–5246.

79. *Life Sci.* **2007**, *80* (9) 813-828.

80. *Eur. Journ. Med. Chem.* **2015**, *93* (26), 373-380.

81. *Nat. Prod. Rep*. **2004** , *21*, 164–179.

82. *Nat. Prod. Rep*. **1988**, *5*, 229.

83. *PLoS Comput. Biol.* **2009**, *5* (4), e1000339.

84. *Gr. J. Epidem. Pub. Health* **2019** *7* (1), 1-5.

85. *Annu. Rev. Microbiol*. **2009**, *63*, 195–221.

86. *PLoS Med*. **2012**, *9*, e1001169.

87. *Liebigs Ann. Chem*. **1986**, *1*, 78-92.

88. *Org. Lett*. **2005**, *7* (8), 1649-1651.

89. *Org. Lett*. **2012**, *14* (20), 5169-5171.

90. *Synlett* **2011**, *4*, 547–550.

91. *J. Nat. Prod*. **2012**, *75* (4), 793.

92. *Tetrahedron Lett*. **2002**, *43* (10), 1793-1795.

93. *Synthesis* **2016**, *48* (11), 1573-1596.

94. *ACS Catal*. **2015**, *5* (11), 6828-6837.

95. *Eur. J. Org. Chem*. **2008**, *7*, 1214-1223.

96. *J. Organomet. Chem*. **1990**, *385*, 147-152.

97. *Tetrahedron Lett.* **1980**, *21* (3), 315-318.

98. *Chem. Pharm. Bull*. **2011**, *59* (12), 1494-1508.

99. *Tetrahedron Lett.* **1994**, *35* (10), 1584.

100. *Synthesis* **2003**, *9*, 1324–1328.

101. *Tetrahedron* **2013**, *69*, 3141-3148.

102. *J. Org. Chem*. **2014**, *79*, 7477–7490.

103. *Helv. Chim. Acta* **1990**, *73*, 922-931.

104. *Tetrahedron* **1992**, *48* (15), 3121-3130.

105. *Org. Lett.* **2008**, *10* (18), 4049-4052.

106. *J. Am. Chem. Soc*. **1979**, *101* (23), 6996-7000.

107. *J. Am. Chem. Soc.* **2016**, *138* (45), 14864–14867.

108. *Org. Lett*. **2007**, *9* (2), 375–378.

109. *J. Am. Chem. Soc*. **1987**, *109*, 1287-1289.

110. *Angew. Chem., Int. Ed*. **2007**, *46*, 4708.

111. *J. Am. Chem. Soc.* **2016**, *138* (45), 14864–14867.

112. *Chem. Rev*. **1989**, *89*, 1841-1860.

113. *J. Am. Chem. Soc.* **2018**, *140*, 4977–4981.

114. *J. Chem. Soc., Chem. Commun*. **1972**, *6*, 354-355.

115. *Tetrahedron Lett*. **1973**, *47*, 4691 – 4694.

116. *J. Am. Chem. Soc*. **1977**, *99* (16), 5453-5461.

117. *J. Org. Chem*. **1997**, *62* (21), 7094-7095.

118. "Organic Chemistry: A Series of Monographs." Volume 37, 1978, p. 221-251.

119. *J. Am. Chem. Soc.* **2002**, *124*, 9812-9824.

120. *J. Org. Chem*. **1996**, *61* (6), 2215-2218.

121. *Chem. Lett.* **1978**, *7* (11), 1243-1244.

122. *Chem. Lett.* **1979**, *8* (9), 1081-1084.

123. *Synthesis* **1987**, *3*, 267-270.

124. *Can J. Chem*. **2005**, *61* (24), 5788-5796.

125. *J. Am. Chem. Soc*. **1992**, *114*, 8751-8752.

126. *Can. J. Chem.* **1996**, *74*, 1480-1489.

127. *J. Org. Chem*. **2005**, *70*, 8431-8436.

128. *Can. J. Chem.* **1997**, *75*, 1264-1280. And also

Polyhedron **2010**, *29* (9), 2035 – 2040.

129. *Chem. Ber*. **1972**, *105* (11), 3532-3541.

130. *Tetrahedron* **2000**, *56* (52), 10101 – 10111.

131. *Org. Lett*. **2013**, *15* (16), 4074-4077.

132. *J. Am. Chem. Soc*. **1955**, *77* (19), 5068-5077.

133. *Helv. Chim. Acta* **2005**, *88*, 3011-3050.

134. *Tetrahedron* **1985**, *41* (19), 3925-3941.

135. *J. Org. Chem.* **1987**, *52* (6), pp 959–974.

136. *Acc. Chem. Res.* **1991**, *24* (5), 139–145.

137. *J. Am. Chem. Soc*. **1977**, *99* (25), 8341-8343.

138. *J. Am. Chem. Soc*. **2015**, *137*, 5837-5844.

139. *J. Am. Chem. Soc*. **1999**, *121* (20), 4894-4895.

140. *Nat. Commun*. **2015**, *6* (6096), 1-8.

141. *J. Am. Chem. Soc.* **1996**, *118* (47), 11982–11983.

142. *Tetrahedron* **2017**, *73* (16), 2316-2322.

143. *Tetrahedron Lett*. **1991**, *32* (48), 7005-7008.

144. *J. Am. Chem. Soc*. **2017**, *139*, 11158–11164.

145. *Org. Lett*. **2016**, *18* (2), 268-271.

146. *Synlett* **2007**, *17*, 2718 – 2722.

147. *Eur. J. Org. Chem*. **2011**, *2011* (26), 5002-5011.

148. *Chem. Eur. J*. **2015**, *21*, 17605–17609.

149. *Tetrahedron* **2006**, *62* (22), 5215-5222.

150. *Synthesis* **2010**, *1*, 67–72.

151. *J. Nat. Prod.* **2019**, *82* (1), 9–15.

152. *J. Am. Chem. Soc*. **1964**, *86*, 1959.

153. *Chem. Commun*. **1999**, 325–326.

154. *Angew. Chem. Int. Ed*. **2013**, *52* (34), 9019-9022.

155. *J. Am. Chem. Soc.* **1988**, *110* (25), 8561–8562.

156. *J. Am. Chem. Soc.* **1989**, *111* (12), 4525–4527.

157. *J. Am. Chem. Soc*. **1989**, *111*, 1759.

158. *Angew. Chem. Int. Ed*. **2012**, *51* (19), 4739-4742.

159. *Chem. Eur. J*. **2015**, *21* (1), 280-289.

160. *Dalton Trans*. **2016**, *45* (2), 448-452.

161. *J. Org. Chem*. **1978**, *43* (20), 3878-3882.

162. *J. Am. Chem. Soc.* **1980**, *102* (11), 3957–3959.

163. *J. Phys. Chem. A* **2002,** *106* (44), 10681-10690.

164. *Chem. Rev.* **1991** *91* (8), 1625-1678.

165. *J. Am. Chem. Soc*. **1998**, *120* (49), 12849-12859.

166. *Arkivoc* **2014**, *2014* (3), 287-296.

167. *J. Org. Chem.* **1997**, *62* (4), 784–785.

168. *J. Chem. Soc., Perkin Trans. 2*, **2001**, *9*, 1785-1792.

169. *Tetrahedron* **2004**, *60* (37), 8093 – 8102.

170. *J. Am. Chem. Soc.* **1997**, *119* (38), 8777–8787.

170. *Bioorg. Med. Chem.* **2015**, *23* (13), 3687 – 3695.

171. *Molec. Pharmacol*. **2015**, *87* (3), 477 – 491.

172. *Synth. Commun*. **2004**, *34* (5), 871 – 888.

173. *Tetrahedron Asym*. **2010**, *21* (3), 346 – 351.

174. *J. Am. Chem. Soc.* **1978**, *100* (7), 2252-2254.

175. *J. Am. Chem. Soc.* **2016**, *138* (32), 10344–10350.

176. *J. Org. Chem*. **1999**, *64* (20), 7675-7677.

177. *J. Am. Chem. Soc.* **1987**, *109* (25), 7925–7926.

178. *J. Am. Chem. Soc.* **1973**, *95* (2), 512-519.

179. *Nat. Protoc*. **2007**, *2* (10), 2451–2458.

180. *Org. Lett.* **2011**, *13* (13), 3514-3517.

181. *J. Am. Chem. Soc*. **1993**, *115* (23), 11028-11029.

182. Nelson, R. V. ICI Americas Inc., 2-Piperidones, US4504664A, **1985**.

183. *J. Med. Chem.* **2008**, *51* (19), 6220-6224.

184. *Molecules* **2012**, *17* (2), 1617-1634.

185. *J. Chem. Soc., Perkin Trans. 1*, **2001**, *21*, 2861-2873.

186. *Synlett* **2019**, *30* (2), 181–184.

187. *J. Chem. Soc. Perkin Trans. 1*, **1996**, *8*, 793 – 802.

188. *Eur. J. Org. Chem*. **2000**, *22*, 3703 – 3711.

189. *Tetrahedron* **2012**, *68* (4), 1253-1261.

190. *J. Org. Chem.* **2008**, *73* (2), 726–729.

191. *Org. Lett.* **2004**, *6* (2), 161–164.

192. *J. Am. Chem. Soc.*, **1963**, *85* (22), 3533–3539. Also, see

J. Chem. Soc (Res.). **1965**, 6753–6761.

193. Smith, March. *Advanced Organic Chemistry* 6th ed. (501-502).

194. *J. Org. Chem.* **1994**, *59* (15), 4172–4178.

195. *Rec. Trav. Chim.* **1985**, *104* (11), 281 – 288.

196. *Org. Lett.* **2005**, *7* (24), 5531–5533.

197. *Eur. J. Org. Chem*. **1999**, *1999* (5), 1201-1211.

198. *J. Am. Chem. Soc.* **2016**, *138* (32), 10344–10350.

199. *Org. Lett.* **2004**, *6* (2), 161–164.

200. *J. Am. Chem. Soc*. **2008**, *130*, 10078–10079.

201. *J. Org. Chem*. **1983**, *48* (18), 2981-2989.

202. *J. Am. Chem. Soc*. **1997**, *119* (2), 443-444.

203. *J. Am. Chem. Soc.* **1981**, *103* (1), 82-87.

204. *Synth. Commun*. **2002**, *32* (11), 1751 – 1756.

205. *Tetrahedron* **1989**, *45* (18), 5877-5886.

206. *J. Org. Chem.* **1990**, *55* (13), 4144–4153.

207. *Angew. Chem. Int. Ed*. **2016**, *55* (10), 3509 – 3513.

208. *Synlett* **1998**, *1998* (8), 801-809.

209. *J. Org. Chem.* **1968**, *33* (7), 2801-2804.

210. *Chem. Eur. J*. **2018**, *24* (33), 8325 – 8330.

211. *J. Am. Chem. Soc*. **2012**, *134* (39), 16111 – 16114.

212. *Tetrahedron Lett*. **2009**, *50* (10), 1097 – 1099.

213. *J. Org. Chem*. **1991**, *56* (3), 1094-1098.

Appendix A: Experimental Details

Synthesis of monoprotected diol 8

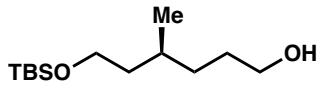

8

Ozone from a generator was bubbled through a solution of the alkene **31** (100.2 mg, 0.3704 mmol, 1.00 equiv.) in dichloromethane and EtOH (1:1; 4.0 mL) at −78 °C for approximately 1 minute until the solution turned blue, indicating all alkene has reacted and excess ozone is present. Oxygen was then bubbled through the solution at −78 °C until the blue color disappeared. Solid sodium borohydride (37.8 mg, 2.03 mmol, 5.00 equiv.) was added at −78 °C, and the reaction mixture was allowed to warm to room temperature and stirred for 3 h. After concentration under reduced pressure, the residue was partitioned between saturated aqueous sodium hydrogen carbonate and Et_2O. The organic layer was washed with brine (20 mL), dried (Na_2SO_4) and concentrated under reduced pressure. Chromatography of the residue eluting with 30% Et_2O in hexanes gave the monoprotected diol **8** (60.6 mg, 0.246 mmol, 66%) as a colorless oil.

Synthesis of alkyl chloride 33

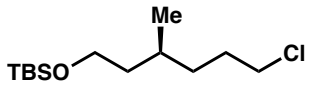

33

To a solution of monoprotected diol **8** (56.5 mg, 0.23 mmol, 1.0 equiv.) in pyridine (37 μL, 0.46 mmol, 2.0 equiv.) and CH_2Cl_2 (1.20 mL) at −78 °C was added a solution of $SOCl_2$ (83 μL, 1.14 mmol, 5.0 equiv.) and pyridine (157 μL, 1.95 mmol, 8.5 equiv.) in CH_2Cl_2 (1.20 mL) via PTFE cannula over 20 minutes with rapid stirring. The reaction mixture was stirred 2 h then quenched at −78 °C with saturated aqueous $NaHCO_3$. The resulting mixture was flooded with water then extracted with 1:1 hexanes:EtOAc (3 x 10 mL), and the combined organic layers were dried over Na_2SO_4, and concentrated to give primary alkyl chloride **33** (62.2 mg, 0.23 mmol, quant.) as a clear, colorless oil: ^{1}H NMR (500 MHz, $CDCl_3$) δ: 4.01 (1H, m), 3.90 (1H, m), 3.60 (2H, m), 1.76-1.51 (4H, m), 1.42-1.28 (2H, m), 1.21 (1H, m), 0.89 (3H, d, *J* = 6.5 Hz), 0.88 (9H, s), 0.04 (6H, s).

Synthesis of tosylate 34

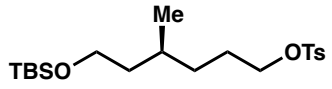

34

To a stirred solution of alcohol **8** (99.3, 0.403 mmol, 1.00 equiv.) in pyridine (1.86 mL) was added p-toluenesulfonyl chloride (192.2 mg, 1.01 mmol, 2.50 equiv.) at 0 °C. After stirring for 2 h at rt, H_2O (10 mL) and Et_2O (10 mL) were added and the organic layer separated. The ethereal layer was washed with 1 N HCl (10 mL), saturated aqueous

$NaHCO_3$ solution (10 mL), and brine (15 mL). The organic layer was dried (Na_2SO_4), filtered, and concentrated. Filtration of the residue over a short pad of silica gel (10% EtOAc in petroleum ether) and evaporation of the solvent gave the pure tosylate **34** as a colorless oil (90.6 mg, 0.226 mmol, 55% yield).

Synthesis of alkyl iodide 35

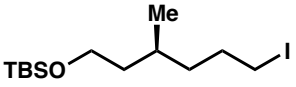

35

A solution of tosylate **34** (40.3 mg, 0.101 mmol, 1.00 equiv.) and NaI (30.2 mg, 0.201 mmol, 2.00 equiv.) in acetone was heated to reflux under Ar (1.5 h) until TLC showed complete consumption of starting material **34**. After cooling to rt, saturated aqueous NaS_2O_3 was added and the mixture was extracted with hexanes (3 x 10 mL), dried (Na_2SO_4), and concentrated to give primary alkyl iodide **35** as a clear colorless oil in high purity without the need for purification (33.9 mg, 0.095 mmol, 95%).

Representative Diels-Alder procedure (screening)

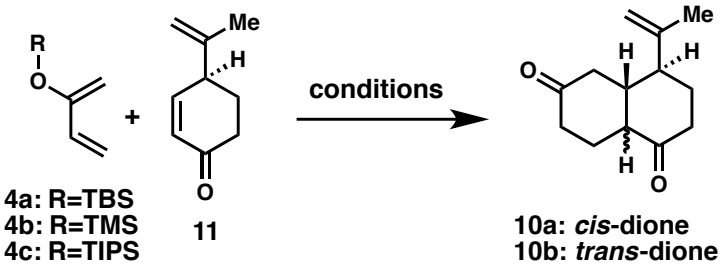

To a solution of enone **11** (13.6 mg, 0.100 mmol, 1.0 equiv.) in 0.50 mL CH_2Cl_2 at 0 °C was added Lewis acid ($EtAlCl_2$, 25 wt% in hexanes, 0.027 mL, 0.05 mmol, 0.5 equiv.)

dropwise. Next a solution of diene **4a** (30.0 mg, 0.13 mmol, 1.3 equiv.) in 0.1 mL CH_2Cl_2 was added over 3 minutes. The solution was stirred under Ar and let warm to rt. After 4 hours (or TLC showed consumption of starting material), the reaction mixture was cooled to -78 °C and quenched slowly with saturated aqueous $NaHCO_3$. The resulting mixture was stirred vigorously and gradually warmed to rt with venting. The aqueous layer was extracted with Et_2O (3 x 20 mL), dried ($MgSO_4$), and concentrated. The residue was subjected to column chromatography. However, no product was isolated by this method.

Synthesis of *trans*- and cis-diones 10a and 10b

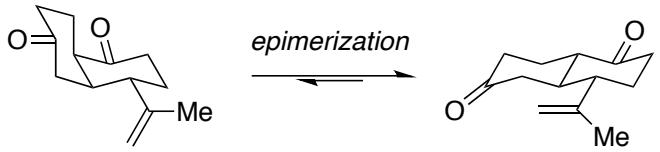

10a **10b**

Representative procedure for 10b

Part A: To a flame-dried 25-mL RBF and stir bar was added enone **11** (272.4 mg, 2.00 mmol, 1.00 equiv.) and diene **4a** (0.60 mL, 479.3 mg, 2.60 mmol, 1.30 equiv.). The flask was capped and sealed with a rubber septum and purged with Ar. Next, dry CH_2Cl_2 was added (8.3 mL) via syringe under Ar and the solution was cooled to -78 °C and kept under a balloon of Ar. To the cooled solution was added a dropwise solution of $HNTf_2$ in CH_2Cl_2 (2.00 mL 0.10 M, 0.20 mmol, 0.10 equiv.) over 5 minutes. The solution was stirred at -78 °C for 3 hours then warmed to -55 °C for 10 minutes followed by gradual quenching with dry Et_3N (0.5 mL) and warming to rt. The solution

was then passed through a short pad of pH 7 silica, washed with CH_2Cl_2, and concentrated to give 664.4 mg of a crude mixture of *cis*-dione **10a,** *trans*-dione **10b,** and *cis*-TBS-silyl enol ether, and multiple side products as a clear oily foam.

Part B: To the crude mixture in a 50-mL flame-dried, vacuum-cooled RBF with a stir bar was added dioxane (24 mL) then aqueous HCl (2.00 mL 12.0 M HCl diluted with 12.0 mL H_2O, 24.0 mmol) over 10 minutes at rt. The mixture was stirred vigorously overnight (18 h) then quenched slowly with saturated $NaHCO_3$ (35.0 mL) and extracted with Et_2O (3 x 35 mL), washed with saturated $NaHCO_3$, then filtered through a fritted funnel with $MgSO_4$/silica and concentrated. The residue was taken up in MeCN, filtered through Celite, and concentrated in order to remove nonpolar silyl impurities. Dry loading on a wide column of silica (140 g) with subsequent flash chromatography (22.5%-30% Et_2O/Hexanes) gave impure *trans*-dione **10b** as a white oily solid (86.7 mg). Further purification by recrystallization in hexanes/CH_2Cl_2 gave (71.3 mg, 0.346 mmol, 17% yield) *trans*-dione **10b** as thin colorless needles: ^{1}H NMR (500 MHz, $CDCl_3$) δ: 4.84 (1H, m), 4.81 (1H, s), 2.58-2.22 (8H, m), 2.10 (1H, dd, *J* = 15.4, 13.1 Hz), 2.02 (1H, dq, *J* = 13.9, 3.8 Hz), 1.83 (2H, m), 1.70 (1H, tdd, *J* = 14.0, 12.0, 4.2), 1.62 (3H, m); ^{13}C NMR (125 MHz, $CDCl_3$) δ: 209.6, 209.5, 144.6, 113.4, 51.95, 51.92, 46.3, 45.5, 41.1, 40.1, 31.8, 25.1, 18.3.

Procedure for 10a

Following Part A of the above procedure (utilizing 0.20 mmol enone **11**), the *cis*-dione **10a** was obtained as a mixture with *cis*-TBS-silyl enol ether by rapid column chromatography (10-30% Et_2O/Hexanes) of the crude mixture. This silyl ether quickly

hydrolyzed in $CDCl_3$, likely due to residual water and acid present in the solvent, and the resulting TBSOH was removed by dissolving the crude mixture in MeCN and filtering through Celite to give partially purified *cis*-dione **10a** (3.0 mg) as a clear, colorless oil (further chromatography led to epimeriation to the *trans*-dione **10b**): ^{1}H NMR (500 MHz, $CDCl_3$) δ: 4.95 (1H, m), 4.87 (1H, s), 2.90 (1H, dt, *J* = 9.6, 4.8 Hz), 2.58 (1H, m), 2.54-2.46 (2H, m), 2.44-2.27 (6H, m), 2.00 (1H, dq, *J* = 14.2 Hz, 4.9 Hz), 1.94-1.85 (2H, m), 1.70 (3H, m); ^{13}C NMR (125 MHz, $CDCl_3$) δ: 212.4, 209.8, 144.9, 113.3, 49.1, 44.1, 43.9, 42.1, 39.7, 37.8, 29.4, 26.0, 19.8.

Synthesis of aldehyde 30a

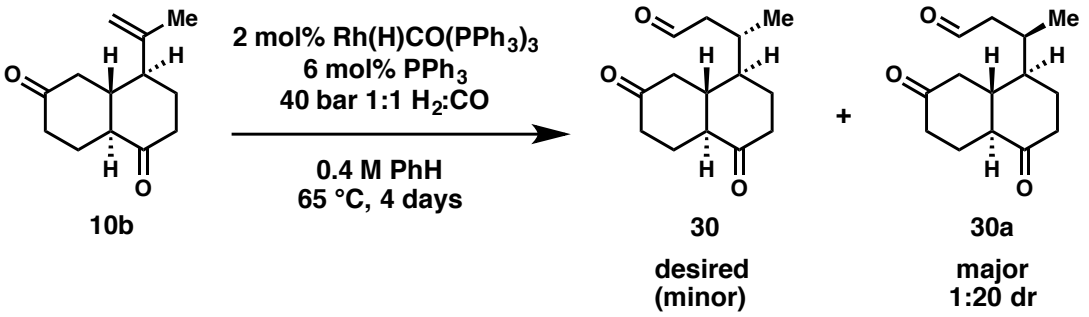

To a 100-mL Parr hydrogenator, was added a ½-dram vial that was equipped with a stir bar and had been charged with a mixture of $RhH(CO)(PPh_3)_3$ (0.7 mg, 8 μmol, 0.02 equiv.), PPh_3 (0.6 mg, 24 μmol, 0.06 equiv.), PhH (0.10 mL), and *trans*-dione **10b** (8.5 mg, 41.2 μmol, 1.0 equiv.). The bomb was sealed, pressurized to 40 bar with 1:1 H_2:CO, and heated to 65 °C. The reaction mixture was removed from heat and pressure after 4 days, but only ~15% conversion was observed. Chromatography on silica with 10-50% EtOAc afforded 2.1 mg diketoaldehyde **30a** (contaminated with PPh_3, ~15% yield).

^{1}H NMR (500 MHz, $CDCl_3$) δ: 9.74 (1H, d, *J* = 2.6 Hz), 2.67 (1H, br ddd, *J* = 13.4, 3.4, 2.0 Hz), 2.43-2.55 (5H, m), 2.27-2.39 (4H, m), 2.11-2.17 (2H, m) 1.77 (2H, d, *J* = 9.9 Hz), 1.63-1.74 (2H, m), (3H, d, *J* = 6.9 Hz); ^{13}C NMR (125 MHz, $CDCl_3$) δ: 209.4, 209.1, 201.2, 52.0, 47.6, 45.5, 45.3, 44.4, 41.1, 40.0, 29.7, 26.3, 25.1, 19.1.

Synthesis of (racemic) oxadiazoline primary allylic ether 66

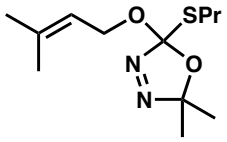

66

To a solution of 3-methyl-2-buten-1-ol **65** (43.1 mg, 0.50 mmol, 1.0 equiv.) and TsOH-H_2O (9.5 mg, 0.050 mmol, 0.10 equiv.) in CH_2Cl_2 (0.5 mL) at was added a solution of oxadiazoline acetate **64** (345.5 mg, 1.50 mmol, 3.0 equiv.) in CH_2Cl_2 (0.50 mL), rinsed with CH_2Cl_2 (0.25 mL). The reaction mixture was stirred at rt until completion (rt, 8 h, shown by NMR of aliquot), then poured directly onto silica (~12 g) and eluted with 1-4% Et_2O/hexanes. Concentration of fractions containing product afforded desired oxadiazoline ether **66** (115.8 mg, 0.426 mmol, 85% yield, ~95% pure) as a clear, colorless oil, contaiminated slightly with irremovable TsOH (~6 mol%): ^{1}H NMR (500 MHz, $CDCl_3$) δ: 5.34 (1H, appar tsept, *J* = 7.1, 1.3 Hz), 4.29 (1H, dd, *J* = 11.1, 7.1 Hz), 4.10 (1H, dd, *J* = 11.1, 7.2 Hz), 2.92 (1H, ddd, *J* = 12.8, 8.2, 6.4 Hz), 2.75 (1H, ddd, *J* = 12.9, 8.1, 6.9 Hz), 1.65-1.78 (2H, m), 1.75 (3H, br s), 1.68 (3H, br s), 1.56 (3H, s), 1.54 (3H, s), 0.99 (3H, appar t, *J* = 6.7 Hz).

Synthesis of (racemic) oxadiazoline tertiary allylic ether 68

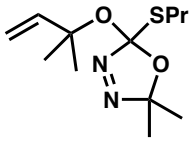

68

To a solution of 2-methyl-3-buten-2-ol **67** (43.1 mg, 0.50 mmol, 1.0 equiv.) and TsOH-H_2O (9.5 mg, 0.050 mmol, 0.10 equiv.) in CH_2Cl_2 (0.5 mL) at was added a solution of oxadiazoline acetate **64** (345.5 mg, 1.50 mmol, 3.0 equiv.) in CH_2Cl_2 (0.50 mL), rinsed with CH_2Cl_2 (0.25 mL). The reaction mixture was stirred for 11 days at rt, then poured directly onto silica (~12 g) and eluted with 1-4% Et_2O/hexanes. Concentration of fractions containing product afforded desired oxadiazoline ether **68** (6.8 mg, 0.025 mmol, 5% yield, ~95% pure) as a clear, colorless oil, contaiminated slightly with irremovable TsOH (~6 mol%): ^{1}H NMR (500 MHz, $CDCl_3$) δ: 6.10 (1H, dd, *J* = 17.5, 10.8 Hz), 5.11 (1H, br d, *J* = 17.5 Hz), 5.01 (1H, dd, *J* = 10.8, 0.5 Hz), 2.87 (1H, ddd, *J* = 12.5, 7.8, 5.7 Hz), 2.69 (1H, ddd, 12.5, 8.0, 6.9 Hz), 1.60-1.77 (2H, m), 1.57 (3H, s), 1.51 (3H, s), 1.50 (3H, s), 1.48 (3H, s), 0.98 (3H, appar t, *J* = 7.4 Hz); ^{13}C NMR (125 MHz, $CDCl_3$) δ: 143.9, 121.7, 112.7, 81.2, 77.3, 33.2, 28.3, 28.1, 24.3, 23.4, 23.1, 13.6.

[2,3]-Wittig procedures for 66 and 68: all [2,3]-Wittig reactions of **66** and **68** were performed in a microwave with pre-set temperatures and durations (1 hour per temp. setting; specifics denoted in Chapter **2**). Each procedure was carried out with 20 mg of

oxadiazoline ether **66** at 0.1 M concentration in the designated solvent unless otherwise noted—oxadiazoline ether **68** was very difficult to acquire and thus used in a lower concentration of 0.3 M (6.8 mg used in reported [2,3]-Wittig rearrangement; see Chapter **2**). Upon cooling after microwave heating, the crude reaction mixture was concentrated under reduced pressure. When NMR yields were obtained, 1,3,5-trimethylbenzene (mesitylene) was utilized as the internal standard (e.g. during optimization). When appropriate, isolation was undertaken using flash chromatography on silica gel, with a gradient of 0-4% Et_2O/hexanes.

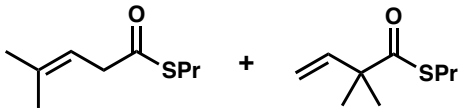

71 **70**

Flash chromatography with 0-10% Et_2O/hexanes to give a mixture of the two (inseparable) β,γ-unsaturated thioesters as colorless oil. In only a single reaction (**68→71**), was one of these thioesters, **71**, obtained as the only identifiable product. **71**: ^{1}H NMR (500 MHz, $CDCl_3$) δ: 5.30 (1H, m), 3.24 (2H, d, *J* = 11.8 Hz), 2.84 (2H, t, *J* = 7.2 Hz), 1.77 (3H, br s), 1.67 (3H, br s), 1.56-1.65 (2H, m), 0.97 (3H, t, *J* = 7.3 Hz); **70**: ^{1}H NMR (500 MHz, $CDCl_3$) δ: 6.02 (1H, dd, *J* = 17.3, 10.6 Hz), 5.19 (1H, br d, *J* = 17.2 Hz), 5.17 (1H, br d, *J* = 10.3 Hz), 2.80 (2H, t, *J* = 7.3 Hz), 1.58-1.67 (2H, m), 1.32 (6H, s), 0.96 (3H, t, *J* = 7.6 Hz).

Synthesis of carbazate hydrazone 73[210]

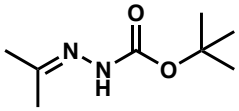

73

To a solution of *tert*-butyl carbazate **72** (2.50 g, 18.92 mmol, 1.0 equiv.) in acetone (76 mL) was added AcOH (1.00 mL, 17.4 mmol, 0.92 equiv.). This solution was heated at reflux overnight. Concentration of the crude reaction mixture followed by flash chromatography on silica with 25-55% EtOAc/hexanes afforded a white powder, found to be *tert*-butyl carbazate acetone hydrazone **73** (3.08 g, 17.88 mmol, 95% yield). NMR data can be found in ref 210.

Synthesis of semicarbazone 74

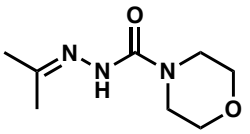

74

Intially following a procedure by Beauchemin et al. for similar transformations,[211] neat *tert*-butyl carbazate hydrazone **73** (0.62 g, 3.6 mmol, 1.0 equiv.) and distilled morpholine (3.6 mL, 1:1 mL/mmol SM) were heated for 3 min at 150 °C in a sealed tube using microwave (μw) radiation. Since starting material was largely recovered (after distilling morpholine), a slightly different procedure inspired by Garland et al.[131] was followed next. To the recovered *tert*-butyl carbazate hydrazone **73** (0.62 g, 3.6

mmol, 1 equiv.) was added $PhCF_3$ (18 mL) and morpholine (0.124 mL, 14.4 mmol, 4 equiv.). This solution was heated to 120 °C in the microwave for incrementally increased amounts of time in a sealed vial until the starting material was completely consumed (20 min; 60 min; 100 min; see Chapter **2**). Unfortunately, not much product remained, but after flash chromatography on silica with 3-4% $MeOH/CH_2Cl_2$, usable amounts of the desired semicarbazone **74** (130.9 mg, 0.36 mmol, 20% yield) were obtained. ^1H NMR (500 MHz, $CDCl_3$) δ: 7.03-7.15 (1H, v br s), 3.68-3.73 (4H, appar t, *J* = 4.8 Hz), 3.54-3.58 (4H, appar t, *J* = 4.9 Hz), 2.00 (3H, s), 1.82 (3H, s).

Synthesis of (racemic) N-morpholino oxadiazoline (*E*)-crotyl ether 76

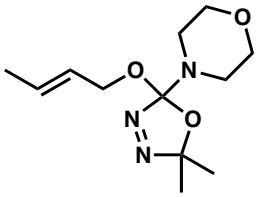

76

To a solution of semicarbazone **74** (36.5 mg, 0.197 mmol, 1.0 equiv.) and (*E*)-crotyl alcohol **75** (42.6 mg, 0.591, 3.0 equiv.) in CH_2Cl_2 (1.90 mL) at rt was added a solution of $PhI(OAc)_2$ () in CH_2Cl_2 (1.38 mL) via syringe pump over 2 hours. The reaction was stirred overnight (16 h), then poured into a separatory funnel. This mixture was washed with saturated aqueous $NaHCO_3$ (4 x 5 mL), brine, then dried with $MgSO_4$, filtered, and concentrated. The residue was chromatographed on silica with 0-15% EtOAc/hexanes to give the desired oxadiazoline crotyl ether **76**, albeit in poor yield (4.5 mg, 0.018 mmol, 9% yield). ^1H NMR (500 MHz, $CDCl_3$) δ: 5.70 (1H, dqt, *J* = 15.3, 6.5, 1.2 Hz), 5.53 (1H, dtq, *J* = 15.3, 6.2, 1.6 Hz), 4.15 (1H, appar ddp, *J* = 11.4, 6.4, 1.2 Hz),

4.08 (1H, appar ddp, *J* = 11.6, 6.3, 1.2 Hz), 3.67-3.76 (4H, m), 2.85-2.92 (2H, m), 2.74-2.81 (2H, m), 1.69 (3H, appar dq, *J* = 6.5, 1.3 Hz), 1.56 (3H, s), 1.51 (3H, s); ^{13}C NMR (125 MHz, $CDCl_3$) δ: 135.7, 129.6, 126.6, 119.0, 66.9, 64.8, 45.9, 24.5, 23.8, 17.8.

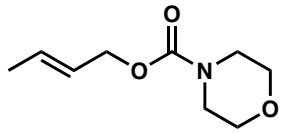

78

Carbamate **78** was obtained as the only identifiable product from the attempted [2,3]-Wittig rearrangement of oxadiazoline **76** (4.5 mg, 0.018 mmol, 1.0 equiv.), a reaction which appeared to have afforded only one major product by TLC (see Chapter **2**). Evaporation of PhF followed by NMR analysis with mesitylene as internal standard revealed a (NMR) yield of 12% for undesired side product, **78**. Also, the SM **76** had been fully consumed and other unidentified products were present, though the diagnostic peaks for [1,2] and [2,3] products were not seen. ^{1}H NMR (500 MHz, $CDCl_3$) δ: 5.78 (1H, dqt, *J* = 15.2, 6.5, 1.1 Hz), 5.60 (1H, dtq, *J* = 15.3, 6.4, 1.5 Hz), 4.53 (2H, appar dp, *J* = 6.4, 1.0 Hz), 3.62-3.68 (4H, appar v br t), 3.47 (4H, appar t, *J* = 4.6 Hz), 1.73 (3H, appar dq, *J* = 6.4, 1.2 Hz).

Synthesis of vinylsilane-tethered alcohol

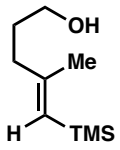

(*E*):(*Z*) = 23:1

This carboalumination-isomeriation reaction was carried out following Negishi's procedure[B] using the same amount of the same SM, TMS-alkyne primary alcohol **97**[A] (2.00 mmol alkyne, 2.00 mmol Cp_2ZrCl_2, 6.00 mmol Me_3Al, 0.25 M CH_2Cl_2, 3.5 days at rt under Ar). The only alteration was the following: instead of quenching with I_2 at -78 °C, this reaction was quenched at brine/ice temperatures (-10 to -20 °C) with saturated aqueous K_2CO_3, filtered through Celite, washed with brine, then dried with $MgSO_4$ and filtered, affording the (*E*)-alkene predominantly. The product **98** was obtained in good yield and purity as a clear pale yellow oil (70% yield, 23:1 (*E*):(*Z*) ratio), without further purification. ^{1}H NMR (500 MHz, $CDCl_3$) δ: 5.24 (1H, br s), [minor (*Z*)-diastereomer peak at 5.20 ppm, 1H, integrates to .0430 (compared to 1.0000 for (*E*)), br s], 3.65 (2H, q, *J* = 6.4 Hz), 2.15 (2H, t, *J* = 7.7 Hz), 1.79 (3H, br s), 1.69-1.75 (2H, m), 1.29 (1H, t, *J* = 5.6 Hz).

Synthesis of vinylsilane-tethered iodide 99

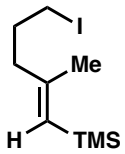

99

(*E*):(*Z*) = 23:1

As mentioned in Chapter **3**, the iodination of **98** was carried out using a procedure employed for a very similar compound in the literature with very little modification.[C] To a solution of **98** (155.6 mg, 0.903 mmol, 1.0 equiv.) in MeCN (0.45 mL) and Et_2O (0.72 mL) at 0 °C was added PPh_3 (284.2 mg, 1.084 mmol, 1.2 equiv.), imidazole (92.2 mg, 1.354 mmol, 1.5 equiv.), and then I_2 (229.2 mg, 0.903 mmol, 1.0 equiv.). The reaction was stirred overnight at rt, then quenched with saturated aqueous $Na_2S_2O_3$, and diluted with H_2O and Et_2O. The organic layer was separated and the aqueous layer extracted with 3 x Et_2O. The organic layers were combined, washed twice with brine, dried with Na_2SO_4, filtered, and concentrated. The residue was chromatographed on silica with pentane twice to separate the product from residual Ph_3P. The alkyl iodide **99** was obtained as a clear colorless oil (130 mg, 0.461 mmol, 51% yield). ^{1}H NMR (500 MHz, $CDCl_3$) δ: [(*Z*)-diastereomer peak at 5.26 ppm partially overlapping adjacent (*E*)-diastereomer peak], 5.24 (1H, s), 3.16 (2H, t, *J* = 7.0 Hz), 2.16 (2H, t, *J* = 6.9 Hz), 1.96 (2H, tt, 7.9, 7.0 Hz), [minor (*Z*)-diastereomer peak at 1.82 ppm, 3H, integrates to .1310 (compared to 3.0000 for (*E*)), d, *J* = 1.2], 1.77 (3H, CH_3, br s), 0.10 (9H, $(CH_3)_3Si$, s); ^{13}C NMR (125 MHz, $CDCl_3$) δ: 152.9, 124.6, 43.0, 31.7, 21.6, 6.5, 0.1.

Synthesis of (racemic) vinylsilane-tethered phosphonate 94

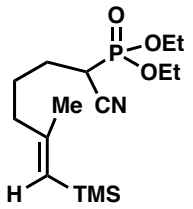

94

(*E*):(*Z*) = 23:1

Inspired by a similar procedure:[D] To a mixture of NaH (60% dispersion, 14.1 mg, 0.352 mmol, 3.52 equiv.) in THF (0.30 mL) and HMPA (0.14 mL) at rt was added a solution of diethyl (cyanomethyl)phosphonate (66.6 mg, 0.376 mmol, 3.76 equiv.) in THF (0.30 mL) with a THF wash (0.17 mL). The resultant mixture was stirred at rt under Ar for 1.5 h, after which it was a pale clear solution. To this solution of phosphonate anion was added a solution of **99** (28.2 mg, 0.100 mmol, 1.0 equiv.) in THF (0.30 mL) with a THF wash (0.18 mL). After 1h at rt, the reaction mixture was concentrated, then Et_2O and H_2O were added. The layers were separated and the aqueous layer extracted with 3 x Et_2O. The combined organic layers were washed with 2 x H_2O and brine, then dried over Na_2SO_4, filtered and concentrated to give the crude product. Chromatography on silica (1.3 g) with 10-35% EtOAc/hexanes afforded pure phosphonate **94** as a clear colorless oil (24.4 mg, 0.0736 mmol, 74% yield).

^{1}H NMR (500 MHz, $CDCl_3$) δ: [(*Z*)-diastereomer peak at 5.25 ppm integrates to 0.0432 (compared to 1.0000 for (*E*)), 1H, sx, *J* = 1.2 Hz], 5.21 (appar br d, *J* = 0.8 Hz), 4.24 (4H, m), 2.91 (1H, ddd (including ^{31}P-^{1}H coupling), *J* = 23.6, 10.0, 5.0 Hz), 2.05-2.20 (2H, m), 1.78-1.93 (3H, m), 1.77 (3H, CH_3, br s), 1.56-1.65 (1H, m), 1.38 (6H, t, *J* = 7.1 Hz), 0.09

(9H, s); ^{13}C NMR (125 MHz, $CDCl_3$) δ: 153.4, 124.5, [116.34/116.27], [64.11/64.05/63.76/63.71], 41.5, 30.6, 29.4, [26.58/26.54], [25.91/25.81], 21.4, [16.46/16.44/16.42/16.40], 0.06.

*Brackets, forward slashes indicate ^{31}P-^{13}C coupling to cause doublet splitting and/or diastereotopic ^{13}C peaks

Synthesis of 93

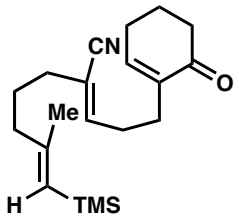

(*E*,*Z*):(*E*,*E*):(*Z*,*Z*) = 18:4:1

To a solution of phosphonate **94** (fragment **A1**, 24.4 mg, 0.0736 mmol, 1.0 equiv.) in $PhCH_3$ (0.80 mL) at -78 °C was (slowly!) added a solution of KHMDS in $PhCH_3$ (0.155 mL 0.5 M, 0.0775 mmol, 1.05 equiv.). The resulting solution was stirred for 1 hour at this temperature, then a solution of enone-tethered aldehyde **95** (fragment **B1**, 11.8 mg, 0.0775 mmol, 1.05 equiv.) in $PhCH_3$ (0.28 mL, then 0.10 mL rinse) was added in a dropwise fashion and the reaction was stirred for 3 h at -78 °C. Saturated aqueous NH_4Cl was then added to quench the reaction and H_2O was added to dissolve solids that remained. This mixture was exracted with 4 x EtOAc, washed with brine, dried over $MgSO_4$, and concentrated under reduced pressure. Chromatography on silica (~1g) with 0-10% EtOAc/hexanes afforded the desired product, **93**, as a clear colorless

oil (15.7 mg, 0.0476 mmol, 65% combined yield of 3 diastereomers—(*E*,*Z*):(*E*,*E*):(*Z*,*Z*) = 18.3:4.2:1).

For combined mixture of diastereomers: ^{1}H NMR (500 MHz, $CDCl_3$) δ: 6.76 [minor (*Z*,*Z*)-diastereomer directly overlapping], 1H, t, *J* = 4.0 Hz), [minor (*E*,*E*)-diastereomer peak at 6.73 ppm, 1H, t, *J* = 4.1 Hz], [minor (*E*,*E*)-diastereomer peak at 6.29 ppm, 1H, appar t, *J* = 6.4 Hz], [minor (*Z*,*Z*)-diastereomer peak at 6.14 ppm partially overlapping with adjacent (*E*,*Z*)-diastereomer, appar t, *J* = 7.4 Hz], 6.11 (1H, appar t, *J* = 7.6 Hz), [minor (*Z*,*Z*)-diastereomer peak at 5.24 ppm, 1H, br s], [minor (*E*,*E*)-diastereomer peak at 5.195 ppm, 1H, br s], 5.185 (1H, s), 2.40-2.48 (4H, m), 2.28-2.39 (4H, m), 2.13-2.20 (2H, m), 2.06 (2H, d, *J* = 7.6 Hz), 1.99 (2H, p, *J* = 6.3 Hz), [minor (*Z*,*Z*)-diastereomer peak at 1.82 ppm, 3H, br s], [minor (*E*,*E*)-diastereomer peak at 1.765 ppm partially overlapping with adjacent (*E*,*Z*)-diastereomer, 3H, br s], 1.76 (3H, s), 1.60-1.69 (2H, m), 0.095 (9H, s), [minor (*E*,*E*)-diastereomer peak at 0.092 ppm partially overlapping with adjacent (*E*,*Z*)-diastereomer, 9H, s], [minor (*Z*,*Z*)-diastereomer peak at 0.08 ppm partially overlapping with adjacent (*E*,*Z*)-diastereomer, 9H, s].

For major (*E*,*Z*)-diastereomer: ^{13}C NMR (125 MHz, $CDCl_3$) δ: 199.2, 153.8, 146.9, 146.4, 138.1, 124.1, 117.7, 115.1, 41.3, 38.4, 33.7, 30.9, 28.4, 26.2, 26.1, 23.1, 21.5, 0.1.

Synthesis of (racemic) α-silyl epoxide 104

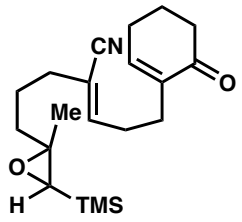

104

Estimated dr (*E*,*Z*):(*E*,*E*):(*Z*,*Z*) = 18:4:1—overlapping diagnostic peaks prevented dr calculation, but stereochemistry assumed from triene SM.

To a flame-dried conical ½-dram vial was added triene **93** (3.1 mg, 0.0094 mmol, 1.0 equiv.) and dry CH_2Cl_2 (75 μL, 0.2 M). This solution was cooled to 10 °C and a separate pre-formed solution of mCPBA in CH_2Cl_2 (47 μL, 0.204 M, 0.0096 mmol, 1.02 equiv.) was added in a dropwise fashion. This mixture was first stirred at 10 °C for 15 min, but no product was observed by TLC so the solution was allowed to warm to rt and stirred until the reaction had reached completion by TLC (rt, 1h). The reaction was quenched with saturated aqueous $Na_2S_2O_3$, cooled to 0 °C, then washed with 1.0 M KOH, H_2O, and brine. After drying with $MgSO_4$ and filtering through a very small plug of $MgSO_4$, the organic layer was concentrated to give the desired **104** as a clear colorless oil in ~quantitative yield and high molar purity (4.3 mg, ~quant.). This was the only observable product, though a small amount of grease and water were observed as well, perhaps causing the >100% calculated yield.

For major (*E*,*Z*)-diastereomer: ^{1}H NMR (500 MHz, $CDCl_3$) δ: 6.76 (1H, t, *J* = 4.1 Hz), 6.13 (1H, t, *J* = 7.6 Hz), 2.40-2.48 (4H, m), 2.37 (2H, appar q, *J* = 5.6 Hz), 2.33 (1H, appar br d, *J* = 7.0 Hz), 2.30 (1H, appar v br d, *J* = 9.1 Hz), 2.15-2.25 (2H, appar o (dtd overlapped?), *J* = 5.4-7.0 Hz), 1.96-2.03 (2H, appar s, *J* = 6.4 Hz), 2.02 (1H, s), 1.55-1.70 (3H, m), 1.41-1.52 (1H, m), 1.29 (3H, s), 0.13 (9H, s).

For major (*E*,*Z*)-diastereomer: ^{13}C NMR (125 MHz, $CDCl_3$) δ: 199.2, 147.2, 146.5, 138.1, 117.6, 114.8, 60.6, 57.8, 39.2, 38.5, 34.1, 30.9, 28.4, 26.1, 24.3, 23.1, 19.8, -1.8.

Synthesis of (racemic) epoxy alcohol 110

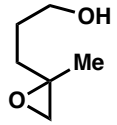

110

First, a solution of TBS-protected epoxy alcohol **118** (1.16 g, 0.503 mmol, 1.0 equiv.) in THF (5.0 mL, 1.0 M) was cooled to 0 °C. Next, a solution of TBAF (6.25 mL, 1.0 M in THF, 6.25 mmol, 1.25 equiv) was added over 15 minutes. The solution was allowed to warm to rt for 4 h with stirring. Upon completion of the deprotection by TLC, the mixture was concentrated and the residue was loaded onto a column with 45 g pH 7 silica with a small amount of CH_2Cl_2. Eluting with 0-70% Et_2O/hexanes afforded epoxy alcohol **110** in good yield and purity, after the column, as a clear colorless oil (0.46 g, 3.96 mmol, 79% yield). ^{1}H NMR (500 MHz, $CDCl_3$) δ: 3.61-3.71 (2H, m), 2.65 (1H, d, *J* = 4.7 Hz), 2.61 (1H, d, *J* = 4.7 Hz), 1.82 (1H, OH, appar t, *J* = 5.5 Hz), 1.57-1.75 (4H, m), 1.33 (3H, s); ^{13}C NMR (125 MHz, $CDCl_3$) δ: 62.6, 56.9, 54.1, 33.0, 28.0, 20.8.

Synthesis of epoxy tosylate

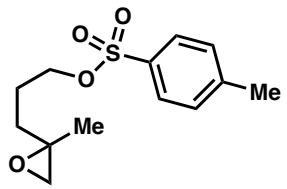

116

To a solution of TsCl (1.19 g, 6.24 mmol, 1.58 equiv.) and DMAP (1.02 g, 8.35 mmol, 2.11 equiv.) in CH_2Cl_2 (16 mL) at rt was added a solution of epoxy alcohol **110** (0.46 g, 3.96 mmol, 1.0 equiv.) in CH_2Cl_2 (4 mL, with 2 x 1 mL rinses). The reaction was stirred overnight, then concentrated under reduced pressure and chromatographed on silica (155 g) with 0-25% EtOAc/hexanes to afford epoxy tosylate **116** as a viscous clear colorless oil (0.68 g, 2.52 mmol, 64% yield). Upon scale-up, starting from 2.29 g **118**, 1.46 g **116** was obtained, resulting in a 52% yield over 2 steps on gram-scale. The neat compound decomposes at rt within 24 h—this is best avoided by storing at -80 °C under an inert gas (e.g. Ar, N_2). ^{1}H NMR (500 MHz, $CDCl_3$) δ: 7.78 (2H, Ar-H, appar d, *J* = 8.3 Hz), 7.34 (2H, Ar-H, appar d, *J* = 8.1 Hz), 4.05 (1H, dt, *J* = 9.1, 6.4 Hz), 4.02 (1H, dt, *J* = 9.8, 6.5 Hz), 2.56 (1H, d, partially overlapping adjacent geminal proton peak, *J* = 5.2 Hz), 2.54 (1H, d, partially overlapping adjacent geminal proton peak, *J* = 5.2 Hz), 2.45 (3H, Ar-CH_3, s), 1.75 (2H, appar p, *J* = 7.4 Hz), 1.52-1.65 (2H, m), 1.27 (3H, s); ^{13}C NMR (125 MHz, $CDCl_3$) δ: 144.8, 133.1, 129.9, 127.9, 70.3, 56.2, 53.6, 32.5, 24.7, 20.9.

Synthesis of epoxy iodide 111 via Finkelstein

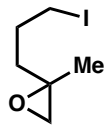

111

To a solution of tosylate **116** (0.68 g, 2.52 mmol, 1.0 equiv.) in dry acetone (6.3 mL, 0.4 M) was added NaI (749.5 mg, 5.00 mmol, 2.0 equiv.) in one portion. The mixture was refluxed under an atmosphere of Ar with rapid stirring for 10 min, during which NaI went into solution, the mixture became cloudy and yellow, and a solid (NaOTs) crashed out of solution. After cooling, TLC showed no SM remained. A solution of saturated aqueous $Na_2S_2O_3$ was then added to the reaction mixture as well as a small amount of H_2O to dissolve solids present. The mixture was then extracted with 3 x hexanes and then 2 x CH_2Cl_2. The organic layers were combined, washed with H_2O and brine, then dried with $MgSO_4$, filtered, and concentratedto give epoxy iodide **111** as a clear colorless oil (0.45 g, 1.99 mmol, 79% yield), with no purification needed. Upon scale-up, 1.46 g **116** afforded 0.89 g **111**, resulting in a 75% yield on gram-scale.

^{1}H NMR (500 MHz, $CDCl_3$) δ: 3.15-3.24 (2H, m), 2.63 (1H, d, *J* = 4.7 Hz), 2.58 (1H, d, *J* = 4.7 Hz), 1.87-2.04 (2H, m), 1.61-1.76 (2H, m), 1.32 (3H, s); ^{13}C NMR (125 MHz, $CDCl_3$) δ: 56.1, 53.7, 37.5, 29.3, 21.0, 6.2.

3-step synthesis of alkene-tethered alkyl iodide 120 from 117

- Step 1: synthesis of **117a** (Wittig)

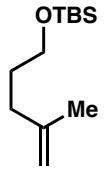

117a

This Wittig olefination of **117** (to **117a**) was inspired by a literature procedure for the analogous transformation of a congener, the O-acetyl-protected keto-alcohol, reported by Lugtenburg et al.[Va] To a rapidly stirring solution of freshly made, vacuum oven-dried $(Ph_3PMe)^+(I^-)$ (25.67 g, 63.5 mmol, 1.44 equiv.) in THF (50 mL) at -30 °C was added (slowly) a solution of nBuLi (39.7 mL, 1.6 M in hexanes) over 15 min. This mixture was warmed to rt and stirred for 6 h, and turned a deep orange color. The ylide solution was then cooled once more to -30 °C and to this mixture was added a solution of ketone **117** (9.529 g, 44.04 mmol, 1.0 equiv.) in THF (20 mL, with 5 mL rinse) over 15 min. The resulting reaction mixture was stirred at rt for 3 days, then was cooled again to -30 °C and quenched with saturated aqueous NH_4Cl. This mixture was extracted with 3 x hexanes and the combined organic layers were washed with H_2O and brine, dried over $MgSO_4$, filtered, and concentrated to give crude product **117a** as a clear yellow non-viscous oil (10.88 g, 85-90% pure, est. ~quant.). NMR data for **117** (and **117a**) can be found at ref 196.

- Step 2: synthesis of **119** (silyl deprotection)[212]

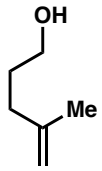

119

To a solution of crude **117a** (10.88 g, assume 44.04 mmol for calculations, 1.0 equiv.) in THF (50.7 mL) at -10 °C was added a solution of TBAF (63.4 mL, 1.0 M in THF, 63.4 mmol, 1.44 equiv.) over 10 min. The reaction mixture was then stirred at rt until completion by TLC (1.5 h). This solution was then concentrated under reduced pressure and passed through a plug of silica (185 g), eluting first with 0.5 L hexanes (tossed) then 1.5 L 40% EA/hexanes (kept), ultimately affording cruded deprotected alcohol **119** as a clear, nearly colorless oil, contaminated with TBSOH and a small amount of EtOAc (8.72 g crude, ~40% pure, est. ~78% yield), but used without further purification in the next reaction. NMR data for **119** can be found at ref 212.

- Step 3: synthesis of **120** (Appel)[213]

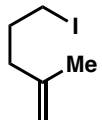

120

This procedure was inspired by the protocol developed by Boyer et al. for the same transformation;[Xa] with the main difference being our use of a MeCN/Et_2O solvent system instead of PhH, since the former worked well for the Appel iodination of similar primary alcohol, **98** (see above). To a rapidly stirring solution of alkene-tethered

primary alcohol **119** (8.72 g crude, ~40% pure, assume 34.56 mmol, 1.0 equiv.), Ph_3P (19.28 g, 73.5 mmol, 2.13 equiv.), and imidazole (9.66 g, 142.0 mmol, 4.11 equiv.) in Et_2O (41 mL) and MeCN (25 mL) at -10 °C under Ar was added I_2 (17.64 g, 69.5 mmol, 2.01 equiv.) in a portionwise fashion. This reaction was stirred until completion by TLC (< 1 h), then quenched with saturated aqueous $Na_2S_2O_3$ and water, extracted with 3 x Et_2O, and the combined organic layers washed with 2 x H_2O and brine, dried over $MgSO_4$, filtered, and concentrated. The crude residue was chromatographed on silica (~250 g) and eluted with 1-1.5 L pentane to afford the desired primary iodide, **120** in good yield and high purity, with ~3% TBSOTBS as the only observed impurity (5.60 g, 97% pure, 25.86 mmol, 59% yield over 3 steps, est. ~75% yield for this step, highest lit. yield for this step was 69%).[Xa] NMR data for **120** can be found at ref 213.

Synthesis of alkene-tethered phosphonate 118

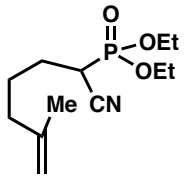

118

To NaH (60% dispersion, 3.64 g, 91.03 mmol, 3.52 equiv.) in a flame-dried 1-L RBF with a stir bar under positive Ar pressure was added HMPA (36 mL) and THF (78 mL). Following, there was added a solution of diethyl (cyanomethyl)phosphonate **100** (17.22 g, 97.24 mmol, 3.76 equiv.) in THF (108 mL, with 14 mL rinse) at rt over 10 min. This deprotonation reaction was exothermic and on this large scale, minor cooling (rt water bath) was required to maintain a reaction temperature of ~rt. After 2.5 h, the

exortherm had ceased. To this solution of the newly formed sodium phosphonate nucleophile was then added a solution of **120** (5.60 g, 97% pure, 25.86 mmol, 1.0 equiv.) in THF (114 mL, with 10 mL rinse) over 5 min. After 2 h stirring at rt, the reaction was complete by TLC and concentrated under reduced pressure (removing THF). H_2O was then added, and the mixture was extracted with 3 x Et_2O, the organic layers combined and washed first with 2 x H_2O, then with brine, then dried over $MgSO_4$, filtered, and concentrated under reduced pressure to give 8.13 g crude product as a clear yellow oil. This residue was chromatographed on silica (600 g) and eluted first with hexanes (to remove oil from NaH dispersion), then with 25%, 40%, and finally 50% EtOAc/hexanes (product mostly eluted towards the end, 40-50%) to afford the desired monoalkylated product, **118**, in good yield and excellent purity (5.32 g, 20.52 mmol, 79% yield, ≥ 98% pure). ^{1}H NMR (500 MHz, $CDCl_3$) δ: 4.75 (1H, br s), 4.70 (1H, br s), 4.19-4.29 (4H, m), 2.91 (1H, ddd, (including ^{31}P-^{1}H coupling), *J* = 23.8, 9.8, 4.8 Hz), 2.02-2.13 (2H, m), 1.78-1.96 (3H, m), 1.72 (3H, CH_3, br s), 1.56-1.67 (1H, m), 1.39 (6H, appar t, *J* = 7.1 Hz).

^{13}C NMR (125 MHz, $CDCl_3$) δ: 144.3, [116.33/116.26], [111.040/111.037], [64.12/64.06/63.76/63.71], 36.8, 30.6, 29.4, [26.55/26.52/25.71/25.61], 22.2, [16.47/16.45/16.42/16.40].

*Brackets, forward slashes indicate ^{31}P-^{13}C coupling to cause doublet splitting and/or diastereotopic ^{13}C peaks

Synthesis of epoxy phosphonate 112 (fragment A2)

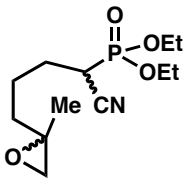

112

To a solution of alkene-tethered phosphonate **118** (1.5557 g, 6.00 mmol, 1.00 equiv.) in CH_2Cl_2 (48 mL) cooled in an ice-water bath to ≤ 10 °C was added a freshly made solution of mCPBA (1.408 g of ~75% mCPBA, 6.12 mmol, 1.02 equiv.) in CH_2Cl_2 (30.6 mL, 0.20 M) over 10 min. The reaction mixture was allowed to warm to rt with rapid stirring and once TLC showed completion (1.5 h, rt), the reaction was quenched with saturated aqueous $Na_2S_2O_3$. After transferring this mixture to a separatory funnel, shaking, and allowing the two phases to separate (adding H_2O if emulsions formed), the organic layer was separated and washed with 2 x saturated aqueous K_2CO_3, H_2O, and brine, then dried over $MgSO_4$, filtered through a plug of $MgSO_4$, and concentrated under reduced pressure. The resulting product, **112**, was obtained as a highly viscous clear colorless oil (1.62 g, 5.88 mmol, 98% yield, ~98% pure). No further purification was needed, though care had to be taken to prevent the absorption of atmospheric H_2O (e.g. using air-tight sealed containers for storage), as this compound appeared to be rather hygroscopic. ^{1}H NMR (500 MHz, $CDCl_3$) δ: 4.19-4.30 (4H, m), 2.87-2.97 (1H, 2 diastereomeric protons, each with appar td splittings partially overlapping each other (including ^{31}P-^{1}H coupling), J_1 = 9.8, 5.0 Hz and J_2 = 9.6, 5.9 Hz)], 2.57-2.63 (2H, 2 diastereotopic geminal (epoxymethylene) protons of each diastereomer, each with d

splittings partially overlapping each other, J_1 = 4.7 Hz, $J_{1'}$ = 4.8 Hz, J_2 = 5.0 Hz, $J_{2'}$ = 5.1 Hz), 1.74-1.99 (3H, m), 1.55-1.68 (1H, m), 1.39 (6H, appar t, J = 7.0 Hz), 1.32 (3H, br s). ^{13}C NMR (125 MHz, $CDCl_3$) δ: [116.22/116.16/116.14/116.09], [64.25/64.19/64.17/64.13/64.11/64.05/63.83/63.78], [56.38/56.34/56.02/55.97], [53.80/53.55], [35.86/35.51], [30.68/30.48/29.53/29.33], [27.08/27.05/26.83/26.80], [23.77/23.67/23.58/23.49], [20.81/20.79], [16.47/16.45/16.42/16.41].

*Brackets, forward slashes indicate ^{31}P-^{13}C coupling to cause doublet splitting and/or diastereotopic ^{13}C peaks

Synthesis of enone-tethered (diethyl) acetal 103

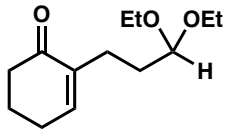

103

A solution of bicyclic vinylogous hemiketal (2.68 g crude; not drawn)—made from literature LAH reduction[E] of bicyclic vinylogous ester **102** (3.35 g, 17.07 mmol)—in abs. EtOH (10 mL, 3mL rinse) was added to a stirring solution of acetyl chloride (1.01 mL, 14.21 mmol, 0.83 equiv. wrt **102** from previous step) in abs. EtOH (120 mL) at ≤ -10 °C over 10 min. This mixture was then allowed to warm to rt. Upon completion by TLC (20 min, rt), the reaction was quenched with saturated aqueous $NaHCO_3$ and extracted with 2 x Et_2O. The combined organic layers were washed with H_2O, then brine, dried over $MgSO_4$, passed through a plug of $MgSO_4$, and concentrated to give 2.61 g crude product, in which NMR analysis indicated no aldehyde was present. This crude

residue was chromatographed on silica (~100 g) and eluted with 5-15% EtOAc/hexanes to afford the desired enone-tethered acetal **103** (1.869 g, 8.26 mmol, 48% yield over 2 steps). NMR data can be found at ref E.[170]

3-step synthesis of allylic acetate-tethered aldehyde 108 from alcohol 105

- Step 1: synthesis of **105** (Luche reduction)

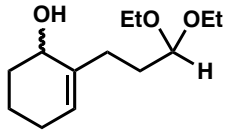

105

To a solution of enone-tethered acetal **103** (181.0 mg, 0.800 mmol, 1.0 equiv.) in MeOH (2.0 mL, 0.4M) at -10 °C was added $NaBH_4$ (45.4 mg, 1.200 mmol, 1.5 equiv.) in portions. The mixture was then stirred until complete consumption of SM was shown by TLC (45 min). The reaction was then quenched with 2.4 mL brine (H_2O added to dissolve solids) and extracted with 4 x CH_2Cl_2; diluting with Et_2O helped break emulsions. The organic layers were combined, dried over $MgSO_4$, filtered, and concentrated to give 167.7 mg crude product (mostly **105**). While both the diethyl acetal **105** and the mixed methyl/ethyl acetal **106** were obtained (in a 1.6:1 ratio), only the NMR data for the former (**105**) is detailed: ^{1}H NMR (500 MHz, $CDCl_3$) δ: 5.54 (1H, appar br t, J = 3.2 Hz), 4.49 (1H, appar t, J = 5.3 Hz), 4.05 (1H, br s), 3.58-3.69 (2H, m), 3.44-3.53 (2H, m), 2.10-2.25 (2H, m), 1.99-2.08 (2H, m), 1.89-1.98 (1H, m), 1.80-1.88 (1H, m), 1.61-1.78 (4H, m), 1.51-1.60 (1H, m), 1.17-1.22 (6H, 2 diastereotopic methyl groups, each with dd splittings partially overlapping each other, J_1 = 4.9, 2.2 Hz, $J_{1'}$ =

5.0, 2.1 Hz); ^{13}C NMR (125 MHz, $CDCl_3$) δ: 138.6, 125.3, 102.8, 67.0, [61.2/60.7], 32.2, 31.9, 29.7, 25.5, 18.0, [15.4/15.3].

*Brackets, forward slashes indicate diastereotopic ^{13}C peaks

- Step 2: synthesis of **107** (acetylation)

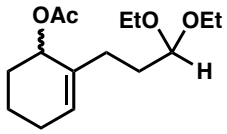

107

To a solution of allylic alcohol-tethered acetal **105**/**106** (167.7 mg, assume 0.80 mmol, 1.0 equiv.) and DMAP (9.8 mg, 0.08 mmol, 0.1 equiv.) in pyridine (16 mL, 0.05 M) under Ar at 0-5 °C was added Ac_2O (3 mL, 32 mmol, 40 equiv.) over 3 min. The mixture was then stirred at this temperature until complete consumption of SM was shown by TLC (1.5 h). The reaction was then diluted with CH_2Cl_2 and quenched by adding 3 M HCl (70 mL, 210 mmol) while the solution was stirring rapidly. After 15 min, the organic layer was separated, washed first with 3 M HCl (20 mL; shaken vigorously), then with saturated aqueous $NaHCO_3$, H_2O, and brine. Following, the organic layer was dried over $MgSO_4$, filtered, concentrated, and then subjected to the subsequent reaction without further purification. While a both the diethyl acetal and the mixed methyl/ethyl acetal were obtained (in a 1.6:1 ratio), only the NMR data for the former is detailed: ^{1}H NMR (500 MHz, $CDCl_3$) δ: 5.72 (1H, appar v br t), 5.28 (1H, appar t, J = 4.1 Hz), 4.46 (1H, appar t, J = 5.8 Hz), 3.59-3.66 (2H, m), 3.44-3.51 (2H, m), 1.91-2.14 (4H, m), 2.06 (3H, s), 1.55-1.84 (6H, m), 1.17-1.22 (6H, 2 diastereotopic methyl groups, each with appar t splittings partially overlapping each other, J_1 = 7.0, Hz, $J_{1'}$ = 7.0 Hz);

^{13}C NMR (125 MHz, $CDCl_3$) δ: 170.9, 135.0, 127.7, 102.5, 69.4, [61.0/60.9], 31.7, 29.1, 29.0, 25.2, 21.4, 18.2, [15.4] (directly overlapping).

*Brackets, forward slashes indicate diastereotopic ^{13}C peaks

- Step 3: synthesis of **108**, fragment **B2** (acetal deprotection)

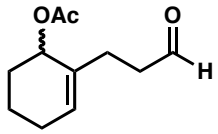

108

To a solution of allylic acetate-tethered acetal (used crude material from Step 2 of **107**, assume 0.8 mmol, 1.0 equiv.) in acetone (8 mL, 0.1 M) at rt was added 3 M HCl (0.53 mL, 1.6 mmol, ~2.0 equiv) in a dropwise manner. After just 5 min, TLC showed no SM remained. After 10 min, the reaction was diluted with EtOAc and quenched with excess saturated aqueous $NaHCO_3$ while stirring on high. The two phases were then separated and the aqueous layer was extracted with 2 x EtOAc. The combined organic layers were washed with brine, dried over $MgSO_4$, filtered, and concentrated to give the desired allylic acetate-tethered aldehyde **108** in a great 3-step yield (134.2 mg, 0.7054 mmol, 88% yield over 3 steps), without any chromatographic purification. ^{1}H NMR (500 MHz, $CDCl_3$) δ: 975 (1H, v br t), 5.72 (1H, appar v br t), 5.28 (1H, appar v br t), 2.46-2.64 (2H, m), 2.26-2.38 (2H, m), 2.06-2.15 (1H, m), 2.07 (3H, s), 1.93-2.03 (1H, m), 1.72-1.85 (2H, m), 1.54-1.68 (2H, m); ^{13}C NMR (125 MHz, $CDCl_3$) δ: 202.1, 170.9, 133.8, 128.7, 69.2, 42.0, 28.9, 26.4, 25.2, 21.4, 18.1.

Synthesis of first model system: complex allylic acetate substrate HWE-2

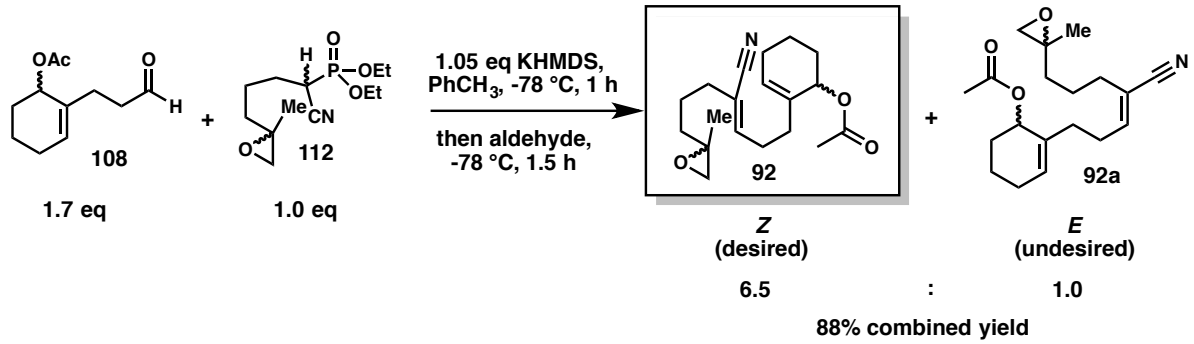

General HWE procedure: To a solution of **112** (8.2 mg, 0.0298 mmol, 1.0 equiv.) in $PhCH_3$ (0.13 mL) at -78 °C was added a pre-made solution of KHMDS in $PhCH_3$ (0.09 mL, 0.35 M, 0.0315 mmol, 1.06 equiv.). After stirring for 1 h at this temperature, a solution of aldehyde **108** (10.1 mg, 0.0531 mmol, 1.78 equiv.) in $PhCH_3$ (0.19 mL) was added dropwise at -78 °C. The HWE reaction mixture was then stirred at this temperature until no phosphonate SM (**112**) was seen by TLC (1.5 h) and then quenched with 1.3 mL saturated aqueous NH_4Cl at -78 °C and allowed to warm to rt. The mixture was then extracted with 4 x EtOAc and the combined organic layers were washed with brine, dried over $MgSO_4$, filtered, and concentrated to afford ~20 mg crude product residue (ratio of (*E*):(*Z*) in crude was 6.5:1). This material was chromatographed on regular silica first, then on pH 7 silica to afford **92** in great combined yield and good purity as a clear colorless viscous oil (8.8 mg, ~95% pure, 0.0263 mmol, 88% combined yield). ^1H NMR (500 MHz, $CDCl_3$) δ: [minor (*E*)-diastereomer peak at 6.31 ppm integrates to 0.1296 (compared to 0.8509 for (*Z*)), (1H, t, *J* = 7.4 Hz)], 6.11 (1H, t, *J* = 7.6 Hz), 5.72 (1H, appar br t, *J* = 3.3 Hz), 5.29 (1H, appar br t, *J* = 4.3 Hz), [minor (*E*)-diastereomer peak at 2.62 ppm with d splitting and partially overlapping adjacent peak (1H, *J* = 5.0 Hz)], 2.60 (1H, d, *J* = 4.8 Hz), 2.58 (1H, d, *J* = 4.7

Hz), 2.46 (2H, appar q, J = 7.6 Hz), 2.17-2.28 (2H, m), 1.95-2.16 (4H, m), 2.08 (3H, s), 1.71-1.84 (2H, m), 1.50-1.69 (6H, m), [minor (*E*)-diastereomer peak at 1.33 ppm partially overlapping adjacent peak (3H, s)], 1.32 (3H, s); ^{13}C NMR (125 MHz, $CDCl_3$) δ: [170.980/170.976], 147.4, 133.9, 129.0, 117.5, 114.7, 69.3, 56.6, [53.72/53.71], [35.61/35.60], 34.1, 32.8, 30.0, [28.98/28.97], 25.2, [23.84/23.83], 21.4, 20.9, 18.2.

*Brackets, forward slashes indicate diastereomeric ^{13}C peaks

Attempted polycyclization of 92

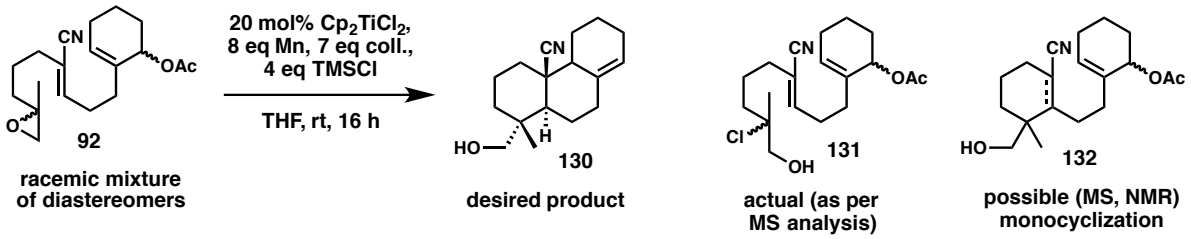

A typical procedure for the attempted polycyclization of **92** entailed the used of 1 eq substrate (5-6 mg, 95-98% pure, dr 5-18:1), 0.2 eq Cp_2TiCl_2, 8 eq Mn, and 7 eq 2,4,6-collidine in THF (0.01-0.05 M) for ~16 h, stirring in a strictly oxygen-free environment. However, whether using Zn or Mn as the terminal reductant, catalytic or stoichiometric Ti(III) as the epoxide reducing agent, or ambient or elevated temperatures, similarly unsatisfactory results (mostly products **131** and **132**) were obtained regardless of the use of similar or drastically different conditions (see Chapter **3**).

Synthesis of epoxy silane substrate

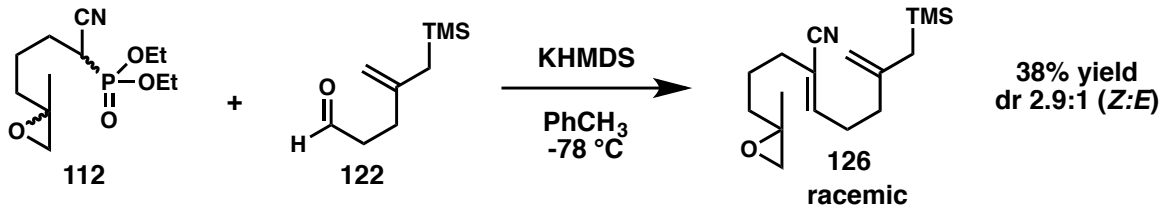

General HWE procedure followed with **112** (0.5 mmol, 1.0 equiv.), **122** (0.5 mmol, 1.0 equiv.), and KHMDS (0.675 mmol, 1.35 equiv.) to give 54.9 mg substrate **126** (38% yield, 95% pure, 2.9:1 dr). ^{1}H NMR (500 MHz, $CDCl_3$) δ: [minor (*E*)-diastereomer peak at 6.35 ppm integrates to 0.2288 (compared to 0.6743 for (*Z*)), 1H, t, *J* = 7.3 Hz], 6.14 (1H, t, *J* = 7.4 Hz), 4.57-4.61 (2H, m), 2.56-2.63 (2H, m), 2.51 (2H, q, *J* = 7.4 Hz), 2.17-2.28 (2H, m), 2.09 (2H, t, *J* = 7.6 Hz), 1.50-1.70 (4H, m), 1.54 (2H, s), 1.32 (3H, s), 0.03 (9H, s).

Attempted polycyclization of simple epox-silane

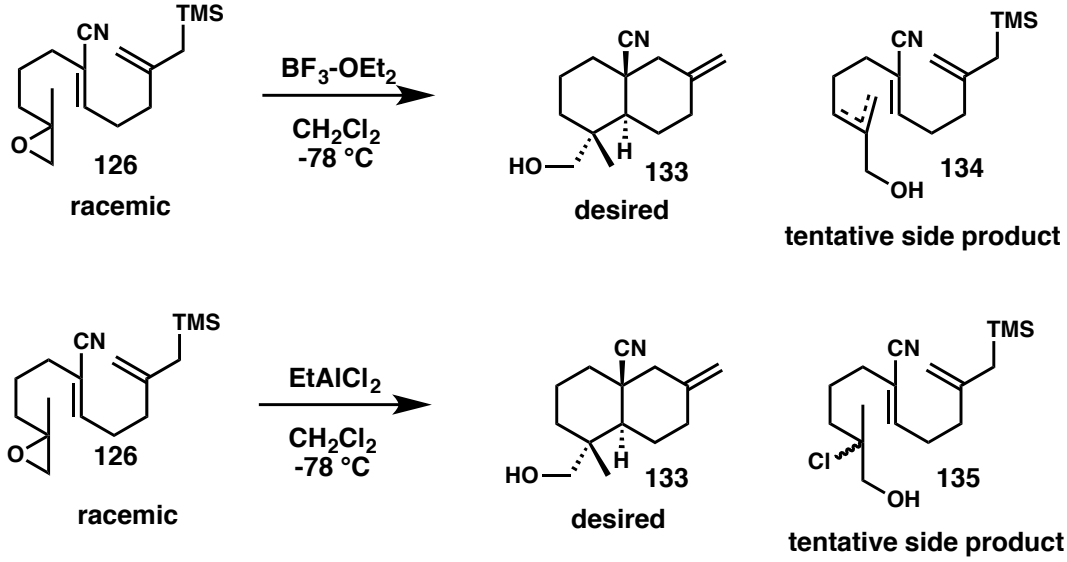

General method for both attempted polycyclizations of substrate **126** (with BF_3-OEt_2 and $EtAlCl_2$): To a solution of the simple allylsilane substrate (8-9 mg, 1 equiv.) in

CH_2Cl_2 (0.02 M) at -78 °C was added Lewis acid (1.5 equiv.) under Ar. The reaction was stirred at this temperature for 2 h, then quenched with saturated aqueous $NaHCO_3$, H_2O, and Rochelle's solution. This mixture was extracted with 3 x EtOAc and the combined organic layers washed with brine, dried with $MgSO_4$, filtered, and concentrated to give 7+ mg crude product. However, in both cases, unproductive epoxide opening predominated (**133**-**135**).

Synthesis of epoxy arene substrate 125

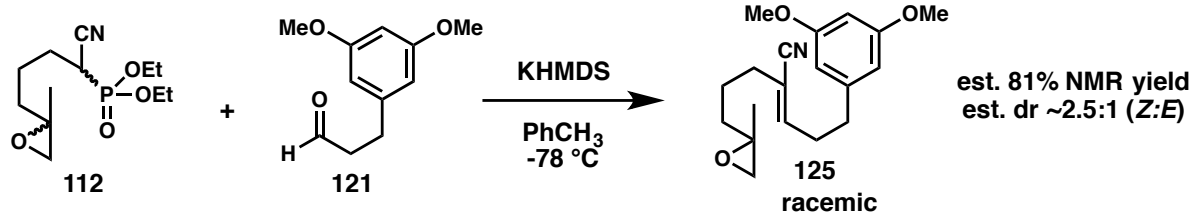

General HWE procedure followed with **112** (1.6 mmol, 1.6 equiv.), **121** (1.0 mmol, 1.0 equiv.), and KHMDS (1.6 mmol, 1.6 equiv.) to give an 81% NMR yield of **125** (dr ~2.5:1). ^{1}H NMR (500 MHz, $CDCl_3$) δ: [peak at 6.26-6.39 ppm integrates to 3.000 and correlates to $4H_E$ + $3H_Z$, and H_Z integrates to 0.6511, 3H, m], 6.13 (1H, t, J = 6.4 Hz), 3.59 (6H, s), 2.55-2.73 (6H, m), 2.13-2.25 (2H, m), 1.55-1.67 (2H, m), 1.45-1.53 (2H, m), 1.30 (3H, s).

Synthesis of epoxy ketone substrate

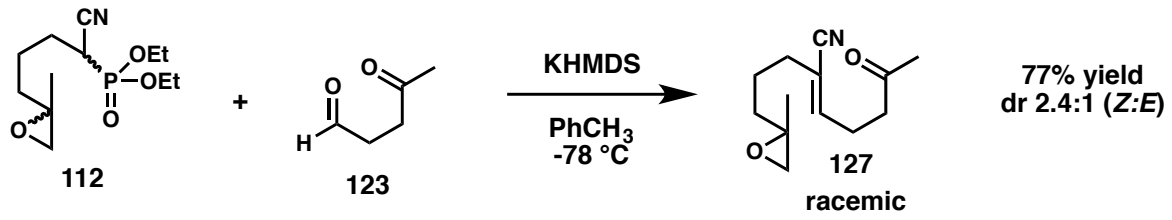

General HWE procedure followed with **112** (1.25 mmol, 1.25 equiv.), **123** (1.0 mmol, 1.0 equiv.), and KHMDS (1.25 mmol, 1.25 equiv.) afforded **127** substrate (0.17 g, 0.768 mmol, 77% yield, 98% purity) after flash chromatography with 15-30% EtOAc/hexanes. ^{1}H NMR (500 MHz, $CDCl_3$) δ: [minor (*E*)-diastereomer peak at 6.27 ppm integrates to 0.4157 (compared to 1.0000 for (*Z*)), 1H, t, *J* = 7.5 Hz], 6.16-6.22 (1H, m), 2.54-2.63 (6H, m), 2.21 (2H, appar td, *J* = 7.5, 3.2 Hz), 2.16 (3H, s), 1.52-1.70 (4H, m), 1.32 (3H, s). ^{13}C NMR (125 MHz, $CDCl_3$) δ: 206.7, 146.3, 117.2, 115.3, 56.5, 53.7, 42.0, 35.6, 34.1, 28.4, 25.5, 23.8, 20.9.

Radical polar-crossover polycyclization of epoxy ketone substrate 127

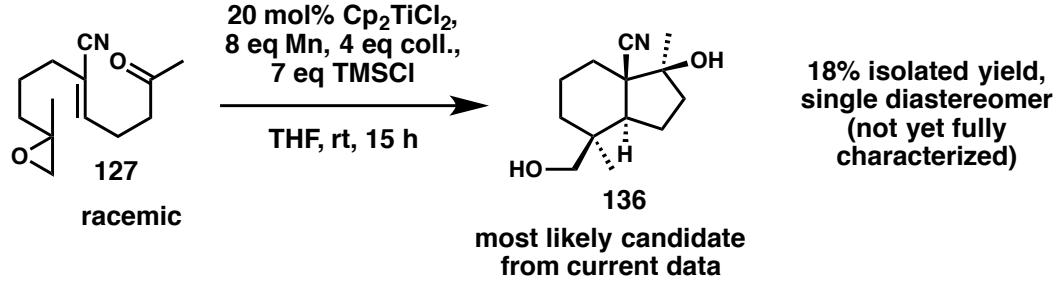

Following the exact procedure for the radical epoxide cyclization-intramolecular aldol sequence published by Cuerva[36] (only 1 example)—with the only changes being the substrate used and the duration (15 h instead of 16 h)—the polycyclization of **127** (10. 8 mg, 0.0488 mmol, 98% pure, 1.0 equiv.) was carried out. No SM remained and the

major product, bicyclic diol **136** (2.0 mg, 0.00896 mmol, 18%) was isolated via chromatography on silica (14.7 mg crude residue loaded onto ~1.5 g silica) by eluting with a slow gradient, starting at 10% and increasing to 30% EtOAc/hexanes, then flushing with 50% EtOAc/hexanes and finally pure (100%) EtOAc. Another ~1-2 mg **136** was also present, however it was not able to be separated from other compounds of similar polarity (not yet identified; possibly other diastereomers).

Appendix B: Supporting Information

^{1}H and ^{13}C NMR spectra for ***trans*-dione 10b**:

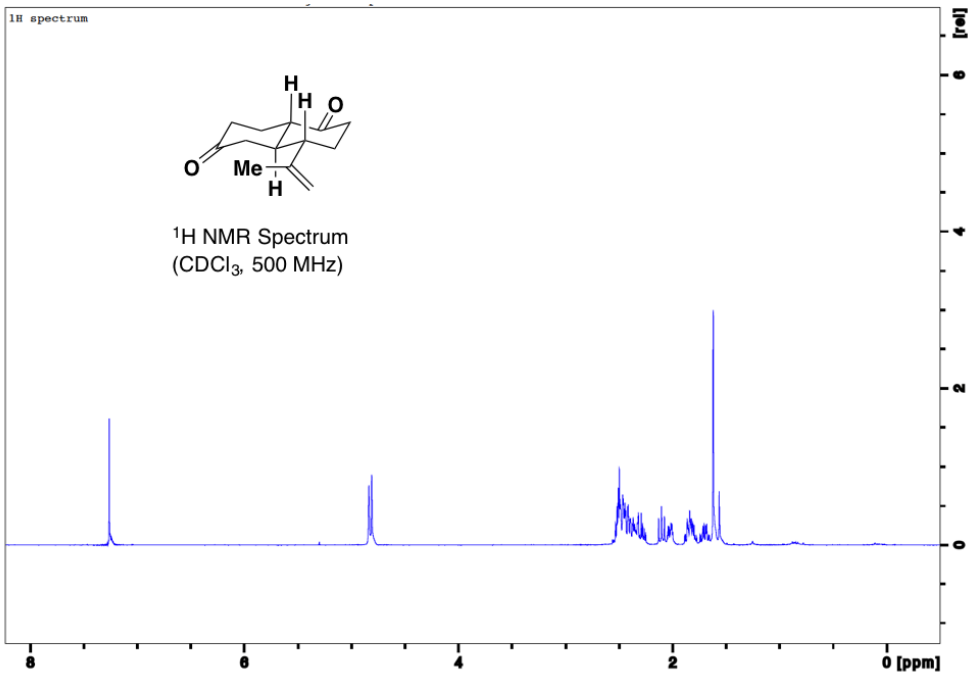

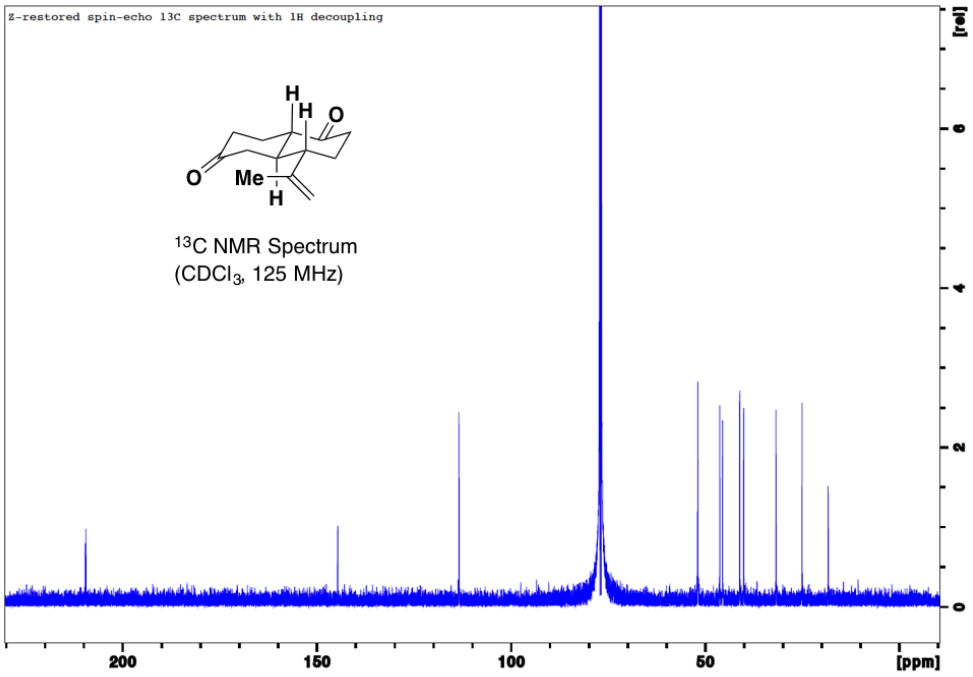

^{1}H and ^{13}C NMR spectra for ***cis*-dione 10a** (epimerizes on silica):

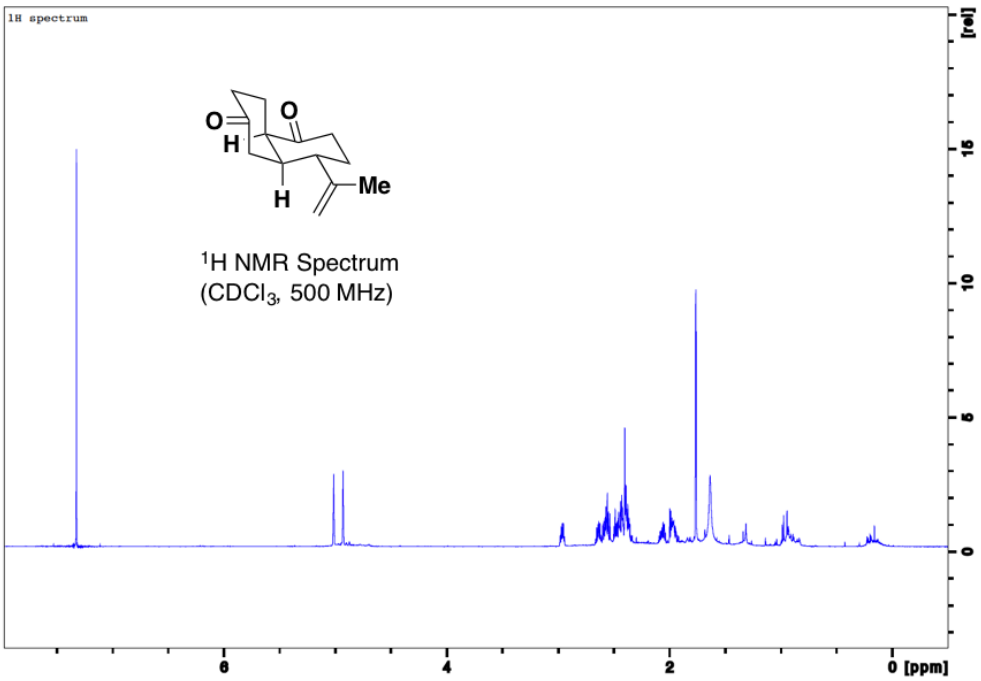

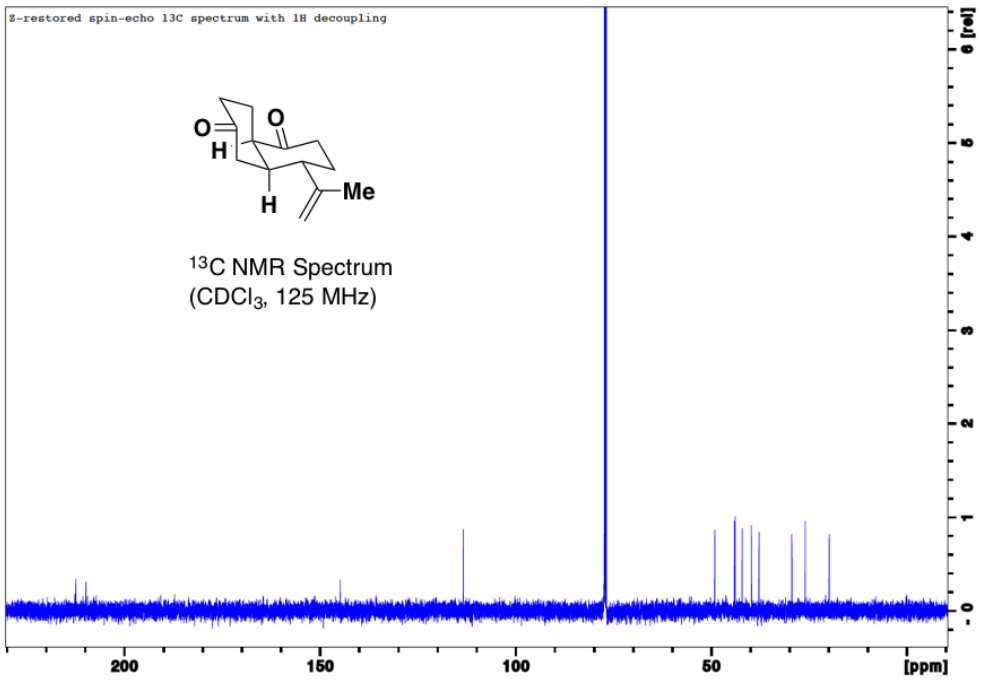

For the aldehyde hydroformylation product, a small amount of Ph_3P and residual solvent remained after extensive chromatography and vacuum distillation due to the small scale of the reaction. Further processing was not undertaken since the preference for the undesired diastereomer was found to be incredibly high (see **1.6**).

^{1}H and ^{13}C NMR spectra for **hydroform prod 30a**:

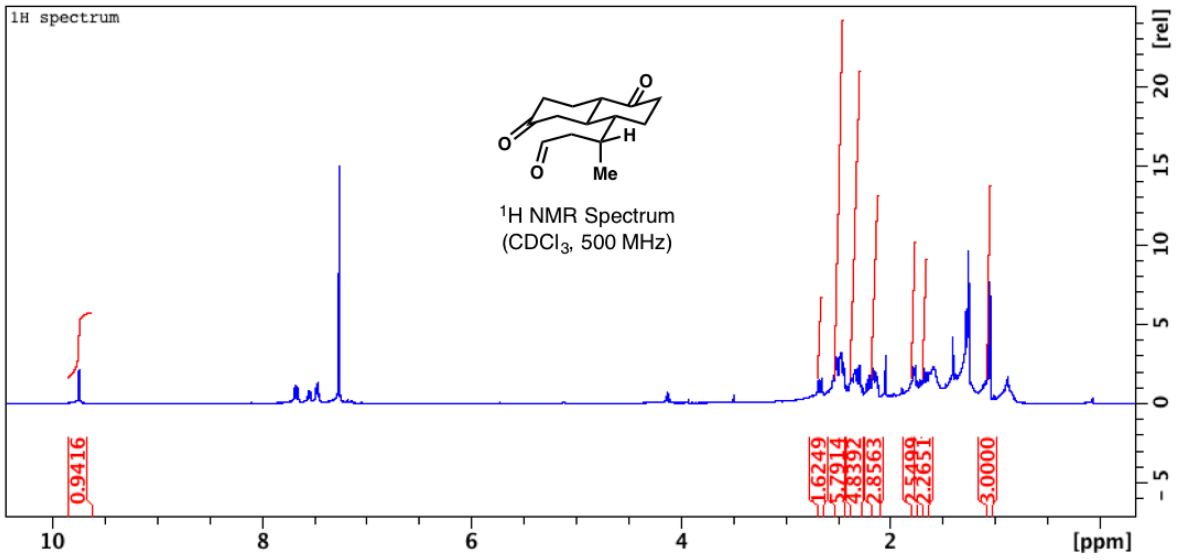

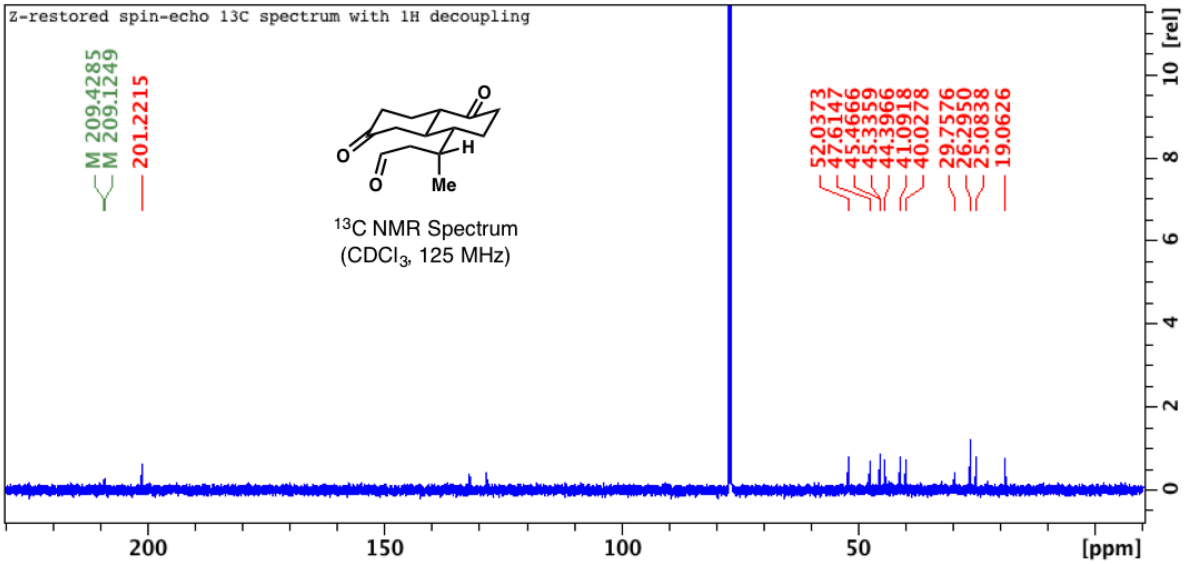

^{1}H NMR spectrum for (racemic) **primary allylic ether of oxadiazoline 66** (~6% TsOH not removable by KOH washes or chromatography):

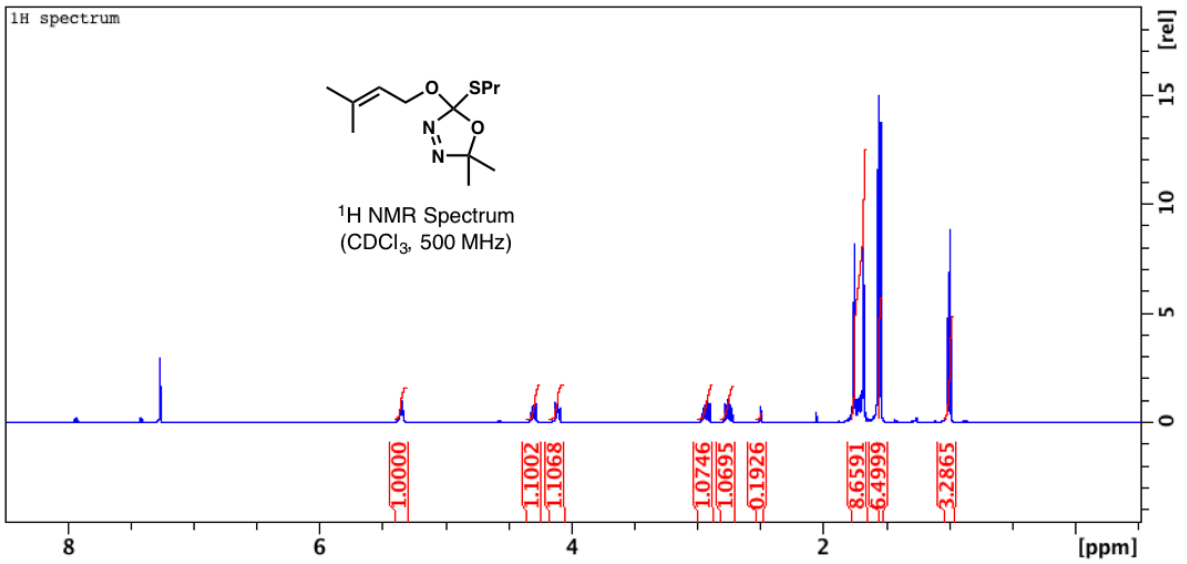

^{1}H and ^{13}C NMR spectra for (racemic) **tertiary allylic ether of oxadiazoline 68** (~6% TsOH not removable by KOH washes or chromatography):

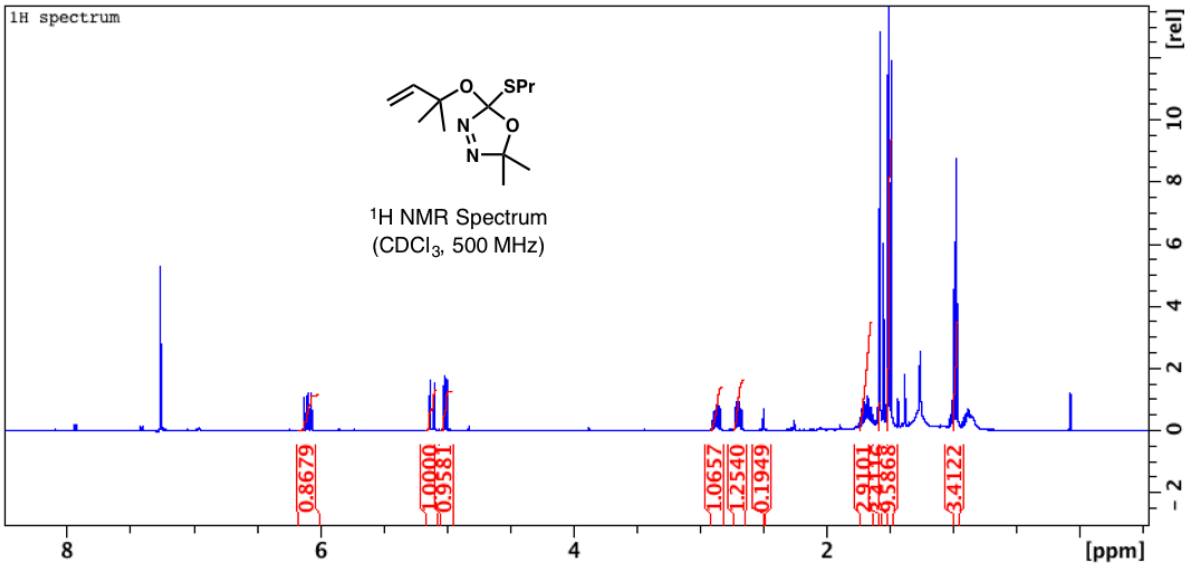

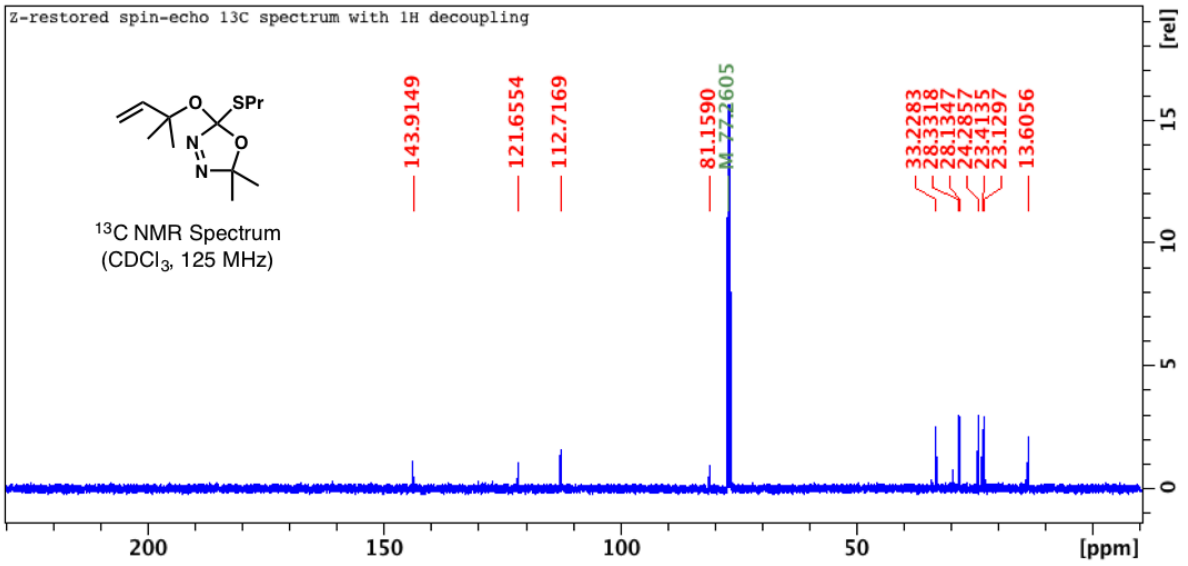

^{1}H and ^{13}C NMR spectra for (racemic) **allylic morpholine oxadiazoline 76**:

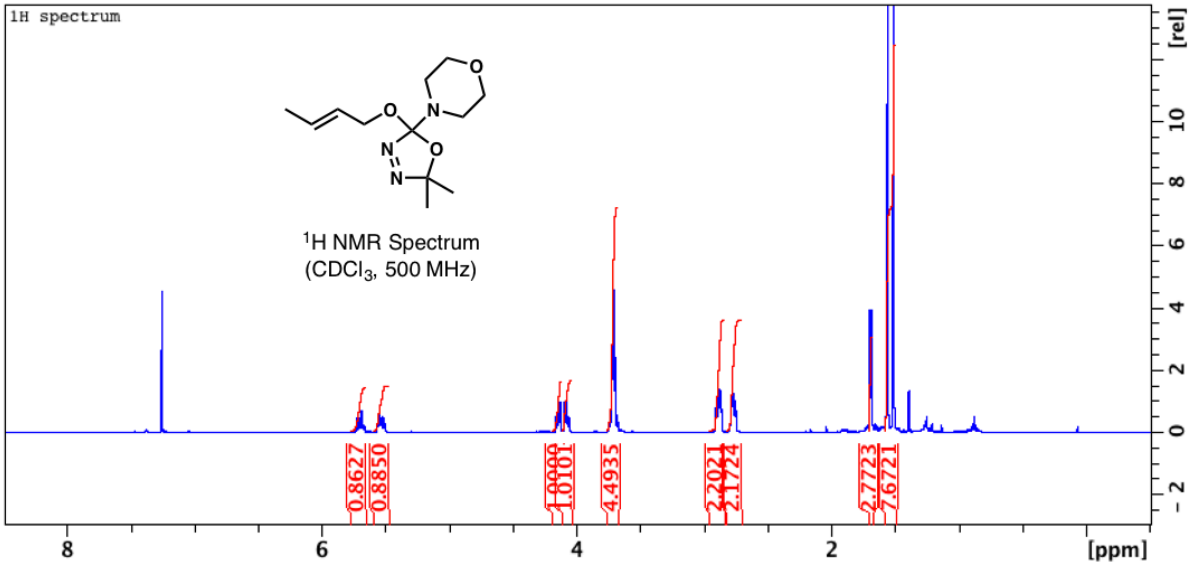

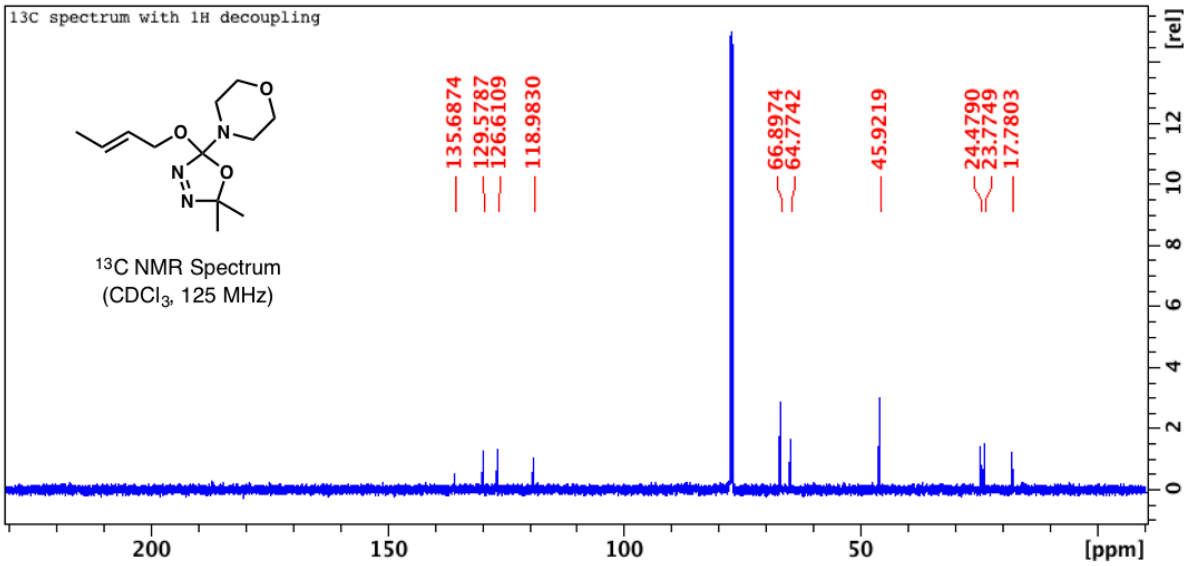

^{1}H NMR spectrum for crude **allylic amide 78 (from 76)—only discernable product**:

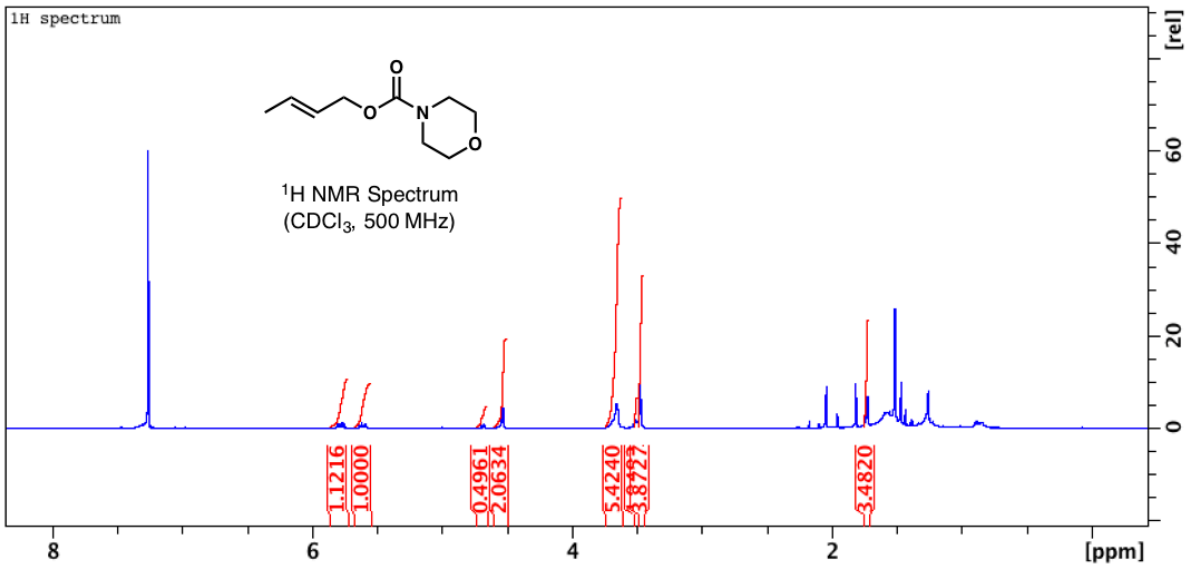

^{1}H and ^{13}C NMR spectra for **vinylsilane alkyl alcohol 98**:

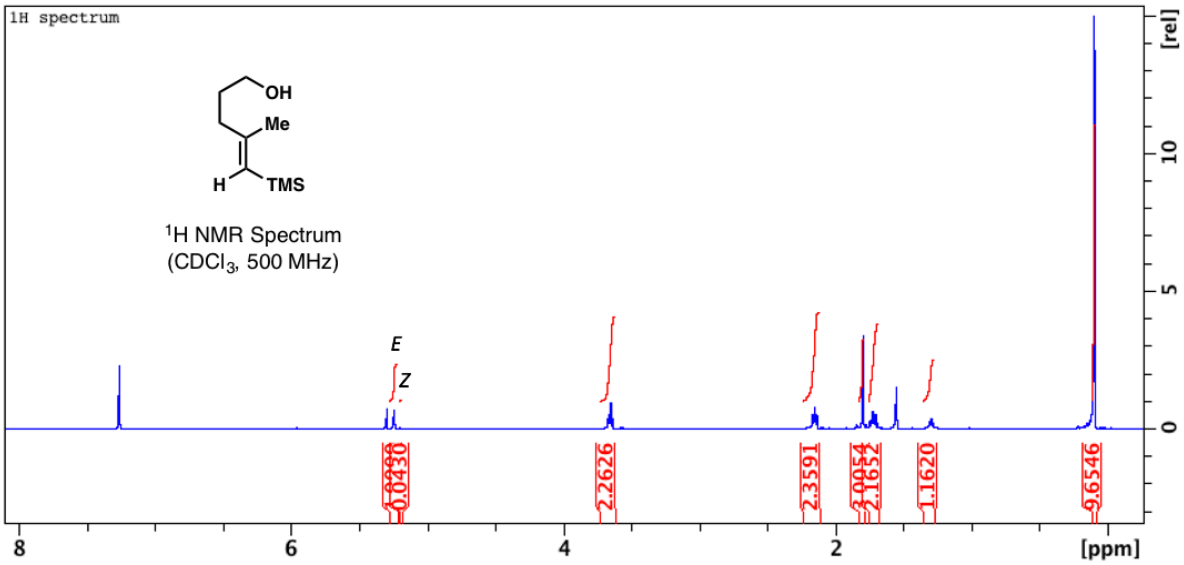

^{1}H and ^{13}C NMR spectra for **vinylsilane alkyl iodide 99**:

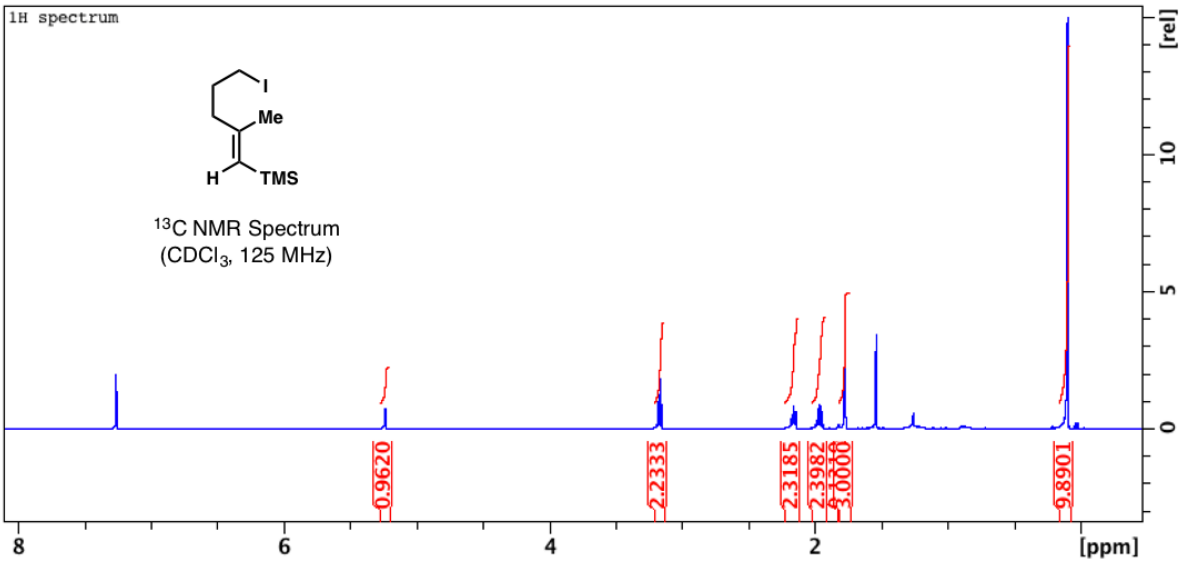

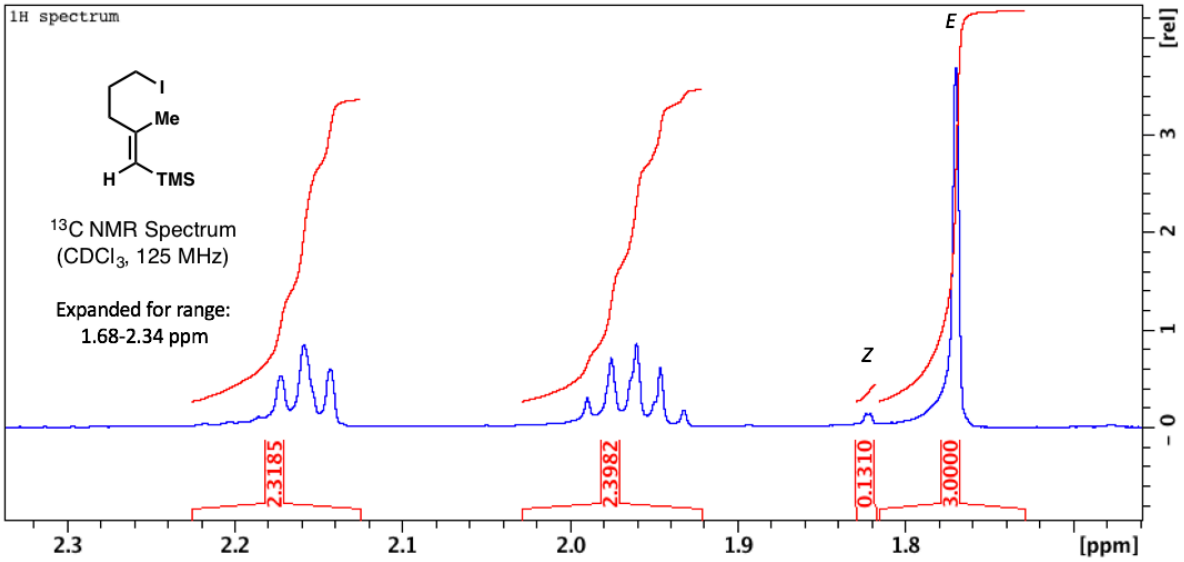
1H spectrum
I
Me
H
TMS
13C NMR Spectrum
(CDCl3, 125 MHz)
Expanded for range:
1.68-2.34 ppm
E
Z
2.3185
2.3982
0.1310
3.0000
2.3
2.2
2.1
2.0
1.9
1.8
[ppm]
[rel]

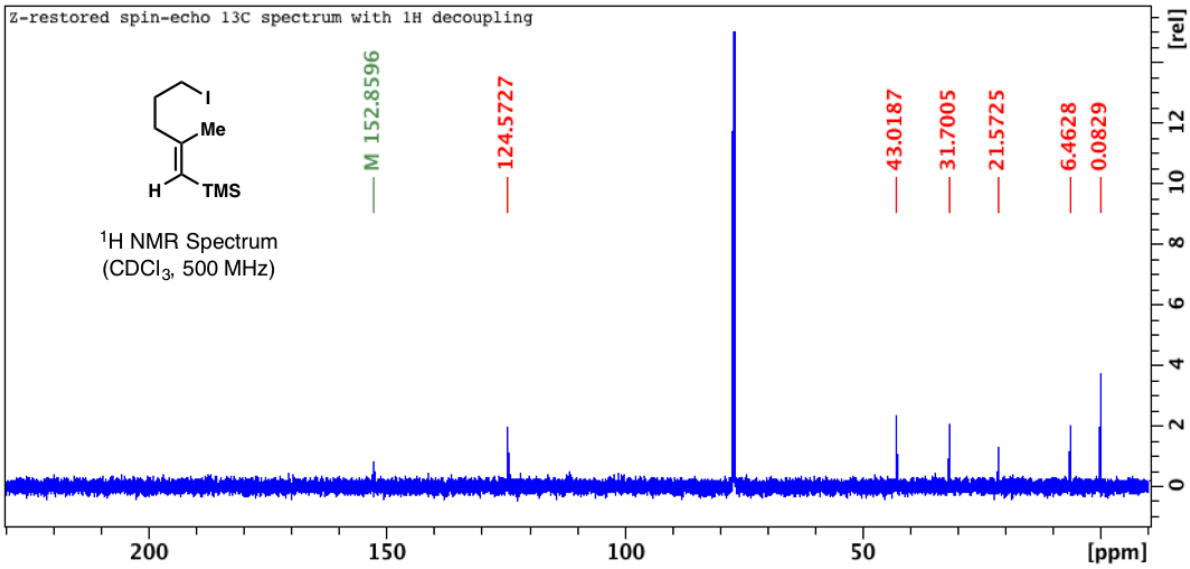
Z-restored spin-echo 13C spectrum with 1H decoupling
I
Me
H
TMS
1H NMR Spectrum
(CDCl3, 500 MHz)
M 152.8596
124.5727
43.0187
31.7005
21.5725
6.4628
0.0829
200
150
100
50
[ppm]
[rel]

^{1}H and ^{13}C NMR spectra for **vinylsilane phosphonate 94**:

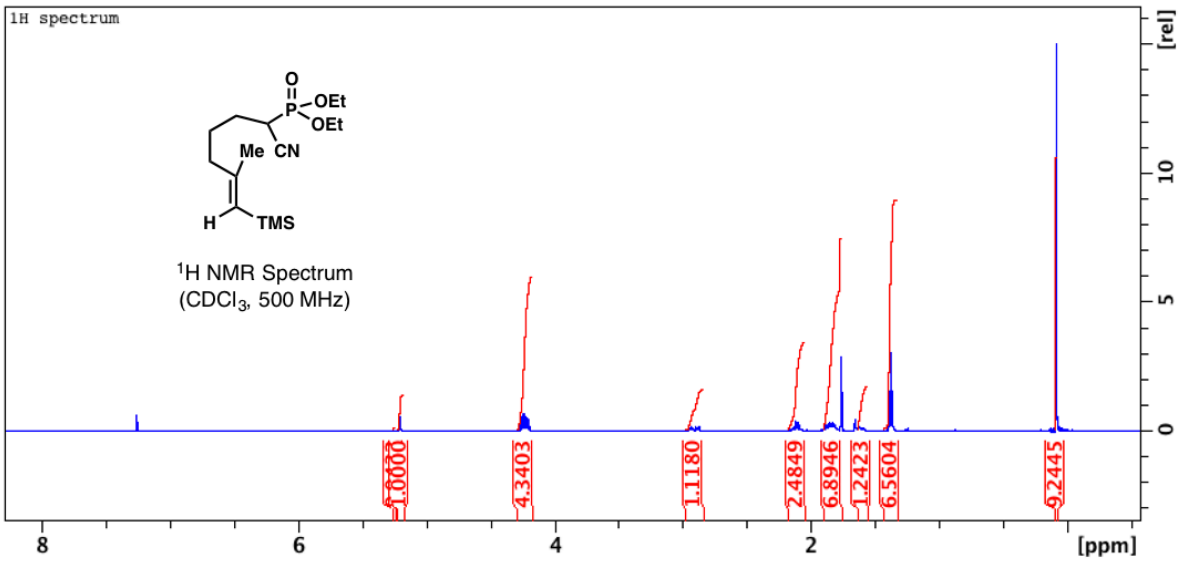

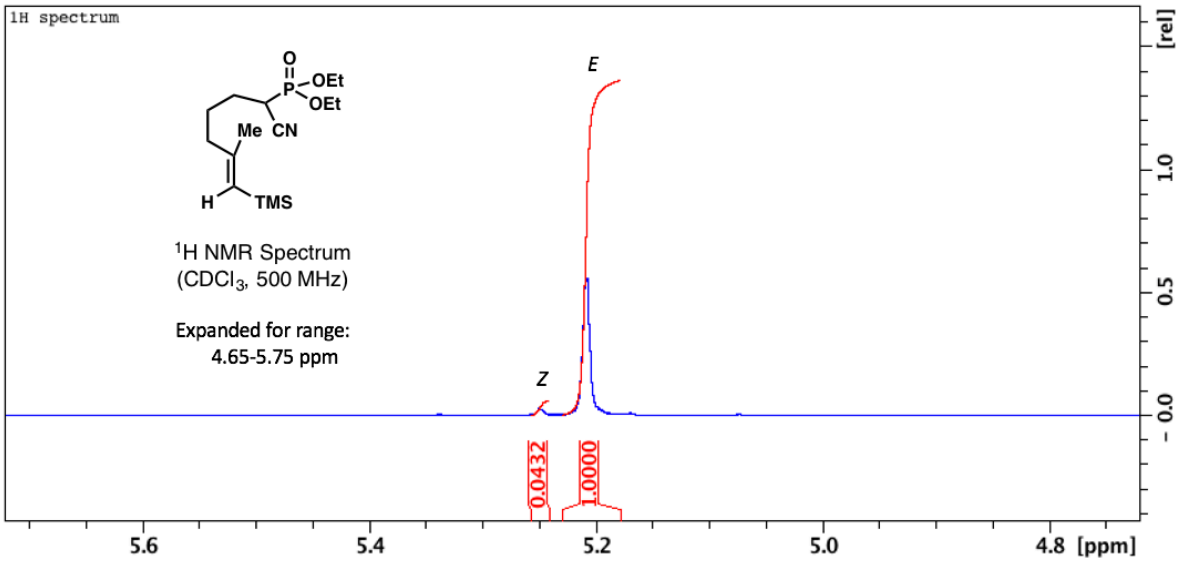

Alkene geometry for (racemic) vinylsilane phosphonate **33**: As shown above, *E*:*Z* ratio = 23:1; inseparable mixture; this ratio was the same as in the spectra of the alkyl iodide **32** and alcohol **31**. Diastereotopic carbons and ^{31}P-^{13}C coupling in ^{13}C NMR: since **33** contains a stereogenic center, the methylenes and methyl groups within the ethyl moieties are diastereotopic. Furthermore, they are 2 and 3 bonds away from the P atom, respectively, causing observable ^{31}P-^{13}C coupling to occur. Therefore, each methylene and each methyl group in the ethyl moieties exhibits a doublet in the ^{13}C NMR (CH_2: 64.07 ppm, d, J = 7.0 Hz; CH_2: 63.73 ppm, d, J = 6.8 Hz; CH_3: 16.45 ppm, d, J = 2.5 Hz; CH_3: 16.41 ppm, d, J = 2.6 Hz), etc.

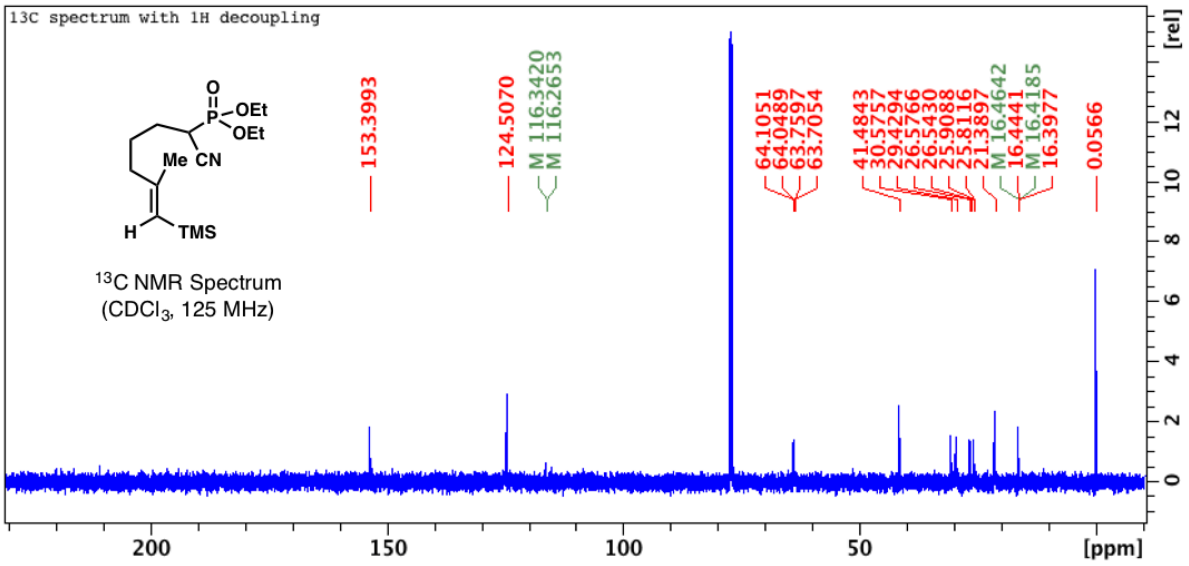

^{1}H and ^{13}C NMR spectra for **vinylsilane triene HWE product 93 (major of 3 distinguishable products)**: Extremely difficult to separate on preparatory TLC plates and even with argentation chromatography.

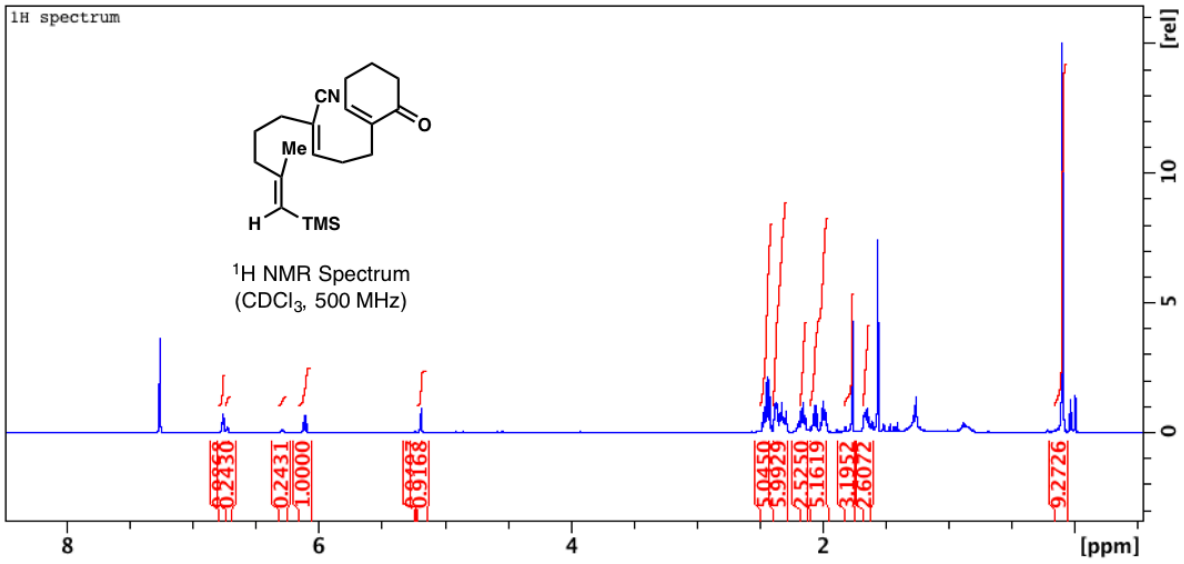

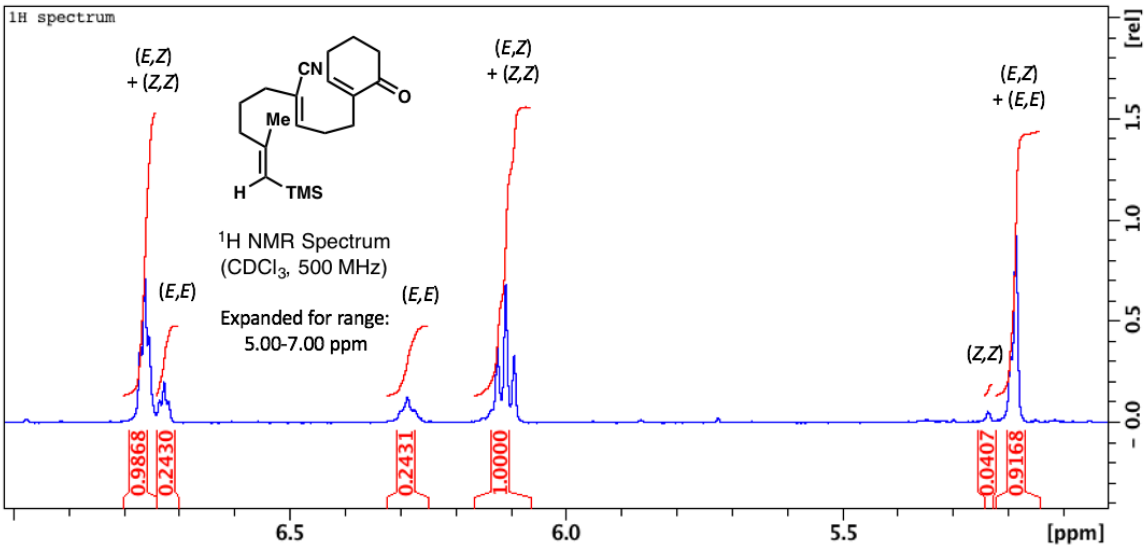

Calculations to determine the ratio of diastereomers in **34**.

i) In comparison of vinylic proton peaks beta to the nitrile:

$D_{(E,E)} = 0.2431$, $D_{(E,Z)} + D_{(Z,Z)} = 1.0000 \rightarrow D_{(E,Z)} + D_{(Z,Z)} = 4.1135(D_{(E,E)})$

$\rightarrow D_{(E,Z)} = 4.1135(D_{(E,E)}) - D_{(Z,Z)}$

ii) In comparison of vinylic proton peaks vicinal to silane:

$D_{(Z,Z)} = 0.0407$, $D_{(E,Z)} + D_{(E,E)} = 0.9168 \rightarrow D_{(E,Z)} + D_{(E,E)} = 22.5258(D_{(Z,Z)})$

iii) Combining solutions of i) and ii):

$D_{(E,Z)} = 4.1135(D_{(E,E)}) - D_{(Z,Z)} = 4.1135(D_{(E,E)}) + (D_{(E,Z)} + D_{(E,E)})/22.5258$

$\rightarrow 4.1579(D_{(E,E)}) = 0.9556(D_{(E,Z)}) \rightarrow$ **$D_{(E,E)} = 0.2298(D_{(E,Z)})$**

iv) Combining solutions of ii) and iii):

$5.3511(D_{(E,E)}) = 22.5258(D_{(Z,Z)}) \rightarrow$ **$D_{(Z,Z)} = 0.23755(D_{(E,E)})$**

v) Determining the diastereomeric ratio from the solutions of iii) and iv):

$D_{(Z,Z)} = 0.23755(D_{(E,E)}) = 0.23755[0.2298(D_{(E,Z)})]$

$\rightarrow 0.05460(D_{(E,Z)}) = 0.23755(D_{(E,E)}) = D_{(Z,Z)}$

Therefore, $D_{(E,Z)} : D_{(E,E)} : D_{(Z,Z)} = 18.32:4.21:1.00$

i.e. **$(E,Z):(E,E):(Z,Z) \approx 18:4:1$**

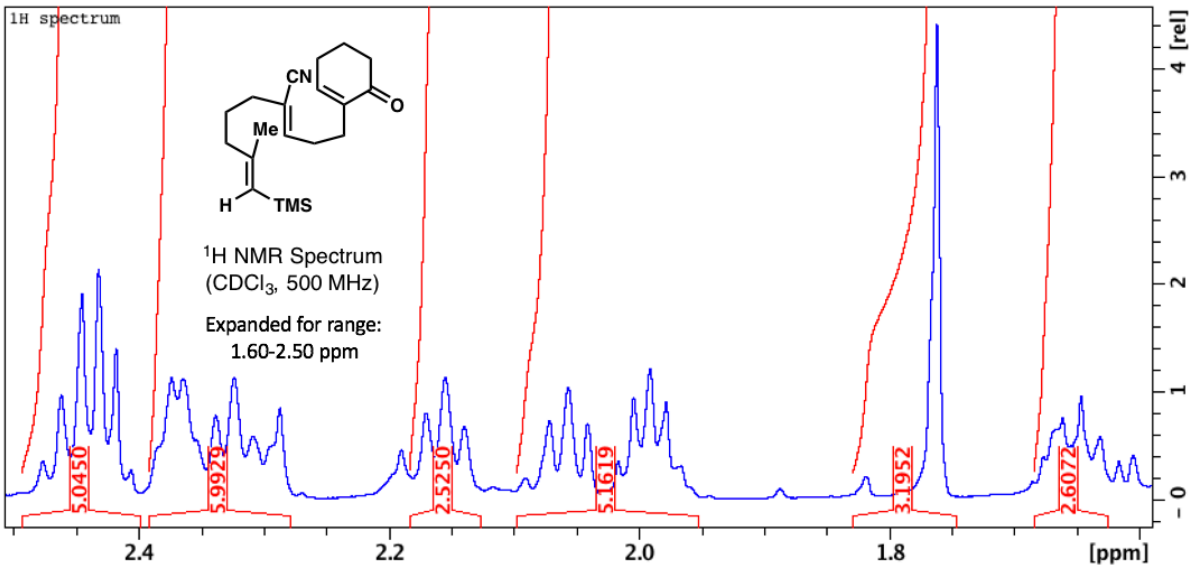
1H spectrum
CN
O
Me
H
TMS
^{1}H NMR Spectrum
(CDCl$_3$, 500 MHz)
Expanded for range:
1.60-2.50 ppm
5.0450
5.9929
2.5250
5.1619
3.1952
2.6072
2.4
2.2
2.0
1.8
[ppm]
4 [rel]
3
2
1
0

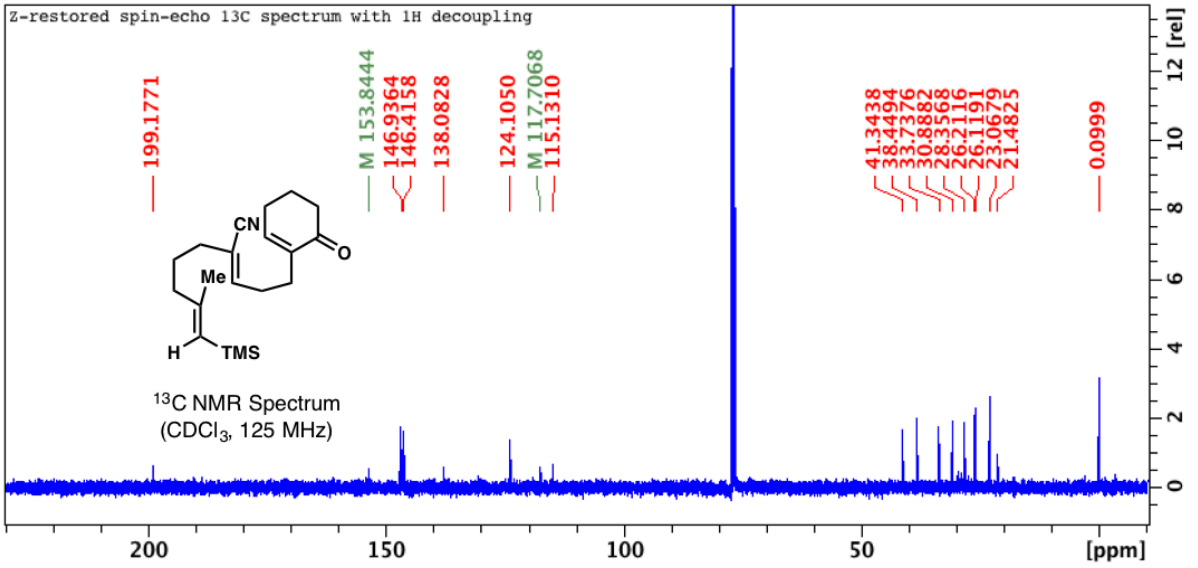
Z-restored spin-echo 13C spectrum with 1H decoupling
199.1771
M 153.8444
146.9364
146.4158
138.0828
124.1050
M 117.7068
115.1310
41.3438
38.4494
33.7376
30.8882
28.3568
26.2116
26.1191
23.0679
21.4825
0.0999
CN
O
Me
H
TMS
^{13}C NMR Spectrum
(CDCl$_3$, 125 MHz)
200
150
100
50
[ppm]
12 [rel]
10
8
6
4
2
0

COSY

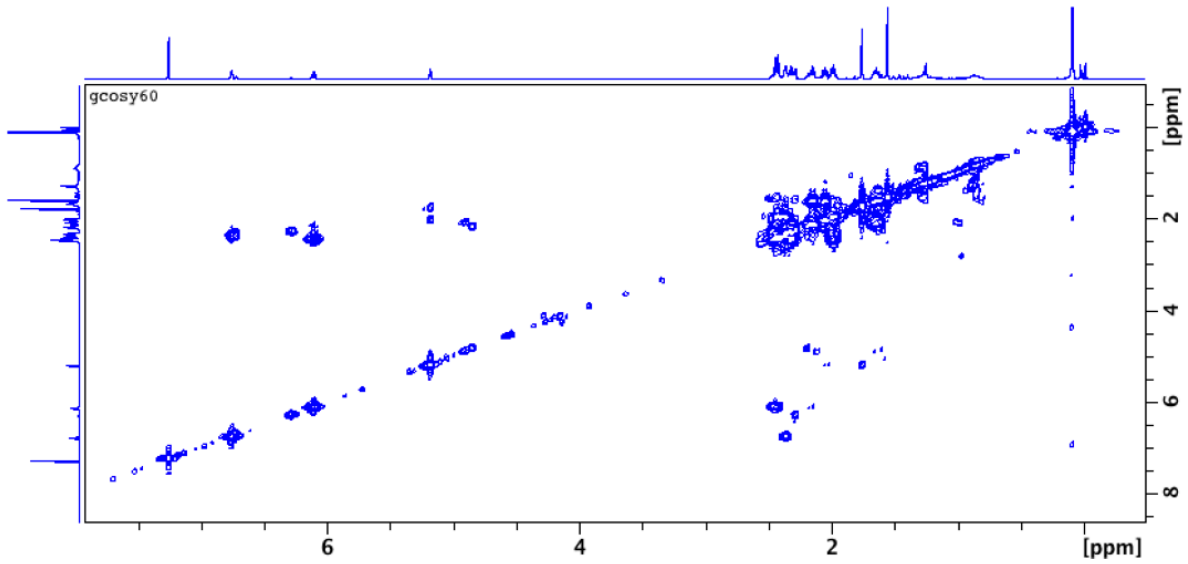

COSY expanded for range: [$^{1}H_{x}$: 1.95-2.12 ppm, $^{1}H_{y}$: 5.00-5.27 ppm]; the vinylic proton geminal to the TMS group (distinguishable by its lack of strong coupling and characteristic chemical shift of 5.17 ppm) show allylic coupling to adjacent allylic methylene protons at 2.06 ppm.

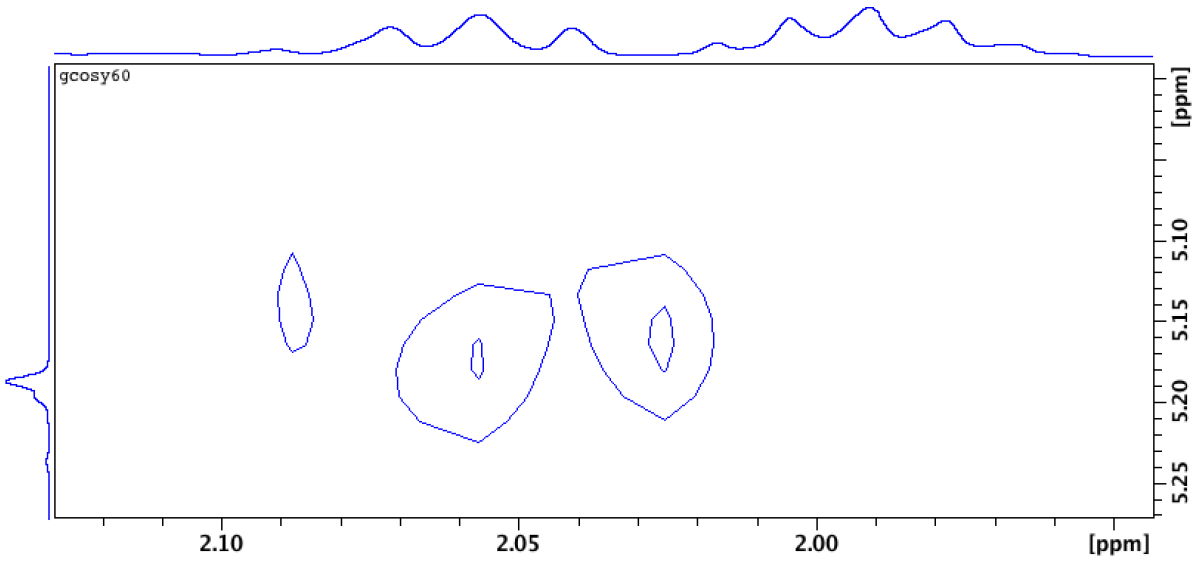

COSY expanded for range: [$^{1}H_{x}$: 1.93-2.23 ppm, $^{1}H_{y}$: 1.51-1.83 ppm]; the allylic methylene protons adjacent to the methyl group at 2.06 ppm show strong coupling to bis(homoallylic) methylene protons at 1.63 ppm, which in turn show strong coupling to the methylene sp^{3} protons beta to the nitrile at 2.15 ppm.

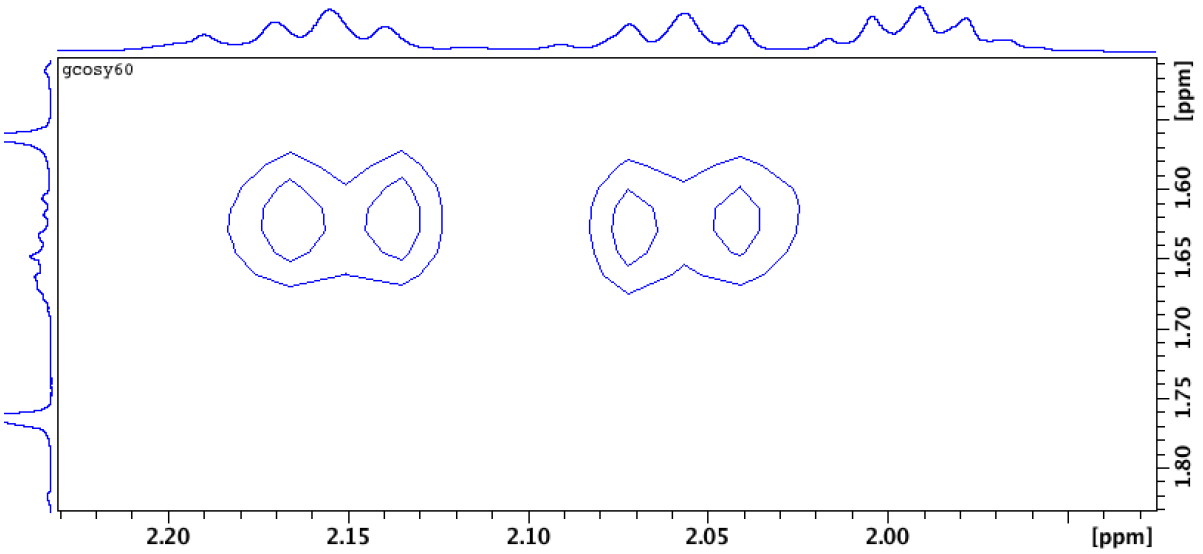

NOESY

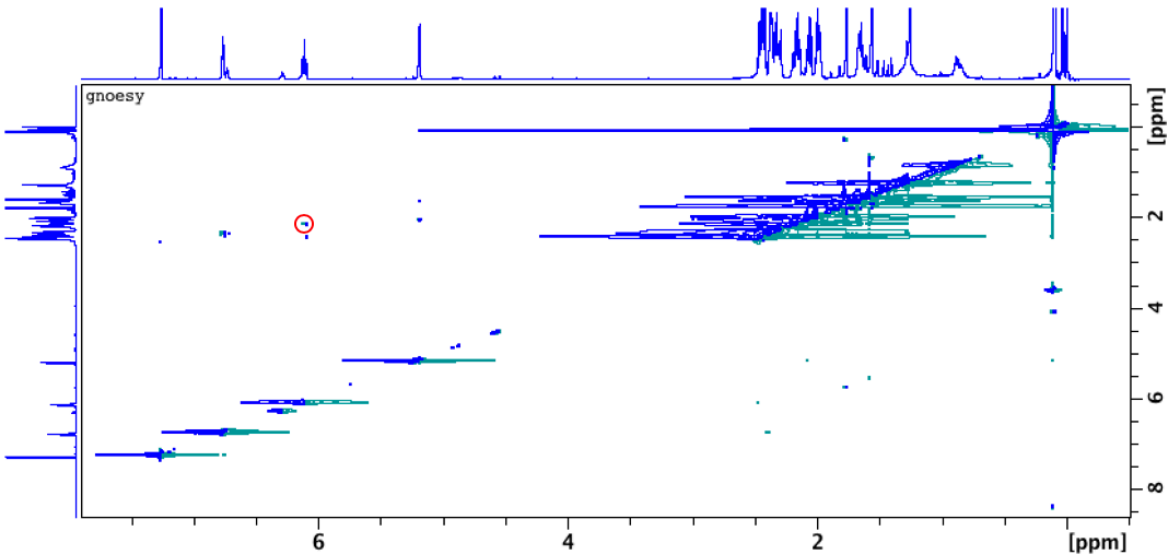

NOESY expanded for range: [$^{1}H_{x}$: 5.92-6.24 ppm, $^{1}H_{y}$: 2.11-2.22 ppm]; The methylene sp^3 protons beta to the nitrile at 2.15 ppm (established in the above COSY data) show a clear strong correlation to the vinylic sp^2 proton beta to the nitrile at 6.10 ppm—much stronger than the correlation between the latter proton and the methylene sp^3 protons gamma to both the nitrile and carbonyl which shows coupling in the COSY and ^{1}H-NMR (causing triplet splitting at the peak with a 6.10 ppm chemical shift).

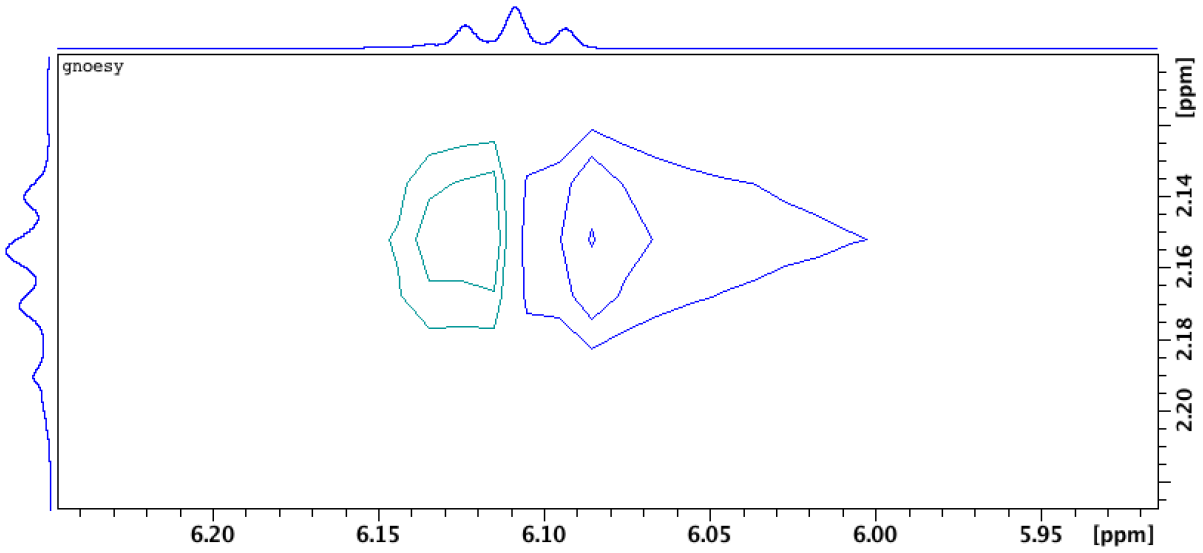

Two pieces of spectral evidence support the assignment of (*Z*)-stereochemistry as the preferred geometry at the α,β-unsaturated nitrile, as expected. First, the β-vinylic proton in (*Z*)-diastereomers in trisubstituted nitriles (α,β-substituted) of this type typically exhibit a chemical shift below that of their (*E*)-diastereomer counterparts. Since the aforementioned β-vinylic protons were observed at approximately 6.1 ppm and 6.3 ppm, and the more upfield peak was found to have a higher relative area under

the curve (i.e. integrated value), the data was consistent with the expected stereochemical outcome. Second, the 2D-NOESY showed a strong correlation between the sp^2 proton beta to the nitrile and the methylene sp^3 protons beta to the nitrile (and no correlation between the methylene sp^3 protons beta to the nitrile and the methylene sp^3 protons gamma to both the nitrile and carbonyl), lending strong support to the notion that the actual stereochemical preference of the HWE aligned with the predicted (and desired) stereochemical outcome, favoring the (*Z*) over the (*E*)-geometry. The NOESY shows a strong correlation between the major product peak (6.1 ppm) and a peak at 2.15 ppm. The COSY reveals the latter peak to be associated with the protons on the sp^3 carbon beta to the nitrile.

^1H and ^{13}C NMR spectra for ***α*-silyl epoxide 104** (all diastereomers integrated in ^1H NMR; major diastereomer peak-picked in ^{13}C NMR):

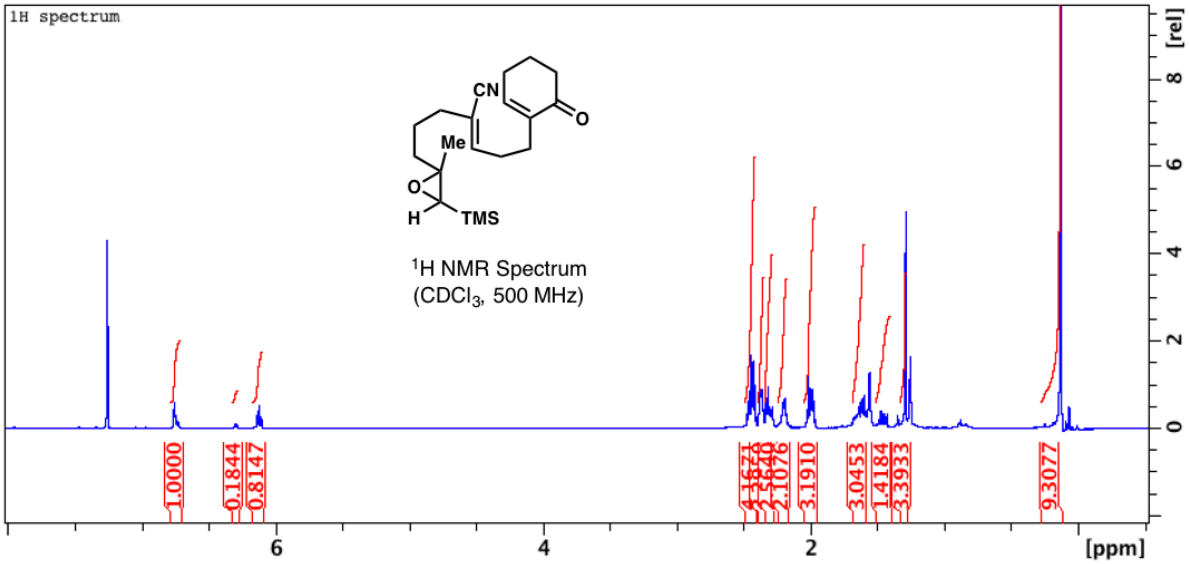

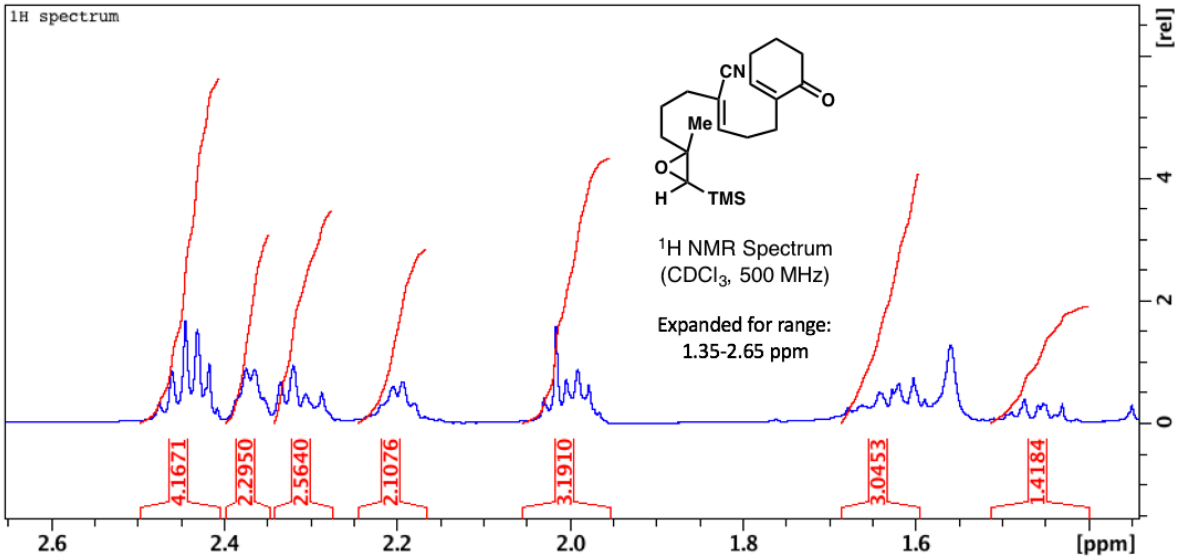
1H spectrum
CN
O
Me
O
H
TMS
^{1}H NMR Spectrum
($CDCl_3$, 500 MHz)
Expanded for range:
1.35-2.65 ppm
4.1671
2.2950
2.5640
2.1076
3.1910
3.0453
1.4184
2.6
2.4
2.2
2.0
1.8
1.6
[ppm]
[rel]

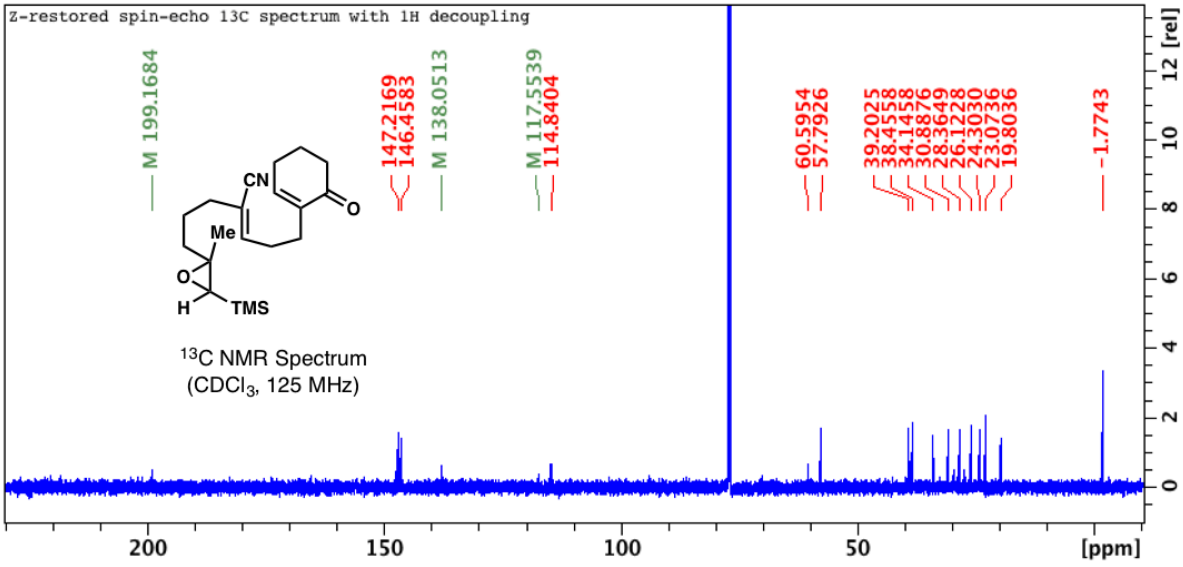
Z-restored spin-echo 13C spectrum with 1H decoupling
M 199.1684
147.2169
146.4583
M 138.0513
M 117.5539
114.8404
60.5954
57.7926
39.2025
38.4558
34.1458
30.8876
28.3649
26.1228
24.3030
23.0736
19.8036
-1.7743
CN
O
Me
O
H
TMS
^{13}C NMR Spectrum
($CDCl_3$, 125 MHz)
200
150
100
50
[ppm]
[rel]

^{1}H and ^{13}C NMR spectra for **epoxy alcohol 110**:

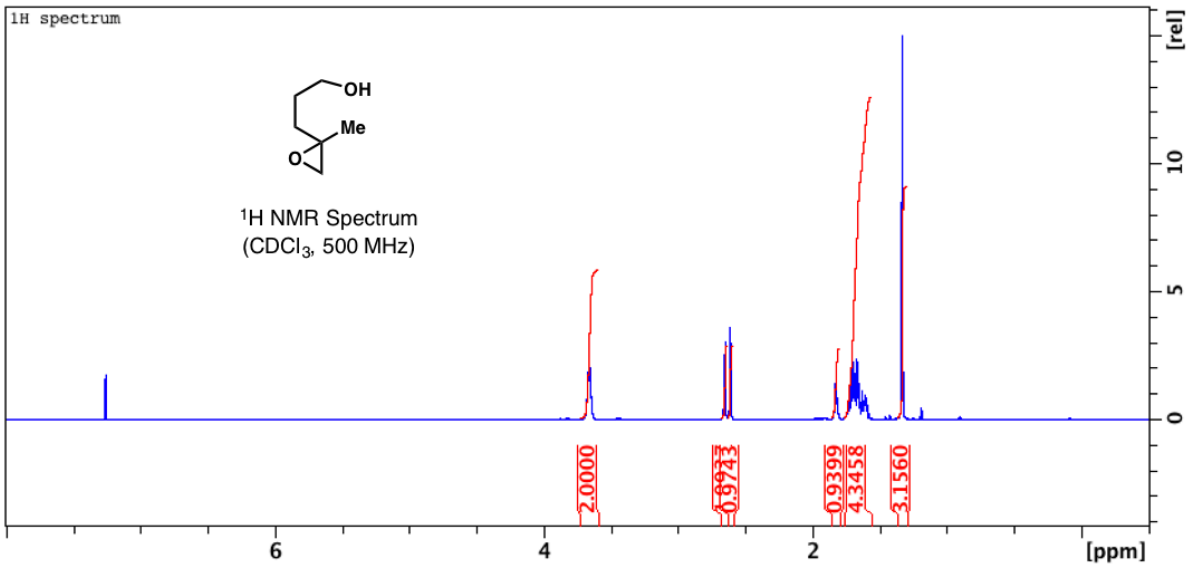

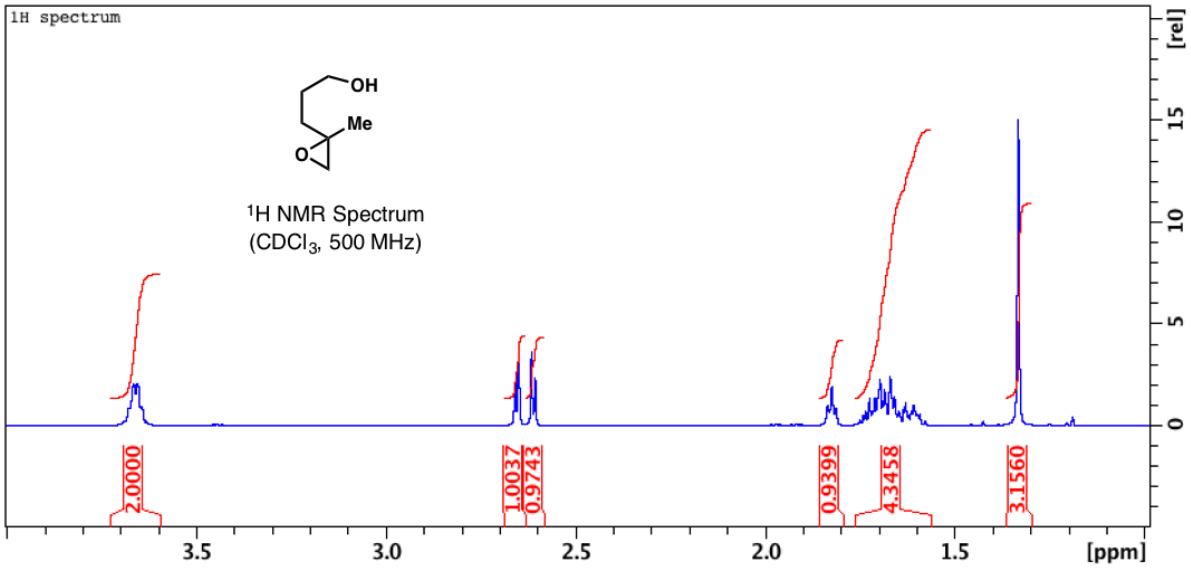

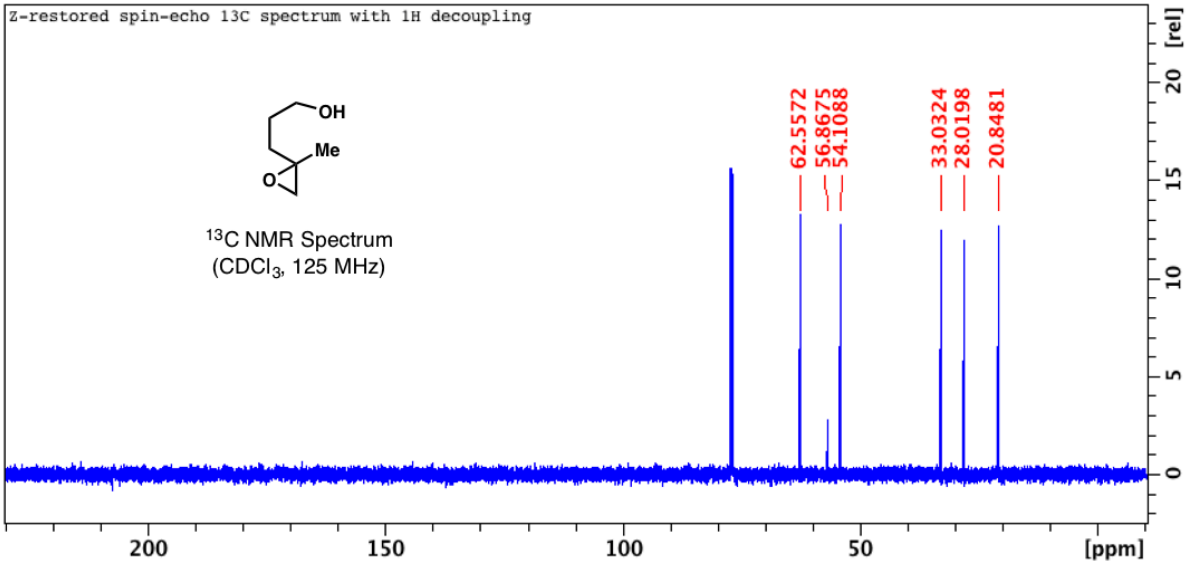

^{1}H and ^{13}C NMR spectra for crude **epoxy tosylate 116** (with lots of residual EtOAc—used in next reaction as is):

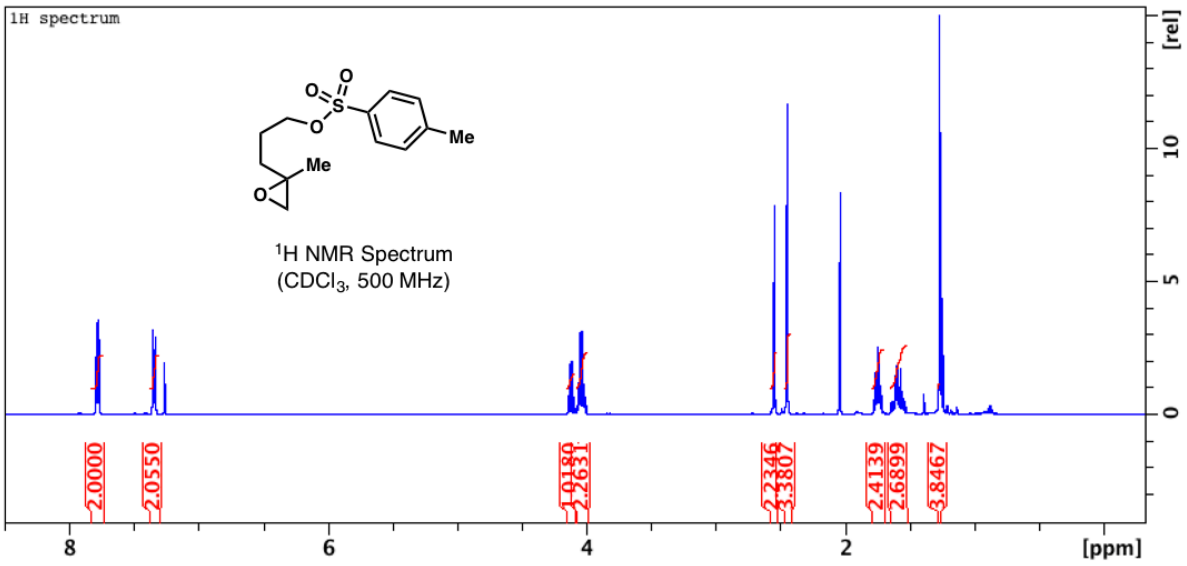

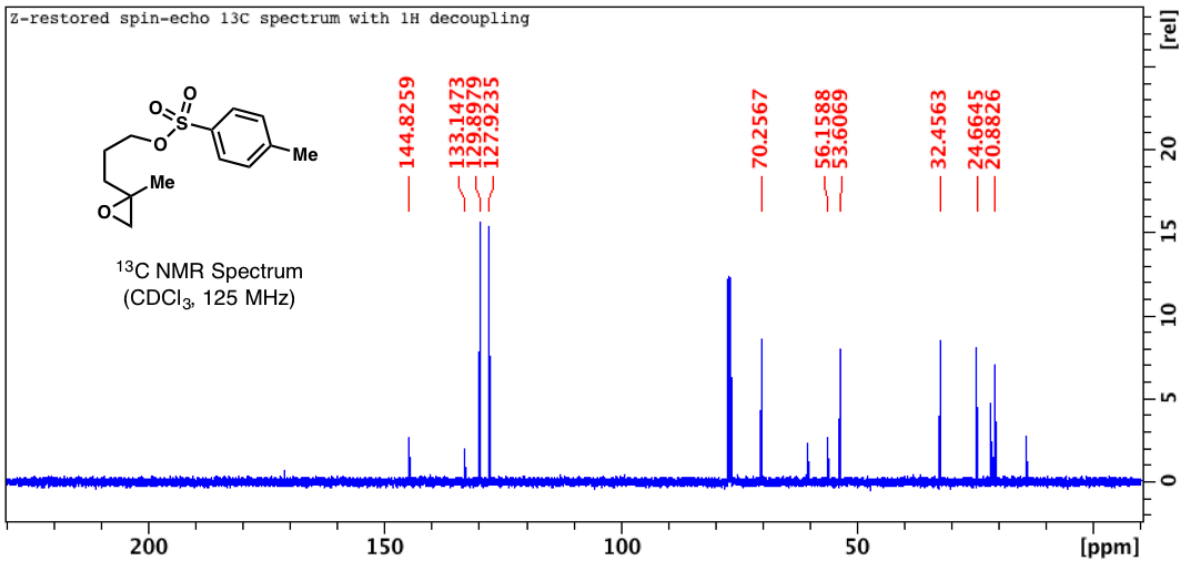

^{1}H and ^{13}C NMR spectra for crude **epoxy iodide 111**:

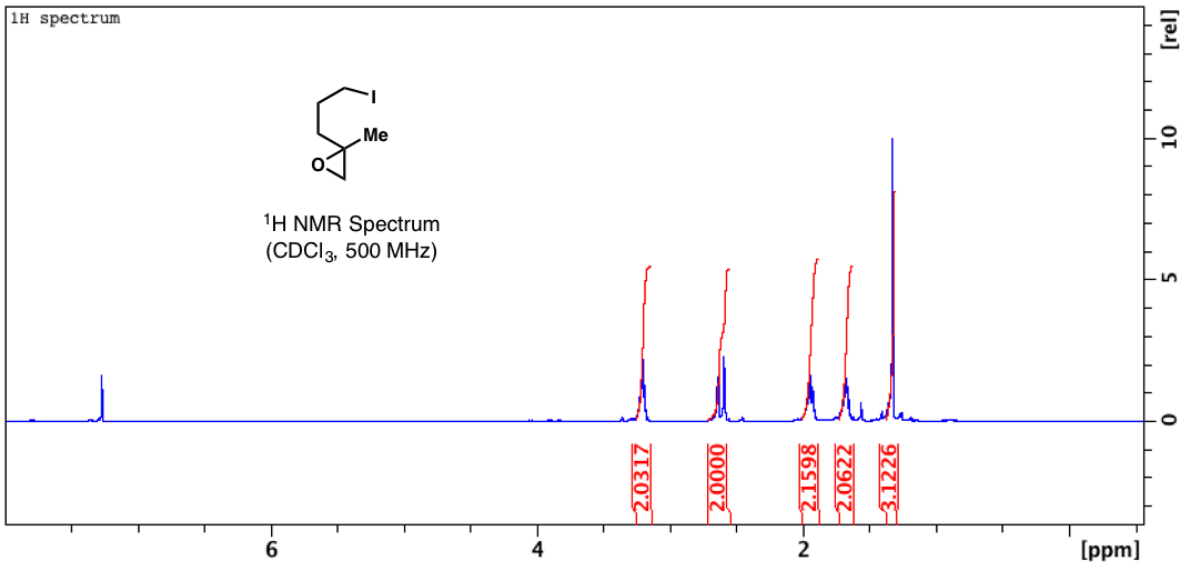

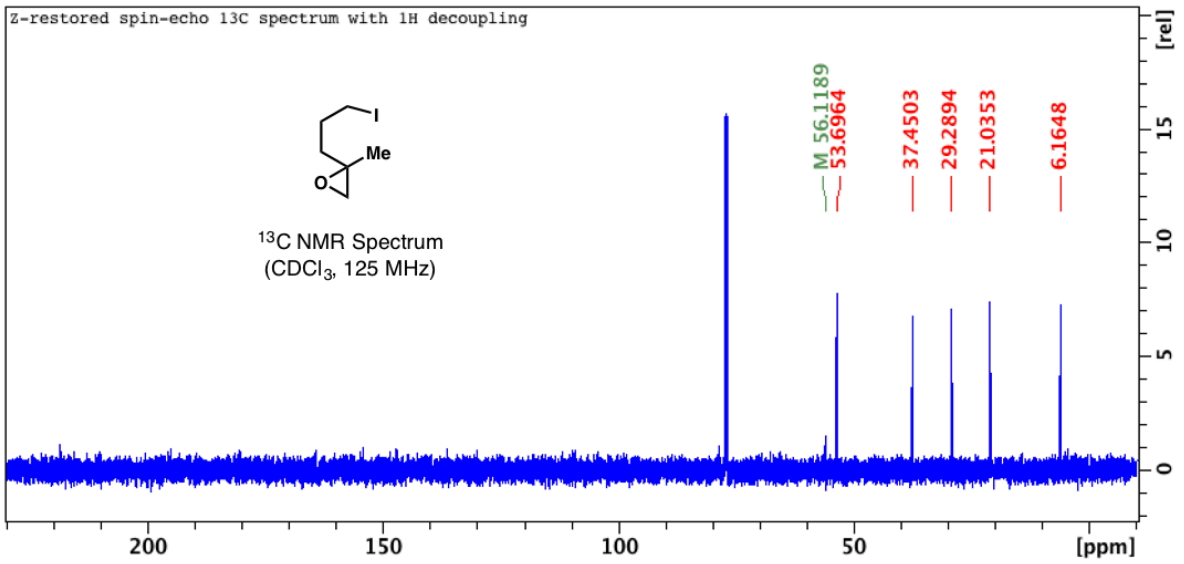

^{1}H and ^{13}C NMR spectra for (racemic) **1,1-disubstituted alkene tethered to phosphonate 118**:

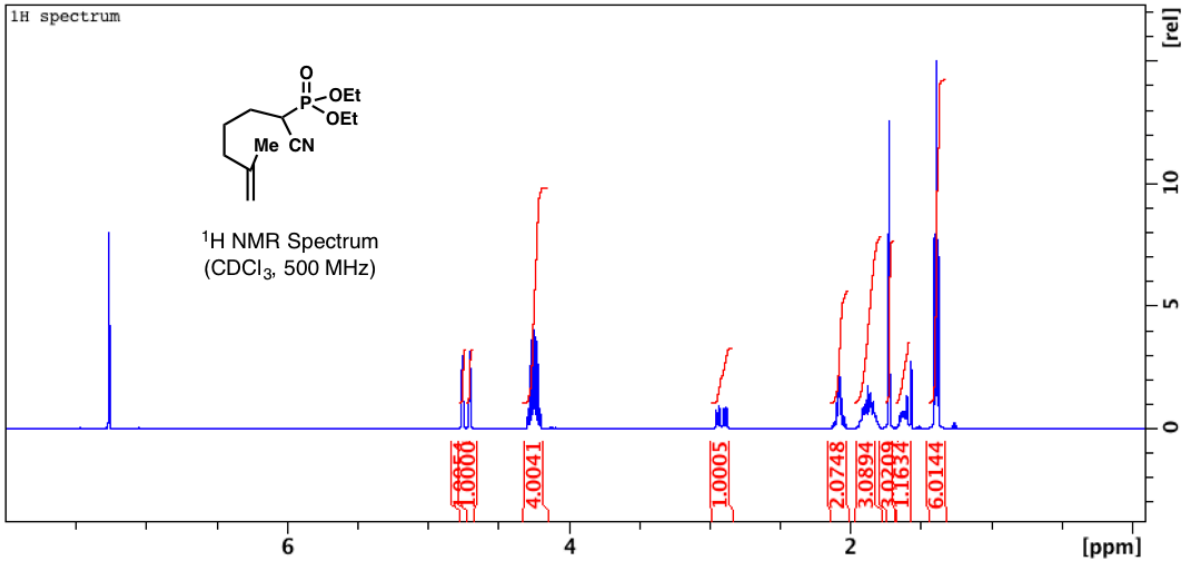

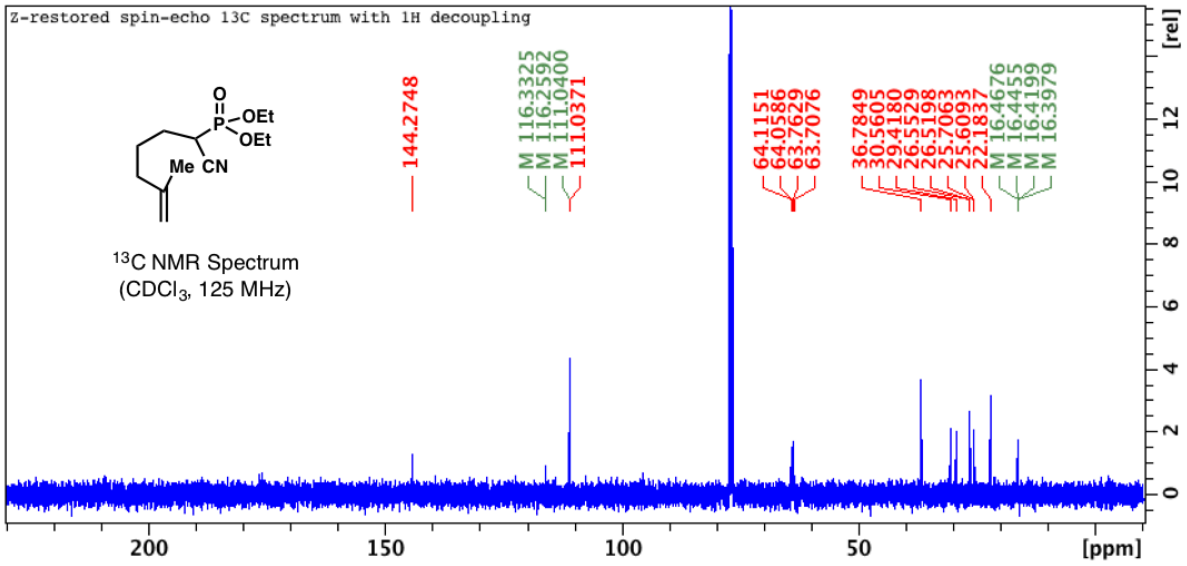

^{1}H and ^{13}C NMR spectra for (completed racemic fragment) **1,1-disubstituted epoxide tethered to phosphonate 112**:

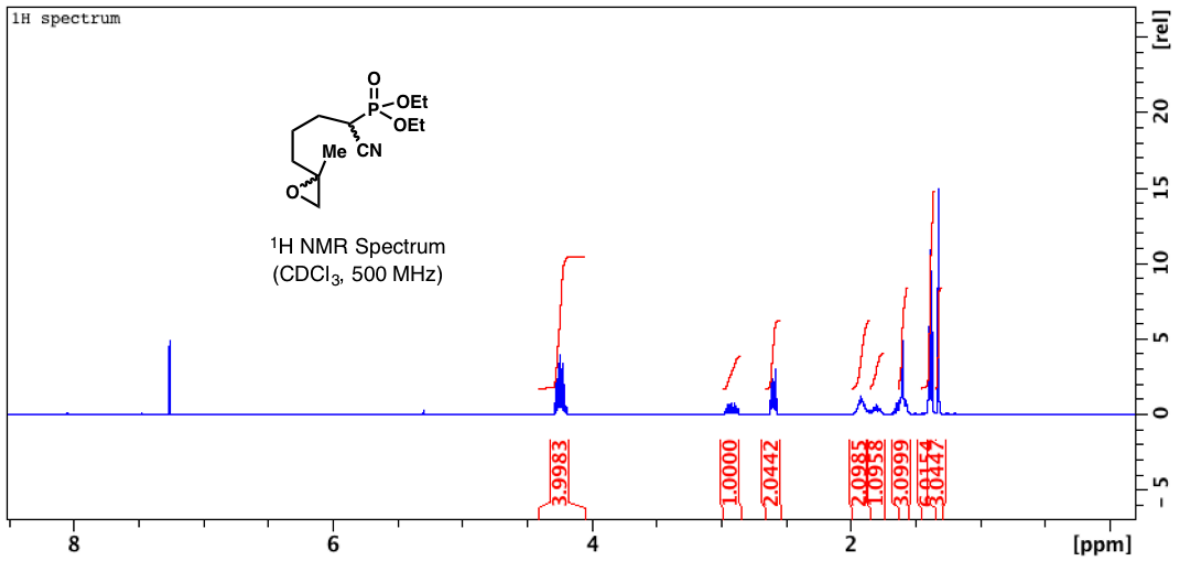

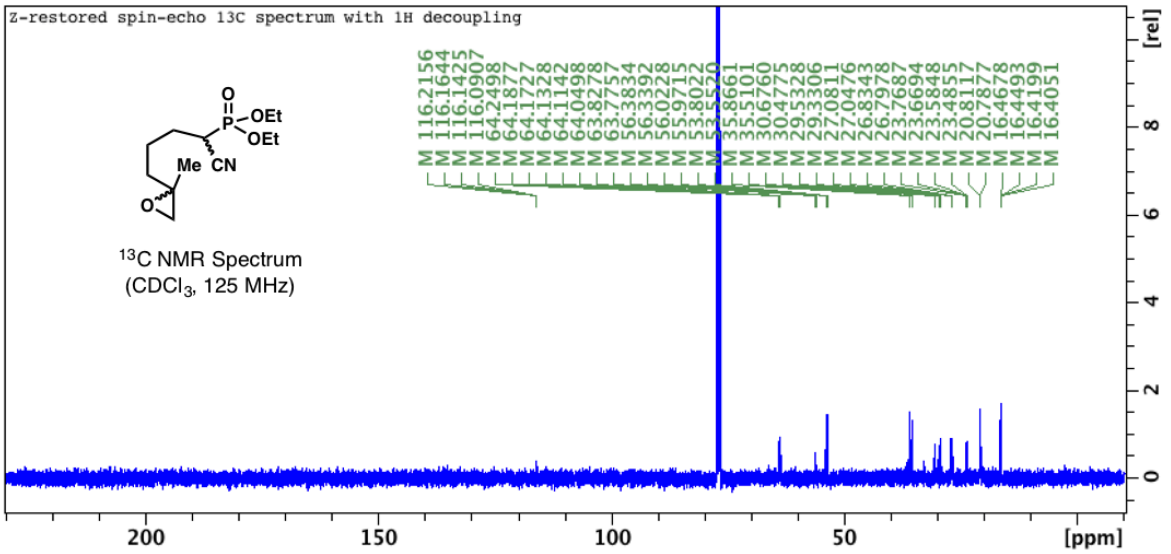
Z-restored spin-echo 13C spectrum with 1H decoupling
M 116.2156
M 116.1644
M 116.1425
M 116.0907
M 64.2498
M 64.1877
M 64.1727
M 64.1328
M 64.1142
M 64.0498
M 63.8278
M 63.7757
M 56.3834
M 56.3392
M 56.0228
M 55.9715
M 53.8022
M 53.5520
M 35.8661
M 35.5101
M 30.6760
M 30.4775
M 29.5328
M 29.3306
M 27.0811
M 27.0476
M 26.8343
M 26.7978
M 23.7687
M 23.6694
M 23.5848
M 23.4855
M 20.8117
M 20.7877
M 16.4678
M 16.4493
M 16.4199
M 16.4051
O
P
OEt
OEt
Me
CN
O
13C NMR Spectrum
(CDCl3, 125 MHz)
[rel]
0
2
4
6
8
200
150
100
50
[ppm]

114-118.5 ppm:

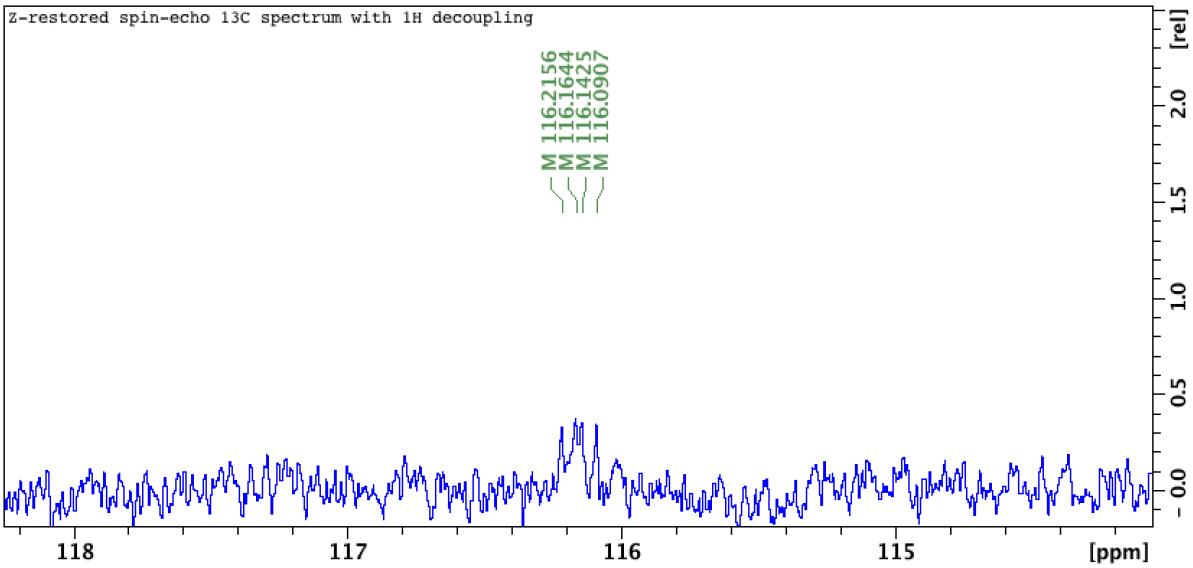
Z-restored spin-echo 13C spectrum with 1H decoupling
M 116.2156
M 116.1644
M 116.1425
M 116.0907
[rel]
- 0.0
0.5
1.0
1.5
2.0
118
117
116
115
[ppm]

48.5-70.0 ppm:

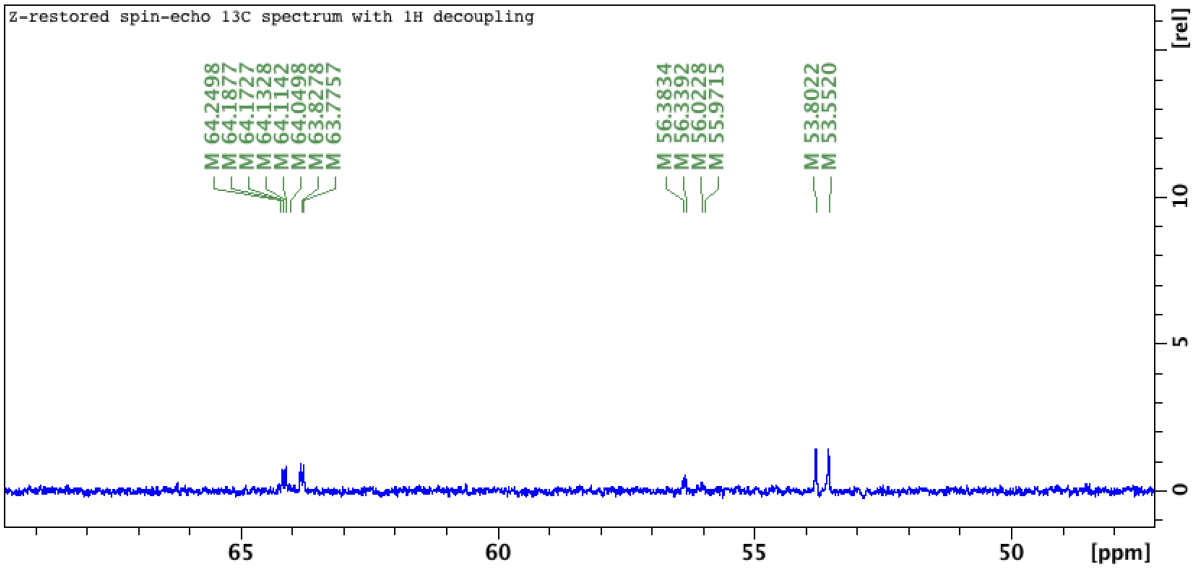

28.5-36.5 ppm:

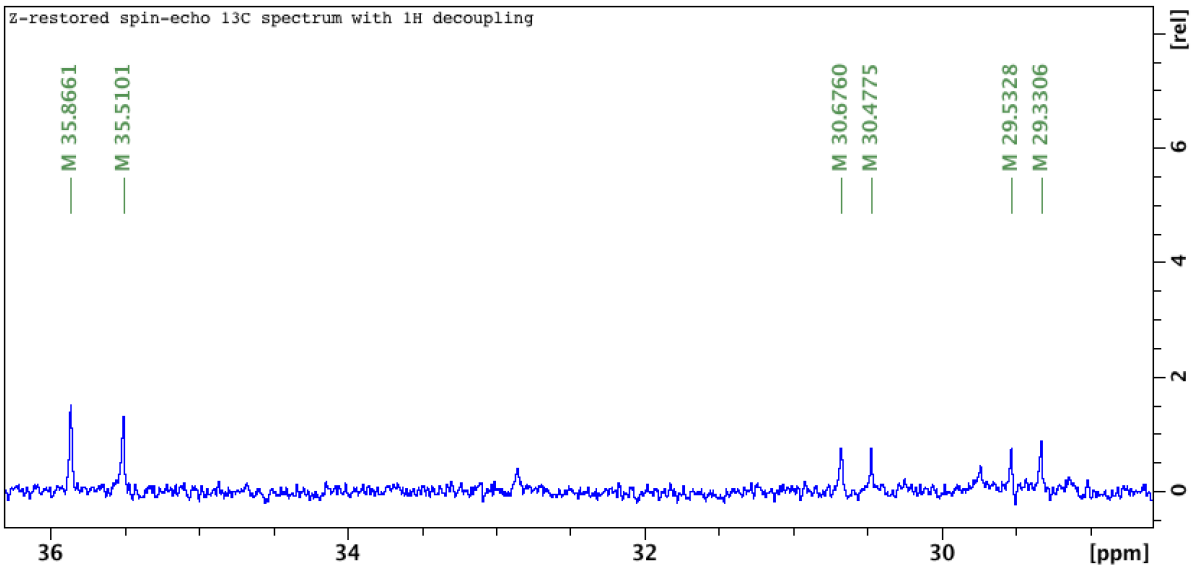

19.5-28.0 ppm:

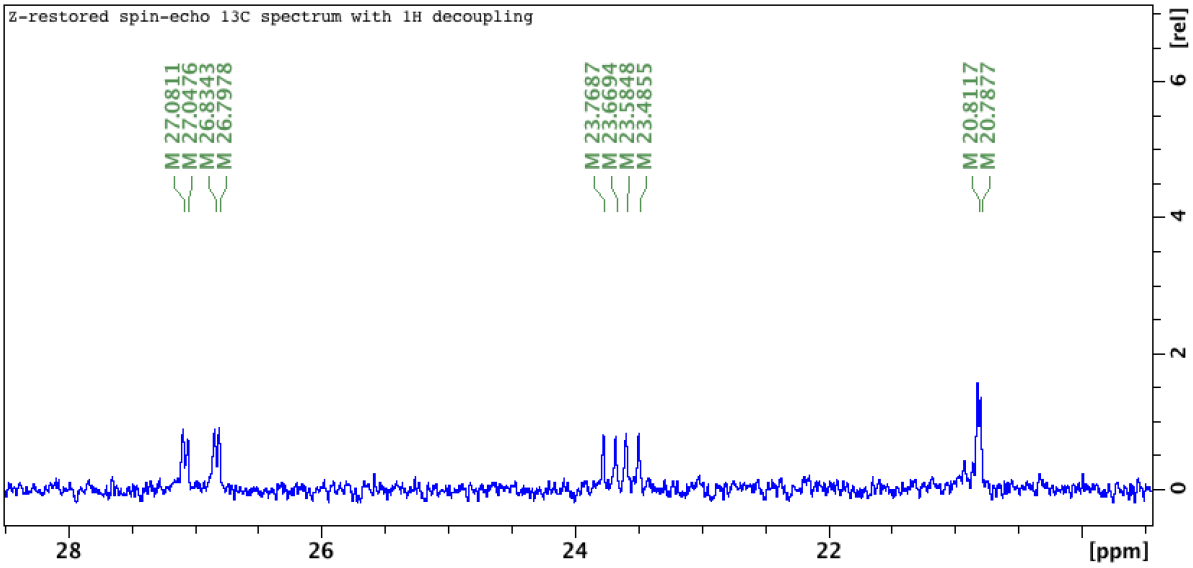

15.80-16.95; two doublets overlapping:

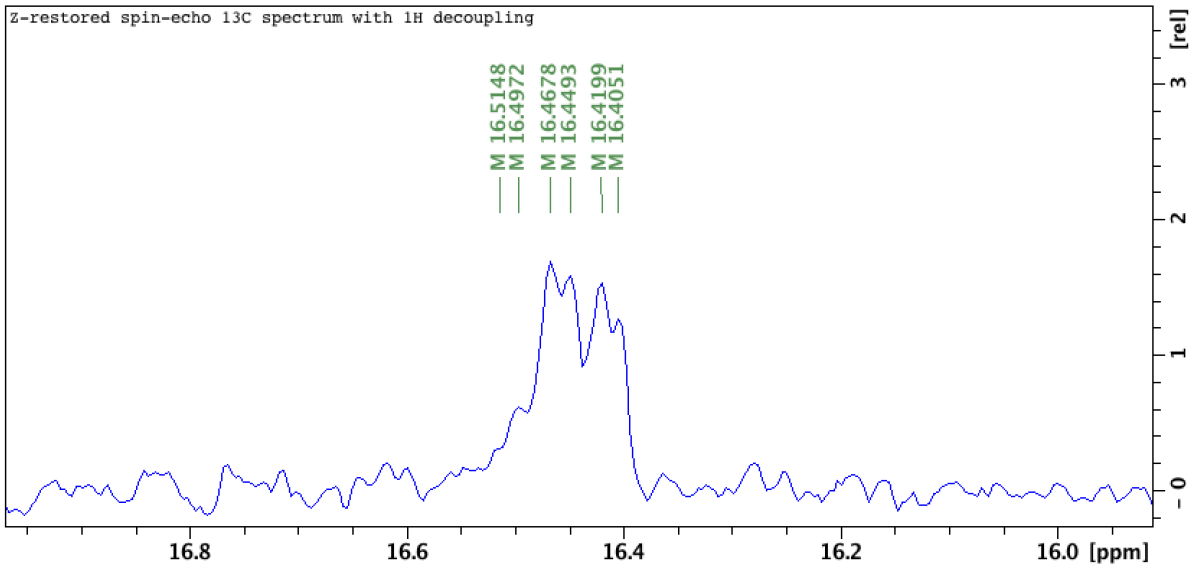

^{1}H and ^{13}C NMR spectra for **cyclic allylic alcohol-acetal 105**:

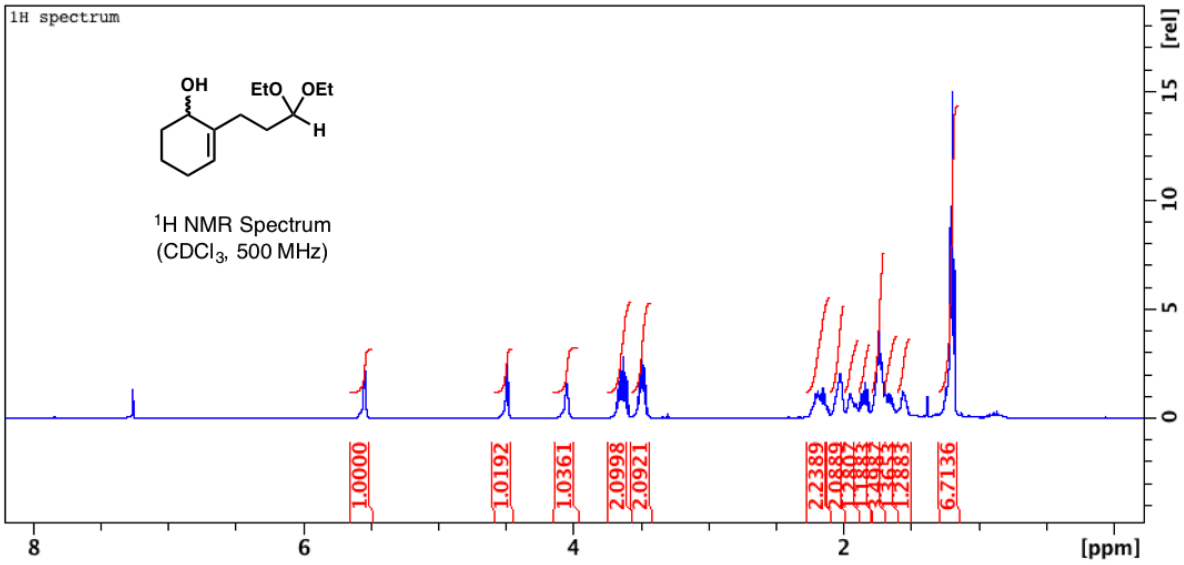

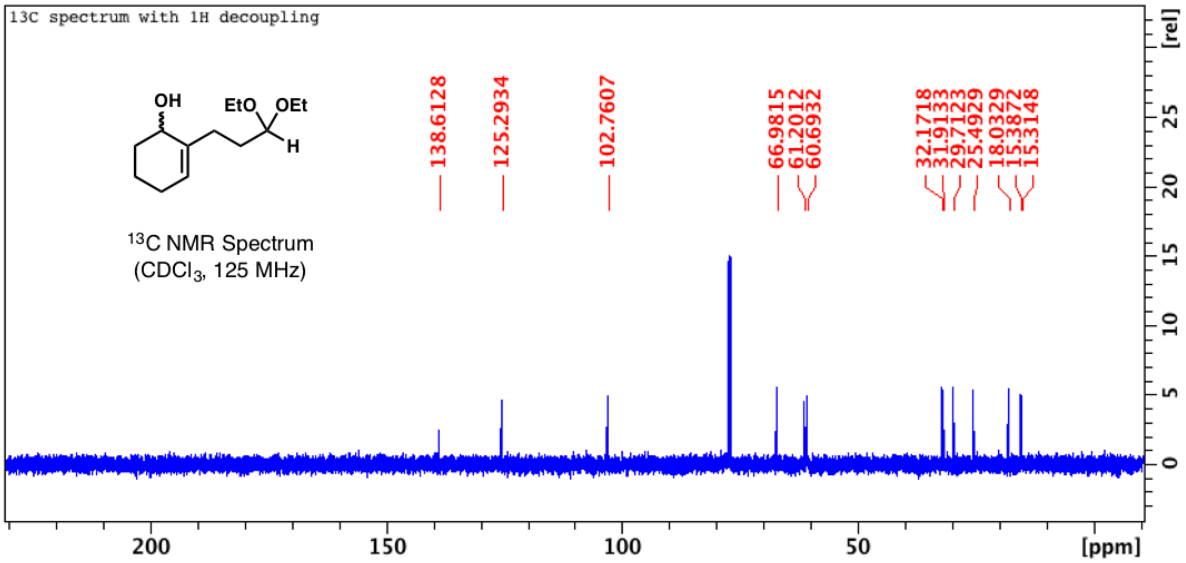

^{1}H and ^{13}C NMR spectra for **cyclic allylic acetate-acetal 107**:

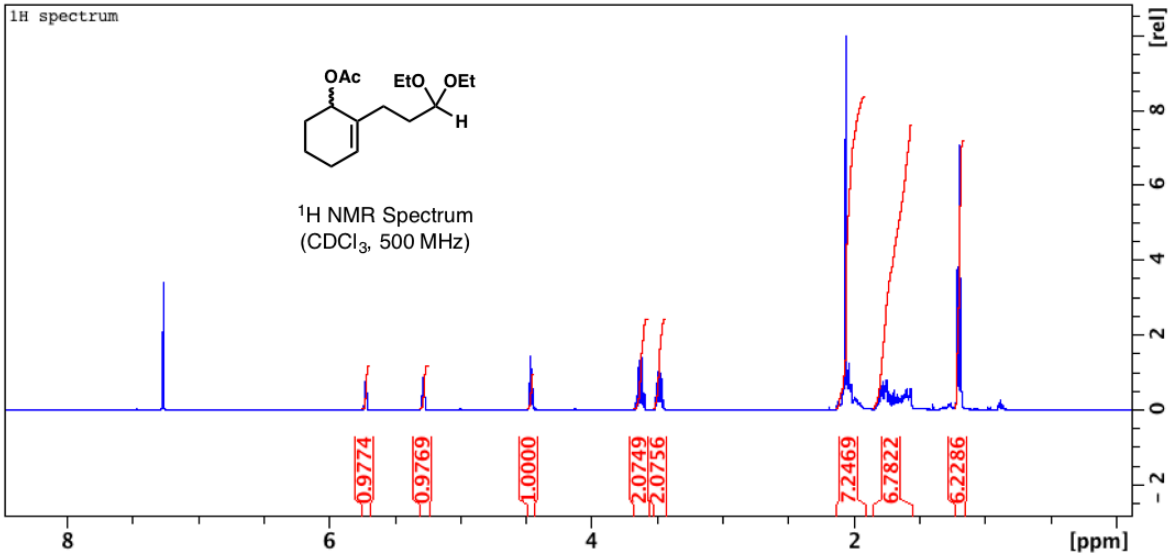

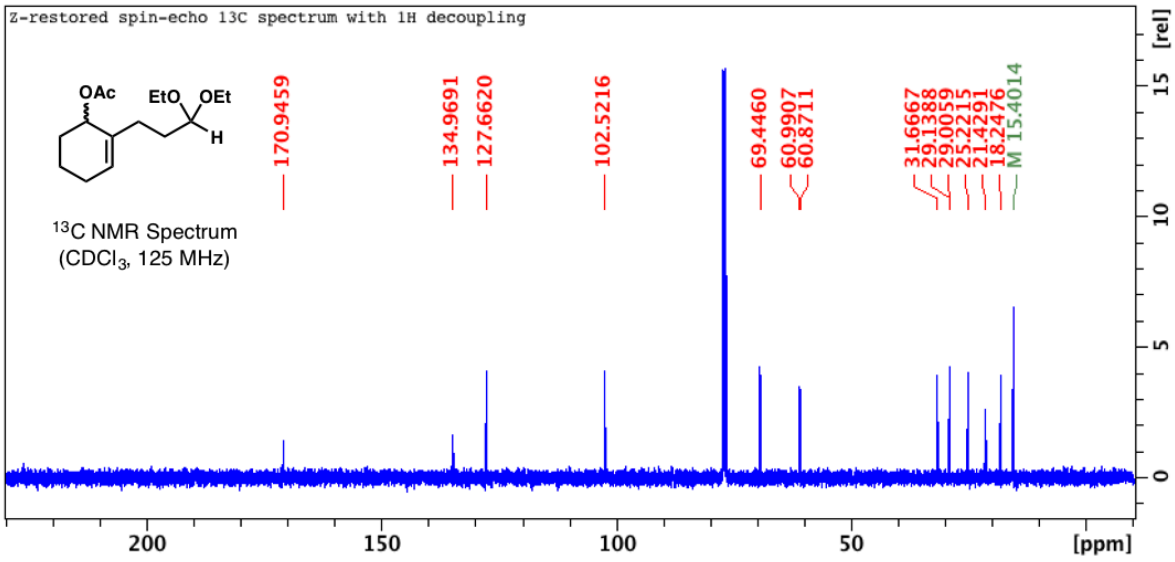

^{1}H and ^{13}C NMR spectra for **cyclic allylic acetate-aldehyde 108**:

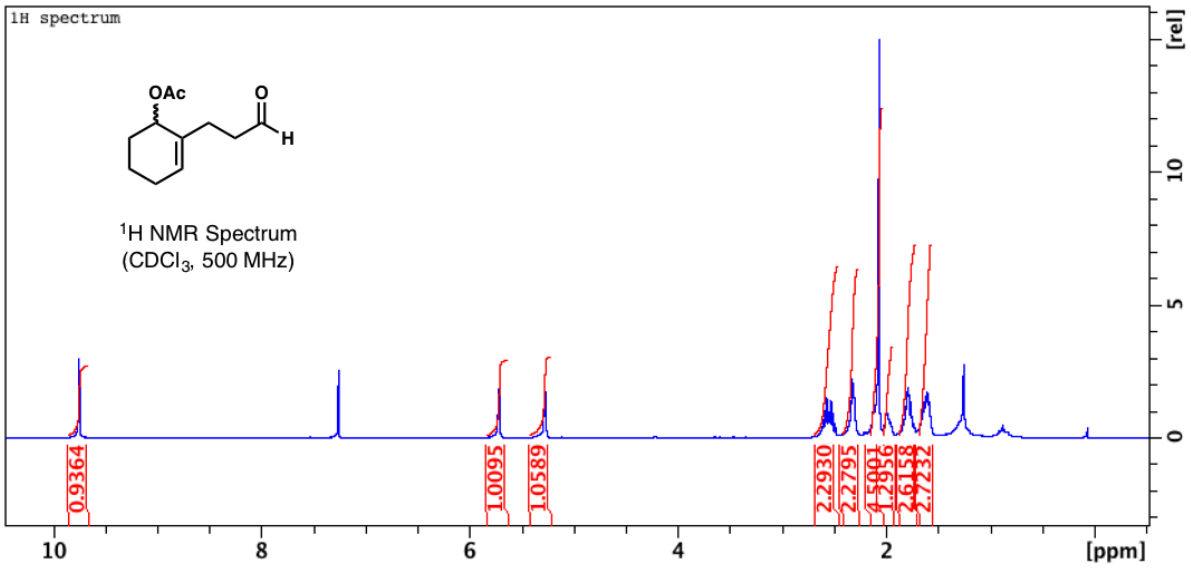

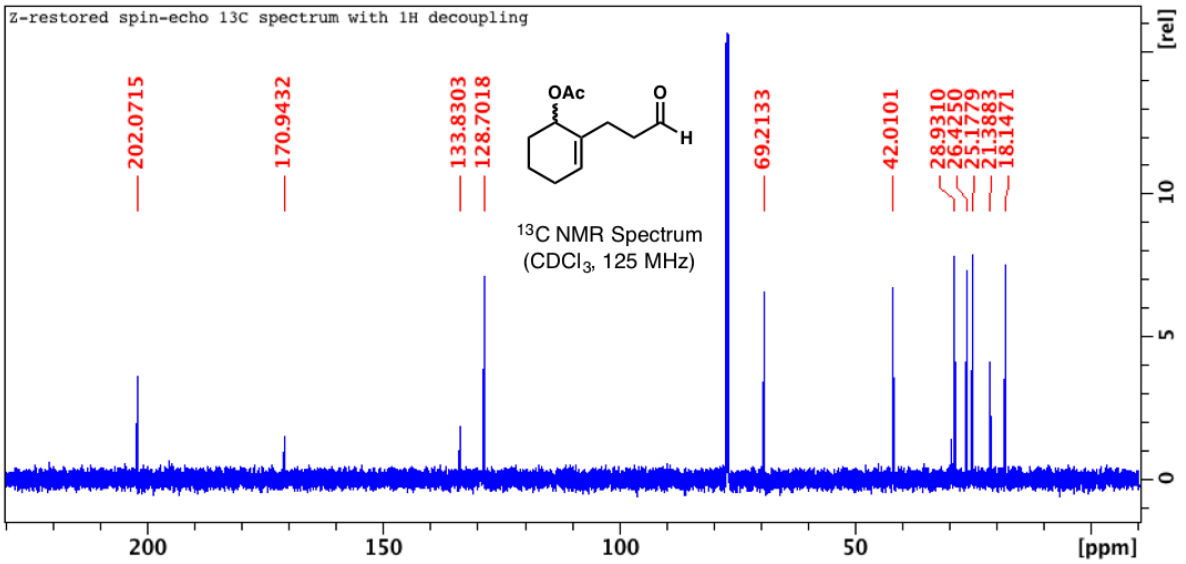

^{1}H and ^{13}C NMR spectra for **epoxide cyclic allylic acetate substrate 92**:

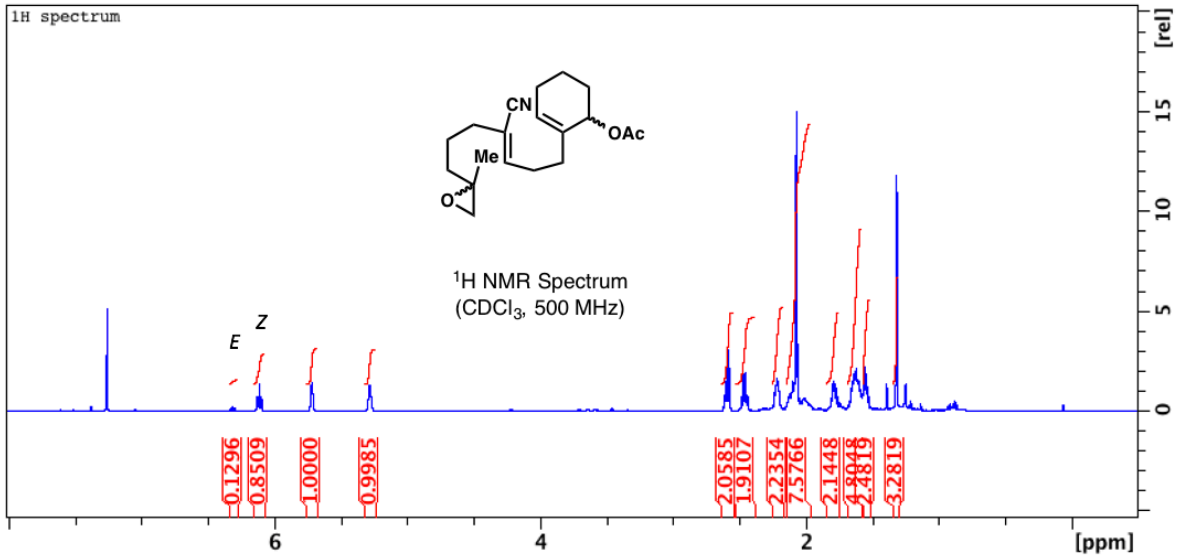

13C NMR: since neither of the chiral centers were set stereoselectively during the synthesis of **92**, both RR/SS and RS/SR diastereomers (that have (*Z*)-stereochemistry at the *α,β*-unsaturated nitrile since this stereocenter was formed as the major double bond isomer in the HWE) are present. The peaks in the carbon spectra of these very similar compounds overlap almost entirely, with differentiation only barely observable at the ester carbonyl carbon (170.976 and 170.980 ppm) and a few other peaks (listed in Appendix A). Also, integrating distinctive peaks gives a *Z*:*E* ratio of 6.6:1. Further characterization data (below) confirmed that the expected and desired (*Z*)-diastereomer was formed preferentially.

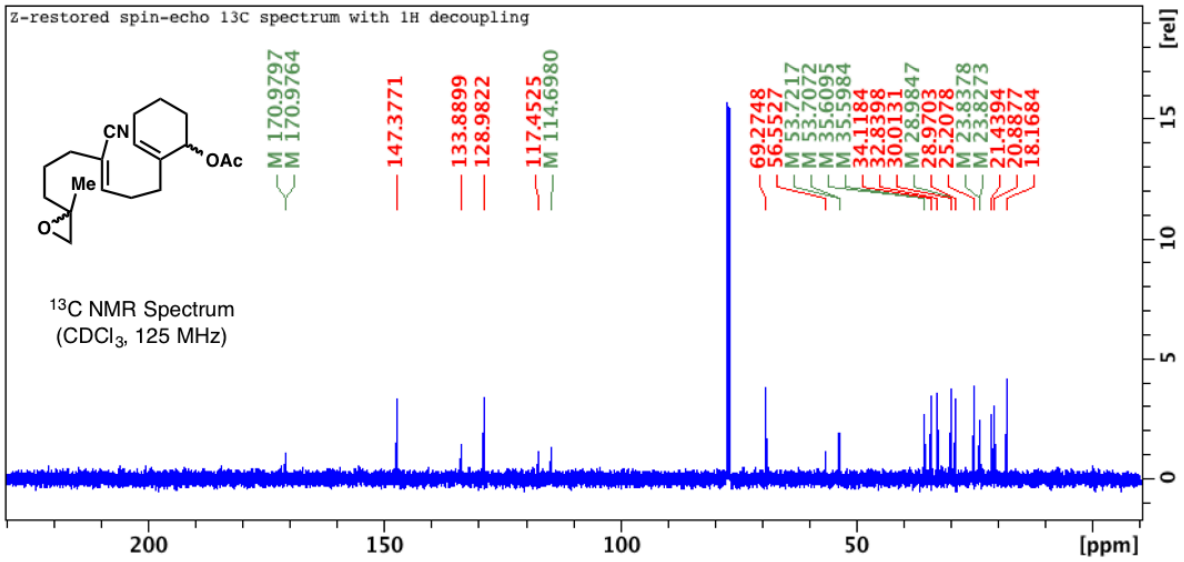
Z-restored spin-echo 13C spectrum with 1H decoupling
M 170.9797
M 170.9764
147.3771
133.8899
128.9822
117.4525
M 114.6980
69.2748
56.5527
M 53.7217
M 53.7072
M 35.6095
M 35.5984
34.1184
32.8398
30.0131
M 28.9847
28.9703
25.2078
M 23.8378
M 23.8273
21.4394
20.8877
18.1684
CN
OAc
Me
O
13C NMR Spectrum
(CDCl3, 125 MHz)
[rel]
0
5
10
15
200
150
100
50
[ppm]

COSY

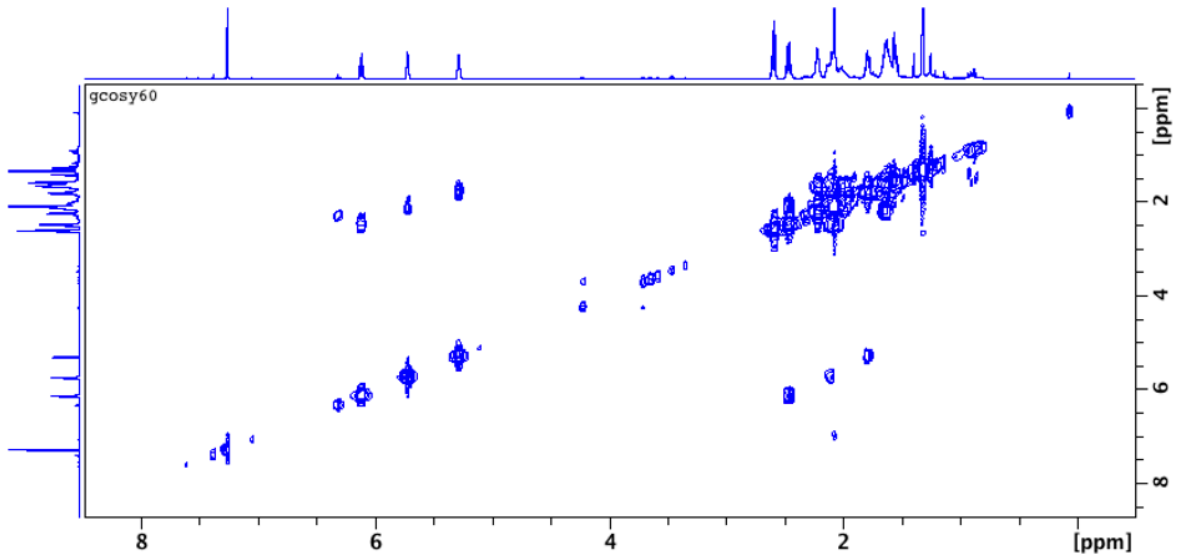
gcosy60
[ppm]
2
4
6
8
8
6
4
2
[ppm]

COSY expanded for range: [$^{1}H_x$: 6.01-6.21 ppm, $^{1}H_y$: 1.95-3.05 ppm]; the allylic methylene sp^3 protons gamma to the nitrile (2.46 ppm) exhibit a strong COSY correlation to the adjacent vinyl proton beta to the nitrile (6.11 ppm).

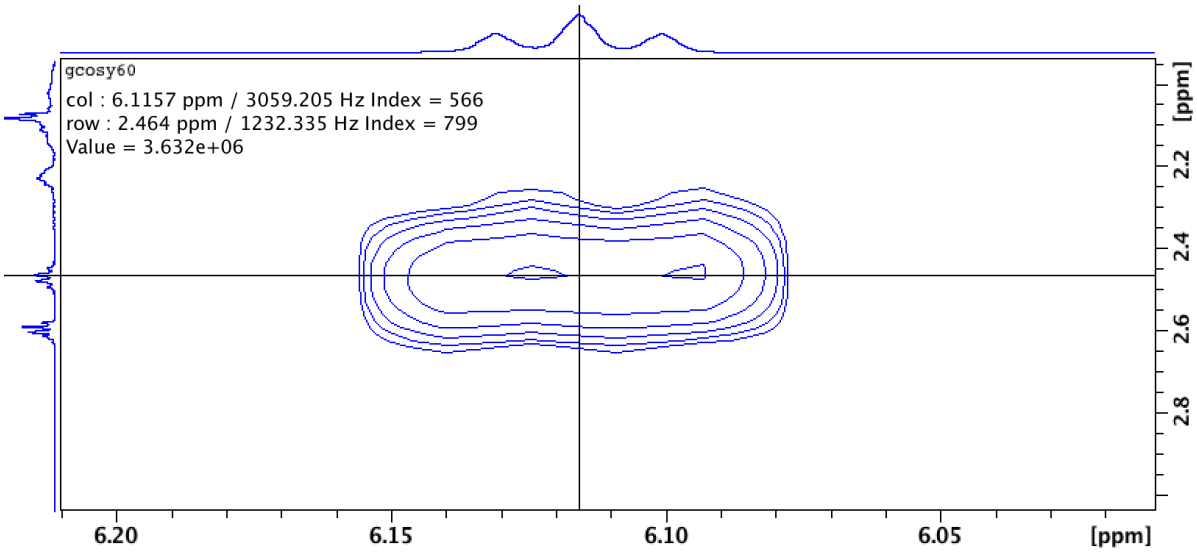

HMBC

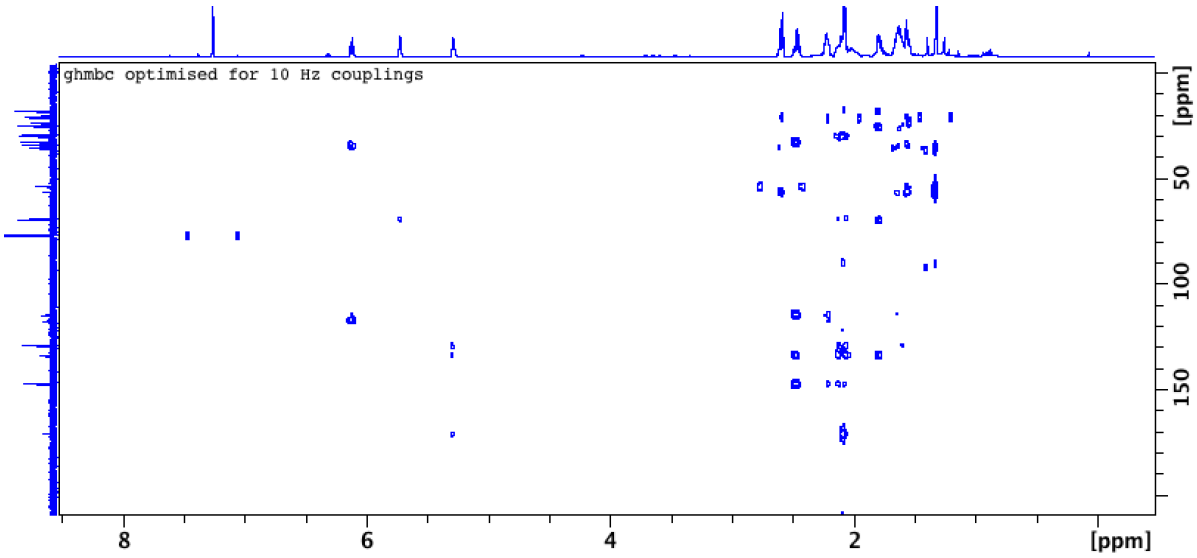

HMBC (opt. 10Hz) expanded for range: [$^{1}H_{x}$: 2.15-6.40 ppm, $^{13}C_{y}$: 112.5-121.0 ppm]; The vinylic proton on the sp^2 carbon beta to the nitrile at 6.11 ppm coupled with the expected coupling constant (J = 7.6 Hz) to the allylic sp^3 methylene protons gamma to the nitrile at 2.46 ppm. The two protons exhibiting a (^{1}H NMR) peak at approximately 2.23 ppm show HMBC correlations to both the nitrile carbon (114.7 ppm) and the quaternary sp^2 carbon (117.5 ppm) α to the nitrile. However, little to no correlation is observed in the COSY between these protons (~2.23 ppm) and the vinylic proton on the sp^2 carbon beta to the nitrile (6.11 ppm), thus providing further evidence that the former protons are the methylene sp^3 protons beta to the nitrile—providing a potential method of determining the stereochemistry of the major diastereomer due to the expected NOESY correlation between these protons and those at 6.11 ppm (discussed below).

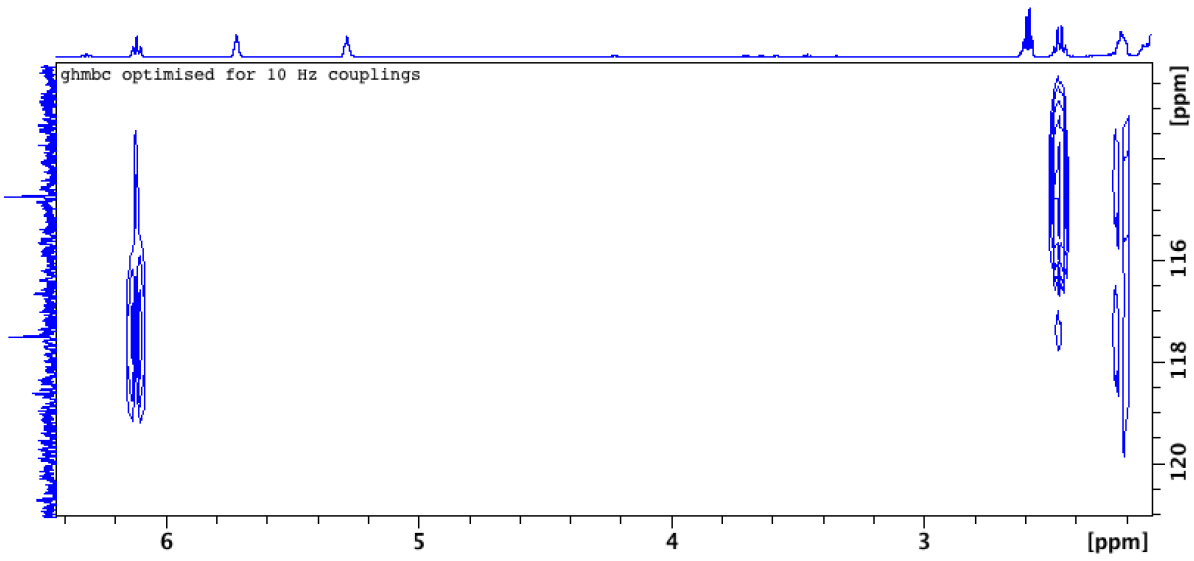

HMBC (opt. 10Hz) expanded for range: [$^{1}H_{x}$: 5.94-6.43 ppm, $^{13}C_{y}$: 23.5-47.0 ppm];

A (3-bond) HMBC correlation is observed between the apparent sp^3 carbon beta to the nitrile (~34.1 ppm; HMQC correlation to peak at ~2.23 ppm, below) and the vinylic proton beta to the nitrile (6.11 ppm).

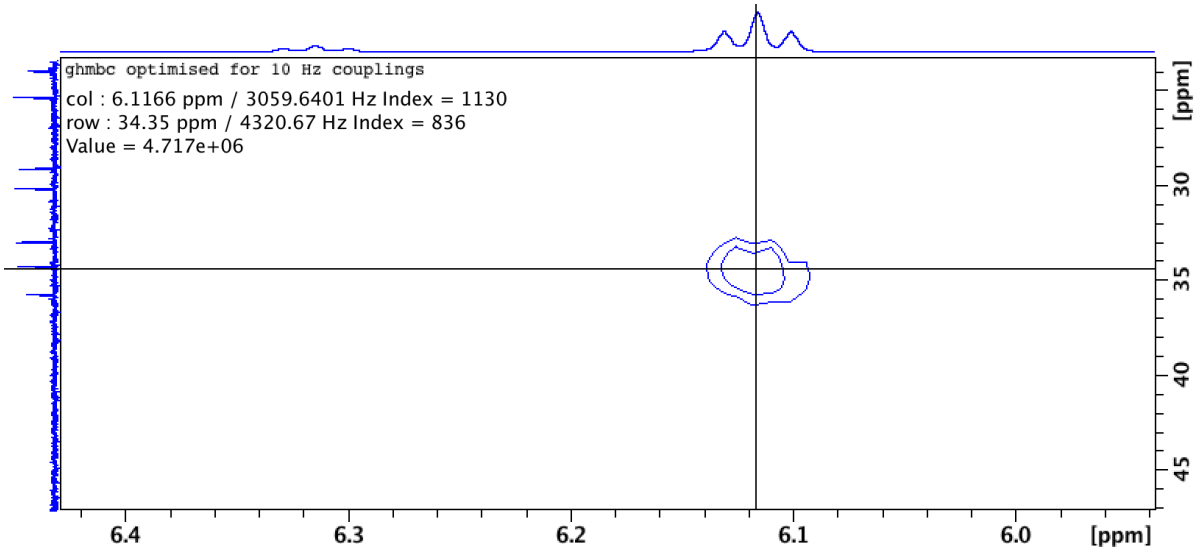

HMBC (opt. 10Hz) expanded for range: [$^{1}H_{x}$: 1.197-2.272 ppm, $^{13}C_{y}$: 109-150 ppm]; As further confirmation that the allylic sp^3 methylene protons beta to the nitrile exhibit the ^{1}H NMR peak at ~2.23 ppm, three HMBC correlations are observed in the spectrum below between these protons (~2.23 ppm) and: 1) the sp^2 carbon beta to the nitrile at 147.4 ppm (3-bond coupling); 2) the sp^2 ("quaternary") carbon alpha to the nitrile at 117.5 ppm (2-bond coupling); and 3) the sp nitrile carbon at 114.7 ppm (3-bond coupling).

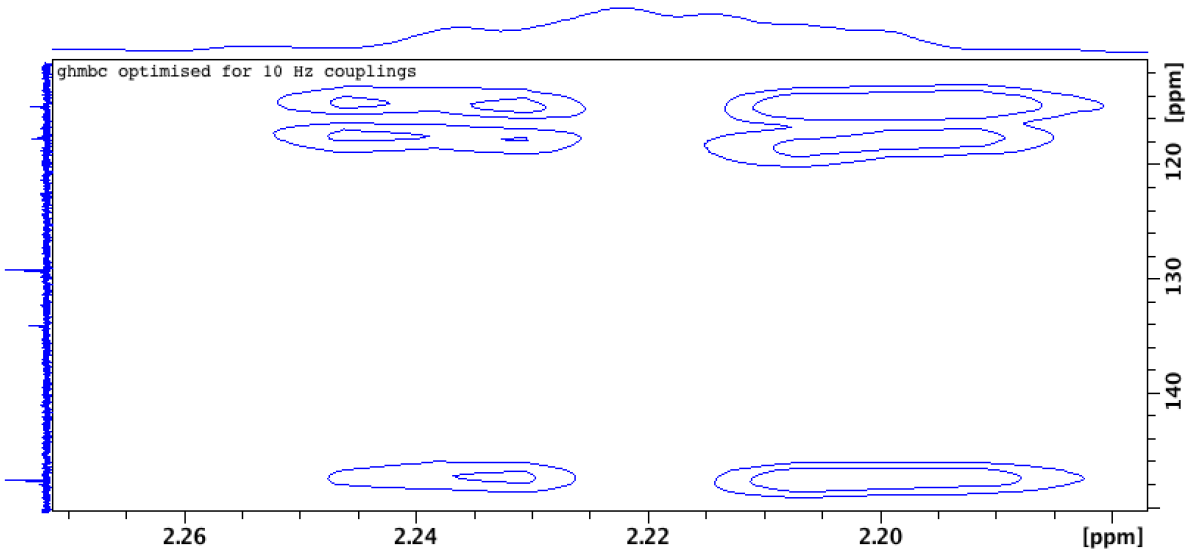

HMBC (opt. 10Hz) expanded for range: [$^{1}H_{x}$: 2.12-2.33 ppm, $^{13}C_{y}$: 31.6-38.7 ppm]; Furthermore, a (3-bond) HMBC correlation is observed between the apparent methylene sp^3 protons beta to the nitrile at ~2.23 ppm and the carbon signals at ~35.6 ppm (discussed below).

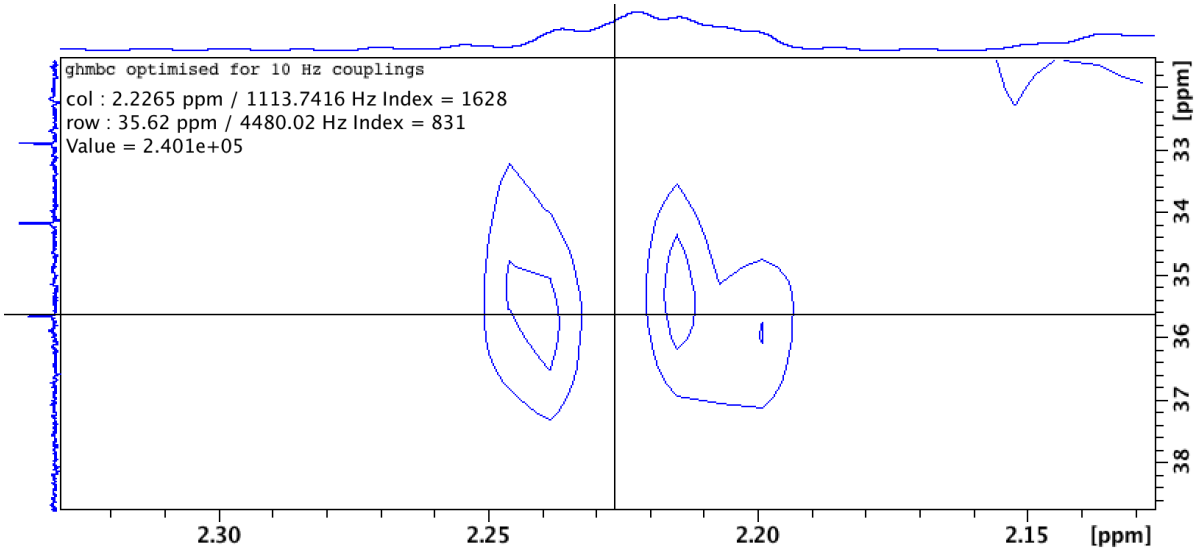

HMBC (opt. 10Hz) expanded for range: [$^{1}H_{x}$: 1.235-1.370 ppm, $^{13}C_{y}$: 30.5-41.5 ppm]; The carbon peaks at ~35.6 ppm (3 bonds from protons at ~2.23 ppm), in turn, show a (3-bond) HMBC correlation to the methyl protons adjacent to the epoxide (1.32 ppm), which also is consistent with the above characterization of the protons at ~2.23 ppm.

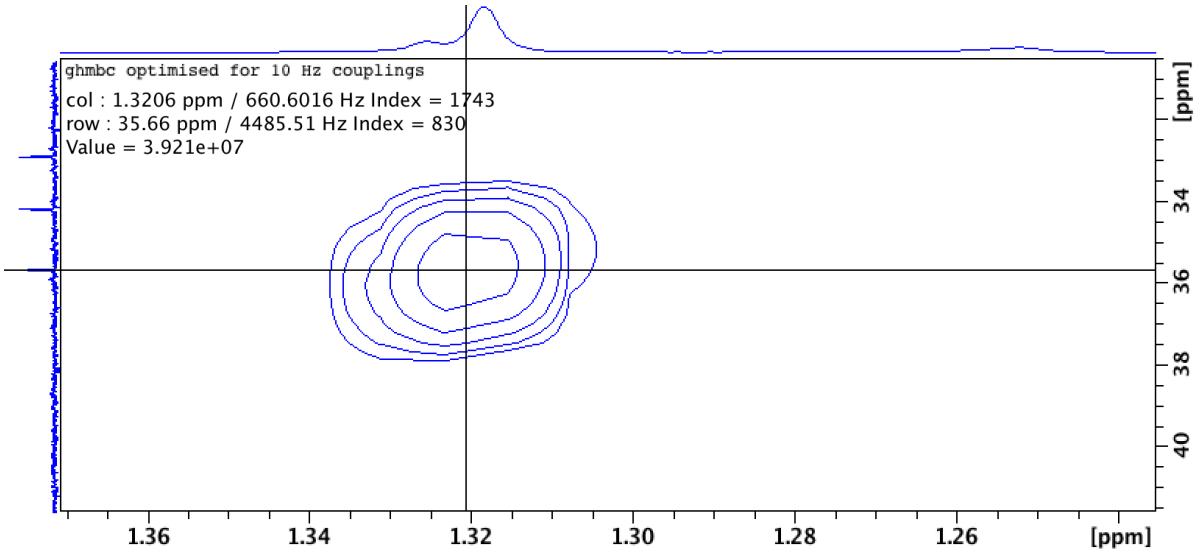

HMQC

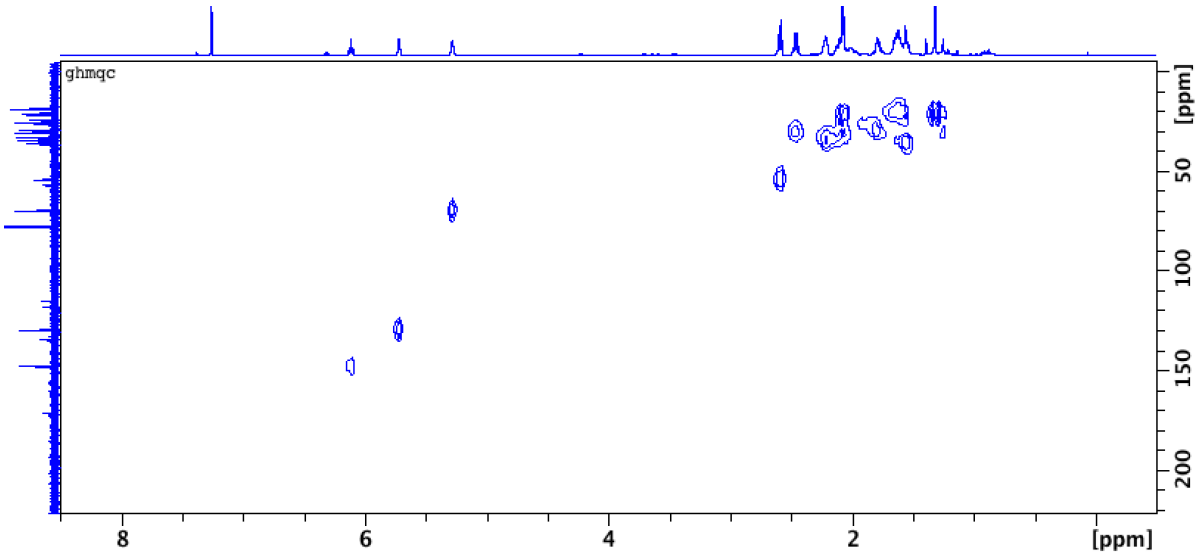

HMQC expanded for range: [$^{1}H_{x}$: 11-46 ppm, $^{13}C_{y}$: 0.3-2.8 ppm]; The HMQC correlation shown between the carbon at 34.1 ppm and the protons at ~2.23 ppm establish direct connectivity between the two.

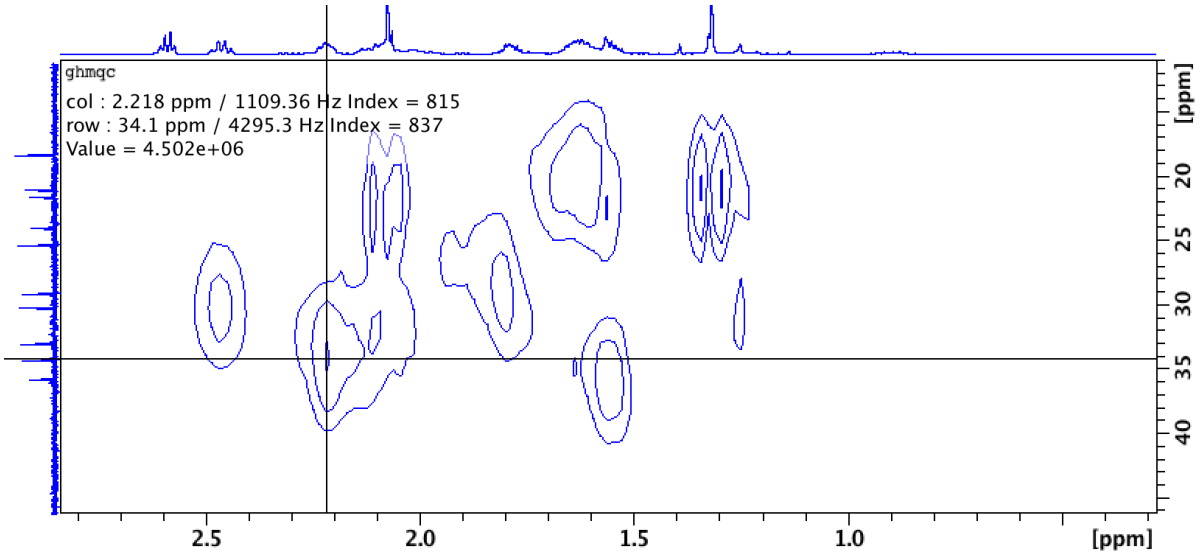

NOESY

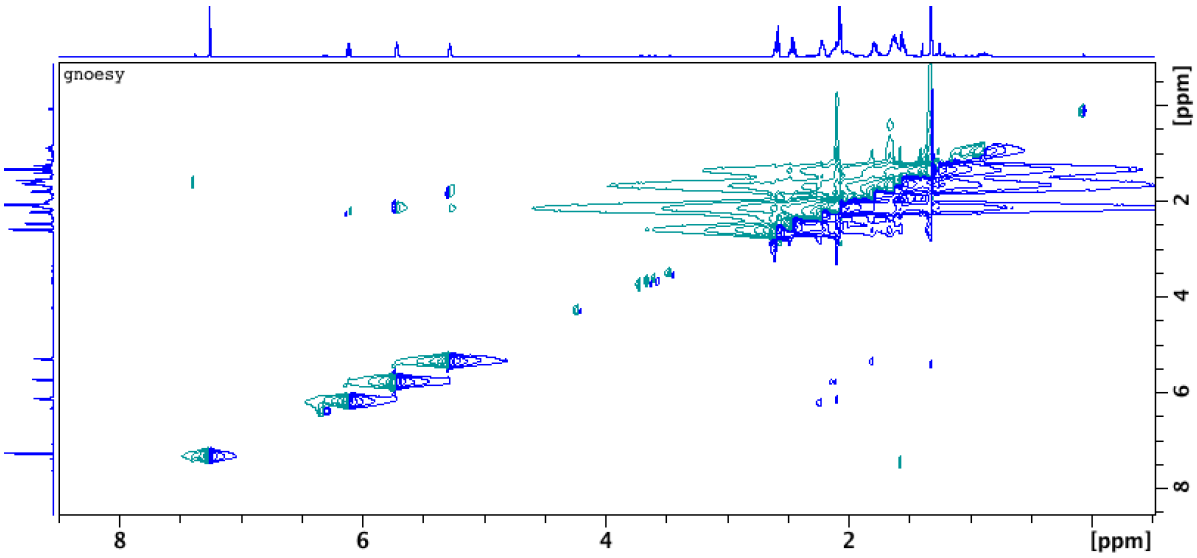

NOESY expanded for range: [$^{1}H_{x}$: 5.18-6.26 ppm, $^{1}H_{y}$: 1.95-2.77 ppm]; The relatively strong correlation between the peaks at 6.11 ppm and ~2.23 ppm, combined with the lack of correlation between the peaks at 6.11 ppm and 2.46 ppm, serve as strong evidence for the characterization of the major diastereomer as (*Z*). Specifically, the methylene sp^3 protons beta to the nitrile (~2.23 ppm) and the vinylic proton on the sp^2 carbon beta to the nitrile (6.11 ppm) are shown to be in close spatial proximity by the NOESY spectra. The lack of correlation between the vinylic proton beta to the nitrile (6.11 ppm) and the allylic sp^3 methylene protons gamma to the nitrile (2.46 ppm)—which show a strong COSY correlation, possess identical coupling constants (J = 7.6 Hz), and exhibit the expected (discernible) triplet and quartet splittings, respectively—further supports this conclusion.

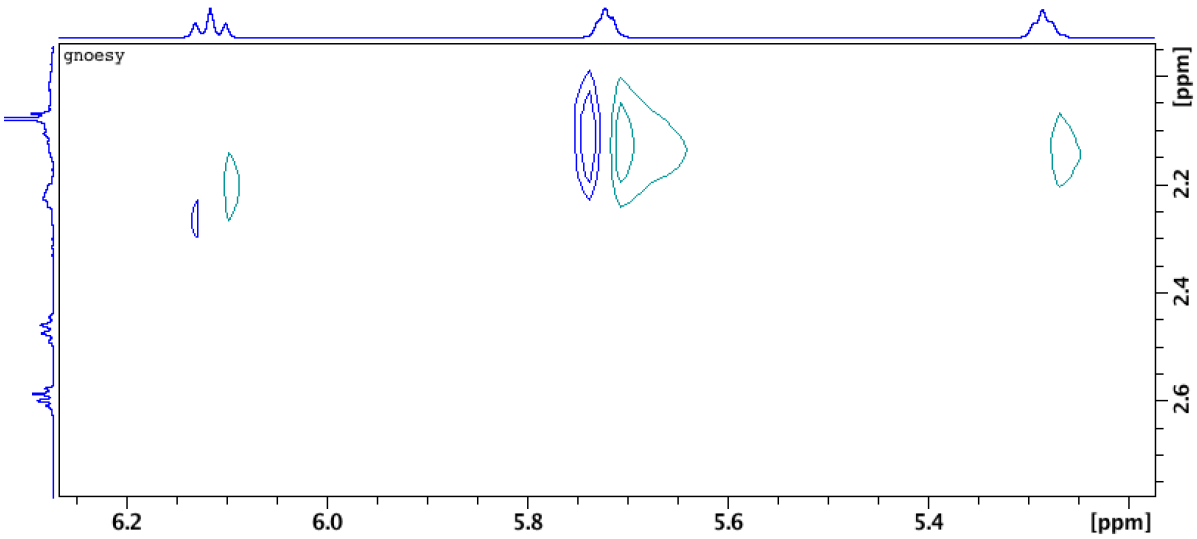

^{1}H NMR spectra for **silane substrate 126**:

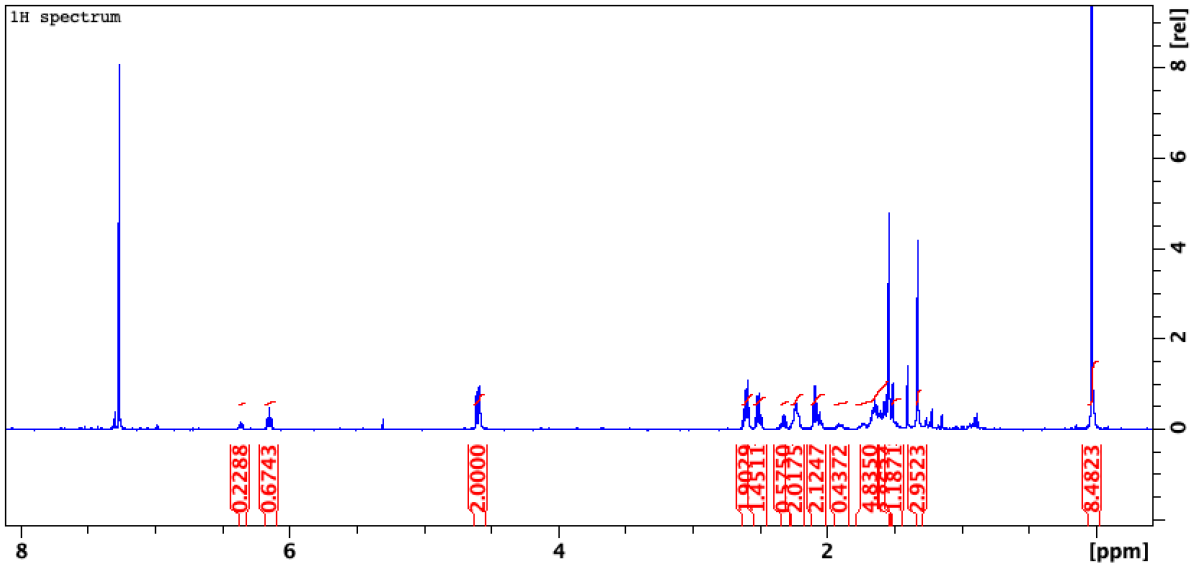

^{1}H and ^{13}C NMR spectra for **epoxy ketone substrate 127**:

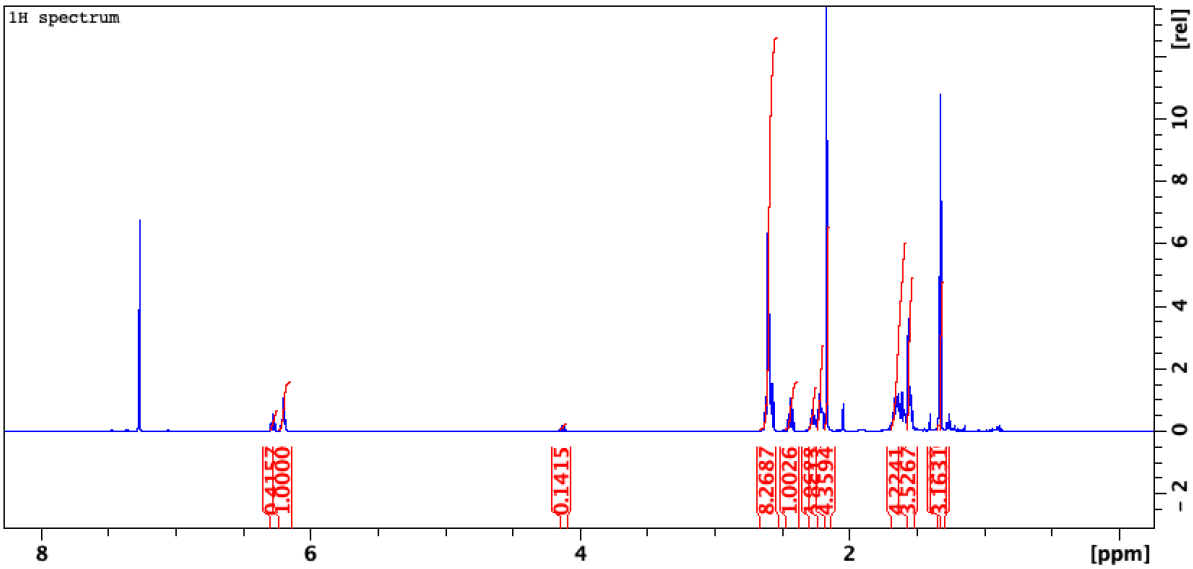

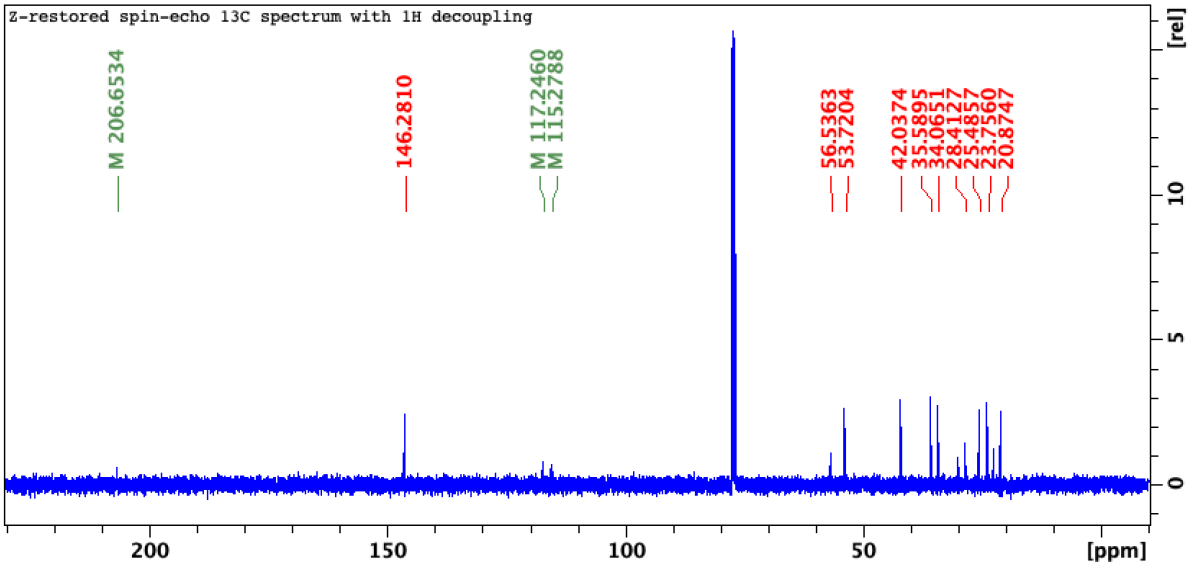
Z-restored spin-echo 13C spectrum with 1H decoupling
M 206.6534
146.2810
M 117.2460
M 115.2788
56.5363
53.7204
42.0374
35.5895
34.0651
28.4127
25.4857
23.7560
20.8747
[rel]
0
5
10
200
150
100
50
[ppm]